5-2021

Evaluation of conventional energy conservation strategies and active thermal insulation wall system and economic analyses.

Li Liu
University of Louisville

EVALUATION OF CONVENTIONAL ENERGY CONSERVATION STRATEGIES AND ACTIVE THERMAL INSULATION WALL SYSTEM AND ECONOMIC ANALYSES

By

Li Liu

B.S. Civil Engineering, Huazhong University of Science and Technology, 2012
M. S. Civil Engineering, University of Louisville, 2017

A Dissertation
Submitted to the Faculty of the
University of Louisville
J.B. Speed School of Engineering
as Partial Fulfillment of the Requirements
for the Degree of

Doctor of Philosophy

in Civil Engineering

Department of Civil & Environmental Engineering
University of Louisville
Louisville, Kentucky

May 2021

EVALUATION OF CONVENTIONAL ENERGY CONSERVATION STRATEGIES AND ACTIVE THERMAL INSULATION WALL SYSTEM AND ECONOMIC ANALYSES

By

Li Liu
B.S. Civil Engineering, Huazhong University of Science and Technology, 2012
M. S. Civil Engineering, University of Louisville, 2017

A Dissertation Approved on

April 16, 2021

by the following Dissertation Committee:

W. Mark McGinley, Dissertation Director

Omid Ghasemi Fare

Thomas D. Rockaway

Hui Wang

ACKNOWLEDGEMENTS

It is definitely not easy to finish this research without the help of my advisor, Dr. W. Mark McGinley. His guidance helped me start the topic of green engineering and building energy efficiency, and develop good research habits. In the past few years, he always encouraged me, pushed me, guided me, especially during this very tough COVID-19 time. I would like to give my appreciation to Dr. Ghasemi Fare, Dr. Rockaway, Dr. Wang, Dr. Sun for their help and guidance, they helped me improve my abilities and skills, as well.

I would like to thank my wife, Han Qiu, for her companion and support. Four years life overseas has brought a lot of fun and inconvenience as well. Through all the highs and lows, we stay together. She gave up her job opportunity, far from our families, friends and country, our loss of loved ones. These experiences make me understand that how precious time is, and seize the moment, make every minute counts. I can not finish this study without her support.

I would like to thank my parents and parents-in-law, my best friends in here, Yan Wu and Allison Chou. Of course, I appreciate the joy the little girl, Nicole Wu, has brought to me. I would like to graciously thank all of you and everyone else that has made opportunity come to fruition.

ABSTRACT

EVALUATION OF CONVENTIONAL ENERGY CONSERVATION STRATEGIES AND ACTIVE THERMAL INSULATION WALL SYSTEM AND ECONOMIC ANALYSES

Li Liu

April 16, 2021

For the past few decades, the importance and the technology of building energy conservation is increasing. In support of this research into energy efficiency, the U.S. Department of Energy has developed simulation models of sixteen buildings representing most commercial buildings in the US. In this research, four of these sixteen prototype models were used in energy conservation analyses variety of energy conservation strategies in the seven US Climate Zones.

To estimate the effectiveness of several common energy conservation measures on yearly building energy use, holistic analyses were conducted using software that accounts for the interactions of the building systems, occupants and the environment, including the impacts of thermal mass. In this investigation, the influence of thermal mass was also evaluated using thermal heat flow models. A novel energy conservation measure, an active thermal insulation wall system (ATIWS) that used circulating fluids in walls, was introduced and the influence of fluid temperature, pipe location and pipe spacing were evaluated using the proposed a series of thermal heat flow analyses.

Some conventional wall configurations and the active thermal insulation wall system were tested using hot box tests. The test results showed good agreement with predictions by thermal heat flow models. The impact of active insulation system was confirmed by the testing program. These tests showed that pipe location, pipe spacing and fluid temperature impacted the performance of active thermal insulation wall system.

To evaluate the viability of the various energy conservation measures investigated, a series of payback analysis was also performed.

Comparisons of energy conservation performance of conventional energy conservation strategies and the ATIWS system were made. Strategies for improved energy behavior of building systems were identified for the four different types of buildings studied, for all seven climate zones. The investigation showed that improving lighting, optimizing HVAC system setpoints, and adopting the active thermal insulation wall system had the greatest impact on energy use.

TABLE OF CONTENTS

ACKNOWLEDGEMENTS iii

ABSTRACT iv

LIST OF TABLES xi

LIST OF FIGURES xiii

CHAPTER 1 INTRODUCTION 1

1.1. The Importance of Energy Conservation in Buildings 1

1.2. Typical Energy Conservation Strategies in Buildings 2

1.2.1. Active Conservation Strategies 2

1.2.2. Passive Energy Conservation Strategies 3

1.3. Holistic Building Energy Analysis Programs 4

1.4. Dissertation Overview 5

CHAPTER 2 BACKGROUND 6

2.1. Literature Review/Energy Conservation Strategies Current Practices 6

2.1.1. Active Design Strategies: HVAC System 10

2.1.2. Active Design Strategies: Lighting 12

2.1.3. Active Design Strategies: Building Control System 13

2.1.4. Passive Design Strategies: Orientation 14

2.1.5. Passive Design Strategies: Opaque 14

2.1.6. Passive Design Strategies: Window/Facades 19

2.1.7. Passive Design Strategies: Thermal Mass 21

2.2. Active Thermal Insulation Wall System (ATIWS) 24

CHAPTER 3 BUILDING ENERGY MODELLING 30

3.1. Simulation Methods Used in This Research 30

3.1.1. OpenStudio (EnergyPlus) Modelling 31

3.1.2. MATLAB Modelling 35

3.1.3. ANSYS Modelling 41

3.2. Evaluation of Conventional Energy Conservation Strategies (Without Thermal Mass) 43

3.2.1. Yearly Energy Consumption Baselines 46

3.2.2. Impact of Wall Insulation 50

3.2.3. Impact of Roof Insulation 52

3.2.4. Impact of Lighting Efficiency 54

3.2.5. Impact of Lighting Demand 56

3.2.6. Impact of HVAC Cooling Coil COP 58

3.2.7. Impact of HVAC Heating Efficiency 59

3.2.8. Impact of Window Glazing System 60

3.2.9. Impact of Window SHGC 63
3.2.10. Impact of HVAC Setpoints 64
3.2.11. Impact of Setpoint Deadband Width 68
3.2.12. Impact of Wall Reflectance 69
3.2.13. Results and Discussion 71
3.3. Energy Conservation Leveraging Thermal Mass Effects 78
3.3.1. MATLAB Model Analysis in Typical Summer/Winter Condition 79
3.3.2. OpenStudio Model Simulation in U.S. Climate Zone Weather Conditions 87
3.3.3. Results and Discussion 92
3.4. Active Thermal Insulation Wall Systems in Typical Summer/Winter Condition 94
3.4.1. Model Descriptions of Active Thermal Insulation (Mass) Wall System and Four Conventional Wall Systems 94
3.4.2. Analytical Results of the Conventional Wall System 98
3.4.3. Analytical Results of Fixed Spacing ATIWS 101
3.4.4. Analytical Results of Variable Spacing ATIWS 108
3.4.5. Discussion 109
CHAPTER 4 TESTING PROGRAM 110
4.1. Specimen Description and Testing Configurations 110
4.1.1. Materials 110

4.1.2. Specimens 112

4.1.3. Sensors 115

4.2. Testing Apparatus 119

4.2.1. Temperature Regimes 121

4.2.2. Testing Matrix 121

CHAPTER 5 TEST RESULTS AND OBSERVATIONS 130

5.1. Test Results of Conventional Wall Specimens 132

5.2. Test Results of Active Thermal Insulation Wall Specimens 134

5.3. Validation of MATLAB Model Simulations 142

5.4. Performance of Active Thermal Insulation Wall System in U.S. Climate Zone Weather Conditions 149

5.4.1. Temperature Conditions 150

5.4.2. Simulation Results 152

5.5. Discussion 161

CHAPTER 6 PAYBACK ANALYSIS 162

6.1. Payback Analysis Assumptions 162

6.1.1. Payback Analysis Assumptions for Conventional Energy Conservation Measures 162

6.1.2. Payback Analysis Assumptions for ATIWS 166

6.2. Payback Analysis Results 174

6.2.1. Large Office 174

6.2.2. Secondary School 181

6.2.3. Standalone Retail 187

6.2.4. Midrise Apartment 192

6.3. Payback Analysis Summary 198

CHAPTER 7 SUMMARY, CONCLUSION AND RECOMMENDATIONS 201

REFERENCES 207

APPENDIX A. Plots of Hot Box Test Results 219

APPENDIX B. MATLAB Code 228

CURRICULUM VITA 236

LIST OF TABLES

Table 3-1: DOE Prototype Buildings 31

Table 3-2: Representative Cities for the Seven Climate Zones 33

Table 3-3: Thermal Properties of Materials 40

Table 3-4: Energy Conservation Strategy Ratings for the Large Office Prototype Based on ESP 72

Table 3-5: Energy Conservation Strategy Ratings for the Secondary School Prototype Based on ESP 73

Table 3-6: Energy Conservation Strategy Ratings for the Standalone Retail Prototype Based on ESP 74

Table 3-7: Energy Conservation Strategy Ratings for the Midrise Apartment Based on ESP 76

Table 3-8: Thermal Properties of Exterior Wall Materials 87

Table 3-9: Simulation Matrix for 16-inch Active Thermal Insulation Wall 101

Table 4-1: Thermal Properties of Materials Used in Tests 111

Table 4-2: List of Specimens (Conventional Wall Specimen) 113

Table 4-3: List of Specimens (Active Thermal Insulation Wall Specimen) 113

Table 4-4: Hot Box Testing Matrix: Phase 1 125

Table 4-5: Hot Box Testing Matrix: Phase 2 126

Table 4-6: Hot Box Testing Matrix: Phase 3 127

Table 4-7: Hot Box Testing Matrix: Phase 4 128

Table 5-1: Measured $T_{in,max}$' and Their Average for Conventional Wall Specimens..... 132

Table 5-2: Measured $T_{in,max}$' and Their Average (Fixed Spacing Active Thermal Insulation Wall) 135

Table 5-3: Measured $T_{in,max}$' and Their Average (Variable Spacing Active Thermal Insulation Wall) 139

Table 5-4: Measured and Predicted $T_{d,\,max}$' and Deviation of the Method 146

Table 5-5: Temperature Condition of Seven Representative Cities by Season (°C) 151

Table 5-6: MATLAB Simulation Results for Active Thermal Insulation Walls in Seven Representative Cities by Season 153

Table 6-1: Available Lighting Bulbs for Baseline Prototypes..... 163

Table 6-2: Available Lighting Bulbs for Lighting Improved Prototypes 163

Table 6-3: Unit Price of Trane Heat Pumps..... 165

Table 6-4: Unit Price of Trane Air Conditioner..... 165

Table 6-5: The Maximum ESP of Wall Insulation in Seven Climate Zones..... 171

Table 7-6: Payback Analysis for the Large Office Prototype in Seven Climate Zones . 176

Table 7-7: Payback Analysis for Secondary School Prototype in Seven Climate Zones 182

Table 7-8: Payback Analysis for Standalone Retail Prototype in Seven Climate Zones 188

Table 7-9: Payback Analysis for Midrise Apartment Prototype in Seven Climate Zones 193

LIST OF FIGURES

Figure 1-1 Energy Consumption by Sector *1*

Figure 1-2 Total Energy Consumption by Sector *1*

Figure 2-1 Active Thermal Insulation Wall System: Direct Exchange *25*

Figure 2-2 Active Thermal Insulation Wall System: With Heat/Cool Sources *25*

Figure 3-1 The Selected Four Prototype Buildings: a) Large Office; b) Secondary School; c) Standalone Retail; d) Midrise Apartment *33*

Figure 3-2 Convective Heat Transfer Rate at Pipe Inner Surface Per Whitaker Correlation *38*

Figure 3-3 Typical 8-inch-Wide CMU MATLAB Model & Meshing *39*

Figure 3-4 Typical 16-inch-Wide CMU MATLAB Model & Meshing *39*

Figure 3-5 Typical 8-inch-Wide Poured Concrete MATLAB Model & Meshing *40*

Figure 3-6 8-inch-Wide CMU ANSYS Model & Meshing: (Left) Isometric View (Right) Top View *41*

Figure 3-7 Total Yearly Energy Consumption Baselines of The Four Prototype in the Seven Climate Zones: a) Large Office; b) Secondary School; c) Standalone Retail; d) Midrise Apartment *47*

Figure 3-8 Figure Heating/Cooling Related Energy of the Four Prototype Baselines in the Seven Climate Zones: a) Large Office; b) Secondary School; c) Standalone Retail; d) Midrise Apartment *48*

Figure 3-9 End Use of the Four Prototype Baselines by Percentage in Climate Zone 5A: a) Large Office; b) Secondary School; c) Standalone Retail; d) Midrise Apartment 49

Figure 3-10 ESP of Wall Insulation Thickness: a) Large Office; b) Secondary School; c) Standalone Retail; d) Midrise Apartment 51

Figure 3-11 Heating/Cooling Related Energy Consumption of Wall Insulation: a) Large Office; b) Secondary School; c) Standalone Retail; d) Midrise Apartment 52

Figure 3-12 ESP of Roof Insulation Thickness: a) Large Office; b) Secondary School; c) Standalone Retail; d) Midrise Apartment 54

Figure 3-13 ESP of Lighting Efficiency: a) Large Office; b) Secondary School; c) Standalone Retail; d) Midrise Apartment 55

Figure 3-14 Lighting Related Energy Consumption of Lighting Efficiency: a) Large Office; b) Secondary School; c) Standalone Retail; d) Midrise Apartment 56

Figure 3-14 ESP of Lighting Demand: a) Large Office; b) Secondary School; c) Standalone Retail; d) Midrise Apartment 57

Figure 3-16 Lighting Related Energy Consumption and Lighting Demand: a) Large Office; b) Secondary School; c) Standalone Retail; d) Midrise Apartment 58

Figure 3-17 ESP of Cooling Coil COP Efficiency: a) Large Office; b) Secondary School; c) Standalone Retail; d) Midrise Apartment 59

Figure 3-18 ESP of Heating Efficiency: a) Large Office; b) Secondary School; c) Standalone Retail; d) Midrise Apartment 60

Figure 3-19 ESP of Window Glazing System: a) Large Office; b) Secondary School; c) Standalone Retail; d) Midrise Apartment Impact of Window Frames 62

Figure 3-20 ESP of U Factor of Window Frames: a) Large Office; b) Secondary School; c) Standalone Retail; d) Midrise Apartment *63*

Figure 3-21 ESP of Window SHGC: a) Large Office; b) Secondary School; c) Standalone Retail; d) Midrise Apartment *64*

Figure 3-22 ESP of Setpoints Scenario 1: a) Large Office; b) Secondary School; c) Standalone Retail; d) Midrise Apartment *67*

Figure 3-23 ESP of Setpoints Scenario 2: a) Large Office; b) Secondary School; c) Standalone Retail; d) Midrise Apartment *68*

Figure 3-24 ESP of Setpoints Deadband Width: a) Large Office; b) Secondary School; c) Standalone Retail; d) Midrise Apartment *69*

Figure 3-25 ESP of Wall Reflectance: a) Large Office; b) Secondary School; c) Standalone Retail; d) Midrise Apartment *71*

Figure 3-26 Ambient Temperature Conditions Used in the MATLAB Analysis *81*

Figure 3-27 Temperature of Wall Surfaces in a Mild Summer Weather with Different Specific Heat for Uninsulated Walls *82*

Figure 3-28 Peak Temperature Time Lag with Different Specific Heat Wall in Summer Weather *84*

Figure 3-29 Peak Temperature Time Lag with Different Specific Heat Wall in Winter Weather *84*

Figure 3-30 Amplitude of Temperature on Interior Surface with Different Specific Heat Wall in Summer Weather *85*

Figure 3-31 Amplitude of Temperature on Interior Surface with Different Specific Heat Wall in Winter Weather *86*

Figure 3-32 Yearly Energy Consumption with Different Wall Configurations (Large Office) *88*

Figure 3-33 Yearly Energy Consumption with Different Wall Configurations (Secondary School) *89*

Figure 3-34 Total Energy Consumption with Different Wall Configurations (Standalone Retail)..... *89*

Figure 3-35 Total Energy Consumption with Different Wall Configurations (Midrise Apartment) *90*

Figure 3-36 Solid Grouted CMU Wall *95*

Figure 3-37 Grouted CMU Wall with Air Gap..... *95*

Figure 3-38 Grouted CMU Wall with Rigid Insulation Insert *96*

Figure 3-39 Grouted CMU Wall with Rigid Reflective Insulation Insert..... *96*

Figure 3-40 General Active Thermal Insulation (mass) Wall Model..... *98*

Figure 3-41 Temperature of CMU Surfaces (Solid Grouted)..... *99*

Figure 3-42 T_d of the Four Conventional Walls in Summer..... *100*

Figure 3-43 T_d of the Four Conventional Walls in Winter..... *100*

Figure 3-44 Isotherm at Time=16.3h of ATIWS Simulation No. 1-5 ..... *103*

Figure 3-45 Temperature Response at Surfaces of ATIWS, Pipe at Middle, Pipe Spacing16 inches, Summer *104*

Figure 3-46 T_d Response of Simulations No 1_1 to 1_9 (Summer, Indoor 22°C, 16 inches Spacing) *105*

Figure 3-47 $T_{d,\ mean}$ with Variable Pipe Location and Fluid Temperature of 16-inch Pipe Spacing in (a) Summer Set Point 22°C; (b) Summer Set Point 24°C; (c) Winter Set Point 22°C; (d) Winter Set Point 24°C *107*

Figure 3-48 $T_{d,\ mean}$ VS. Pipe Spacing (Fluid Temperature 16°C, Indoor 24°C in Summer, Indoor 22°C in Winter) *109*

Figure 4-1 CMU Blocks: 8-inch Half Block (Left), 16 inch Knockout Block (Right) *111*

Figure 4-2 Insulation Materials: 1-inch R-5 XPS Insulation (Left), 1-inch R-5 Reflective Inserts (Right) *112*

Figure 4-3 Black Steel Pipes (Left) and Connection Detail (Right) *112*

Figure 4-4 Specimen Casting (Conventional Wall Specimen) *114*

Figure 4-5 Specimen Casting (Active Thermal Insulation Wall Specimen) *115*

Figure 4-6 OMEGA T Type Thermocouple (Left) and OMEGA HFS-5 Heat Flux Sensor (Right) *116*

Figure 4-7 Thermocouple Locations on Pipes before Grouted (Demonstration) *116*

Figure 4-8 Specimens Sensor Layout: CONVL_1, CONVL_2, CONVL_3, CONVL_4, ACTV_1, ACTV_2, ACTV_3, ACTV_4, ACTV_5, ACTV_6, ACTV_7, ACTV_8, ACTV_9 (A, B, C, D, E, F, G, H, I, J, K, L, M) *118*

Figure 4-9 Hot Box Test Apparatus Demonstration (by Sketchup) *120*

Figure 4-10 Hot Box Test Apparatus Demonstration *120*

Figure 4-11 Specimens Tested in Hot Box Test Phase One: Three Replicants of CONVL_1 (A, B & C) *122*

Figure 4-12 Specimens Tested in Hot Box Test Phase Two: CONVL_2, CONVL_3, CONVL_4 (A, B & C) *123*

Figure 4-13 Specimens Tested in Hot Box Test Phase Three: ACTV_4, ACTV_5, ACTV_6 (A, B & C) *124*

Figure 4-14 Specimens Tested in Hot Box Test Phase Four: ACTV_1, ACTV_2, ACTV_3, ACTV_7, ACTV_8, ACTV_9 (A, B, C, D, E, F) *125*

Figure 5-1 Temperature Response of The Three Solid Grouted Specimen Replicates... *130*

Figure 5-2 Temperature Response of 16-inch Active Thermal Insulation Specimens in Summer Condition with Indoor Temperature of 22°C..... *137*

Figure 5-3 Temperature Response of 16-inch Active Thermal Insulation Specimens in Summer Condition with Indoor Temperature of 24°C..... *137*

Figure 5-4 Temperature Response of 16-inch Active Thermal Insulation Specimens in Winter Condition with Indoor Temperature of 22°C..... *138*

Figure 5-5 Temperature Response of Variable Spacing Active Thermal Insulation Specimens in Summer Condition with Fluid Temperature of 16℃ and Indoor Set Point of 22℃ *141*

Figure 5-6 Temperature Response of Variable Spacing Active Thermal Insulation Specimens in Winter Condition with Fluid Temperature of 16℃ and Indoor Set Point of 22℃ *141*

Figure 5-7 MATLAB Model Validation of Solid Grouted Specimen Test No.1_1 Temperature Response..... *143*

Figure 5-8 MATLAB Model Validation of Solid Grouted with Air Gap Specimen Test No.2_1 Temperature Response..... *143*

Figure 5-9 MATLAB Model Validation of Solid Grouted with Insulation Inserts Specimen Test No.2_3 Temperature Response *144*

Figure 5-10 MATLAB Model Validation of Solid Grouted with Reflective Inserts Specimen Test No.2_5 Temperature Response *144*

Figure 5-11 MATLAB Model Validation of Solid Grouted with Reflective Inserts Specimen Test No.2_6 (Flipped) Temperature Response *145*

Figure 5-12 MATLAB Model Validation of 16-Inch Active Thermal Insulation Wall Specimen Test No.3_9 Temperature Response *145*

Figure 5-13 MATLAB Simulation of the Five Proposed Wall's Performance in Climate Zone 1A *155*

Figure 5-14 MATLAB Simulation of the Five Proposed Wall's Performance in Climate Zone 2A *156*

Figure 5-15 MATLAB Simulation of the Five Proposed Wall's Performance in Climate Zone 3B *156*

Figure 5-16 MATLAB Simulation of the Five Proposed Wall's Performance in Climate Zone 4C *157*

Figure 5-17 MATLAB Simulation of the Five Proposed Wall's Performance in Climate Zone 5A *157*

Figure 5-18 MATLAB Simulation of the Five Proposed Wall's Performance in Climate Zone 6A *158*

Figure 5-19 MATLAB Simulation of the Five Proposed Wall's Performance in Climate Zone 7 ..... *158*

Figure A-1 Temperature Response of The Three Solid Grouted Specimen Replicates .. *219*

Figure A-2 Temperature Response of The Solid Grouted with Air Gap Specimen (Both Directions) *220*

Figure A-3 Temperature Response of The Solid Grouted with Insulation Insert Specimen (Both Directions) *220*

Figure A-4 Temperature Response of The Solid Grouted with Reflective Insert & Air Gap Specimen (Both Directions) *221*

Figure A-5 Temperature Response of The Active Thermal Insulation Specimen (16-inch specimen, pipe near interior) in Summer Condition (Test No.3_1, No.3_2, No.3_3) *221*

Figure A-6 Temperature Response of The Active Thermal Insulation Specimen (16-inch specimen, pipe near interior) in Summer Condition (Test No.3_4, No.3_5)..... *222*

Figure A-7 Temperature Response of The Active Thermal Insulation Specimen (16-inch specimen, pipe near interior) in Winter Condition (Test No.3_6, No.3_7, No.3_8)..... *222*

Figure A-8 Temperature Response of The Active Thermal Insulation Specimen (16-inch specimen, pipe in middle) in Summer Condition (Test No.3_9, No.3_10, No.3_11)..... *223*

Figure A-9 Temperature Response of The Active Thermal Insulation Specimen (16-inch specimen, pipe in middle) in Summer Condition (Test No.3_13) *223*

Figure A-10 Temperature Response of The Active Thermal Insulation Specimen (16-inch specimen, pipe in middle) in Winter Condition (Test No.3_14, No.3_15, No.3_16)..... *224*

Figure A-11 Temperature Response of The Active Thermal Insulation Specimen (16-inch specimen, pipe near exterior) in Summer Condition (Test No.3_17, No.3_18)..... *224*

Figure A-12 Temperature Response of The Active Thermal Insulation Specimen (16-inch specimen, pipe near exterior) in Summer Condition (Test No.3_19, No.3_20)..... *225*

Figure A-13 Temperature Response of The Active Thermal Insulation Specimen (16-inch specimen, pipe near exterior) in Winter Condition (Test No.3_21, No.3_22)..... *225*

Figure A-14 Temperature Response of The Active Thermal Insulation Specimen (8-inch specimen) in Summer Condition (Test No.4_1, No.4_3) 226

Figure A-15 Temperature Response of The Active Thermal Insulation Specimen (8-inch specimen) in Winter Condition (Test No.4_2, No.4_4)..... 226

Figure A-16 Temperature Response of The Active Thermal Insulation Specimen (24-inch specimen) in Summer Condition (Test No.4_7, No.4_9, No.4_11)..... 227

Figure A-17 Temperature Response of The Active Thermal Insulation Specimen (24-inch specimen) in Winter Condition (Test No.4_8, No.4_10, No.4_12)..... 227

CHAPTER 1

INTRODUCTION

1.1. The Importance of Energy Conservation in Buildings

According to statistics published by International Energy Agency (IEA), over the past two decades the total world energy consumption has continued to grow. An estimate by the Energy Information Administration (EIA) indicates that the energy used in both the commercial and residential sectors are mostly building related. Data published by EIA (Figure 1-1) shows that these two sectors accounted for about 40% (or about 40 quadrillion Btu) of the total U.S. energy consumption in 2018. As shown in Figure 1-2, (World Energy Balance: Overview 2018 edition), the residential and public services sectors accounted for about 30% of total world energy consumption in 2016. Thus, building energy efficiency plays an increasingly important role in sustainable world development.

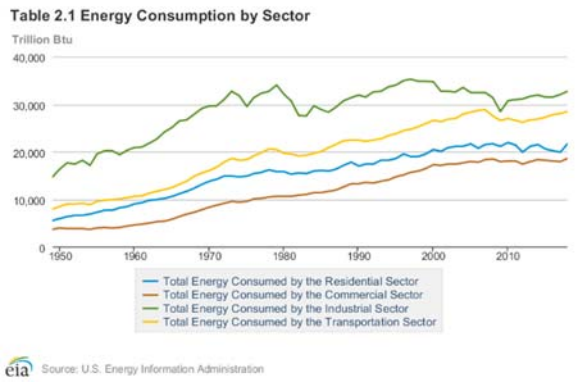

Figure 1-1 Energy Consumption by Sector

https://www.eia.gov/totalenergy/data/browser/?tbl=T02.01#/?f=A

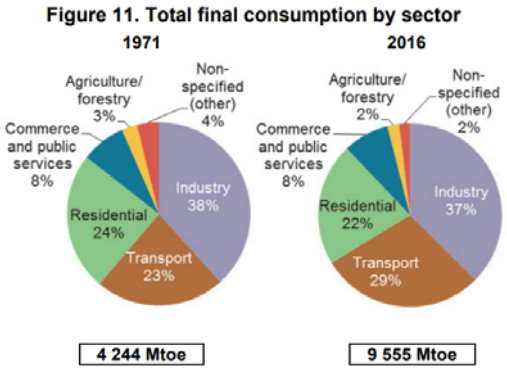

Figure 1-2 Total Energy Consumption by Sector

https://webstore.iea.org/download/direct/2263?fileName=World_Energy_Balances_2018_Overview.pdf

1.2. Typical Energy Conservation Strategies in Buildings

Energy conservation strategies were classified as either active or passive. The former includes optimizing the building systems that provide heating, ventilation, and air conditioning, and lighting, while the latter generally focusses on improving the building envelope in an effort to manage energy losses and gains. These two types of energy conservation strategies, along with development of renewable energy sources (mainly solar panels) are expected to help meet the zero-energy consumption of the whole building (X. Sun, Gou, & Lau, 2018). There are also a number of hybrid strategies that use mechanical energy to enhance renewable energy sources such as: heat recovery ventilation, economizer ventilation, solar thermal systems, radiant facades, and ground source heat pumps. But generally, these hybrid strategies are categorized with the active design strategies.

There are also energy efficiency practices that focus on reducing the building life cycle energy use and environmental impact, like the use of concrete that has recycled CO_2 embedded within its volume (Lenz, 2015). These technologies also address energy consumed during production of the construction materials. However, these are beyond the scope of this dissertation.

1.2.1. Active Conservation Strategies

Generally, active energy conservation strategies make uses of purchased energy and active building services systems to keep the building comfortable. These strategies include forced-air HVAC systems, heat pumps, radiant panels or chilled beams, electric lighting and so on. Active energy conservation strategies can be rather comprehensive. Common active energy conservation measures in buildings are:

a) Energy efficient systems: improved efficiency of the HVAC, lighting, or vertical transportation systems,
b) On-site renewable energy generation: the application of solar panels, ground coupled heat pumps (GCHPs), etc.,
c) Energy storage systems: thermal or electrical storage, e.g., latent heat storage systems, batteries, and
d) Intelligently manage/control systems: optimized HVAC/lighting schedules.

1.2.2. Passive Energy Conservation Strategies

Passive energy conservation strategies aim to maximize the use of natural sources, in most cases, passive conservation strategies do not involve mechanical or electrical systems. Passive design can include consideration of location, landscape, orientation, shading, insulation, thermal mass, internal layout, openings for penetration of solar radiation, visible light and ventilation. When it comes to specific measures in buildings, the following strategies can be considered (Sadineni, Madala, & Boehm, 2011):

a) Walls: passive solar walls, lightweight concrete walls, ventilated or double skin walls, walls with latent heat storage
b) Fenestration: improve in glazing materials and technologies, advanced frames
c) Roofs: improved lightweight roofs, ventilated and micro-ventilated roofs, vaulted and domed roofs with large half rim angles, solar-reflective/cool roofs, green roofs, photovoltaic roofs, well insulated roofs, evaporative cooling roof
d) Insulations: advance insulation materials (for example, transparent insulation material)

e) Thermal mass or Phase Change Materials (PCMs): larger thermal mass brings benefit to building energy conservation in most cases, the result would be opposite in rare cases

f) Infiltration and airtightness: for example, appropriate window ventilation

Conclusions differ among researchers when it comes to which is more effective, active, or passive energy conservation strategies. Some suggest that active strategies are much more cost-effective than passive strategies for the buildings they studied (X. Sun et al., 2018). Others found the opposite (Kang, Ahn, Park, & Schuetze, 2015; Sozer, 2010). Apparently, the results vary with the configuration of the building and it is not practical to assume a universal conclusion for different building conditions. For different weather conditions and building configurations, the impacts of energy conservation strategies vary greatly. Therefore, holistic analysis for each building being considered is required to evaluate each strategy on specific buildings.

However, passive building energy conservation strategies are often related to urban, architectural design and engineering issues, and are therefore easier to apply than active strategies (Park, Kang, Ahn, & Schuetze, 2015). Furthermore, passive conservation strategies usually affect the performances of the active conservation strategies.

1.3. Holistic Building Energy Analysis Programs

The effectiveness of energy conservation strategies is best evaluated through sensitivity analysis using holistic building energy simulation software. There are a number of popular whole-building energy performance simulation tools that were developed by the U.S. Department of Energy (DOE), including EnergyPlus. Other software like DOE-2, Building Design Advisor, SPARK, ESP-r (Fumo, 2014), TRNSYS, BLAST. There are also

software developed by commercial companies such as DesignBuilder, Trane TRACE, Carrier HAP, IES and VE (Crawley, Hand, Kummert, & Griffith, 2008). Each has its advantages and disadvantages. EnergyPlus (including several user interfaces such as OpenStudio and DesignBuilder) is accepted by most authorities and has been extensively and validated by the research community. For instance, in a case study of a six step methodology for calibration of building simulation models, EnergyPlus showed excellent correlation to measured data, with a mean bias error of -4.2% for the HVAC electrical consumption data (Fumo, 2014). Research by Westphal and Lamberts also indicated a maximum of 20% error in monthly building energy use predicted by the EnergyPlus program, but only a 1% error in predicted yearly energy usage (Fumo, 2014).

Openstudio is a user-friendly graphical user interface (GUI) based on EnergyPlus, and it includes a SketchUp plug-in for improved visualization. Thus, in this research, OpenStudio software was used for the whole building energy consumption simulations.

1.4. Dissertation Overview

In the following dissertation, Chapter 2 describes a literature review of previous investigations of building energy conservation strategies. Chapter 3 describes the numerical modelling of a variety of conventional energy conservation strategies on prototype buildings. In Chapter 4, a testing program used to validate the numerical model of a novel active energy conservation system is described. Chapter 5 describes the result of the testing program and discusses the results of the modelling and testing programs. Payback analyses of energy conservation strategies is conducted and shown in Chapter 6. Conclusions and recommendation are presented in Chapter 7.

CHAPTER 2

BACKGROUND

2.1. Literature Review/Energy Conservation Strategies Current Practices

There are a variety of energy conservation strategies, and researchers have conducted a number of investigations to observe their impact on building energy consumption. A concept of Net Zero Energy Building was proposed years ago, is that a building with net zero energy consumption, meaning the total amount of energy used by the building on an annual basis is equal to the amount of renewable energy created on the site. A case study into an office building in Tianjin, China by Z. Zhou et al.(Zhou et al., 2016) in 2016 described the implementation of the Net Zero Energy Building (NZEB). The first thing to note is that the difference between actual solar radiation intensity during the testing period and the data of the standard year given in the e-QUEST software, along with other factors, led into a roughly 40% gap between the actual solar electricity generation and the actual building energy consumption. Thus Z. Zhou et al. identified the importance of collecting more recent solar radiation intensity data and adding this data to simulation software. The paper revealed the case study building cost ￥17300 /m^2 to operate, which is 70% higher than that of an ordinary energy efficient building. But the author also stated that the NZEB investigated achieved about a 27.4% energy savings compared to conventional buildings after one year of operation, and contributed to a payback period of

nine years despite the high cost of solar photovoltaic (PV) system and unsatisfied windows.

J. Kneifel and D. Webb(Kneifel & Webb, 2016) developed and validated a regression model predicting the energy performance of a net zero energy residential test facility (NZERTF) in cities located in varying climates. The model showed good agreement with EnergyPlus predicted trends in both energy production and net building consumption, although energy consumption estimations varied greatly. This model was able to provide quick energy estimates of variety of the target NZERTF configurations, both production and consumption, in an effort to ensure the net consumption (production is no less than consumption) of the building is zero, for a given level of insolation and outdoor dry bulb temperature.

To encourage the growth of green buildings, S.A.A. Shazmin et al.(Shazmin, Sipan, Sapri, Ali, & Raji, 2017) developed property tax assessment incentive models through the evaluation of their effects on the tax revenue of local authorities and amount of tax imposed on properties for the taxpayers based on a survey in Malaysia. The revealed existing two types of incentives (financial and structural) by local authorities (in Spain, Romania, Italy, Bulgaria, U.S., Canada, Malaysia and India) had no definite and uniform basis and were restricted by financial capabilities. S.A.A. Shazmin et al. believed that although the amount of reduction for each green envelope component would differ from place to place and building to building, these property tax assessment reduction and exemption models they developed were generally compatible and applicable to countries that adopted improved values as the basis of property tax assessment calculations, since these incentive models do not require any financial expenses from local authorities for implementation. They claimed the significance of these models since they can help create public awareness and indirectly

educate the public the benefit of green buildings, and then encourage them to participate in sustainable buildings and environment.

X. Sun et al.(X. Sun et al., 2018) investigated the first zero energy building (ZEB) in South-east Asia located in Singapore. In this study, energy conservation strategies were classified as either active or passive conservation strategies. The former included optimizing the building systems that provide heating, ventilation, and air conditioning, and lighting, while the latter generally focused on the building envelope to manage energy losses and gains. These two types of energy conservation strategies typically are combined with renewable energy sources (mainly solar panels) in an effort to control energy demand to levels needed achieve zero energy consumption of the whole building. In the building studied, there was a 40% energy reduction for lighting energy after retrofits replaced existing T5 fluorescent light with LED panels (X. Sun et al., 2018). The building also integrated a daylighting system consisted of mirror ducts, light shelves and light pipes, which allowed daylighting deeper into the floor plan. For windows, the coating the window glass with ultra-violet (UV) film were used to reduce UV rays and heat from the sun, without comprising the visibility. Other retrofit strategies included the application of a solar chimney for non-air-conditioned areas to enhance natural air movement using buoyancy principle, and use of a green roof and green wall system. Even though these strategies saved energy, the overall payback period of the zero energy retrofit was over 40 years, due to the high capital costs.

It was shown that the most cost-effective active strategy was more efficient lighting, followed by more efficient air conditioning systems. The most cost-effective passive

strategy was lighting and lighting controls. In general, X. Sun et al. concluded that active strategies were much more cost-effective than passive strategies (X. Sun et al., 2018).

X. Li et al. (Li et al., 2019) in 2019 identified three key factors for achieving advanced net zero energy buildings (NZEBs): minimizing the energy demands of building, enhancing on-site renewable energy supply, load matching (LM) based on the dynamic behaviors of occupant and the previous two factors. Heat storage (HS) and cold storage (CS) were used in their research to optimize load matching and heat insulation solar glass (HISG) was used to improve natural lighting and minimize solar gain impacts on electrical consumption. X. Li et al.(Li et al., 2019) also discussed additional ways to minimize energy demand of buildings: (1) energy-efficient and environment-friendly architectural design, including improved building envelopes (e.g. thermal insulation, window glazing, reflective/green roof, etc.), (2) high efficiency appliances, (3) high efficient HVAC systems (including adopting ground-source heat pumps, or thermal-driven absorption heat pumps that integrate space cooling and heating, etc). (4) Occupant energy-conservation behavior and (5) smart control systems. X. Li et al.(Li et al., 2019) revealed that use of these systems were sufficient to reach the net zero energy use target but were not economically feasible (resulted in negative of net present value during system lifetime) in Singapore's current economic conditions. This also proved that although NZEBs can be achieved, the best economic performance with the current state of art technology was obtained where the goal was to reduce energy consumption, not to achieve net zero.

Additional evaluation studies on energy conservation strategies are discussed in following chapters.

2.1.1. Active Design Strategies: HVAC System

Research, investigations have shown energy consumed by the HVAC system is impacted significantly by occupant behavior. Occupants determine the thermostat set point and whether to open windows to achieve better thermal comfort (Fabi et al., 2013). Furthermore, an analysis of a number of Hawaiian buildings showed that improving the effciency of lighting or HVAC systems produced lower energy savings than for higher heating demand climates, thus suggesting that HVAC or lighting system efficiency improvements may not translate in significant energy savings in all climates (McGinley & Liu, 2021).

Using holistic energy analysis, researchers have shown annual energy consumption and peak design loads are more sensitive to internal loads, fenestration characteritics (windows), temperature set points and HVAC equipment efficiency (Based on DOE2 simulations of an office building in Hong Kong (Tian, 2013)). Based on a sensitivity analysis, it was also shown that the total annual energy use in a UK school building was sensitive to occupant acitivity and numbers, classroom equipment load and hours of use, heating schedules and set point temperatures (Tian, 2013).

Research has also found that raising the set point temperatures (in summer) can substantially reduce the peak electricity demand as well as total energy use (L. Yang, Yan, & Lam, 2014). They also showed that increases in thermostat set point ranges can also decrease energy consumption based on analyses of office building energy use (Hoyt, Arens, & Zhang, 2015). Additional research found that thermostat set point controls can significantly impact yearly building energy consumption (Yu et al., 2017).

M.A. Fayazbakhsh et.al. studied the effect of set point hysteresis (HVAC deadband) on building energy consumption with 150 minute duration scale tests, and analytical model evaluations. They found the overall energy consumption for cooling decreased by 6.6% when the high and low set point of 26±1.0°C (deadband 2.0°C) was compared to high and low set points of 26±1.8°C (deadband 3.6°C) (Fayazbakhsh, Bagheri, & Bahrami, 2015).

In 2017, A. Rackes and M.S. Waring (Rackes & Waring, 2017) investigated the energy saving potential of multiple alternative ventilation strategies in U.S. office buildings in different climate zones. They assessed the impacts of economizing (Econ), demand controlled ventilation (DCV), supply air temperature reset (SR), and/or a doubled ventilation rate (Rackes & Waring, 2017). Baseline building configurations were small office buildings with a constant air volume (CAV) HVAC system and medium office buildings with variable air volume (VAV) HVAC system. The average of small-CAV office showed 5-25% energy saving potential by changing CAV to DCV with the heating source switched to natural gas. They also found that for the medium-VAV office, the savings increased to 6-42%, due to the benefit provided by Econ and SR settings. In colder climate zones, adding DCV to medium-VAV office with Econ and SR was also often effective in the same ranges as described above (Rackes & Waring, 2017). It should be noted that envelope characteristics were not important predictors of energy use impacts other than the infiltration influence on DCV savings in small offices. However, thermal resistance (R values) of the building envelope did played a role in the less insulated small-CAV office configuration when both Econ and DCV were used, or the lower insulated medium-VAV office configuration when SR was used (Rackes & Waring, 2017). It also pointed out heating degree days (HDD) were one of the most significant factors impacting

energy used, in both the small office and medium office building configurations, the difference was, in small office, occupant density was equally important, while in medium office, the other key factor was zone temperature setpoints (Rackes & Waring, 2017).

J. Laverge et al. (Laverge et al., 2011) developed a simulation model based on a detached residential house that was representative of an average Belgian dwelling. They used this model to investigate the energy saving potential and impacts on indoor air quality of four different demand controlled ventilation strategies, including vent hole (based on relative humidity), fan (based on presence), trickle (based on CO_2) or a combination of these three. The baseline model used a mechanical exhaust ventilation system and basic air leakage. It was shown that when only any one of the system alternatives were applied to the baseline model, there would be an energy savings potential of about 25%, whereas the combined system had an energy saving potential of 60% (Laverge et al., 2011).

2.1.2. Active Design Strategies: Lighting

For a NZEB building studied by X. Sun et al.(X. Sun et al., 2018), there was a 40% energy reduction for lighting energy after replacing T5 fluorescent lights with LED panels. But some research by U.S. Department of Energy (DOE)(DOE, 2011) didn't show signifcant differences between commercially available LED lights and T8 lights. This means that LED lights do not always produce lower lighting energy consumption, it depends on the efficiency of the lamp itself.

In the building studied by X. Sun et al.(X. Sun et al., 2018) also integrated a daylighting system to guide daylight into deeper floor plan to reduce the demand for lighting. This system was consisted of mirror ducts, light shelves and light pipes, which could reduce energy consumed by lights.

A. Boyano et al.(Boyano, Hernandez, & Wolf, 2013) investigated the effect of lighting, building orientation, U factors of windows and external walls in office buildings in Tallinn (a cold climate), London (a moderate climate) and Madrid (a warmer climate). Two scenarios with different lighting control systems were addressed. They showed that a lighting control system that decreased the continuous on time of 12 hours to demand control (with as low as 4.6 hours on time per day), could help reduce the lighting energy by about 50% in Tallinn and London, and about 25% in Madrid. It has also shown that a higher glazing percentage will further reduce the energy consumption for lighting. They concluded that energy saved in lighting can often increase the energy consumed by other building systems, especially in cold climates (Boyano et al., 2013).

Geun Young Yun et al. investigated the effect of occupancy and lighting use patterns on energy consumption in four office buildings. Lighting energy savings of up to 30% was found when lighting controls considered daylighting (Yun, Kim, & Kim, 2012). Lei Xu et.al showed similar results with a reduction of 23% when lighting systems accounted for daylight controls (based on studies on two office buildings) (Xu et al., 2017). They included occupancy sensors on their lighting system controls (Xu et al., 2017).

2.1.3. Active Design Strategies: Building Control System

Stephen Treado and Yan Chen (Treado & Chen, 2013) investigated the importance and effectiveness of building control systems in building energy consumption/savings. In their research, a weighted building design index (BDI) and a so a building operating index (BOI) was proposed to describe the energy behavior of a building. They claimed about 50% of energy consumption of a building was affected by building operations. Although this

idea is rather abstract, but it can still be used as a reference when assessing the energy conservation potential of a building.

2.1.4. Passive Design Strategies: Orientation

Although a case study in European office buildings based on Energyplus simulations by A.Boyano et at. showed an energy conservation potential due to the orientation of the building between 3%~6% (Boyano et al., 2013), the orientation of a building is often determined by the owner and site constraints.

2.1.5. Passive Design Strategies: Opaque

Analysis by Guohui Feng et.al. of an office building in Shenyang (a cold region in China), showed that the total heat loss of the envelope was about 60~70% through exterior wall, 10% through building roof, and 20~30% is through exterior doors and windows (Feng, Sha, & Xu, 2016).

Haie Huo et.al. investigated the energy performance of an uninsulated room (16.2 m^2, 240 mm brick wall with 20 mm internal and external plaster and 200 mm reinforced concrete roof and floor with 20 mm internal and external plaster) in four different climatic regions in China. The effective R value of wall assembly was 0.37 m^2K/W while the roof R value was 0.18 m^2K/W. They found that the heat loss through the roof is about 30% of total (with a larger portion found for hotter cities), about 5% through floor (with a larger portion in hotter cities), and about 10% through windows (with a smaller portion in hotter cities). The remainder was through the walls (Huo, Shao, & Huo, 2017).

Junlan Yang and Jiabao Tang used energy simulations to compare the energy consumption of a newly built apartment building (medium sized) in Germany with varying

configurations. This research focused on the total energy consumption of three wall insulation materials (mineral fiber, polyurethane and vacuum insulation panel). The energy consumption was taken as the sum of unit area of material and the heat loss calculated (under the weather conditions of Essen, Germany) through the insulation over 30 years. It was shown that there is an optimum insulation thickness for each material needed to achieve the lowest total energy consumption. This results was also shown by E. Rodrigues, et al. (Rodrigues et al., 2019). Yang and Tang also showed that the energy payback time primarily depends on the heat transfer coefficients of the material (J. Yang & Tang, 2017).

P. Tsikraa and E. Andreou (Tsikra & Andreou, 2017) investigated 238 school buildings across Greece. They conducted an in-depth investigation and simulation of elementary school built in 1995 in the city of Litochoro (a mild C Climatic Zone). Heating and cooling loads of the building were 52.34 and 1.97 KWh/m^2 respectively. They showed that solar gains account for 18.9% of the annual heat gains. It was indicated that the non-favorable orientation of building reduced the structures' ability to harvest solar energy. It was also suggested that a shading strategy could reduce cooling loads of the school but would increase the heating loads more. However, if the buildings were south orientated, total energy loads decreased. It was concluded that unfavorable orientations are difficult to be shaded effectively. Additional internal insulation applied on the walls (U value to 0.28 W/m^2K from 0.463 W/m^2K) only reduced total energy consumption by 0.45%, but when an additional 5 cm thickness of insulation was applied on roof an approximately 15% energy savings resulted.

A study by D. Tudiwer and A. Korjenic (Tudiwer & Korjenic, 2017) investigated the effect of greening façade walls of an office building of the Municipal Department

MA48 and a school Kandlgasse 39. The “green” façade wall had a green plant system attached on the exterior side, consequently, the thermal resistance of the greening system consisted of the resistance of wall material, an interior air film and the exterior part (green plant system). This investigation showed that the greening system can not only reduce the heat flux through the wall system in summer and winter, but the greening system also helped reduce the fluctuation rate of the surface temperature. The authors also found the thermal resistance of a greening system depends on its construction and ventilation gap, thus the results can’t be generalized to all greening systems. It appears that the “greening system” impacts several major factors: thermal mass increases caused by the green plant and soil, reflectance value increases due to the green plants, the added air gap layer and ventilation through the gap. The research by D. Tudiwer and A. Korjenic (Tudiwer & Korjenic, 2017) did not explain to what extent the above factors impact the energy use individually.

L.Y. Zhang et.al. investigated the effects of insulation thickness and the construction sequence of external walls of an office building in five representative cities in different climate zones in China. It was found that the wall construction sequence had only a minor impact. They also found that increases in insulation thickness can help decrease the heating/cooling energy consumption, but had only a minor impact beyond a certain insulation thickness (Zhang et al., 2017). Pengfei Jie et. al. found similar results (Jie et al., 2018).

Pengfei Jie et.al. published analytical research of an optimization model for determining the insulation thickness of envelopes. This research showed that there is a

critical value of insulation thickness for walls and roofs, from the perspective of global cost saving or pollutant emission reduction (Jie et al., 2018).

Another element of heat loss through the building envelope is the impact of thermal mass and radiant heat transfer. Thermal resistive wall assemblies have been studied (McGinley & Liu, 2021) and showed that increases in the thermal resistance of mass exterior wall assemblies could help decrease total energy consumption, only in some cases. Increases in the thermal resistance of exterior walls can provide significant reductions in energy use in buildings when the thermal resistances are initially low (well below the prescriptive code compliant insulation levels). Furthermore, research by Huygen and Sanders has shown that heat loss through air cavities is predominately by radiation (Nathaniel C. Huygen & Sanders, 2019). This impact needs to be studied further. In this investigation, the effectiveness of CMU walls insulation inserts with reflective barriers will be evaluated. This system will place insulation inserts (with reflective barriers) in the hollow portion of a CMU wall. It is expected that much higher thermal resistance will be achieved with these inserts when compared to similar inserts without the radiant barrier.

M. El Mankibi et al.(El Mankibi, Zhai, Al-Saadi, & Zoubir, 2015) analyzed thermal behaviors of multi-layer living walls using MATLAB, Simulink and TRNSYS “TYPE36” to identify the most efficient wall configurations. They targeted conventional walls with phase change materials (PCMs), ventilated/unvented cavities and with a glazing outer layer. They indicated that for the wall system (wood siding + 1” foam insulation + plywood + wood stud ass. + drywall), interior side located PCMs with a narrow melting range and a melting point close to the heating and cooling setpoints achieved the best performance in peak load reduction and annual savings. They also showed that this system had a significant

effect on cooling (as high as 80% reduction in both peak load and annual consumption) while the impact on heating was minor (less than 5% under most circumstances). However, their investigation did not consider is that the optimal set point zone was very narrow (less than ±0.5 °C) and that any improper operation or offset of the setpoint will significantly lower the energy savings. In addition, this investigation showed that for a given wall system, PCMs located in middle showed a roughly 10% less reduction of energy savings compared to interior side located PCMs, but had better compatibility and fault tolerance. They thus concluded that center located PCMs could be a more widely applicable choice. Similar conclusion was made in this research when investigating the location of pipes. The investigation suggested that a cavity behind a glazing layer with air induced from the indoor environment also could reduce heating energy use, but had a limited impact on peak heating load.

Through analyses of buildings under the weather conditions of sixteen different Mediterranean locations, E. Rodrigues, et al.(Rodrigues et al., 2019) attempted to determine optimal U values for buildings in different climate zones. Their results showed that when the U value was larger than an optimum value, smaller the U values (lower thermal transmittance), the lower the building energy consumption. However, when U values were lower than an optimum value, smaller U values actually increased energy consumption. The specific value that describes this change in performance was defined the ideal U value by the authors, and this varied with climate zones and other factors.

P. Ramamurthy et.al. monitored the temperature and the yearly heat flux through the five types of roofs with varying insulation thickness in Northeastern US. This research showed that doubling the insulation, significantly reduced (~50%) the heat flux (Q)

transferred through the roof regardless of the roof reflectance, under steady state conditions. They also found roofs with high reflectance (white membranes) significantly reduced the cooling load during warm months, while black roofs were not very effective in reduce heating loads during winter. They did find that roof insulation thickness can have a great influence on reducing the heating loads during the wintertime (Ramamurthy, Sun, Rule, & Bou-Zeid, 2015).

Linfang Zhang et al.(Zhang;, Jin;, Liu;, & Zhang;, 2017) published their work simulating the building energy conservation potential of the application of green lawns and roofs. PHOENICS software was used to establish 3D building block models with/without green lawns and roof to investigate the temperature distribution of external surface (walls and roofs) of buildings and the surrounding environment. Linfang Zhang et al. stated that green lawn reduced the peak temperature of outdoor environment temperature at the height of 1.5 m by 2-4°C in hot summers, while a green roof had little impact on the 1.5 m height environment. The green roof was a favorable choice for cooling the roof in summer, and showed a 3-4°C reduction in roof temperatures. It was also mentioned that a green roof could protect the ecological environment and reducing dust and noise, while more research on the payback analysis and the impact on human comfort by air humidity influenced by green roof still needs to be done.

2.1.6. Passive Design Strategies: Window/Facades

Bo-Eun Choi et.al. evaluated the energy performance and economic efficiency of a variety of building construction variations, such as window-to-wall ratio, U-factors and g-values (solar energy transmittance of glass, similar to solar heat gain coefficient, SHGC), on a business/office building with a gross floor area of 2,325 m^2 in Korea (a temperate

climate with hot summers and cold winters). It has shown that with the increase of window-to-wall ratio, the change in heating load of a prototype building is small while the cooling load had about an 10% increase. It was also found that solar heat gain coefficient (SHGC) of windows sometimes plays a more important role than window U-factors (Choi, Shin, Lee, Kim, & Cho, 2017). It remains unclear whether this conclusion is valid for all climate zones.

K. Allen et al. (Allen, Connelly, Rutherford, & Wu, 2017) investigated the potential of "switchable glazing" on reducing energy consumption of buildings. By responding to an applied stimulus such as heat (thermochromism), electricity (electrochromism) or light (photochromism), the switchable glazing was designed to regulate the amount of transmitted solar and long-wave radiation (300-3000 nm) in an effort to reduce the heat transferred from ambient to indoor environment. They studied a type of thermochromism glazing (thermotropic (TT) windows). The intent of these systems was to reduce the amount of solar radiation entering a building during hot periods by adding a mixing layer of hydrogel and polymer that becomes translucent and diffusely reflects light when the temperature of the layer was higher than a designated temperature and vice versa. This TT window system had been shown to have a total energy consumption saving potential of 33% in Palermo in Italy. However, in places that heating was needed in winter, this system could lead to a higher heating load since it reduced the heat flux into the building compared to normal non-switchable glazing systems. However, in the climate investigated, the TT windows only showed better overall performance than Low-E windows when horizontal. In vertical applications (30° or 60° tilt window systems), TT windows did not show any improved performance.

(Y. Sun, Wilson, & Wu, 2018) In 2018, Y. Sun et al. (Y. Sun et al., 2018) studied the effect of using several different types of transparent insulation material (TIM) on facades. TIMs were classified as glazing-perpendicular structure (capillary, honeycomb, parallel slat array structure, etc.), glazing-parallel structure, mixed structure and homogeneous structure. Y. Sun et al., indicated that the energy conservation potential of these systems varied with location and building configuration and savings ranging from -1.8% to 26% for cooling, and 3.7% to 40% for heating were found (note some HIMs provided higher thermal resistance). Another advantage of a TIM was its optical characteristics. The light transmitted through the capillary TIM was more evenly distributed throughout the room without obvious sun patches, compared with clear glass. Light from lower sunlight altitude were found to spread over larger area and deeper into the room, which reduces the fixed lighting demand and thus the electricity bills for lighting. But despite the potential of improved performance of daylight distribution and energy savings, TIMs can interrupt views out of and into a building and this needs to be considered by designers (Y. Sun et al., 2018). In addition, they found that avoiding the use of low R value frames can guarantee a better performance of window systems.

2.1.7. Passive Design Strategies: Thermal Mass

M. Liu and P. Heiselberg (Liu & Heiselberg, 2019) investigated the total cost, total energy consumption, thermal comfort, etc. of a nearly zero energy building under different control systems. This research took advantage of the thermal mass of the building and tried to decrease the electricity consumption during high price periods by adjusting set-points during high price periods, or in response to weather predictions. Although the yearly energy costs were slightly increased from € 0.499 m^2 to € 0.52 /m^2 per year, the system provided

better performance of energy demand flexibility, with decreased power demands of around 0.005 kW/m^2 during high price periods. These findings prove that thermal mass of a building impact peak energy use.

Suresh B. Sadineni et.al. investigated the impacts of a variety of energy conservation strategies and emphasized the importance of improvement of building envelopes as a passive energy conservation strategy. They indicated that building thermal mass (including phase change material) is more effective in places where the outside ambient air temperature differences between the days and nights are high (Sadineni et al., 2011). They also determined that air tightness and building envelope infiltration are also very important in energy conservation (Sadineni et al., 2011). However, as newer code provisions for new construction require much lower infiltration rates, this envelope characteristic will not be addressed in this investigation.

A study of the significance of thermal mass was conducted by Jevgeni Fadejev et al. (Fadejev, Simson, Kurnitski, & Bomberg, 2017). The authors compared the heating and cooling load of two buildings with same U value (0.15 W/m^2K but different thermal masses (the building material differed from wood to concrete). In the Warsaw Poland climate, the higher thermal mass reduced cooling need by 16% on the first day but this the percentage dropped to about 5% over time. An energy recovery system modelled for floor and wall insulation was also investigated. It consisted of a thermal storage tank, circulation pumps, piping system and a pump control schedule. The circulating liquid with a flow rate of 1 kg/s was embedded at 50 mm depth in the concrete floor slab and produced a reduction of 10% in energy used when heating and an increase of 29% when cooling.

E. Rodrigues, et al.(Rodrigues et al., 2019) stated that the effect of thermal mass of buildings varied from climate conditions, methodologies, parameterization and control settings. The lack of common metrics for describing thermal mass also brought difficulties to the evaluation of any thermal mass effects. In their research of a building in Milan, Italy, with the same U value of 0.34 W/m^2K, higher thermal mass reduced heating demand by 10% and cooling demand by 20 %. However, in a study of a building in Belfast, Ireland, heavyweight walls increased the energy consumption. These results suggest that the thermal mass of building has an optimum value and bigger is not necessarily better. They generally concluded that increases of thermal mass increased the cooling energy demand and reduced the heating energy demand for warmer climates but may increase the heating energy demand for colder climates. D. Olsthoorn et al. investigated the impact of thermal mass on building energy consumptions. In their study, four ways of using thermal mass were introduced, including surface (ventilate indoor air during night to reduce cooling demands), forced-air (air ventilation through wall cavities), hydronic (fluid through walls, roofs or floors), electrical (electric heating of a mat below a thermally heavy layer). The effect of these measures showed peak energy demand reductions of as high as 100%, and energy cost savings of 92% cost. This varied with buildings and climate configurations (Olsthoorn, Haghighat, Moreau, & Lacroix, 2017). However, the effectiveness of these systems were highly limited by the convective and radiative heat transfer rate between the thermal mass and the interior air (Olsthoorn et al., 2017), but this effect does not include the barrier effect of an active thermal wall system.

2.2. Active Thermal Insulation Wall System (ATIWS)

ATIWS system incorporates a pipe system into external walls of buildings circulates fluid through them. A pump circulates the fluid through pipes either embedded under the ground (shown in Figure 2-1), or through a heat exchanger attached to a system that can heat/cool the fluid, such as ground coupled heat pumps (shown in Figure 2-2), solar panels, or thermal storage systems. For the convenience of discussion, the system in Figure 2-1 is described as ATIWS DX (ATIWS with direct ground coupling), the system in Figure 2-2 was described as ATIWS/ground coupled heat pump (GCHP). The ATIWS DX system provides a direct heat exchange with the fluid and the ground. The fluid temperature will be around the same temperature as the soil temperature (typically the annual air temperature of the location under consideration). The ATIWS/GCHP system uses a GCHP to provide heat of cooling, therefore, the fluid temperature is variable.

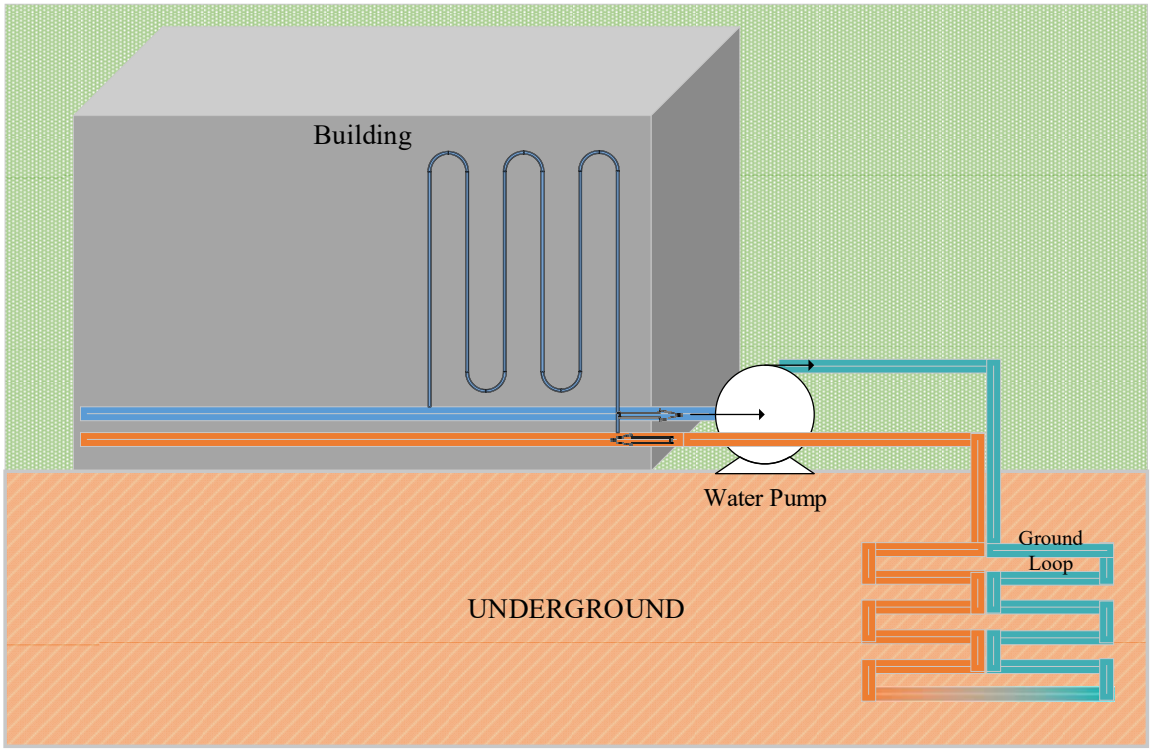

Figure 2-1 Active Thermal Insulation Wall System: Direct Exchange

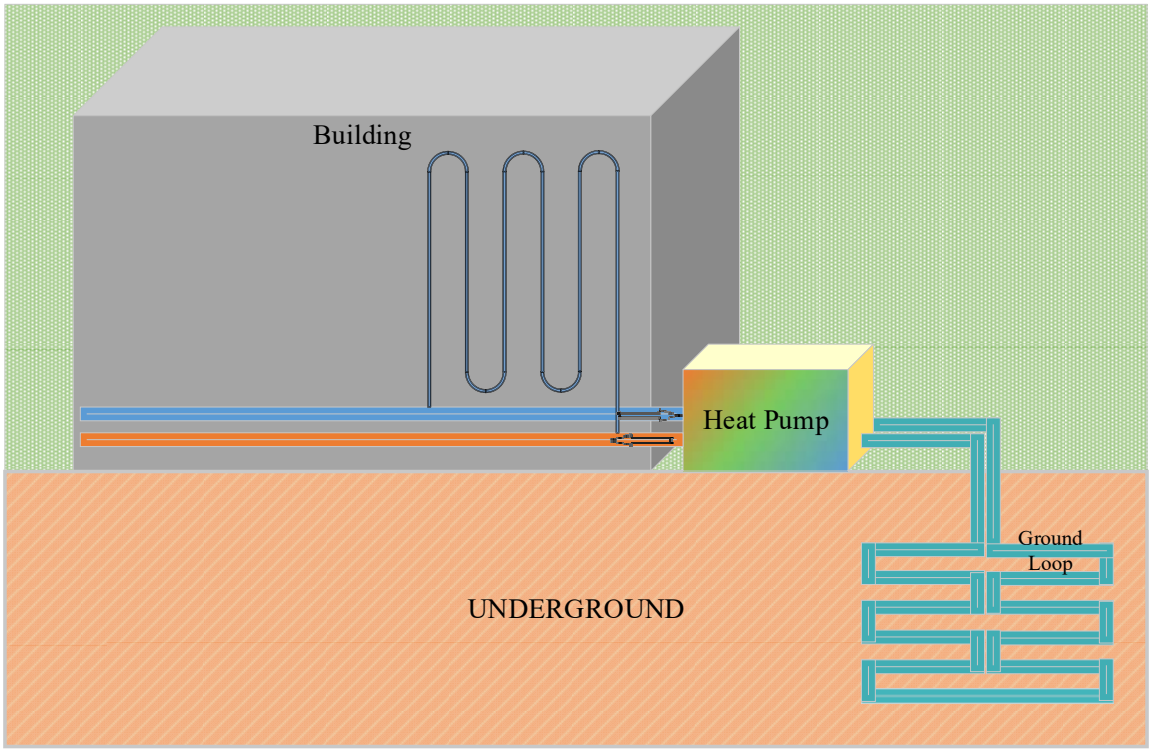

Figure 2-2 Active Thermal Insulation Wall System: With Heat/Cool Sources

Active thermal insulation wall system (ATIWS) introduces an "active thermal insulation (ATI)" layer into the structure of the external walls of the building by embedding pipes inside and circulating fluid through it. As per the Climate.gov, in 2019, the average temperature across global land and ocean surfaces was 14.85°C. The mean annual soil temperature was around 16°C. As suggested by T. Kusuda, ground temperature at an any significant depth equals the average annual air temperature at the site (Andujar Marquez, Martinez Bohorquez, & Gomez Melgar, 2016). At the depth of 3 meters or deeper, the variation of ground temperature is generally within 1.5°C of the average annual air temperature.

Similar to the ATIWS we proposed, research showed that pipe embedded system can significantly reduce heat loss or excess gain through external walls (Kisilewicz, Fedorczak-Cisak, & Barkanyi, 2019). The use of geothermal and solar energy are of great interest of many researchers. Compared with other heating or cooling systems, this system uses clean energy (e.g., shallow ground water, solar energy) to maintain indoor thermal comfort and is more environmentally friendly. The ATIWS takes advantage of thermal mass (Olsthoorn et al., 2017) thermal barrier effect (Krecké, 2004), and other elements in favor of building energy conservation. The other end of circulating fluid could be connected directly with a pipeline embedded in soil or a heat exchanger.

In fact, single embedded pipe layers are not the only option for novel wall systems. Researchers have investigated using a variety of different types of layers in conventional wall systems, including air cavity layers (Chen et al., 2018; El Mankibi et al., 2015; Ghaith*, Shakhshir, Nour, & Lagtah, 2017), phase change material (PCM) layers (Baetens, Jelle, & Gustavsen, 2010; El Mankibi et al., 2015; Konuklu, Ostry, Paksoy, & Charvat, 2015), embedded pipes layers (Atam & Helsen, 2016a, 2016b; Bottarelli et al., 2015; Villarino, Villarino, & Fernández, 2017), to name just a few. Based on these published results, it appears that embedded pipes increase the total thermal mass of wall and other energy sources can be utilized be coupled to them to assist in heating and cooling.

In support of the use of active thermal mass systems, a number of studies using pipe circulation systems in floors or walls have been conducted with ground coupled heat pumps (Andujar Marquez et al., 2016; Krzaczek & Kowalczuk, 2011; Villarino et al., 2017; Xie, Zhu, & Xu, 2012) or without (Kisilewicz et al., 2019; Šimko, Krajčík, Šikula, Šimko, & Kalús, 2018). In these studies, active thermal insulated walls, floors or roofs were found to

be effective in reducing the heat flux through the building envelope, essentially acting as a thermal barrier, and transferring heat from the indoor environment to the exterior of the buildings, or transferring heat for the exterior environment to the interior as a heating system. The implementation of these systems varied in these studies. Geothermal or solar energy (or a combination) have been used as heat source, heat exchangers and phase change materials (PCMs) were also employed in some of the research.

In support of the development of the ATIWS, the study of ground coupled heat pumps (GCHP) has been conducted by many researchers. For example, the work by M. Bottarelli et.al (Bottarelli et al., 2015), by J. I. Villarino (Villarino et al., 2017) and by E. Atam (Atam & Helsen, 2016a, 2016b). GCHPs includes a ground heat exchanger (embedded under the ground), a radiant floor, and a heat pump (absorb energy from geothermal supplies to supply the radiant floor). Using this configuration of an active layer system, a system similar to GCHP was formed.

Xie et al. conducted research regarding to an active pipe-embedded building envelope for utilizing low-grade energy sources (Xie et al., 2012). The embedded-pipe wall consisted of two 120 mm brick layers, a sandwich layer (concrete layer with pipe embedded), and internal and external wall surfaces. This wall system was analyzed under a typical hot summer weather condition. The heat transfer through the wall was significantly reduced compared to a similar wall without the pipe system. They found that a 1°C change in fluid temperature led to a reduction of about 2.6 W/m^2 in heat flux through the wall, while for a 50 mm of reduction in pipe spacing, a 2.3 W/m^2 reduction in heat flux occurred (Xie et al., 2012). However, this preliminary study was with limited value since it did not consider its performance under various weather conditions, nor compare its

thermal performance with conventional walls. Therefore, the practicability of this system cannot be properly assessed.

T. Kisilewicz et al. investigated the thermal performance of an experimental residential building equipped with ATIWS in Nyiregyhaza, Hungary (Kisilewicz et al., 2019). The ATIWS was coupled with a ground heat exchanger. The polyethylene (PE) pipes embedded in wall were mainly horizontally placed. In their study, an equivalent U value for their ATIWS was calculated based on local climate conditions. The standard transmittance value of the wall was 0.282 W/m^2K, however, the equivalent U value of the ATIWS was 0.047 W/m^2K for November and 0.11 W/m^2K in March (Kisilewicz et al., 2019). The average temperature in cold season in Nyiregyhaza during the research was -8.42 °C and in hot season was 25.65 °C. The approximate ground temperature on site at a depth of 2 meters ranged from 8-11 °C. There tests showed a 53% reduction in heat loss in February and 81% in November.

M. Šimko simulated the thermal performance of thermal active wall with variable configurations with embedded pipes(Šimko et al., 2018). This research compared the behavior of several types of thermally active walls, with pipes embedded in different locations in the wall. They showed a 50% reduction in peak heating energy demand when pipes were located concrete core and 63% reduction in heating energy needed when the pipes were located just beneath the interior surface (Šimko et al., 2018). The thermal energy exchange in the active walls was limited by thermal conductivity around the pipes, although the thickness of the concrete did not have a substantial effect (Šimko et al., 2018).

In this study, the impact of ATIWS on building energy conservation will be further investigated. Specifically, aspects such as pipe location, pipe spacing and fluid temperature

will be investigated in an effort to further fine the system application for typical North American building configurations. There is also a need to define the economic viability of these systems in the North American market.

CHAPTER 3

BUILDING ENERGY MODELLING

3.1. Simulation Methods Used in This Research

To evaluate the variety of energy conservation strategies investigated during research, two methods were used: a holistic building analysis using OpenStudio (EnergyPlus) and envelope cross section thermal heat flow analysis using MATLAB. As mentioned previously, the OpenStudio/EnergyPlus program can conduct a comprehensive analysis of energy flow within typical building systems across a range of different building configurations. However, this program does not perform well in the following two aspects: observing the heat transfer through wall sections and analyzing buildings with complex wall behaviors. Consequently, another modeling method was needed for investigating the mechanism of how thermal mass influences energy movement through building envelopes. MATLAB is a proprietary multi-paradigm programming language and numerical computing environment developed by MathWorks. Targeted thermal heat flow analyses can be performed since the MATLAB code and these were developed by the author. To validate the MATLAB model, an ANSYS Workbench model was developed to confirm the MATLAB codes. The analytical results of MATLAB model and ANSYS Workbench model turned out to be very similar. Since the ANSYS Workbench analysis was time consuming, only one validation run was conducted.

3.1.1. OpenStudio (EnergyPlus) Modelling

As in indicated earlier, further research was needed to achieve a comprehensive understanding of the impact of various energy conservation strategies for building energy consumption for various climatic conditions and building configurations. This was conducted on a series of building prototypes.

DOE have published sixteen prototype buildings to facilitate energy studies for buildings that are representative of typical US construction. The surface and wall surface/volume ratio of the sixteen prototypes were listed in Table 3-1. Of these prototypes, a number were typically constructed with mass exterior wall systems. These mass wall buildings include configurations like the Small Office, Large Office, Stand-alone Retail, Supermarket, Large Hotel and Hospital configurations (Deru et al., 2011). In the US, Secondary Schools are also often constructed with mass exterior wall systems.

Table 3-1: DOE Prototype Buildings

Building Type Name	Floor Area (ft^2)	Number of Floors	Surface / Volume Ratio	Wall Surface / Volume Ratio
Large Office	498,588	12	0.027	0.021
Medium Office	53,628	3	0.056	0.031
Small Office	5,500	1	0.119	0.039
Warehouse	52,045	1	0.055	0.019
Stand-alone Retail	24,962	1	0.076	0.026
Strip Mall	22,500	1	0.059	0.033
Primary School	73,960	1	0.104	0.028

Secondary School	210,887	2	0.056	0.018
Supermarket	45,000	1	0.069	0.019
Quick Service Restaurant	2,500	1	0.131	0.058
Full Service Restaurant	5,500	1	0.107	0.035
Hospital	241,351	5	0.034	0.02
Outpatient Health Care	40,946	3	0.079	0.042
Small Hotel	43,200	4	0.071	0.044
Large Hotel	122,120	6	0.057	0.039
Midrise Apartment	33,740	4	0.074	0.049

For this study, four prototype buildings were chosen to represent the yearly energy use behavior of typical US buildings which use mass exterior wall systems. The DOE Large Office prototype was chosen to cover high-rise buildings with small surface/volume and wall surface/volume ratios. To represent institutional buildings, the Secondary School prototype was chosen. The Stand-alone Retail prototype is a good representation of a commercial building with a relatively high surface/volume ratio and low wall surface/volume ratio. The Midrise Apartment prototype was chosen as a medium rise building with high surface/volume and wall surface/volume ratios. The shapes of the four prototypes were presented in Figure 3-1.

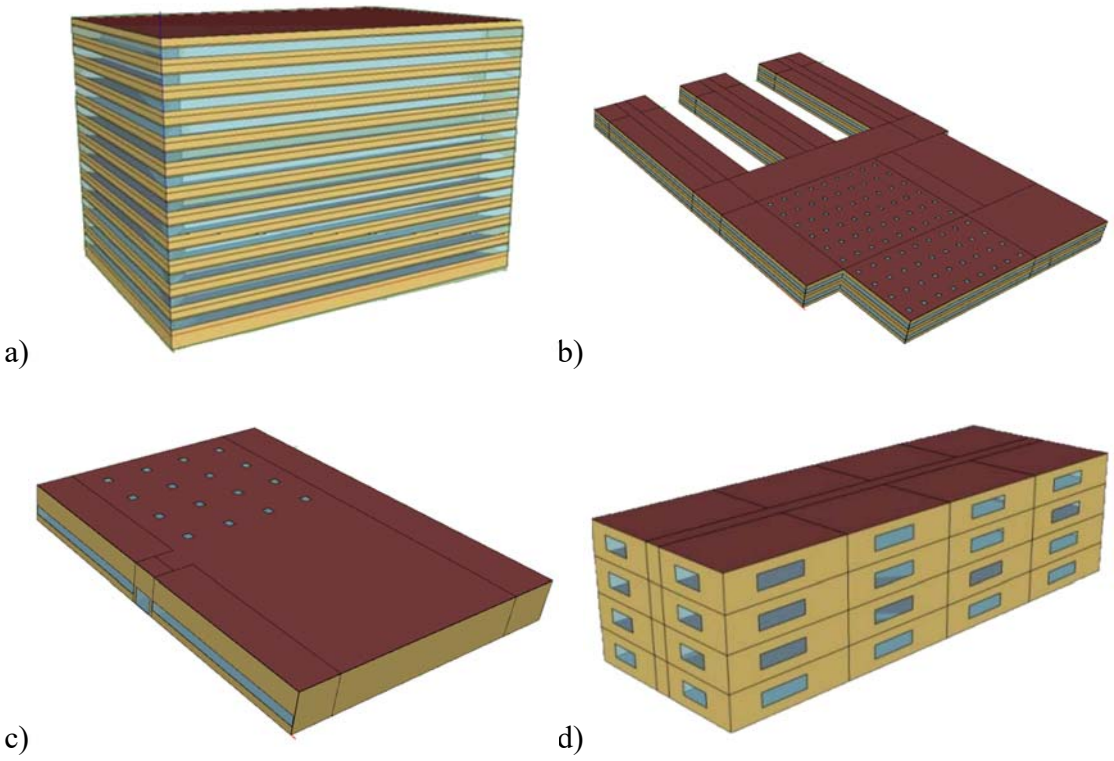

Figure 3-1 The Selected Four Prototype Buildings: a) Large Office; b) Secondary School; c) Standalone Retail; d) Midrise Apartment

These four protypes were used to assess the energy conservation potential of twelve different energy conservation strategies in the climates of the seven cities listed in Table 3-2. The weather in each of these cities are deemed by the DOE to be representative of the seven common climate zones in the US (Deru et al., 2011).

Table 3-2: Representative Cities for the Seven Climate Zones

City	State	Zone
Miami	Florida	1A
Houston	Texas	2A
Las Vegas	Nevada	3B

Seattle	Washington	4C
Chicago	Illinois	5A
Minneapolis	Minnesota	6A
Duluth	Minnesota	7

A base line configuration was also evaluated for each prototype in each of the climate zones using the EnergyPlus and OpenStudio GUI software. Each baseline model of four DOE prototype buildings were loaded directly from the OpenStudio Building Component Library using the ASHRAE 90.1-2013 model configuration. These were the latest OpenStudio models of the prototype buildings published by DOE. However, each baseline building model was adjusted so that their exterior wall assembly configuration met the prescriptive U-factor requirements for mass walls per ASHRAE 90.1-2016, for each climate zone.

Various configurations of each prototype model were evaluated to investigate the impact that changes in lighting systems, HVAC systems, fenestrations (windows), control temperature set points, exterior wall assembly configurations (mass, coatings, R values) were evaluated using the EnergyPlus/OpenStudio holistic building energy modelling program. The ambient temperature was taken as the published hourly weather data from each of the seven representative cities. The weather data files of more than 2100 locations, including locations in the seven representative cities were published by EnergyPlus.

The total yearly energy consumption for each configuration was also used to conduct a payback analysis to examine the effect of these strategies on energy use. This

evaluation allowed an assessment of the most cost-effective energy conservation strategy to be made.

3.1.2. MATLAB Modelling

MATLAB transient thermal models were developed to observe the instantaneous heat flux through an exterior mass wall during typical 24-hour period diurnal ambient temperature variations. In OpenStudio simulations, the weather file were taken as the recorded historical hourly ambient temperature conditions. In the MATLAB simulations, the exterior temperature was assumed to be a sine curve, assuming lowest temperature occurred at 4 am and the highest temperature occurred at 4 pm. Indoor temperature boundary conditions was 22°C or 24°C, and varied with cases.

It should be noted that for the model simulations that were validated in the hot box tests, the ambient driving temperature was set as the 24-hour sine diurnal temperature curve (plus a half-hour warm up). For the simulations that studied impact of system configuration variations such as the influence of pipe locations, the ambient driving temperature was assumed to be two cycles of a 24-hour sine diurnal temperature curve, the results of the first 24-hour was not recorded since it was taken as a conditioning of the wall system. This was done to minimize the impact of initial condition on the results.

The governing PDE provided by the MathWorks (*Partial Differential Equation Toolbox™ User's Guide*, 2020) describing the temperature gradient (u) throughout a generic wall section is:

$$\rho C \frac{\partial u}{\partial t} - \nabla \cdot (k \nabla u) + h(u - u_{\infty}) = f$$

Where ρ is the material density, C is the thermal capacity, ∇ is the Nabla symbol, k is the thermal conductivity, h is the film coefficient, u_{∞} is the ambient temperature, and f is the heat source. As indicated previously, the ambient temperature was set to be a simplified diurnal sine curve. However, in the MATLAB transient thermal model, the ambient temperature at the surface of the wall cannot be defined as a function with variable values when convection governs. Thus, an air film at the exterior and interior surfaces was assumed to be present. As was commonly done in analysis of thermal movement through walls, the R values of air films on the exterior (0.03 m^2K/W) and interior (0.12 m^2K/W) surface to the wall were added to get a total wall assembly R value (ASHRAE, 2019). Boundary conditions were applied on the rear surfaces of air films. In this manner, convection at the wall surfaces is simulated by conduction. Boundary condition at the inner surface of pipe was convections. This is the surface where the heat exchange between fluid and pipe occurs. Therefore, the convective heat transfer rate at pipe inner surface must be determined.

In this research, the pipe inner diameter (D) was 0.01905 m (0.75 inch). When fluid (water) temperature was 20°C, the density (ρ) of the fluid was 997 kg/m^3, dynamic viscosity (μ) was 1002 × 10^{-6} kg/s·m, specific heat capacity (c_p) was 4.182 kJ/kg·K, thermal conductivity (k) was 0.598 W/m·K, thus the Prandtl number (Pr) was:

$$Pr = \frac{c_p \mu}{k} = 6.998$$

The Reynolds number (Re) of fluid depends on the mean velocity of the fluid (V). For simpler calculation, assume the V was 0.25 m/s. In practice, the mean velocity of fluid would be higher than this value.

$$Re = \frac{\rho V D}{\mu} = 4756$$

Therefore, a Whitaker correlation of Nusselt number (SIEDER & TATE, 1936; Tosun, 2002; WHITAKER, 1972) was given as:

$$Nu = 0.015 Re^{0.83} Pr^{0.42} (\mu/\mu_\omega)^{0.14}$$

The $\mu/\mu_\omega \approx 1$ since the fluid temperature throughout the pipeline was assumed to not vary significantly. This correlation was valid when:

$$0.48 \leq Pr \leq 592 \quad 2300 \leq Re \leq 1 \times 10^6 \quad 0.44 \leq \mu/\mu_\omega \leq 2.5$$

The Nu value also defined the convective heat transfer rate (h_c) at the pipe inner surface in the form of:

$$Nu = \frac{h_c D}{k} \quad or \quad h_c = \frac{Nu \cdot k}{D}$$

Dynamic viscosity and thermal conductivity of water vary with temperature. The values can be found from The Engineering Toolbox (EngineeringToolBox, 2004b, 2018). Therefore, the relationship between the convective heat transfer rate and the fluid temperature was derived and shown in Figure 3-2.

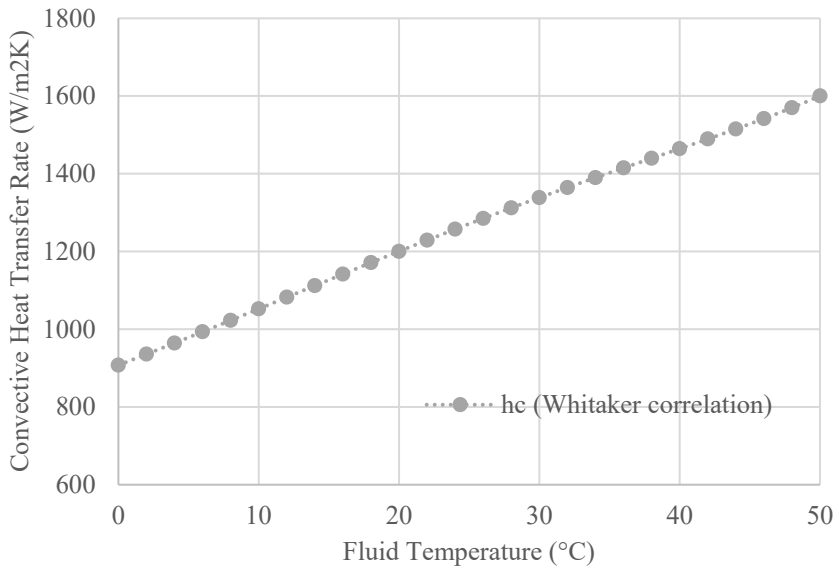

Figure 3-2 Convective Heat Transfer Rate at Pipe Inner Surface Per Whitaker Correlation

The correlation equation for h_c was:

$$h_c = 0.0002T_{fld}^3 - 0.044T_{fld}^2 + 15.59T_{fld} + 903.59$$

The temperature of water (T_{fld}) is in ℃, convective heat transfer rate (h_c) is in W/m^{2}K. Valid when $0 \leq T_{fld} \leq 50$ ℃.

Using this relationship, the h_c value used in MATLAB simulations was determined. Notice that for water, when fluid temperature raises, the h_c value increases roughly in linear manner.

To improve the accuracy of the simulation results and perform as many simulations as possible in limited time frame, the maximum meshing size was 5.08 mm (0.2 inch), with a solution time step of 60 seconds. A typical mesh of an 8-inch (0.2032 m) wall section with pipes embedded in middle is shown in Figure 3-3, and a 16-inch (0.4064 m) example

is shown in Figure 3-4. A typical 16-inch-wide poured concrete wall with insulation was shown in Figure 3-5.

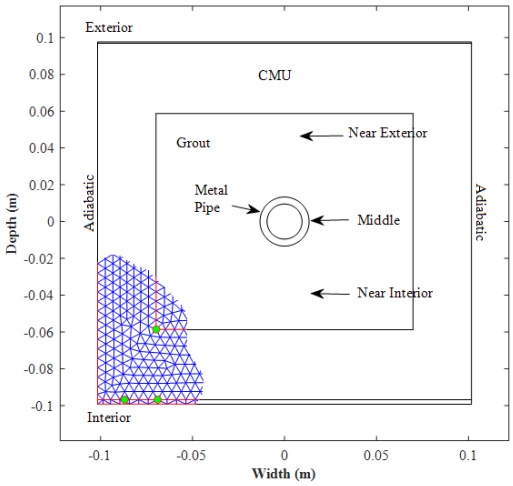

Figure 3-3 Typical 8-inch-Wide CMU MATLAB Model & Meshing

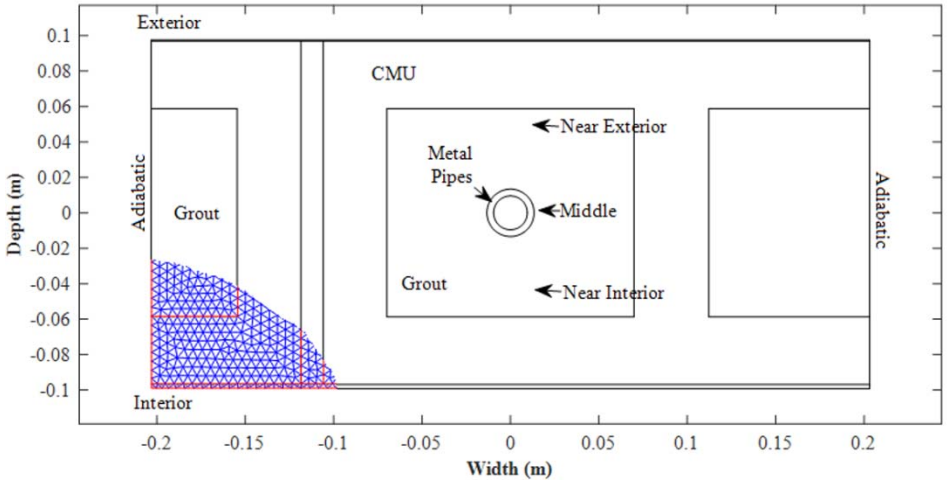

Figure 3-4 Typical 16-inch-Wide CMU MATLAB Model & Meshing

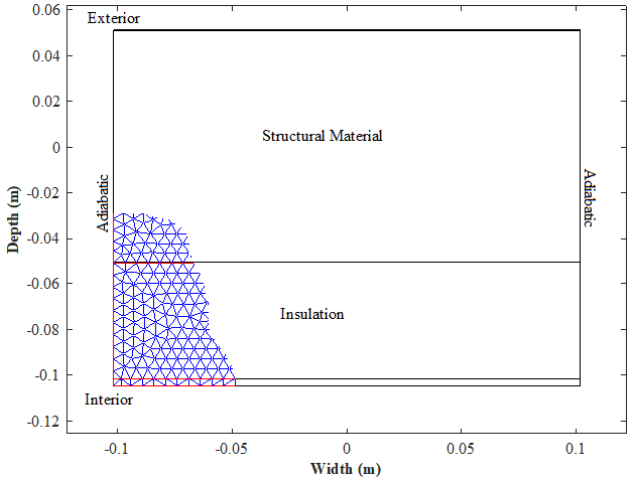

Figure 3-5 Typical 8-inch-Wide Poured Concrete MATLAB Model & Meshing

All other models, including the poured concrete uninsulated wall models, CMU walls with air gaps, etc., were similar to the examples shown above. Thermal properties of materials used in simulation was shown in Table 3-3, unless stated otherwise.

Table 3-3: Thermal Properties of Materials

Material	Density kg/m^3 (lb/ft^3)	Thermal Conductivity W/mK (BTU/h·ft·°F)	Specific heat J/kgK (BTU/lb·°F)
Concrete	1682 (105)	0.73 (0.42)	960 (0.23)
Grout	2000 (124.85)	1.41 (0.82)	800 (0.19)
Insulation	30 (1.87)	0.026 (0.015)	1200 (0.29)
Black Steel Pipe	8050 (502.55)	31.75 (220.14)	510.69 (0.12)
Copper Coil	8960 (559.35)	385 (222.60)	385.11 (0.092)

Again, the exterior temperatures (ambient driving temperature) was taken as a diurnal sine curve with the lowest temperature occurring at 4 am and the highest temperature at occurring at 4 pm. The lowest and highest ambient temperature are listed with the results of each simulation later in this report.

The following factors were to describe the performance of different wall configurations: temperature response at the interior surface of wall (T_{in}), the average ($T_{in,\ mean}$), maximum ($T_{in,\ max}$) and minimum ($T_{in,\ min}$), temperature difference between the interior surface of wall and indoor set point (T_d), the average ($T_{d,\ mean}$), and the maximum ($T_{d,\ max}$) and minimum ($T_{d,\ min}$).

3.1.3. ANSYS Modelling

The ANSYS Workbench mass wall models used the Transient Thermal analysis system module in Workbench. These ANSYS Workbench wall models were only used to validate the accuracy of MATLAB simulation model, since this simulation was more time consuming, these simulations were conducted only on representative wall configurations. Material properties were taken as the same as MATLAB model definitions as in Table 3-3. Screenshots of a simulation of 8-inch-wide pipe embedded CMU were shown in Figure 3-6.

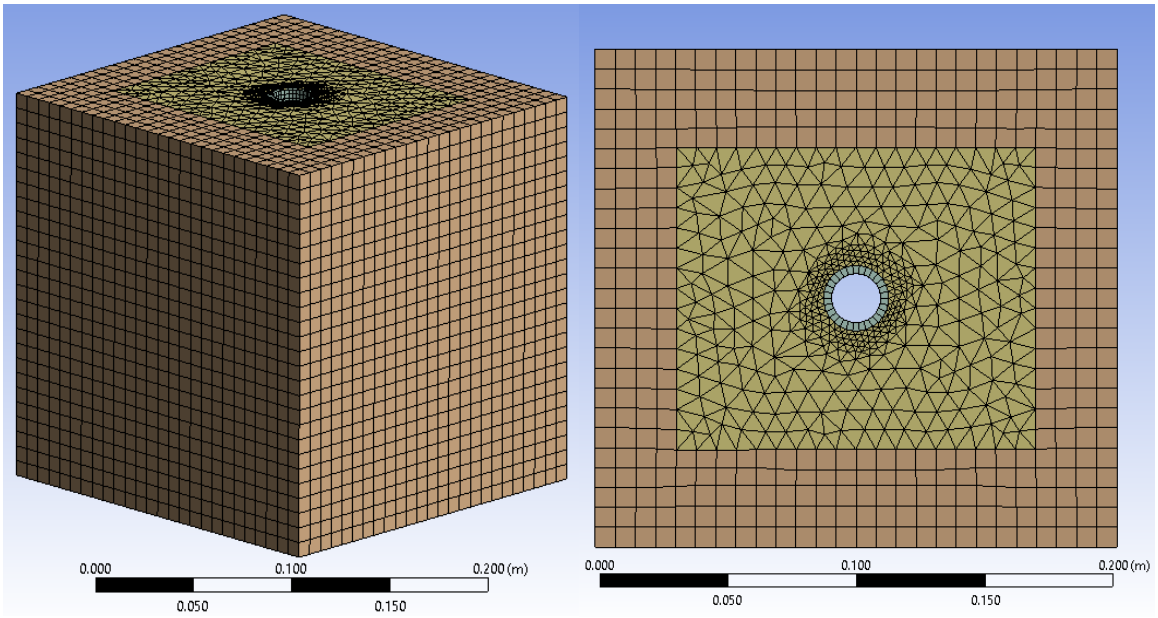

Figure 3-6 8-inch-Wide CMU ANSYS Model & Meshing: (Left) Isometric View (Right) Top View

Since the ANSYS Workbench models were used to verify the MATLAB models, the same ambient and indoor temperatures were applied on the exterior and interior surfaces, respectively. The maximum mesh size was 8 mm, and the area near the pipe used smaller meshing to pick up the higher temperature gradients in this area. The analysis time step was 60 seconds.

In MATLAB model simulations, air films were used to imitating the convection performance at the surfaces, in ANSYS Workbench model simulations, convection boundary conditions were applied at the surfaces instead. The temperature response of the ANSYS and MATLAB models were very similar, predicted heat flux of the simulations were within 15%. This difference was believed caused by the difference in meshing size and difference in numerical solvers.

As will be shown later in this chapter, when pipe fluid temperatures were held at 16°C and Mild Summer exterior temperatures were used (see Figure 3-26 – later in this Chapter), Ansys predicted the average temperature difference between wall interior surface and indoor set point ($T_{d,\,mean}$) value was -1.85°C, the heat flux through the interior surface of wall was 15.13 W/m^2 (heat from indoor to wall surface), heat flux through the inner surface of pipe was 404.66 W/m^2 (heat from wall to fluid). As a comparison, these values obtained from MATLAB simulations were: -1.72°C, -17.34 W/m^2, -374.91 W/m^2, respectively. Note that the sign difference was due to different software definitions, the directions of heat flow were the same in the two simulation methods.

There appears to be good agreement between the two methods, at least partially validating the MATHLAB model.

3.2. Evaluation of Conventional Energy Conservation Strategies (Without Thermal Mass)

Heat flux or Thermal Trasmittance (U) is proportional to the reciprical of the thermal resistance (1/R). The increasing insulation requirements defined in the the newer building codes make the DOE prototype models (baseline) generally well insulated and these requirements vary with climate zones (ASHRAE, 2013, 2019). Thus, to estabilish a comprehensive understanding of the effect that wall insulation has on energy performance, the insulation thickness in the exterior walls were set 0% of the persciptive climate zone baseline value (uninsulated), 50% of the baseline, 200% of the baseline for all prototype buildings, in each climate zone. In a manner similar to wall insulation, the insulation thickness on exterior roofs were set to 0%, 50%, 200% of the baseline configuration for each prototype, in each climate zone. The R values of wall and roof insulation are shown in figures in Chapter 3.2.2 and 3.2.3.

Based on previous investigations by the DOE, luminaire efficacy of the majority of T8/T12 flurescent lamps (in minimum code compliant configurations) are between 55~70 lm/W (DOE, 2009, 2010, 2011). Thus, to cover the range of typical lighting efficiencies commercially available, lighting system efficiencies were set to 10% lower, 10% higher and 20% higher than mimimum baseline model lighting efficiency. In addition, researchers have shown that lighting schedules effected by occupant detection or daylight linked control can save up to 30% of total lighting energy or more (Boyano et al., 2013; X. Sun et al., 2018; Yun et al., 2012). In this research, a change in lighting demand was used to simulate the lighting time/schedule reductions provided through occupancy sensors and use of natural lighting. Thus, the lighting peak demand periods of workday lighting

schedules were set to 10%, 20%, 30% lower than baseline models to simulate this reduction in lighting energy demand.

Changes in efficiency of HVAC systems are typically were small, usually less than 20%, unless very costly changes are made. Thus, to simulate the impact of reasonable changes in HVAC system energy efficiency, the Coefficienct of Performance (COP) of the cooling coils of HVAC systems were set to 10%, 20% better and 10% worse than the baseline model settings to evaluate the influence on cooling. The gas burner efficiency were set to 5%, 10% better and 5% worse than the baseline (0.8) to evaluate the influence on HVAC efficincy on heating energy.

The windows in the four prototype baseline models are double-glazed systems, and the U factors of window glass are normally limited by energy codes to be between 2 to 4 W/m^2K, depending on climate zone. As prescriptive reqirements, windows of the buildings were assumed to vary from single glazing to double glazing systems with designated thickness of glasses. To evaluate the impact of window U factors on building energy consumption, window glass and air gap were altered to different thicknesses that are avaiable on market. Configurations and their U factors are shown in Chapter 3.2.7.

The Solar Heat Gain Coefficient (SHGC) value of window glass was also considered, since this value is usually influenced by the color or tint of glasses. The SHGC value of window are set to be 0.05 higher, 0.1 higher and 0.05 lower than minimum code prescribed baseline window SHGC value (which varied from 0.218 to 0.469 depending on climate zone).

In order to comprehensively investigate the influence of windows, the U factor of window frames was also considered seperately in this research. Since there is general reqirement on fenestration but no specific requirement on U factors of window frames in ASHRAE and IECC codes, the U factors of window frames were set to 10 W/m^2K, 5 W/m^2K, 1 W/m^2K, for each building and climate configuration.

HVAC systems account for about 30% of the yearly energy consumption in buildings (this varies with climate and prototype). Many researchers have studied the energy consumption impact of HVAC systems and found that factors such as occupant behavior, window operability, heating/cooling schedule, set point settings, deadband range, ventilation triggers, and HVAC equipment configurations were found to affect the energy consumption signifcantly (Andersen et al., 2016; FABI et al., 2013; Fayazbakhsh et al., 2015; Hoyt et al., 2015; Laverge et al., 2011; Rackes & Waring, 2017; Tian, 2013; L. Yang et al., 2014; Yu et al., 2017). Based on the results of this research, HVAC control set point and deadband were considered in this investgation, as these parameters have been shown to be cost efficient or even no-cost energy conservation modifications of typical HVAC systems. The baseline HVAC systems of the four prototype buildings are set to heat at 21.11°C(70°F) and to cool at 23.89°C(75°F) during the run period with a deadband width of 2.78°C(5°F). In some thermal zone divisions, set points varied because these rooms were for used for different purposes, for example, Standalone building front entry. To observe the impact of set points, the peak cooling and heating set points on weekdays were set 1°C higher, 2°C higher or 1°C lower than the baseline model. To investgate the impact of deadband width, cooling set points were set 0.5°C higher and heating set points were set 0.5°C lower than the baseline levels (an increased deadband of 1.0°C). Deadbands were

also increased by 2.0°C and decreased by 1.0°C (“SR-3”) from the baseline values. Note that to ensure occupant comfort, set point range changes were limited.

For buildings with mass exterior walls, reflectance of the exterior surface of the wall was assumed be 0.3 in all seven climate zones. This value was the default reflectance value of the baseline models. The reflectance of exterior wall was also set to 0.1, 0.5 and 0.7 to observe the impact of this reflectance value on building energy usage.

3.2.1. Yearly Energy Consumption Baselines

The yearly energy consumption of the four baseline prototypes (Large Office, Secondary School, Standalone Retail, Midrise Apartment) for the seven climate zones were shown in Figure 3-7. This figure showed that the yearly energy consumption in cold regions (Climate Zones 6A and 7), was higher than in warmer regions for the Secondary School, Standalone Retail, and Midrise Apartment prototypes. However, the yearly energy consumption results were different for the Large Office prototype. Here, Climate Zone 7 has lower yearly energy consumption than some of the warmer climate zones. This suggested that this building may be internal load dominated. Figure 3-8 showed the heating/cooling related energy consumption of the baseline prototypes.

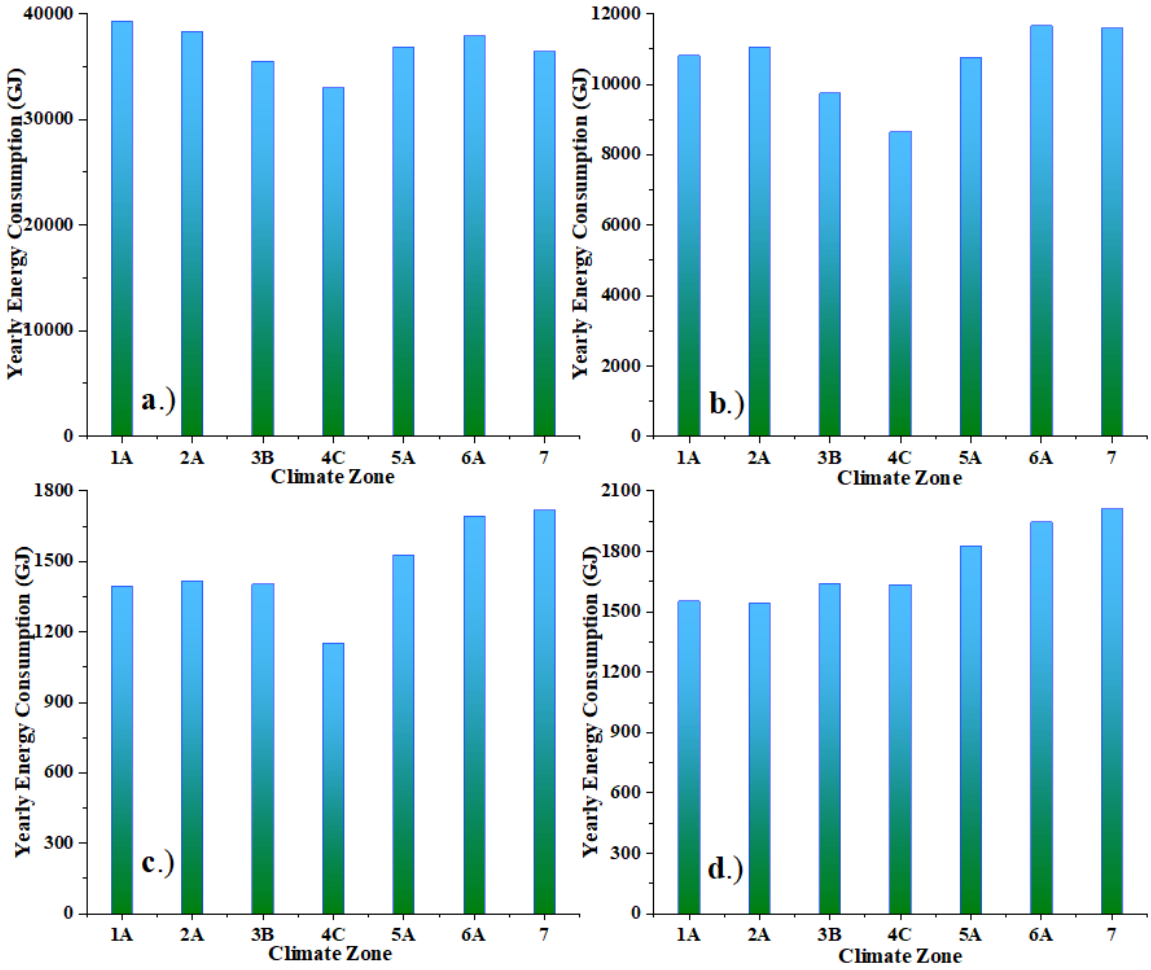

Figure 3-7 Total Yearly Energy Consumption Baselines of The Four Prototype in the Seven Climate Zones: a) Large Office; b) Secondary School; c) Standalone Retail; d) Midrise Apartment

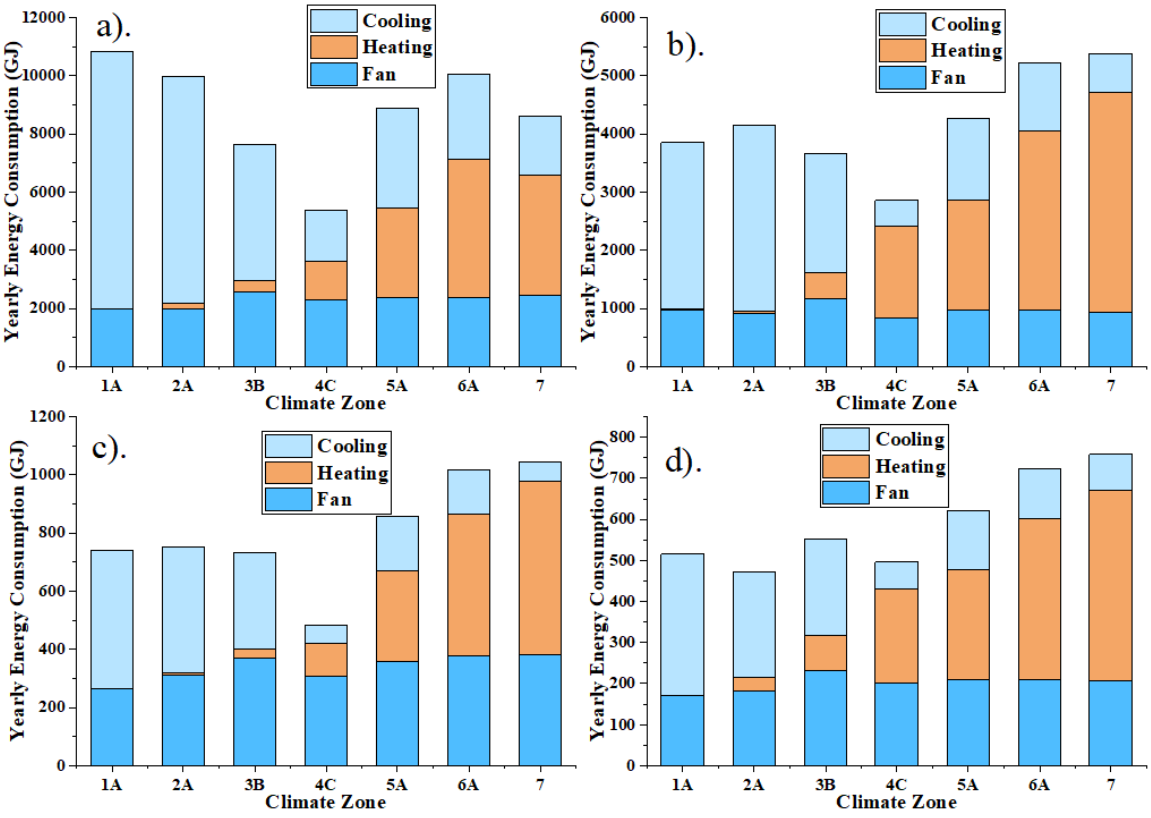

Figure 3-8 Figure Heating/Cooling Related Energy of the Four Prototype Baselines in the Seven Climate Zones: a) Large Office; b) Secondary School; c) Standalone Retail; d) Midrise Apartment

Energy usage by percentage of the four prototype baseline models in Climate Zones 5A were shown in Figure 3-9. These energy use profiles were representative of each type of building, showing the percentage of energy consumed by each building systems.

These analyses showed that heating and cooling accounts for about 18% to 33% of yearly energy consumption in the building prototypes. Further, for buildings with more interior equipment, such as the Large Office prototype, the heating and cooling energy percentage was lower. The difference in the percentage of energy end uses create the variation in performance of the four prototypes, when different energy conservation measures were incorporated. For example, the proportion of energy consumption for heating and cooling in the Large Office was the smallest among the four prototypes,

therefore the percentage changes in insulation R values had the least effect on energy consumption for this prototype. In addition, variation of building function and thus use schedules impact interior heat gains due to occupancy. This also impacted the response of the building prototypes.

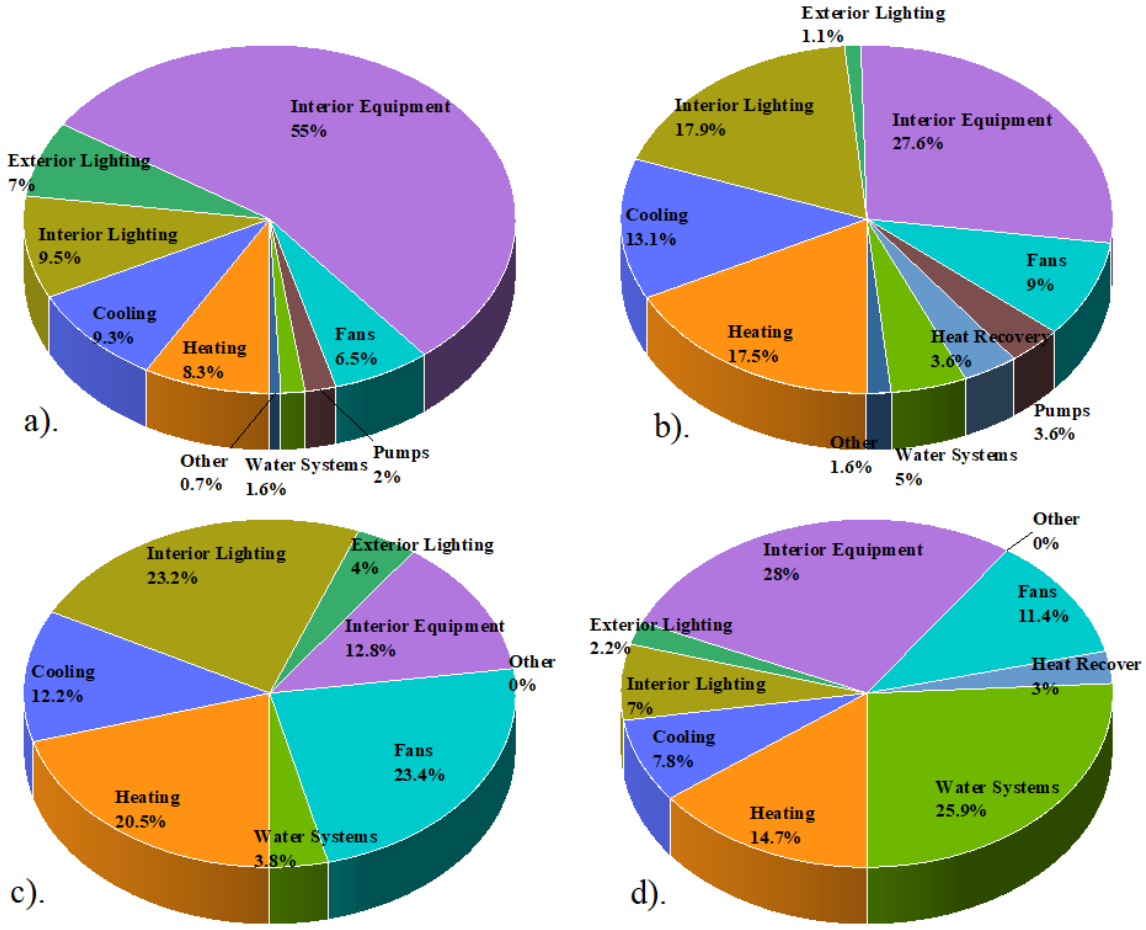

Figure 3-9 End Use of the Four Prototype Baselines by Percentage in Climate Zone 5A: a) Large Office; b) Secondary School; c) Standalone Retail; d) Midrise Apartment

In the following analysis, energy saving potential (ESP) was used to evaluate the impact of the energy conservation strategies on the four prototype buildings in the seven climate zones. The predicted yearly energy consumption from the simulations with different energy conservation strategies were listed in this chapter section by section. ESP is the percentage difference between the baseline and the yearly energy consumption of the

building with the proposed changes and indicates how much energy by percentage the proposed energy conservation strategy could save. A higher ESP means less energy was consumed for the prototype with the proposed change. This indicates that the strategy has a greater influence on building energy consumption. In this chapter, the plotted solid points located on the x axis showed the yearly energy consumption baselines (0% ESP). As a reminder, a positive ESP means the specific measure saves energy, and a negative ESP means more energy consumed for the proposed building configuration.

3.2.2. Impact of Wall Insulation

The energy saving potentials (ESP) of the four prototypes (Large Office, Secondary School, Standalone Retail, Midrise Apartment) in the seven climate zones with different thicknesses of wall insulations were shown in Figure 3-10. Note that the solid points on the zero % line are the baselines. It can be observed from these figures that, in general, insulation of exterior walls has a higher energy saving potential in cold regions than in warm regions, building codes required buildings in cold regions to have thicker insulation. However, for the four prototype buildings studied, ESP changes only by a relatively small amount in Climate Zones 1A, 2A and 3B, with relatively large increases in insulation thickness. In Climate Zone 1A, the yearly energy consumption only changes by 1.2%, 4.3%, 13.2%, 11.4%, with over a 200% increase (from baseline requirements) in wall insulation. However, lower insulation amounts for the four prototype buildings in Climate Zones 4C, 5A, 6A, 7 results in a large building energy consumption increase. The curves follow the equation of:

$$ESP = (a \cdot R_{wall} - b)/(R_{wall} + c);$$

In which R_{wall} means the insulation R value of wall in m^2K/m, a, b, c are constants.

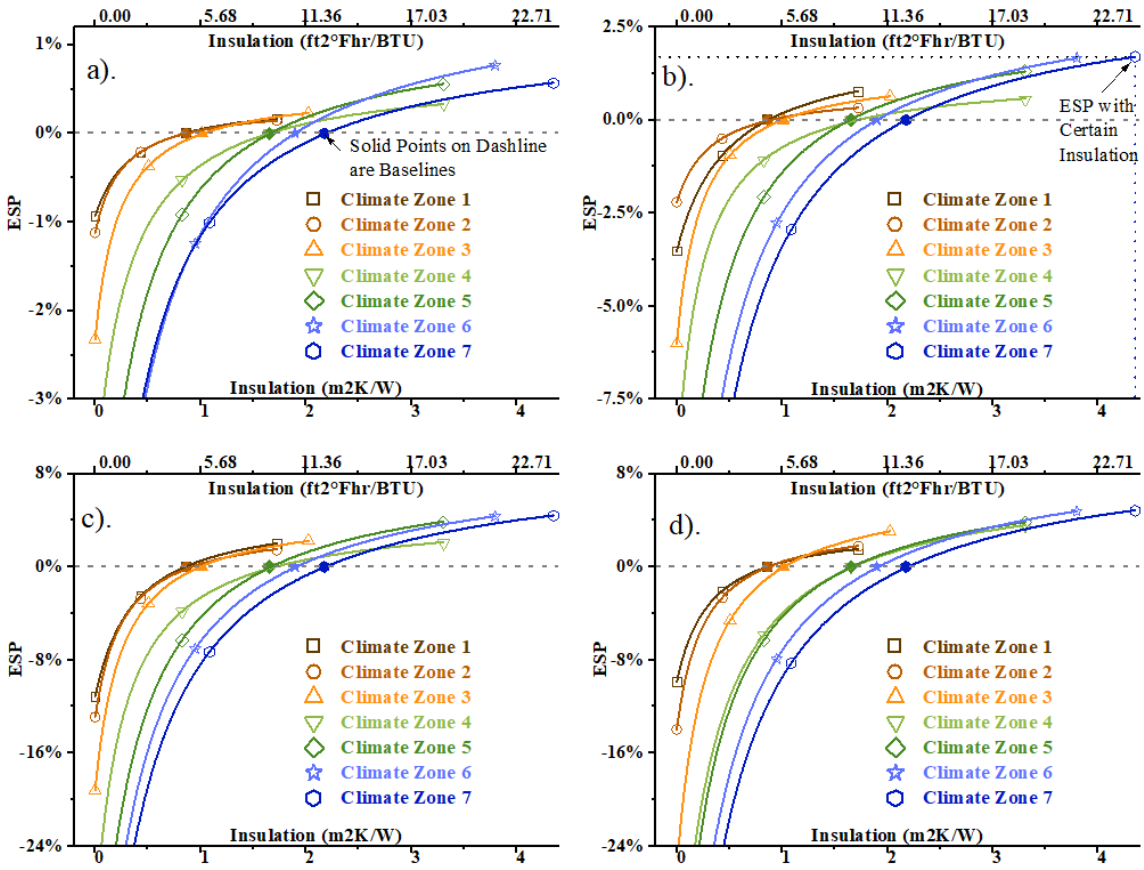

Figure 3-10 ESP of Wall Insulation Thickness: a) Large Office; b) Secondary School; c) Standalone Retail; d) Midrise Apartment

Additional effects can also be seen in these analyses, although thicker insulation (better insulation) showed a higher ESP, and optimum insulation thickness was not shown for any of the seven climate zones. Thicker insulation always reduced yearly energy consumption. However, there are two obvious trends shown in the results. Firstly, as the thickness of wall insulation increases, the smaller the reduction it produces in total energy consumed. This indicates that increases in thermal insulation are much less effective at higher R values. Secondly, with the increase of insulation thickness, energy demand for heating, cooling and fans decreases, except in Climate Zones 4C and 7 (see Figure 3-11). In Climate Zones 4C and 7, better insulation led to a small increase in cooling demand for

the four prototype buildings, except that cooling demand of secondary school in Climate Zone 4C and standalone retail in Climate Zone 7 was the least with 50% of the baseline insulation thickness. Note that for roof insulation, this increase in heating energy was not seen. This suggests that in cases where a lot of cooling is required but heating demand is low, the best solution may be to use insulation levels below the baseline levels.

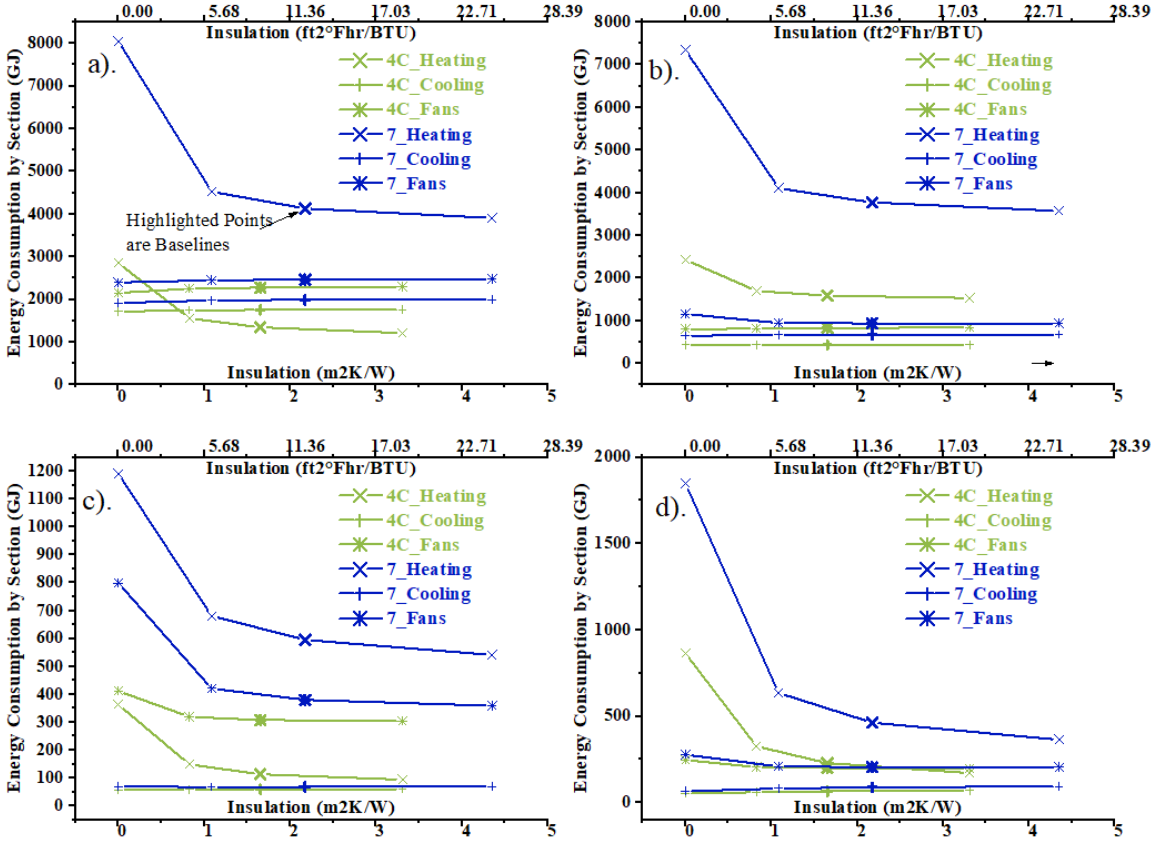

Figure 3-11 Heating/Cooling Related Energy Consumption of Wall Insulation: a) Large Office; b) Secondary School; c) Standalone Retail; d) Midrise Apartment

3.2.3. Impact of Roof Insulation

Energy saving potentials (ESP) of the four prototype buildings (for the seven climate zones) with different thicknesses of roof insulation were shown in Figure 3-12. Note that the solid points on the zero % line are the baseline conditions.

Results of roof insulation analyses showed similar trends to the wall insulation results. Buildings in cold regions require more insulation and insulation thickness has more influence on total yearly energy consumption in these climates. However, these analyses showed that for low-rise buildings (the Secondary School, Standalone Retail and to a lesser extent the Midrise Apartment), the ESP of roof insulation was higher than that for wall insulation. In contrast, for high-rise buildings (Large Office) the effects of the two were similar. These results were explained by the differences in the surface to volume ratio of wall and roof. The lower this ratio (such as in a high-rise building), the lower the impact heat loss through the envelope had on yearly energy consumption. The curves in Figure 3-7 follow the equation:

$$ESP = \left(a \cdot R_{roof} - b\right)/\left(R_{roof} + c\right);$$

In which R_{roof} means the insulation R value of roof in m^2K/m, a, b, c are constants.

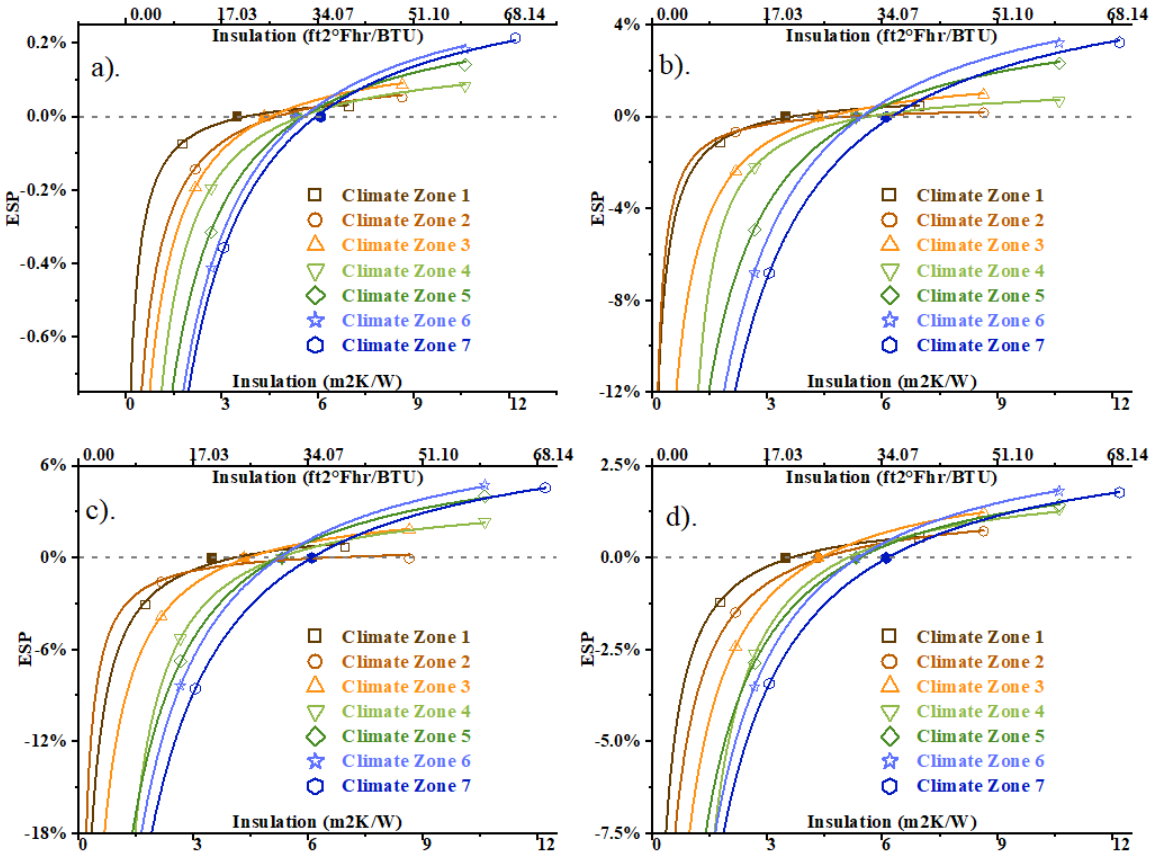

Figure 3-12 ESP of Roof Insulation Thickness: a) Large Office; b) Secondary School; c) Standalone Retail; d) Midrise Apartment

3.2.4. Impact of Lighting Efficiency

The ESPs' of the four prototypes in the seven climate zones with different lighting efficiencies were shown in Figure 3-13. Lighting efficiencies were described as a percentage of the baseline models.

As expected, improvements in lighting efficiency increases the ESP in all seven climate zones studied. The increase in ESP was linearly related to lighting efficiency. Additionally, the percentage change is positively related to the ratio of energy for lighting to yearly energy consumption. In Figure 3-14, energy consumed by lighting, heating, cooling and fan for the four prototypes in Climate Zones 1A, 4C and 7 were shown to illustrate this variation. It is also worth noting that with the increase of lighting efficiency,

energy for lighting, cooling, and fan decreases, but energy demand for heating increases. Lights in buildings produce heat, therefore improvement in lighting efficiency or decrease in lighting demand will reduce the amount of heat generated by lights, thus the building will require more heating or less heating.

This analysis showed that every 10% increase in lighting efficiency brings around 1% ESP in all climate zones for Large Office prototype, a range of 1.5% to 2.4% ESP for different climate zones for Secondary School prototype, a range of 1.3% to 3.9% ESP for the Standalone Retail prototype, and a range of 0.4% to 1.1% ESP for Midrise Apartment prototype.

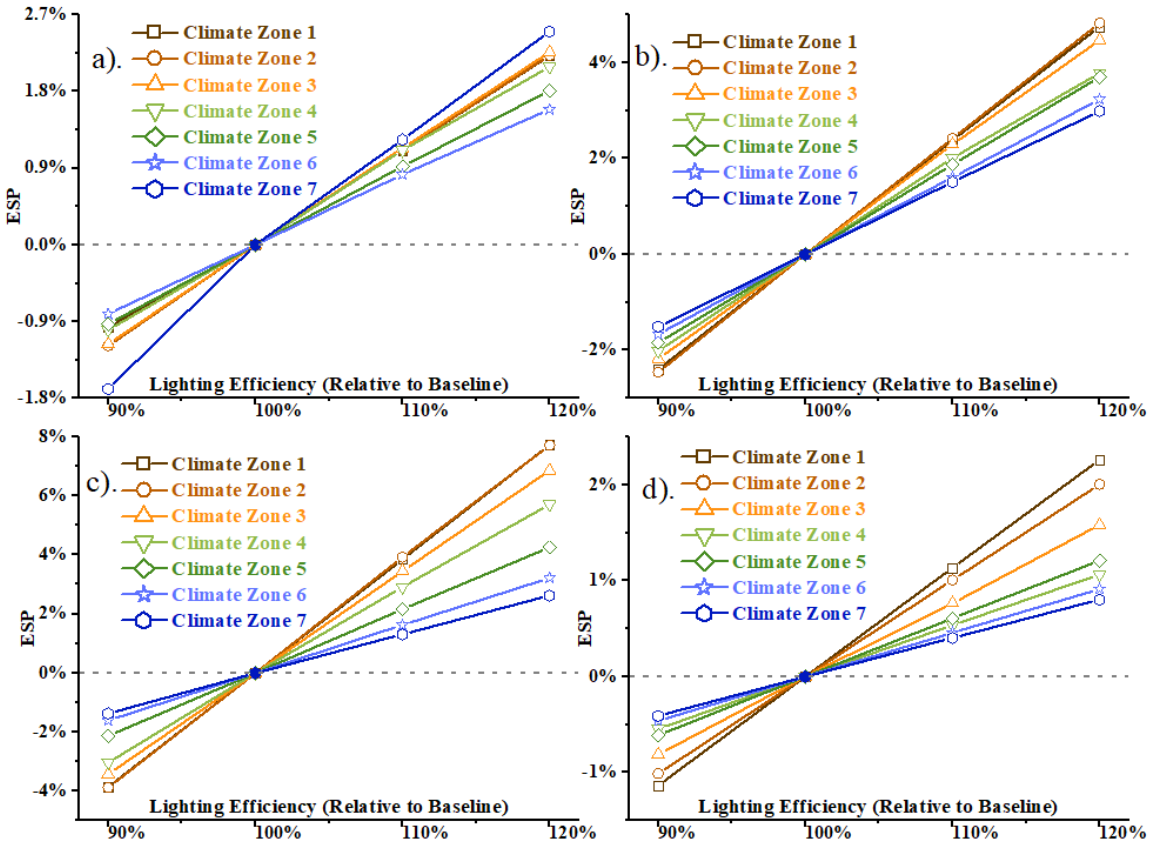

Figure 3-13 ESP of Lighting Efficiency: a) Large Office; b) Secondary School; c) Standalone Retail; d) Midrise Apartment

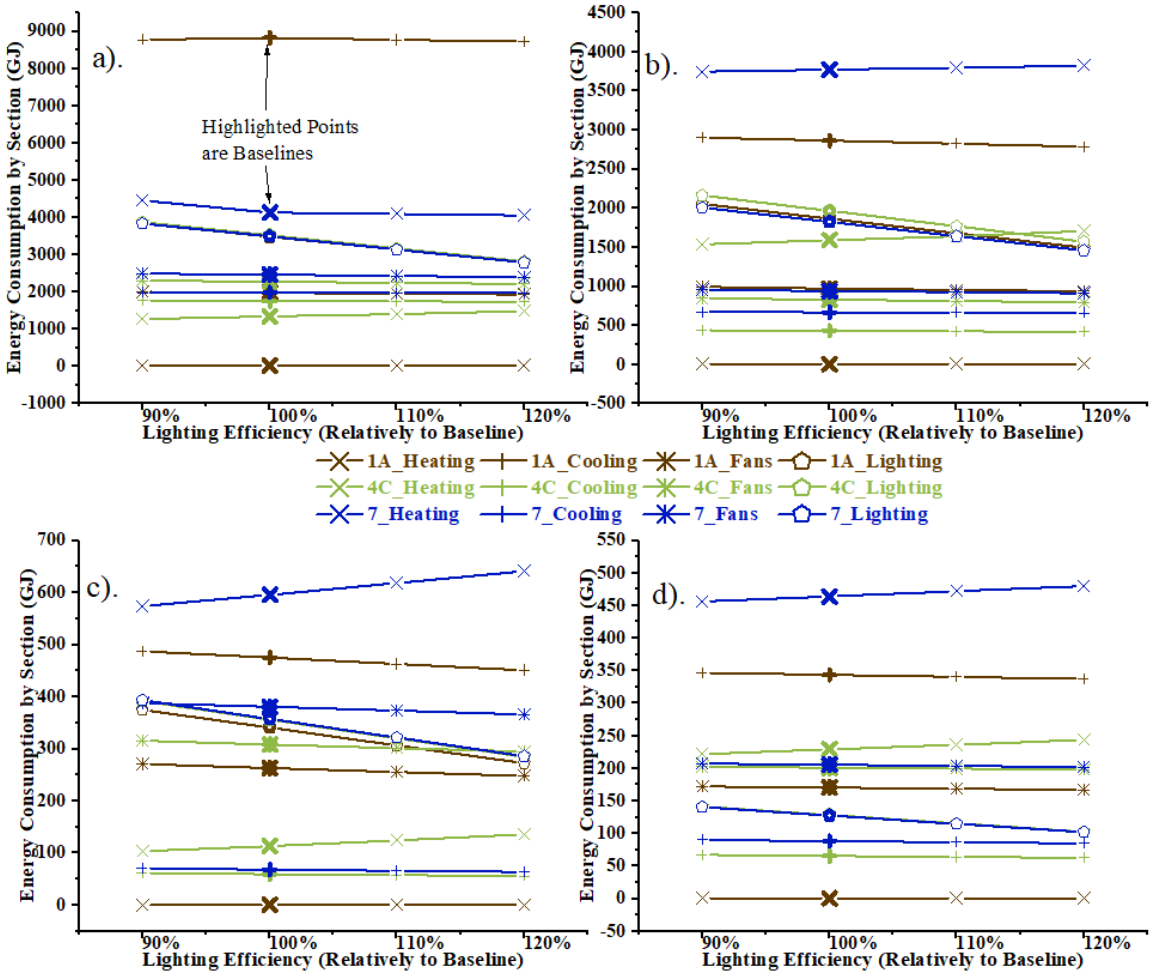

Figure 3-14 Lighting Related Energy Consumption of Lighting Efficiency: a) Large Office; b) Secondary School; c) Standalone Retail; d) Midrise Apartment

3.2.5. Impact of Lighting Demand

The variation of ESP with different lighting demand for the four prototype buildings were shown in Figure 3-15, for all seven climate zones. Note that lighting demand variation was described as a percentage of the baseline models. The difference between lighting efficiency and lighting demand was described previously in Chapter 3.2.

Unsurprisingly, the impacts of reduced lighting demand were similar to the results for improved lighting efficiency. When peak lighting demand decreased by 10%, ESP increases by around 0.7% in all climate zones for the Large Office prototype, a range of

1.1% to 1.5% ESP in different climate zones for the Secondary School prototype, a range of 1.0% to 2.9% for the Standalone Retail prototype, and a range of 0.2% to 0.6% for the Midrise Apartment prototype. In Figure 3-16, the energy consumed by lighting, heating, cooling and fans for the four prototypes in Climate Zones 1A, 4C and 7 are shown to indicate the range of energy being consumed by these systems. Decreases in lighting demand, results in a reduction of energy for lighting, cooling, and fans, but energy demand for heating increases.

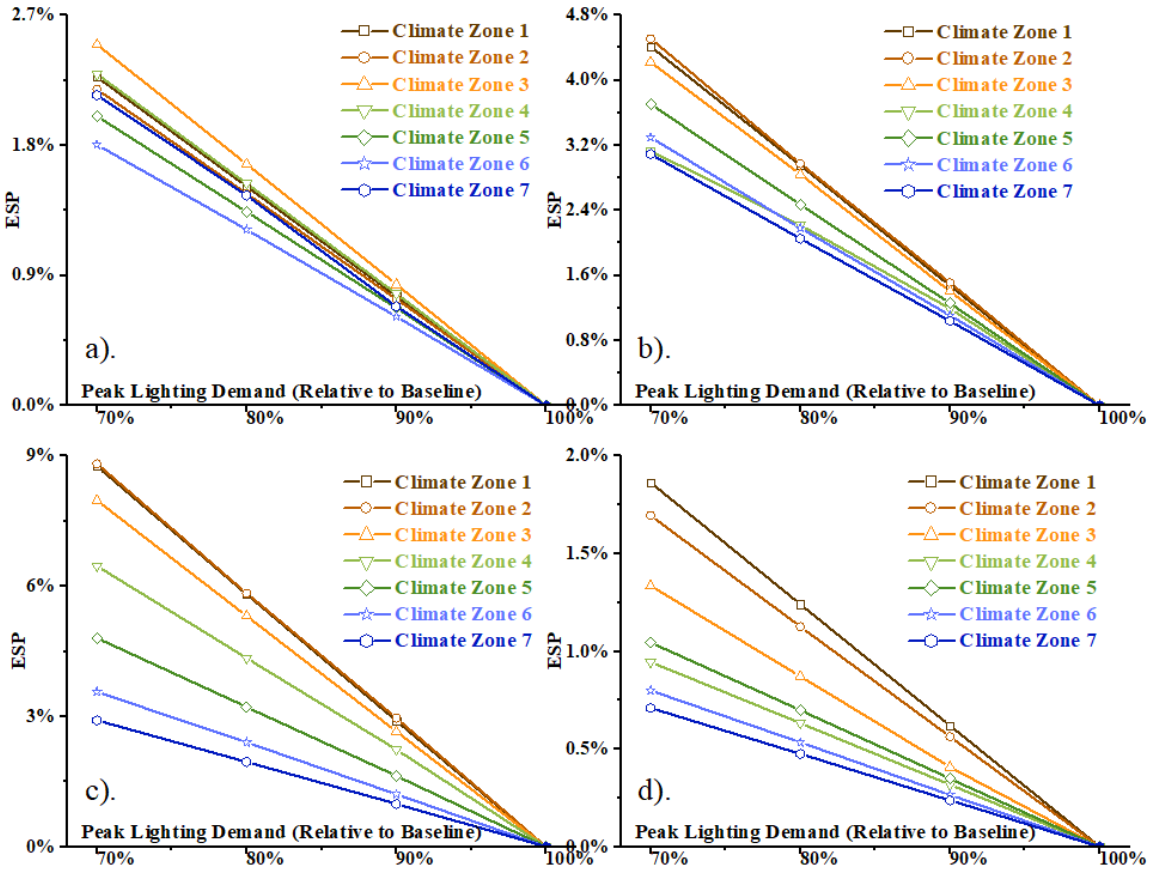

Figure 3-15 ESP of Lighting Demand: a) Large Office; b) Secondary School; c) Standalone Retail; d) Midrise Apartment

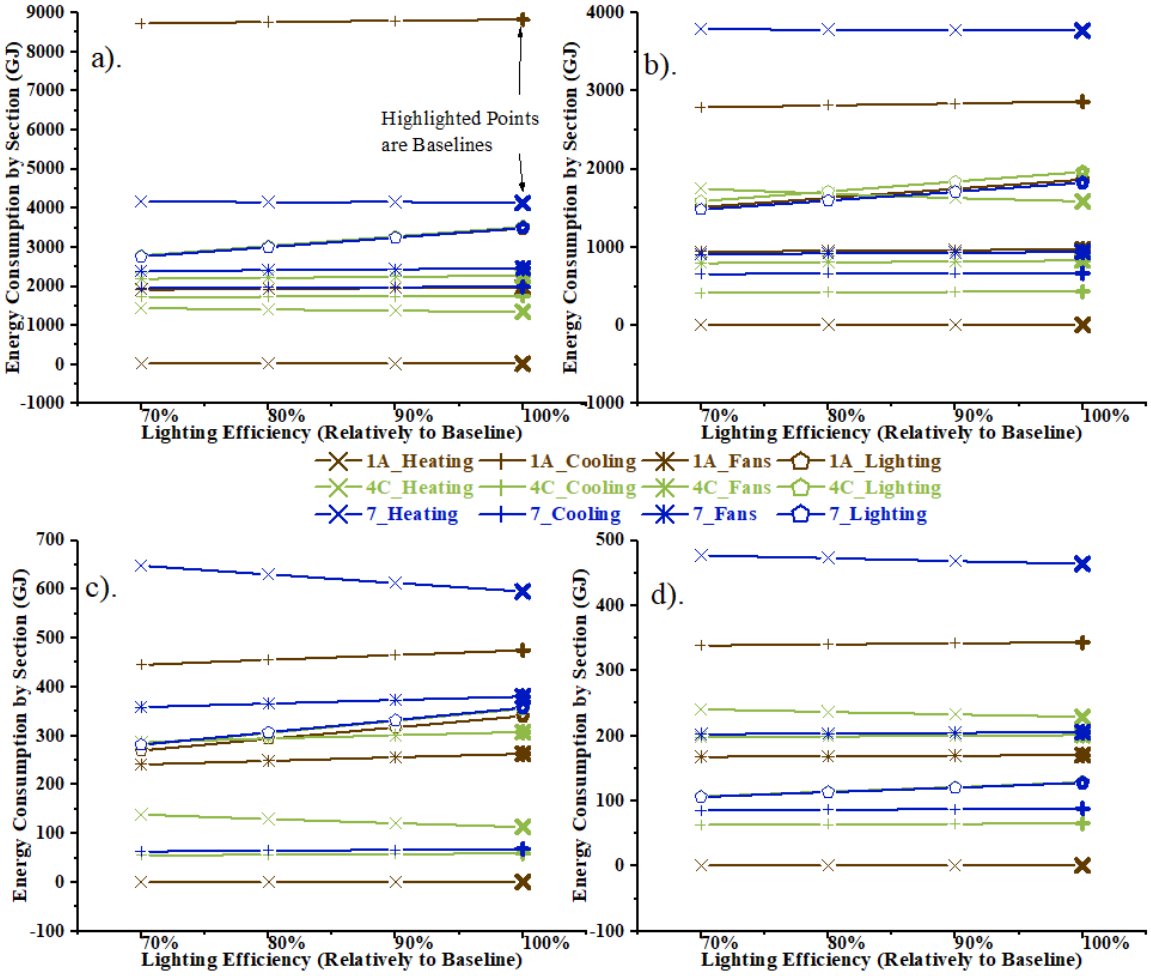

Figure 3-16 Lighting Related Energy Consumption and Lighting Demand: a) Large Office; b) Secondary School; c) Standalone Retail; d) Midrise Apartment

Note that in the Figure 3-16 above, heating demand in Climate Zone 1A is minor, thus not shown.

3.2.6. Impact of HVAC Cooling Coil COP

Variation of the ESP of the four prototypes buildings in the seven climate zones with different HVAC cooling and coil (COP) efficiencies were shown in Figure 3-17. Note that HVAC coil (COP) efficiencies were described as a percentage of the baseline models, and the baseline COP's vary with thermal zones for each building as per the baseline

models published by DOE. The values were not listed here but are considered in the payback analysis chapter.

Cooling coil efficiency has the most impact on the performance of the Standalone Retail and Secondary School prototypes, and has the least impact on the Midrise Apartment prototype. This is consistent with the percentage of cooling energy used by each of the four prototypes.

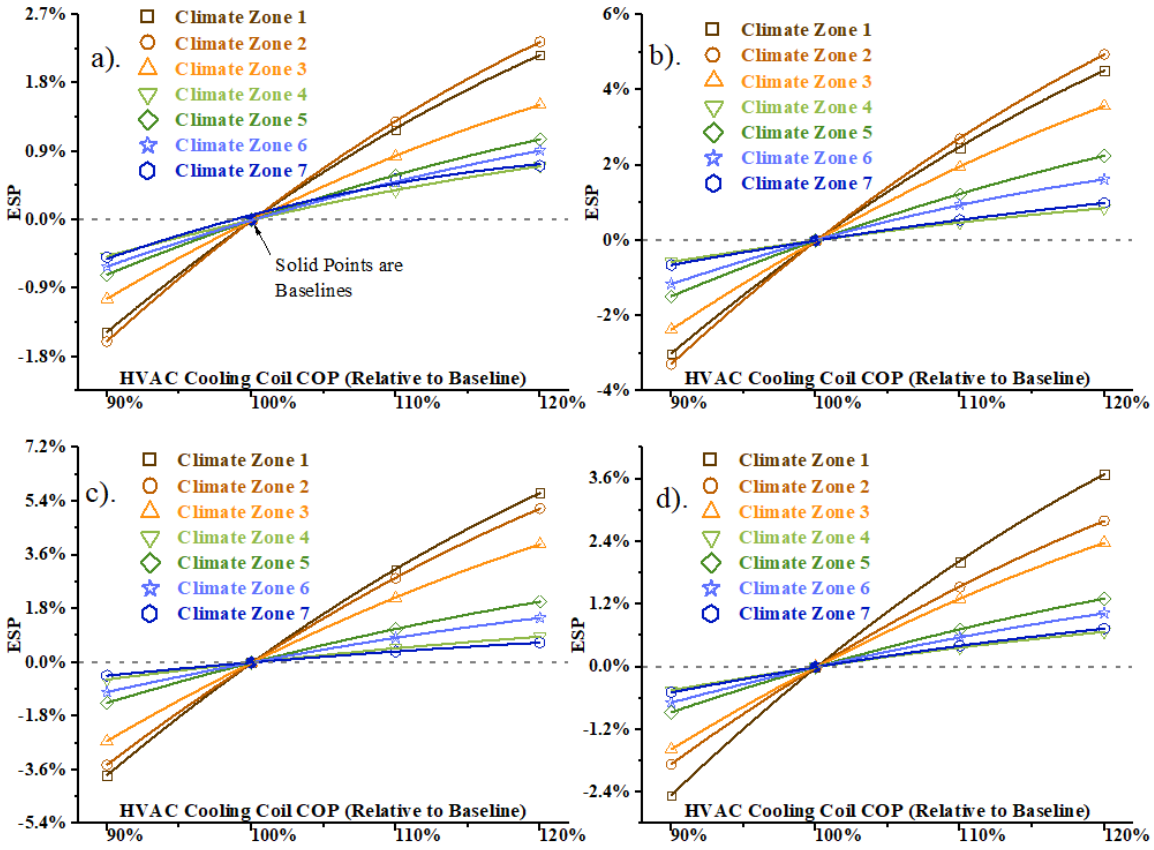

Figure 3-17 *ESP of Cooling Coil COP Efficiency: a) Large Office; b) Secondary School; c) Standalone Retail; d) Midrise Apartment*

3.2.7. Impact of HVAC Heating Efficiency

Variation of the ESP of the four prototypes buildings, in the seven climate zones with different air condition/boiler efficiencies were shown in Figure 3-18. Note that heating efficiencies were described as a percentage of the baseline models and the heating

efficiencies vary with the different thermal zones as per the baseline models published by DOE. The values were not listed here but are considered in the payback analysis chapter.

Heating efficiency has the most impact on the performance of the Standalone Retail and Secondary School prototypes, and has the least impact on the Large Office prototype. This is consistent with the percentage of heating energy use by the four prototypes.

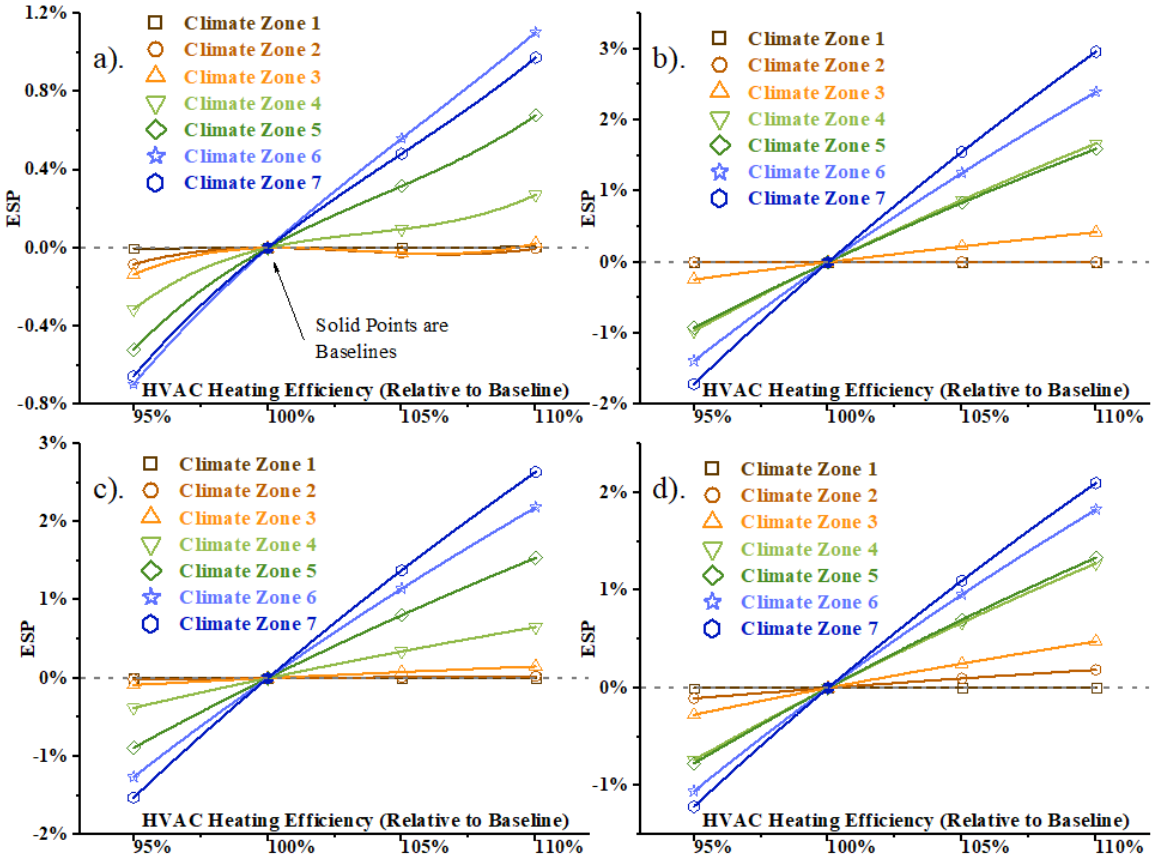

Figure 3-18 ESP of Heating Efficiency: a) Large Office; b) Secondary School; c) Standalone Retail; d) Midrise Apartment

3.2.8. Impact of Window Glazing System

Variation of the ESP with window glazing thermal transmittance (U-Factor) for the four prototypes buildings in the seven climate zones were shown in Figure 3-19.

It should be noted that the U factor for the baseline double-glazing system was around 3 W/m^2K, and when glass thickness was doubled, the U factor will not improve much. However, U factors of the single-glazing system is quite different from double-glazing systems. In this research, a single-glazing system ($U=5.7$ W/m^2K) and double-glazing systems ($U<3.5$ W/m^2K) were analyzed. Examination of these figures shows that in the colder climate zones, the U factor of the windows has a greater impact than in warm regions. Since the U factors of different double-glazing systems do not change much, the difference in ESP with various double-glazing systems is often within 1%. However, the single-glazing window systems show considerable increases in energy use in colder climate zones. That is because the existence of the air gap in double-glazing systems. The ESP for decreasing U factors of window glazing systems show the least impact with the Standalone Retail prototype buildings, due to its relatively low window/wall ratio. The ESP plots show higher impacts of window U-factor reductions with the Secondary School and Midrise Apartment prototypes, which is consistent with their window/wall ratio. However, the ESP impact is low on the Large Office prototype which has the largest window/wall ratio. This is because the proportion of heating and cooling energy consumption in Large Office is low, and U-factor of the window glazing system mainly affects heating and cooling energy use.

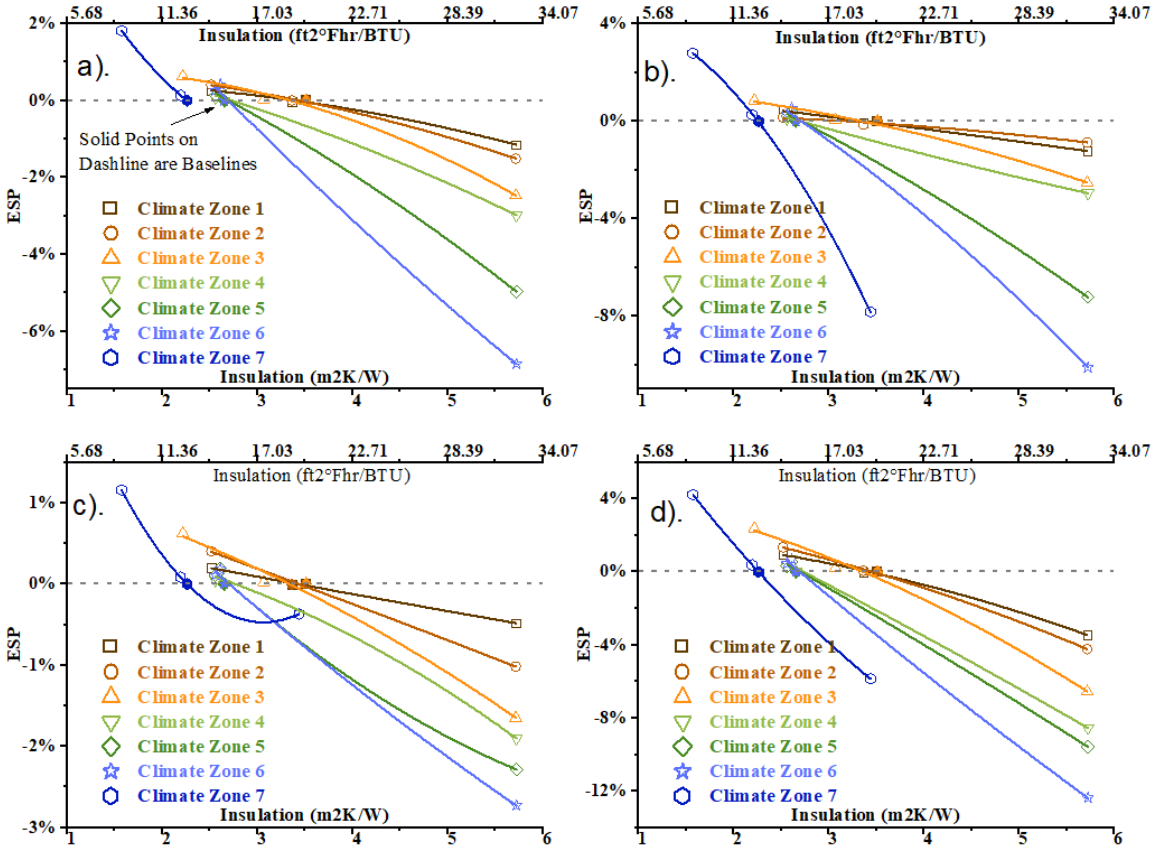

Figure 3-19 ESP of Window Glazing System: a) Large Office; b) Secondary School; c) Standalone Retail; d) Midrise Apartment Impact of Window Frames

Variation in ESP of the four prototypes in the seven climate zones, with variable window frame U-factors, were shown in Figure 3-20. It can be seen that U-factors of the window frames change yearly energy consumption less than about 0.5%, for all four prototypes. This is due to the small amount of the envelopes that the frames represent. As stated earlier in Chapter 3.2, there is general requirement on fenestration, but the U factor of window frames is not mandatorily restricted. The results in this section are only for reference uses.

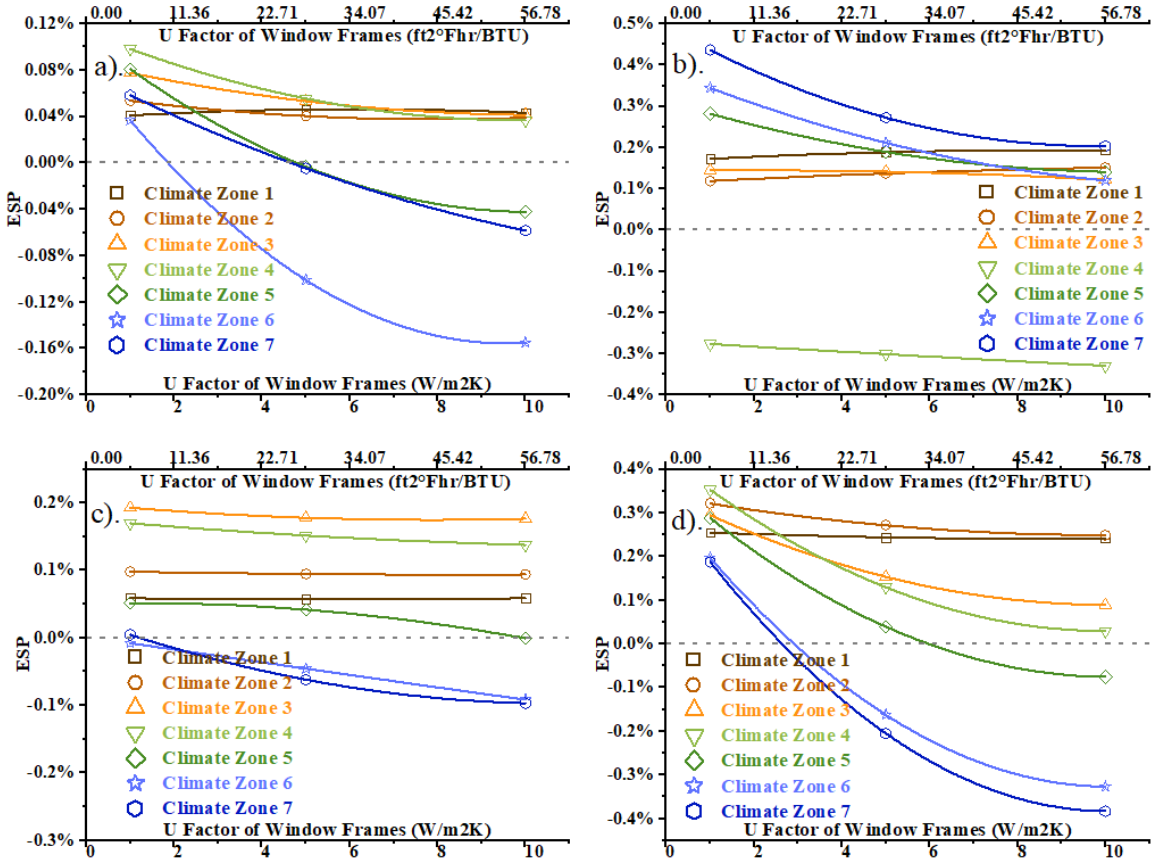

Figure 3-20 *ESP of U Factor of Window Frames: a) Large Office; b) Secondary School; c) Standalone Retail; d) Midrise Apartment*

3.2.9. Impact of Window SHGC

The variation in the ESP of the four prototypes in the seven climate zones with changes in window glass SHGC values were shown in Figure 3-21. Higher SHGC glass transmits more solar heat to the indoor environment, thus, reducing heating demand, but increasing cooling demand. The net reduction in heating and increase in cooling consumption led to different results in yearly energy consumption. In general, a lower SHGC resulted in a higher ESP. However, for only the Standalone Retail prototype in Climate Zones 5A, 6A, 7 and Midrise Apartment prototype in Climate Zone 7, higher SHGC values resulted in higher ESP. The optimum SHGC values for the Large Office and Midrise Apartment prototypes in Climate Zone 6A, and the Secondary School prototype in

Climate Cone 4C appears to be around 0.45. But overall, the ESP is less than 0.8% in all cases studied.

Note that Standalone Retail and Midrise Apartment have larger surface/volume ratio and larger wall surface/volume ratio. The author believes that higher surface/volume ratio increases the heat dissipation of buildings, thus higher SHGC's will be less inclined to "overheat" the buildings during summer but supplement the heating demand in winter in colder climate zones.

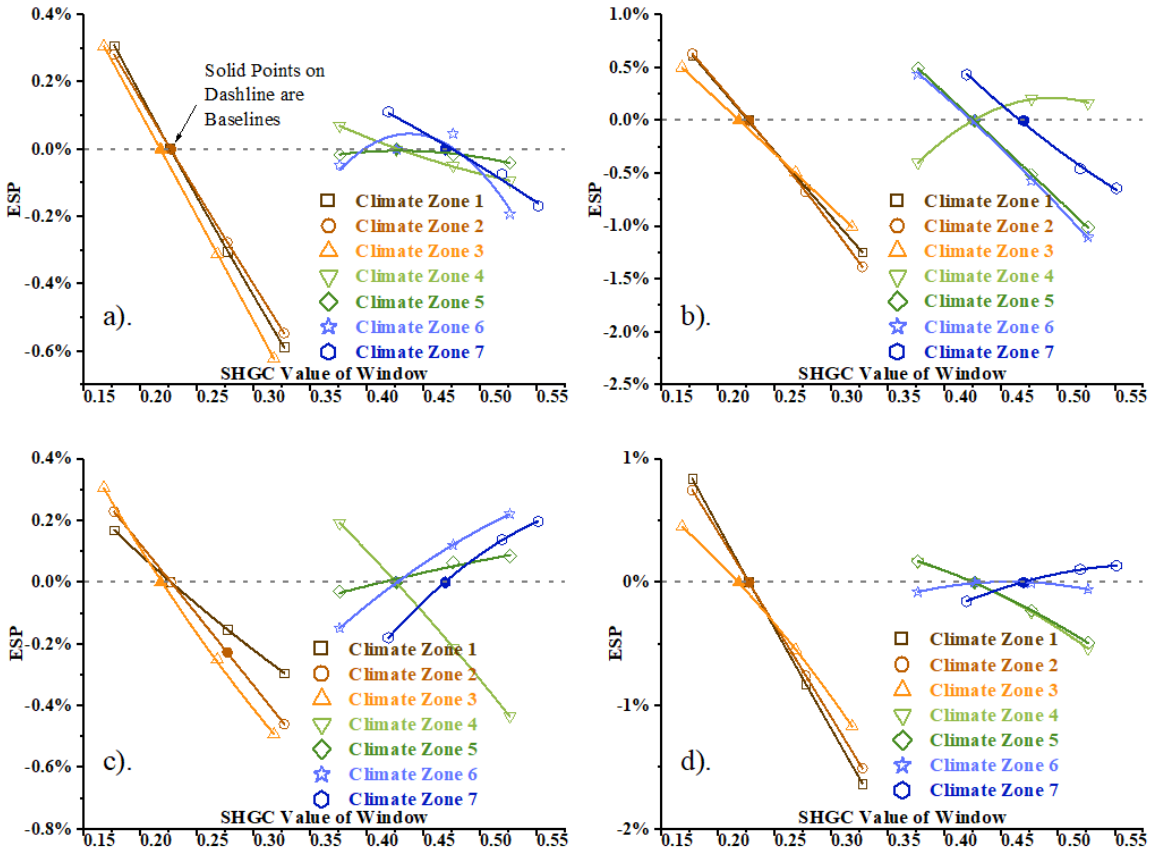

Figure 3-21 ESP of Window SHGC: a) Large Office; b) Secondary School; c) Standalone Retail; d) Midrise Apartment

3.2.10. Impact of HVAC Setpoints

The variation of ESP of the four prototypes in the seven climate zones with different HVAC setpoints were shown in Figure 3-22 and Figure 3-23. Setpoints of baseline models

were designated as 0 on the graphs. The baseline setpoints for each prototype varied as described in the DOE prototype building descriptions. In the Large Office prototype, thermostat settings for the basement were 15.6°C, 24°C (heating, cooling) in summer and 21°C, 24°C (heating and cooling) in the winter. Thermostat settings for main data center in both summer and winter was 18°C, 27°C (heating, cooling). The thermostat settings for office areas were 21°C, 24°C (heating, cooling). The office areas were cooled by a chiller and heated by boilers, instead of via an air conditioner or heat pump. In the Secondary School prototype, baseline thermostat settings for the auditorium were 15.6°C, 24°C (heating, cooling) in summer, and 21°C, 29.44°C (heating, cooling) in winter. The baseline thermostat settings for the restrooms and classrooms were 15.6°C, 24°C (heating, cooling) in summer and 21°C, 29.44°C (heating, cooling) in winter. The classrooms were cooled by chillers instead of an air conditioner or heat pump. In the Standalone Retail prototype, baseline thermostat settings for the retail office and warehouse spaces were 15.56°C, 23.89°C (heating, cooling) in summer and 21.11°C, 29.44°C in winter (heating, cooling). The baseline thermostat settings for the retail core areas were 15.6°C, 23.89°C (heating, cooling) in summer and 21.11°C, 29.44°C (heating, cooling) in winter. The baseline thermostat settings for the retail entry were 15.56°C, 100°C (heating, cooling) in summer, and 16°C, 100°C (heating, cooling) in winter. In the Midrise Apartment prototype, the baseline thermostat settings for the apartments were 21.7°C, 24.4°C (heating, cooling) and 15.6°C, 23.9°C for office in summer and 21.1°C, 29.4°C, in the winter (heating, cooling).

The impact of offset HVAC setpoints were evaluated through two sets of scenarios. The first scenario (Scenario 1) the set points were offset throughout the year, up by 1°C or 2°C, and down uniformly by 1°C (thereby increasing the range by 2 or 3°C). The results

of these analyses were shown in Figure 3-22. The second scenario (Scenario 2) focused on only setpoints in two seasons: winter and summer. In this scenario, the setpoints were offset up by 1°C in summer and down by 1°C in winter, up by 2°C in summer and down by 2°C in winter, or down by 1°C in summer and up by 1°C in winter. These results of these analyses were shown in Figure 3-23. Current convention suggests that setpoints of buildings can be shifted above the baseline, or default settings, to save energy. Scenario 1 was intended to verify whether this conclusion is correct or not. Conventional energy conservation practices suggest that shifting the setpoint up in summer and down in winter to would reduce both cooling and heating demands. Scenario 2 was intended to verify this practice.

In Scenario 1, the relationship between setpoint offset and ESP is close to linear in the studied range, with the except of the Standalone Retail prototype. For the Large Office, Secondary School and Midrise Apartment prototypes, the higher that the setpoints are offset in warmer climate zones, the higher the ESP. For the Secondary School prototype in Climate Zone 4C, the Standalone Prototype in Climate Zone 7, and the Midrise Apartment in Climate Zones 6A and 7, the lower offsets of the setpoints produced higher ESP's. There was an optimum setpoint offset found in Large Office prototype in Climate Zones 4C and 7, the Secondary School prototype in Climates Zones 6A and 7, the Standalone Retail prototype in Climate Zones 1A, 2A, 3B, 4C, 5A, 6A and 7, and the Midrise Apartment prototype in Climate Zone 5A. These optimums varied with prototype and climate zones.

Conventional practice would suggest setpoints need to be higher in warmer climate zones (or lower in colder climate zones) to save energy, but this study proves that this idea is not correct. In this study, the variations of ESP suggest that the sum of the changes in

both heating and cooling is important and both must be accounted for. Two other building characteristics that impact this variation is surface volume ratio and the ratio of energy consumed by heating and cooling. When setpoints were offset at higher values, the cooling demand during hot days was decreased undoubtfully in warmer climate zones, however, the heating demand during mild days or cold days was increased, thus the yearly energy consumption remains unclear since it is a sum of both cooling and heating all year round. That explained the variation of ESP with the setpoint offset.

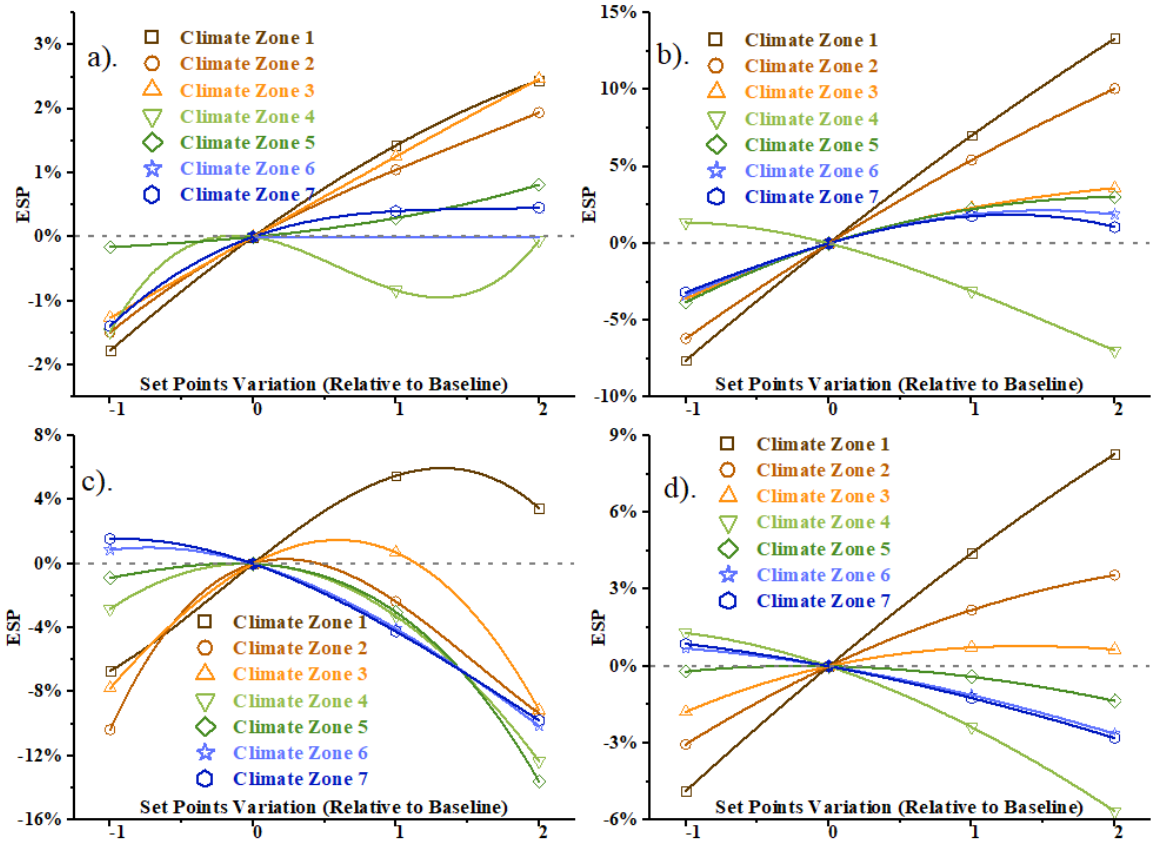

Figure 3-22 ESP of Setpoints Scenario 1: a) Large Office; b) Secondary School; c) Standalone Retail; d) Midrise Apartment

The results of the Scenario 2 were similar to Scenario 1, offsetting the setpoints can contribute an ESP of as high as 6%. However, in warmer regions like Climate Zone 1A, 2A and 3B, the four prototypes (except Standalone Retail) have higher ESP's in Scenario

1. In colder regions like Climate Zone 5A, 6A and 7, all the four prototypes investigated have higher ESP in Scenario 2. In Scenario 2, the energy saving potential of the four prototypes is higher when setpoints are shifted only by 1°C, rather than by 2°C. This proves that it may not be energy-efficient to change setpoints much over 1 °C. This would also make it easier to ensure human comfort is satisfied. These analyses also show that optimum setpoints settings vary with weather conditions and building types.

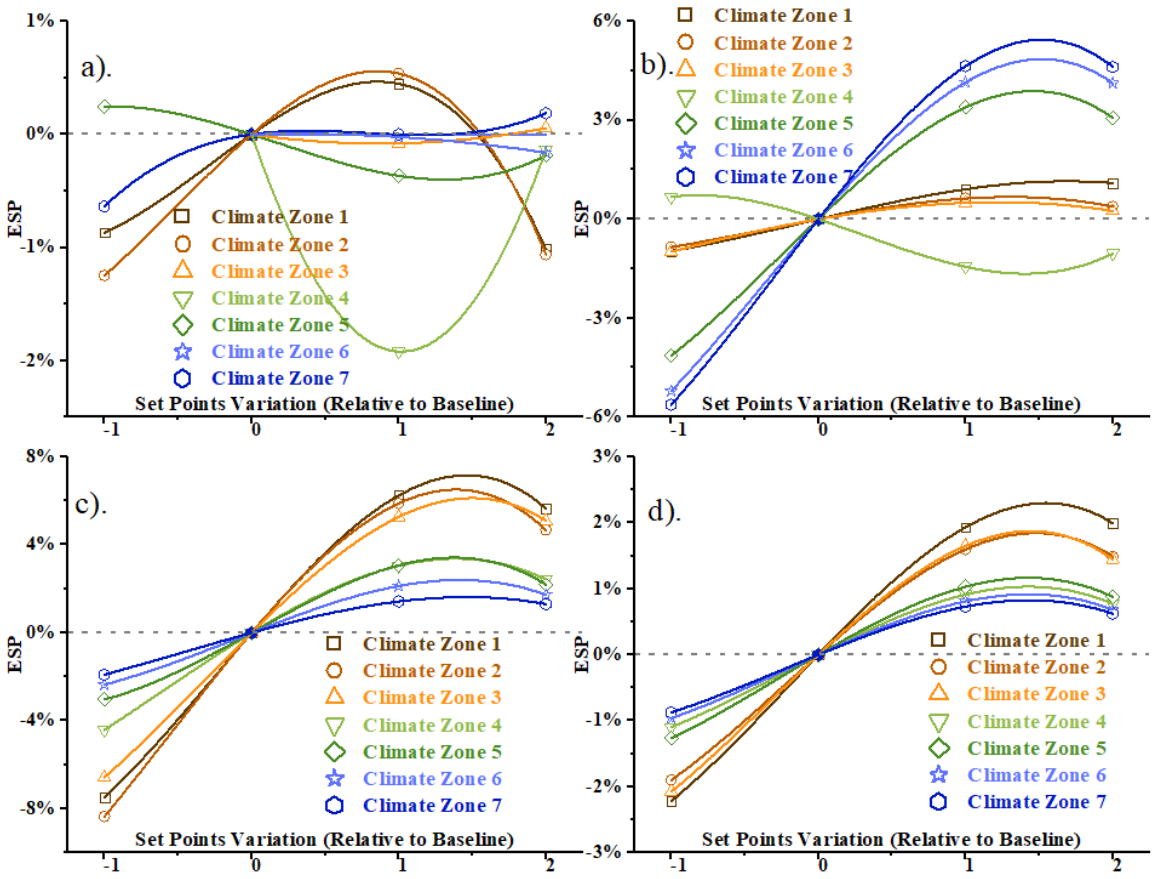

Figure 3-23 ESP of Setpoints Scenario 2: a) Large Office; b) Secondary School; c) Standalone Retail; d) Midrise Apartment

3.2.11. Impact of Setpoint Deadband Width

Variation of the yearly ESP of the four prototypes in the seven climate zones with various deadband widths were shown in Figure 3-24. The increase of deadband width corresponds to an increase in ESP. When deadband width was increased by 1°C, ESP

increased by 0.8% to 1.4% for the Large Office, 1.3% to 4.9% for the Secondary School, 3.1% to 6.5% for the Standalone Retail, 2% to 2.8% for the Midrise Apartment prototypes. Note that the increase in deadband width allows the indoor temperature to vary over a wider range, so the HVAC system will reduce the heating and cooling run times.

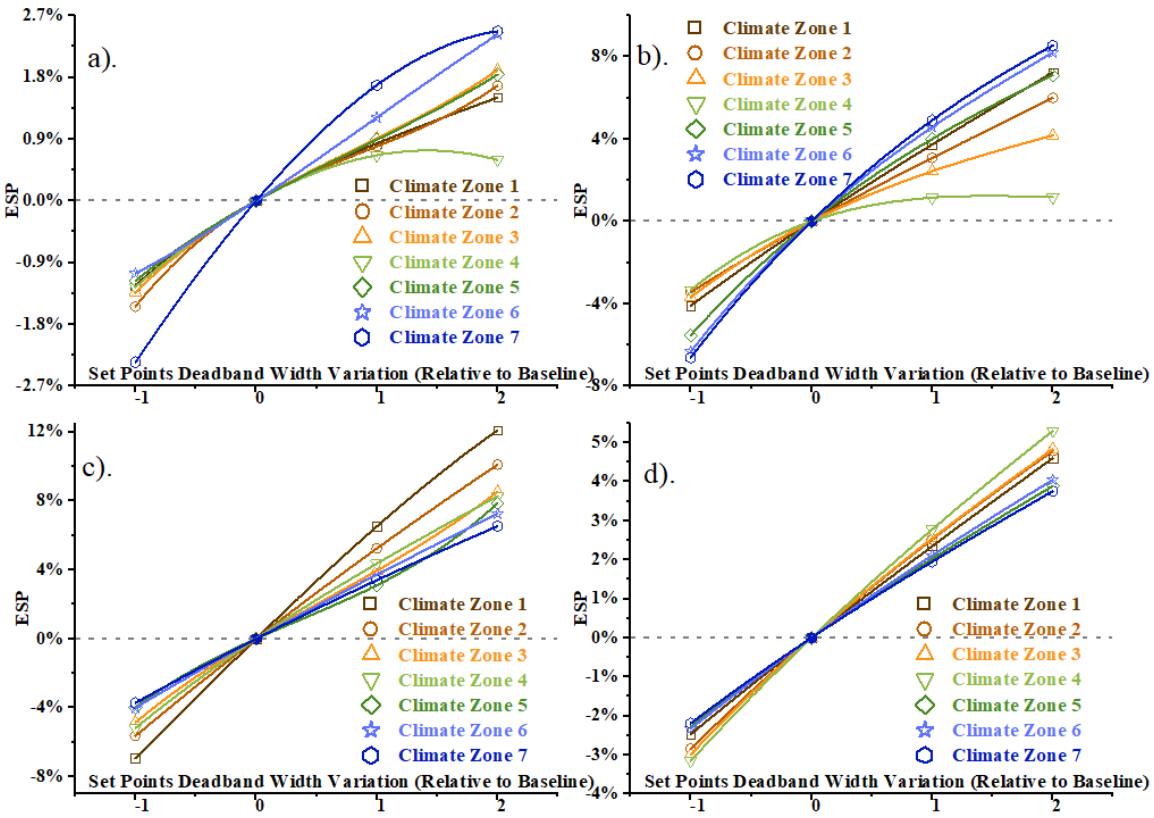

Figure 3-24 *ESP of Setpoints Deadband Width: a) Large Office; b) Secondary School; c) Standalone Retail; d) Midrise Apartment*

3.2.12. Impact of Wall Reflectance

Variation of ESP of the four prototypes in the seven climate zones with different exterior wall reflectance values were shown in Figure 3-25. In warmer climate zones (Climate Zones 1A, 2A and 3B), higher reflectivity of the walls means a higher ESP for all the four prototype buildings. In the other four climate zones studied (Climate Zones 4C, 5A, 6A, 7), the trends of the four prototypes are not consistent. For the Large Office prototype in Climate Zones 4C, 5A, 6A, reflectance value increases produce an ESP

decrease. In Climate Zone 7 for the Large office prototype, the highest ESP occurs when reflectance values are around 0.5. For the Secondary School prototype in Climate Zone 4C, a reflectance value increase produces an ESP decrease. For the same prototype in Climate Zones 5A, 6A, 7, an increase in reflectance produces an ESP increase. For the Standalone Retail prototype in Climate Zone 4C, a reflectance value increase will produce an EPS increase, while in Climate Zones 5A, 6A, 7 the result is just the opposite. For the Midrise Apartment prototype in Climate Zones 4C, 5A, 6A and 7, increase in reflectance will always reduce the ESP.

Overall, wall reflectance affects buildings with higher surface volume ratios, such as the Midrise Apartment and Standalone Retail prototypes, more than buildings with lower surface volume ratio, such as the Large Office prototype. By investigating the results of Standalone Retail and Midrise Apartment prototypes, it can be observed that, although Standalone Retail prototype has smaller surface volume ratio, it has a higher ESP due to the higher ratio of heating to cooling energy in the yearly energy consumption. It appears that this impact is a result of the balance between surface volume ratio and cheating/cooling energy ratios.

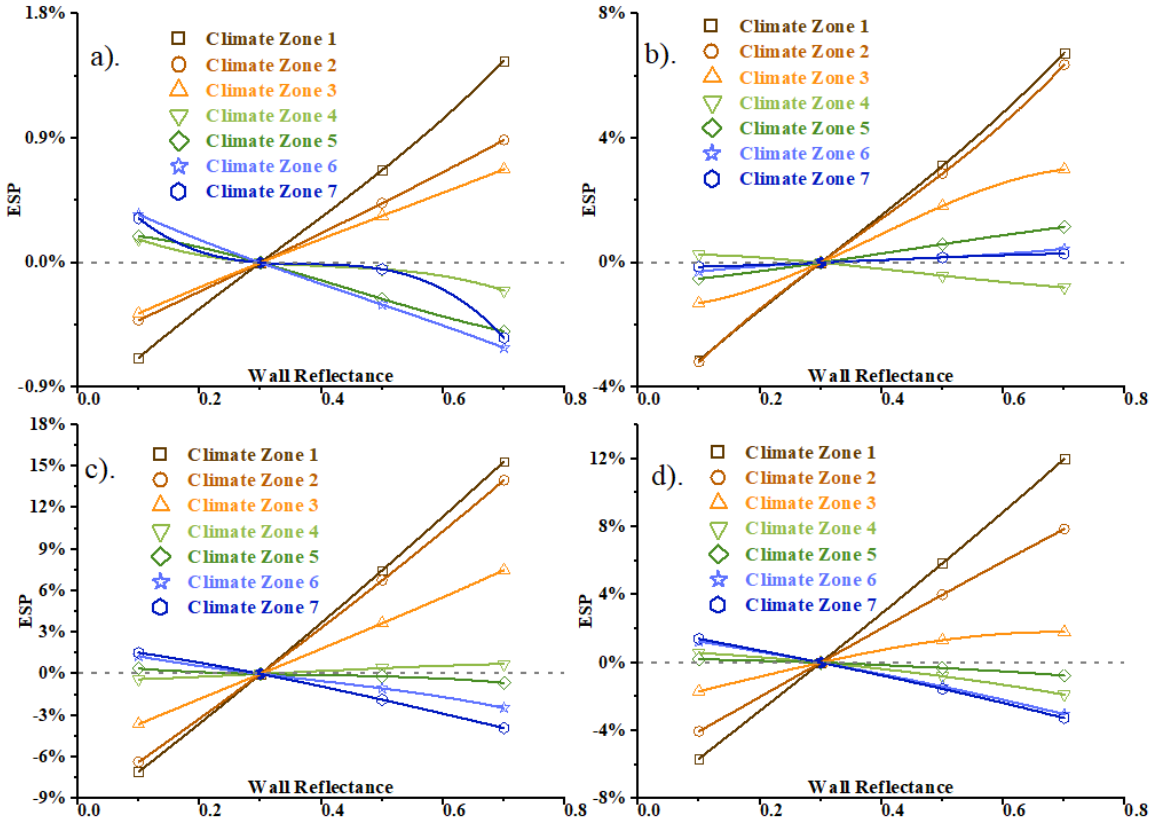

Figure 3-25 ESP of Wall Reflectance: a) Large Office; b) Secondary School; c) Standalone Retail; d) Midrise Apartment

3.2.13. Results and Discussion

Based the analyses presented in the preceding sections for the proposed energy conservation strategies, it can be seen that the effectiveness of these strategies was related to weather conditions. Some of the proposed energy conservation strategies were only slightly impacted by climate, including improved lighting efficiency, reduced lighting demand, and widened deadband. However, the effectiveness of many of these strategies varied significantly with climate zones, some even had the opposite effect in colder versus warmer climate zones.

For the Large Office prototype, broadened deadband width, improved lighting efficiency, and reduced lighting demand show higher ESP in all climate zones with the

values around 2%. In addition, in colder climate zones, improving HVAC cooling efficiency by 20% (ESP of around 0.8%), improving HVAC heating efficiency by 10% (ESP of around 0.8%), doubling wall insulation (ESP of around 0.6%), improving window glass U factors (only in Climate Zone 7) all show positive ESP values. In warmer climate zones, improving HVAC cooling efficiency by 20% (ESP of around 1.8%), increasing HVAC setpoint by 2°C (change setpoint to 23°C~26°C, also results in positive ESP values of around 2%. All other strategies were shown to be less effective (with ESP values less than 0.5%). These results were summarized in Table 3-4.

Table 3-4: Energy Conservation Strategy Ratings for the Large Office Prototype Based on ESP

Strategy	Large Office						
	1A	2A	3B	4C	5A	6A	7
Double Wall Insulation	ø	ø	ø	ø	★	★	★
Double Roof Insulation	ø	ø	ø	ø	ø	ø	ø
Improve Lighting Efficiency by 20%	★★★	★★★	★★★	★★★	★★	★★	★★★
Reduce Peak Lighting Demand by 30%	★★★	★★★	★★★	★★★	★★★	★★	★★★
Improve HVAC Cooling Efficiency by 20%	★★★	★★★	★★	★	★★	★	★
Improve HVAC Heating Efficiency by 10%	ø	ø	ø	ø	★	★★	★
Double Window Glass & Air Gap Thickness	ø	ø	★	ø	ø	ø	★★
Improve Window Frame Resistance	ø	ø	ø	ø	ø	ø	ø
Ajust Window SHGC	ø	ø	ø	ø	ø	ø	ø
Shift Setpoint by 1 or 2°C	★★★	★★	★★★	ø	★	ø	ø
Widen Setpoint Deadband by 1 or 2°C	★★	★★	★★	★	★★	★★★	★★★
Change Wall Reflectance within 0.1 to 0.7	★★	★	★	ø	ø	ø	ø

Note:

1. ESP between 0% and 0.5% are considered as less effective, marked as ø
2. ESP between 0.5% and 1% marked as ★

3. ESP between 1% and 2% marked as ★★
4. ESP larger than 2% marked as ★★★

For the Secondary School prototype, broadened deadband width, improved lighting efficiency, reduced lighting demand, and improved HVAC cooling efficiency were considered effective in all climate zones with ESP values ranging from about 1% to 8%. In addition, in colder climate zones, use of double wall insulation (ESP of around 1.6%), double roof insulation (ESP of around 2.5%), improving HVAC heating efficiency by 10% (ESP of around 2.2%), increasing setpoints by 1°C (change setpoint to 22°C~25°C) (ESP around 2%), and improved window glass U factor in Climate Zone 7 (ESP around 2%). In warmer climate zones, increasing setpoints by 2°C (change setpoint to 23°C~26°C) (ESP 12%), and increasing wall reflectance to 0.7 (ESP around 1.3%) can reduce yearly energy consumption. All other strategies were considered as less effective (ESP less than 1%). These results were summarized in Table 3-5.

Table 3-5: Energy Conservation Strategy Ratings for the Secondary School Prototype Based on ESP

Strategy	Secondary School						
	1A	2A	3B	4C	5A	6A	7
Double Wall Insulation	ø	ø	ø	ø	★	★	★
Double Roof Insulation	ø	ø	★	ø	★★	★★	★★
Improve Lighting Efficiency by 20%	★★★	★★★	★★★	★★	★★	★★	★★
Reduce Peak Lighting Demand by 30%	★★★	★★★	★★★	★★	★★	★★	★★
Improve HVAC Cooling Efficiency by 20%	★★★	★★★	★★	ø	★★	★	ø
Improve HVAC Heating Efficiency by 10%	ø	ø	ø	★	★	★★	★★
Double Window Glass & Air Gap Thickness	ø	ø	ø	ø	ø	ø	★★
Improve Window Frame Resistance	ø	ø	ø	ø	ø	ø	ø

Ajust Window SHGC	ø	ø	ø	ø	ø	ø	ø
Shift Setpoint by 1 or 2°C	★★★	★★★	★★	★	★★	★	★
Widen Setpoint Deadband by 1 or 2°C	★★★	★★★	★★★	★	★★★	★★★	★★★
Change Wall Reflectance within 0.1 to 0.7	★★★	★★★	★★	ø	★	ø	ø

Note:

1. ESP between 0% and 1% are considered as less effective, marked as ø
2. ESP between 1% and 2% marked as ★
3. ESP between 2% and 4% marked as ★★
4. ESP larger than 4% marked as ★★★

For the Standalone Retail prototype, broadened deadband width, improved lighting efficiency, and reduced lighting demand worked in all climate zones (ESP of 2.5% to 12%). In addition, in colder climate zones, doubling wall insulation (ESP of around 4%), doubling roof insulation (ESP of around 4%), improving HVAC heating efficiency by 10% (ESP of around 2%) all improved energy efficiency. For warmer climate zones, improving HVAC cooling efficiency by 20% (ESP of around 5%), increasing setpoints by 1°C (change setpoint to 22°C~25°C) (ESP around 5%), increasing wall reflectance to 0.7 (ESP around 2.5%) also improve energy efficiency. All other strategies were considered as less effective (ESP less than 2%). These results were summarized in Table 3-6.

Table 3-6: Energy Conservation Strategy Ratings for the Standalone Retail Prototype Based on ESP

Strategy	Standalone Retail						
	1A	2A	3B	4C	5A	6A	7
Double Wall Insulation	★	ø	★	★	★	★★	★★
Double Roof Insulation	ø	ø	ø	★	★★	★★	★★
Improve Lighting Efficiency by 20%	★★	★★	★★	★★	★★	★	★
Reduce Peak Lighting Demand by 30%	★★★	★★★	★★	★★	★★	★	★

Improve HVAC Cooling Efficiency by 20%	★★	★★	★	ø	★	ø	ø
Improve HVAC Heating Efficiency by 10%	ø	ø	ø	ø	ø	★	★
Double Window Glass & Air Gap Thickness	ø	ø	ø	ø	ø	ø	ø
Improve Window Frame Resistance	ø	ø	ø	ø	ø	ø	ø
Ajust Window SHGC	ø	ø	ø	ø	ø	ø	ø
Shift Setpoint by 1 or 2°C	★	ø	ø	ø	ø	ø	ø
Widen Setpoint Deadband by 1 or 2°C	★★★	★★★	★★★	★★★	★★	★★	★★
Change Wall Reflectance within 0.1 to 0.7	★★★	★★★	★★	ø	ø	ø	ø

Note:

1. ESP between 0% and 2% are considered as less effective, marked as ø
2. ESP between 2% and 4% marked as ★
3. ESP between 4% and 8% marked as ★★
4. ESP larger than 8% marked as ★★★

For the Midrise Apartment prototype, doubled wall insulation and broadened deadband width were energy conservation strategies that work in all climate zones (ESP of 1.5% to 5.5%). In addition, in colder climate zones, doubled roof insulation (ESP of around 1.5%), improving HVAC heating efficiency by 10% (ESP of around 1.5%), doubled window glazing & air gap thickness (in Climate Zone 7 only) (ESP of around 4%), all improved energy efficiency and had ESP's greater than 1%. In warmer climate zones, improving lighting efficiency by 20% (ESP of around 1.8%), reducing lighting demand during peak by 30% (ESP of around 1.6%), improving HVAC cooling efficiency by 20% (ESP of around 2.9%), doubling window glazing & air gap thickness (in Climate Zones 2A and 3B ONLY) (ESP of 1.9%), raising set points by 2°C (change set point to 23°C~26°C, (ESP around 4%), and increasing wall reflectance to 0.7 (ESP around 1.4%) all improved

energy efficiency. All other strategies were considered as less effective (ESP less than 1%). These results were summarized in Table 3-7.

Table 3-7: Energy Conservation Strategy Ratings for the Midrise Apartment Based on ESP

Strategy	Midrise Apartment						
	1A	2A	3B	4C	5A	6A	7
Double Wall Insulation	★	★	★★	★★	★★	★★★	★★★
Double Roof Insulation	ø	ø	★	★	★	★	★
Improve Lighting Efficiency by 20%	★★	★★	★	★	★	ø	ø
Reduce Peak Lighting Demand by 30%	★	★	★	ø	★	ø	ø
Improve HVAC Cooling Efficiency by 20%	★★	★★	★★	ø	★	★	ø
Improve HVAC Heating Efficiency by 10%	ø	ø	ø	★	★	★	★★
Double Window Glass & Air Gap Thickness	ø	★	★★	ø	ø	ø	★★★
Improve Window Frame Resistance	ø	ø	ø	ø	ø	ø	ø
Ajust Window SHGC	ø	ø	ø	ø	ø	ø	ø
Shift Setpoint by 1 or 2°C	★★★	★★	ø	★	ø	ø	ø
Widen Setpoint Deadband by 1 or 2°C	★★★	★★★	★★★	★★★	★★	★★★	★★
Change Wall Reflectance within 0.1 to 0.7	★★★	★★★	★	ø	ø	★	★

Note:

1. ESP between 0% and 2% are considered as less effective, marked as ø
2. ESP between 2% and 4% marked as ★
3. ESP between 4% and 8% marked as ★★
4. ESP larger than 8% marked as ★★★

Examination of the analyses presented in the previous sections showed that, for all the four prototype buildings, warmer regions required more cooling energy while colder regions required more heating energy. For the Large Office prototype, the ranking of total yearly energy consumption according to climate zone was (highest to lowest): 1A, 2A, 6A,

5A, 7, 3B, 4C. For the Secondary School prototype, the climate zone energy use order was 6A, 7, 2A, 5A, 1A, 3B, 4C. For the Standalone Retail, the climate zone energy use order was 7, 6A, 5A, 2A, 3B, 1A, 4C. For the Midrise Apartment, the climate zone energy use order was 7, 6A, 5A, 3B, 4C, 2A, 1A. The heating and cooling related energy use roughly followed the same sequence as total yearly energy consumption. It was clear that buildings in 4C required the least energy among the seven climate zones, due to the mild weather in Climate Zone 4C.

Examination of the analyses also showed that the Large Office prototype consumed more energy in warmer climate zones, while the other three investigated prototypes consumed more in colder climate zones. Examination of Figure 3-3 shows that cooling demand of the Large Office prototype exceeded that of the other three prototypes. The surface volume ratio of the Large Office, Secondary School, Standalone Retail, Midrise Apartment prototypes were 0.027, 0.056, 0.076, 0.074, respectively. This suggests that higher surface volume ratio allows for greater heat dissipation and thus lower cooling demand. However, these higher surface volume ratios are not good for heat preservation. Buildings with high surface volume ratio tend to consume more energy in colder climate zones than warmer climate zones, while buildings with low surface volume ratio tend to consume more energy in warmer climate zones.

In general, two types of energy conservation strategies work generally better in colder regions. The first are related to the HVAC systems, such as improving the HVAC heating efficiency or adjusting the HVAC setpoints. The other types of effective (although less so) energy conservation strategies are those designed to alleviate heat dissipation such as increases in insulation, deceases in U factors of windows, etc. In colder regions,

buildings with under insulated roofs need up to 2 times more energy than baseline to maintain the same human comfort level, while buildings with under insulated walls need about 70% more that the baseline. However, many energy conservation strategies work better in buildings in warmer regions, including improving the SHGC of glazing systems increasing wall reflectance, improving lighting efficiency, lighting schedule optimization, and employment of cooling coils with better efficiency. In short, strategies intended to reduce heat generation or heat flow into the indoor environment performed well in warmer regions.

Finally, it was shown that a few strategies work in all climate zones, for example, expanding the deadband width.

In conclusion, to minimize the yearly energy consumption, in colder regions, buildings should be designed to reduce their surface/volume ratio, employ good insulation in building envelopes, and increase deadband width. In warmer regions, buildings should be designed to increase their surface/volume ratio, employ reasonable amounts of insulation, increase deadband width, improve lighting efficiency or reduce lighting demand, and to have improve reflectivity in their envelopes.

3.3. Energy Conservation Leveraging Thermal Mass Effects

Compared to the energy conservation strategies discussed previously, the influence of thermal mass on energy performance of buildings is more difficult to determine. Researchers have proved that thermal mass can help reduce total energy consumption of buildings (Fadejev et al., 2017; Rodrigues et al., 2019). However, thermal mass does not have a proportional impact, that is, “the bigger the better”, is not necessarily true (Fadejev et al., 2017). Many factors may affect the impact of thermal mass on building energy use

including weather patterns, the shape of buildings, thermostat settings, etc. In the previous analysis, the walls were considered to have a rather constant thermal mass. In the analyses presented in this section, the impact of thermal mass on yearly energy consumption was investigated in more detail for the four prototypes over the in the seven Climate Zones using holistic energy modelling.

As analyzed in the previous section, the OpenStudio/EnergyPlus program can conduct a comprehensive analysis of energy flow within typical building systems, across a range of different building prototypes. However, this program does not perform well in the following two aspects: observing the heat transfer through the wall section, analyzing buildings with complex walls. Consequently, MATLAB modeling method was needed. Using the MATLAB models, the relationship of thermal mass and total heat flux through the wall throughout the day can be described.

3.3.1. MATLAB Model Analysis in Typical Summer/Winter Condition

3.3.1.1. Description for MATLAB Thermal Mass Models

MATLAB models of sections of typical exterior mass walls were created to simulate the heat transferred through typical building envelopes constructed of concrete or masonry materials. The energy flow within two types of multilayer mass wall systems were analyzed using this MATLAB model. The first type of wall was an insulated wall system. The typical cross section of this wall type is shown in Figure 3-4, the second was an uninsulated wall system, which was the same as the insulated wall system except that the insulation layer was removed.

Thermal properties of insulation and the structural material (concrete) were shown in Table 3-3, except that to investigate the impact of thermal mass of structural material,

the specific heat was assumed to vary from 560 to 960 to 1360 J/kgK (low, middle or high thermal mass, abbreviated as “LM”, “DM”, “HM”). The assembly U factor was assumed to vary from 2.244 W/m^{2}K (insulated, “Insu”) to 0.290 W/m^{2}K (uninsulated, “Unin”). This analysis can reveal the effect of thermal mass instead of a combination of thermal mass and U factors. These generic wall system models were used to be representative of the typical range of exterior mass walls used in building construction. It should be noted that masonry wall systems are very similar to concrete walls, if grouted solid.

To observe the thermal performance of the wall sections over a wider temperature range, Climate Zone 5A was chosen as a representative of the seven Climate Zones in the U.S., since buildings in Climate Zone 5A have relatively large demand for both heating and cooling. Further, the average high and low temperatures during the summer and winter weather data for Climate Zone 5A were used as peak (high) and valley (low) temperatures of the diurnal curve as described previously in Chapter 3.1.2. These curves are identified as Mild Summer and Mild Winter.

To investigate the performance of the proposed wall sections in extreme weather conditions, the extreme high and low temperature during the summer and winter weather data for Climate Zone 5A were used as peak and valley temperatures of the diurnal curves as ambient temperature conditions. These were identified as Extreme Summer and Extreme Winter. The driving ambient diurnal temperature curves were shown in Figure 3-26. Indoor air temperatures were assumed to be a constant 22 °C. The interior surface of air film was thus set as 22 °C.

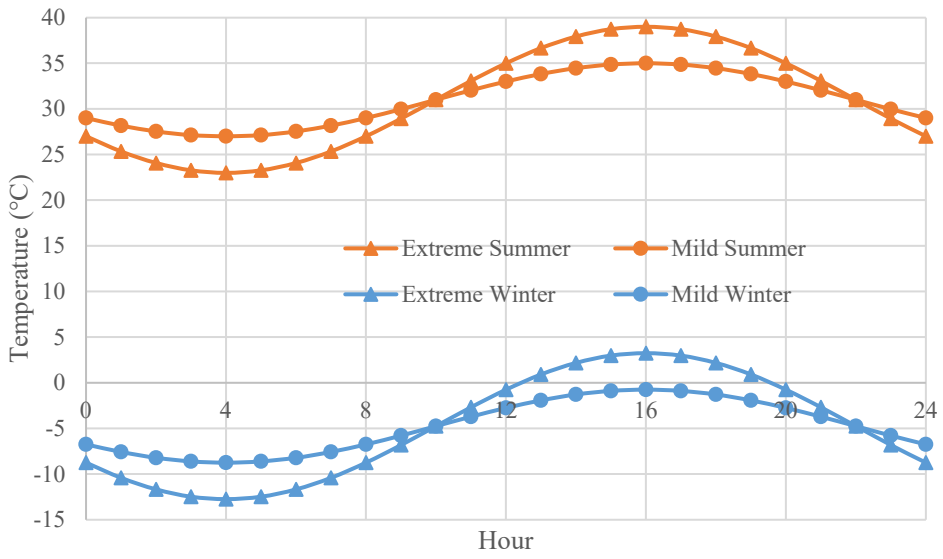

Figure 3-26 Ambient Temperature Conditions Used in the MATLAB Analysis

In the MATLAB model, the temperature response at both the interior and exterior surfaces of the wall assembly were investigated. The difference between temperature at the interior surface of wall and the interior surface of internal air film was used as an indicator of heat flux into the building. The less heat transferred into the building during the summer, the less yearly cooling demand. Similarly, the less heat loss from the building during the winter, the less yearly heating demand.

3.3.1.2. Analytical Results for MATLAB Thermal Mass Models

The surface temperatures predicted by the MATLAB models for the Mild Summer temperature regime were shown in Figure 3-27 and were representative of the four temperature regimes. In this figure, the exterior surface and indoor surface temperatures of the wall assemblies were shown for different material specific heats.

Besides the $T_{in,\,mean}$ etc., the amplitude of T_{in} was defined as T_{AMPL}, and the time delay between peak ambient (exterior) surface temperature and peak interior surface temperature was defined as T_{LAG}. The thermal transmittance (U-factor) of the wall systems

was held constant in this analysis since the impact of U-factor of wall has been studied previously.

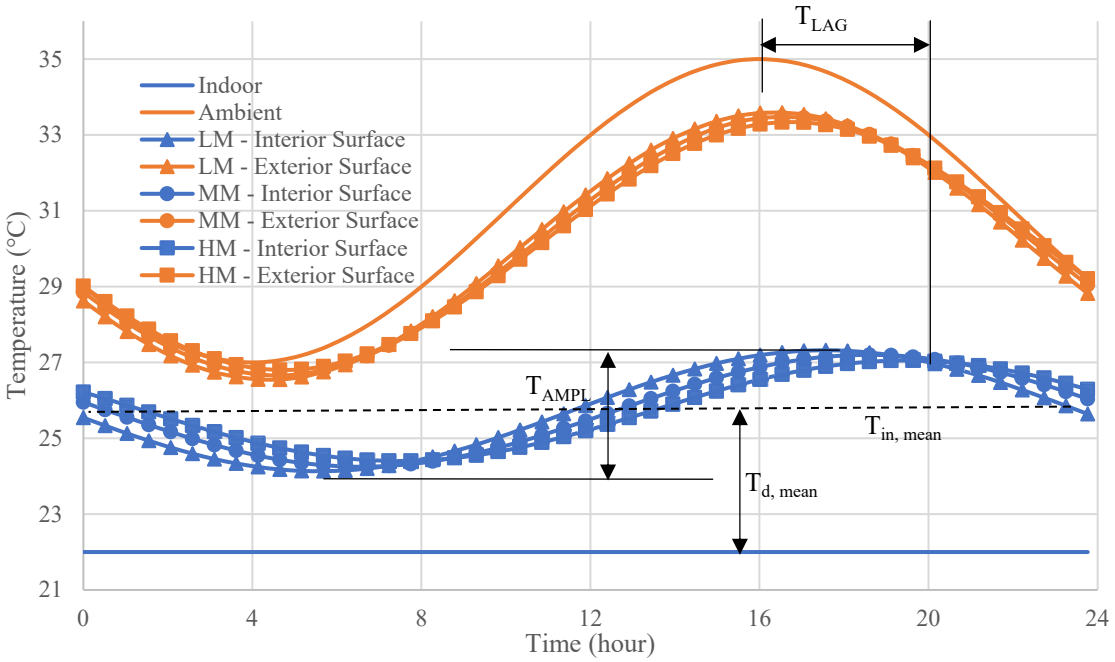

Figure 3-27 Temperature of Wall Surfaces in a Mild Summer Weather with Different Specific Heat for Uninsulated Walls

As can be seen in Figure 3-27, increases in thermal mass (as represented by specific heat) increased the T_{LAG}, and decreased the T_{AMPL} values. However, $T_{in,\ mean}$ and T_d remained almost the same when thermal mass varies. The increase in peak lag will shifted the peak building energy consumption and facilitated use of off-peak energy, but the total heating or cooling energy use remained essentially unchanged.

In the analysis, the indoor temperature was set to a fixed value. In actual building operations, the HVAC system control is operated over a range of temperatures (the deadband). Thus, the interior temperature will not be constant. Furthermore, when interior temperatures are within the deadband range there will be no heating or cooling energy demand. The interior surface temperatures must force the interior ambient beyond the

deadband range to result in heating or cooling. Thus, the variation in interior surface temperature cannot directly be correlated to energy demand. Holistic modeling is needed to define these relationships.

The effect of thermal mass on the delaying peak temperature and reducing the temperature amplitude were shown in Figures 3-28, 3-29, 3-30, and 3-31. Figures 3-28 and 3-29 showed the variation of T_{LAG} with different specific heats defined, for both summer and winter exterior temperature regimes. These figures showed that the delay for peak interior surface temperature increased roughly linearly with increases in thermal mass, at least in the range investigated. It should also be noted that the delay in time were almost identical in winter and summer for a defined wall configuration, and this effect did not vary with insulation thickness. With a proper thermal mass design, the time that the peak temperature occurs on the interior surface of the envelope can be shifted several hours. This later characteristic offers the potential for off peak energy conservation for cooling or heating in off peak demand times.

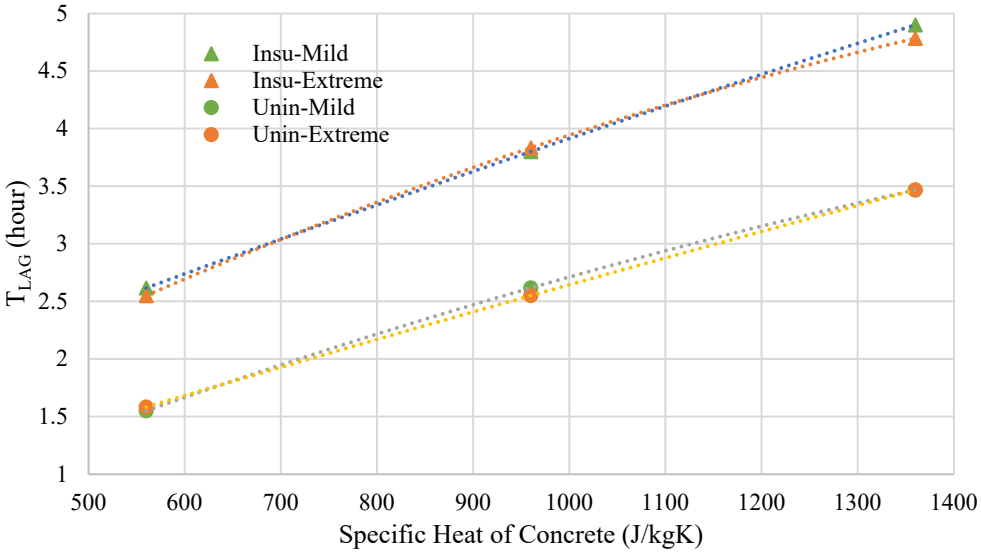

Figure 3-28 Peak Temperature Time Lag with Different Specific Heat Wall in Summer Weather

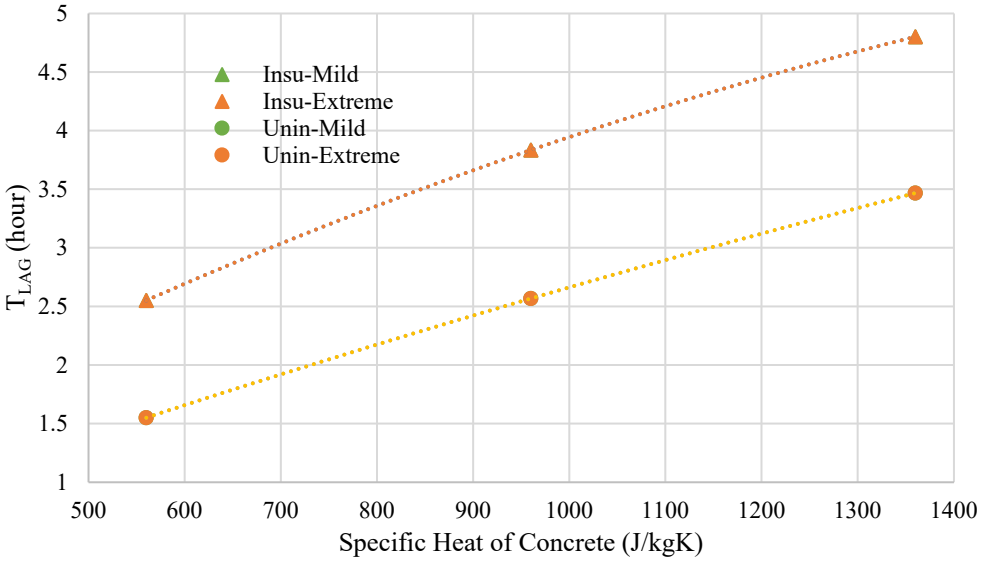

Figure 3-29 Peak Temperature Time Lag with Different Specific Heat Wall in Winter Weather

As mentioned above, these simulations showed no noticeable change (less than 0.3%) in the average temperature of the interior surface of envelope ($T_{in,\ mean}$) as thermal mass varies, for all exterior temperature regimes. Thermal mass appeared not to significantly affect the total energy required for heating or cooling if the indoor temperature is maintained at a fixed value (not within a range). Although, this may not be the case if

the dead band of the HVAC controls are considered. Figure 3-30 and 3-31 showed the amplitude of interior surface temperature of envelope in summer and winter conditions. The graphs showed that, as thermal mass increases, the temperature range at the interior surface becomes smaller. The thermal mass appears to be resisting the change in temperature. In the uninsulated cases, this effect is more significant, which shows the importance of thermal mass when the thermal transmittance (U factor) is high.

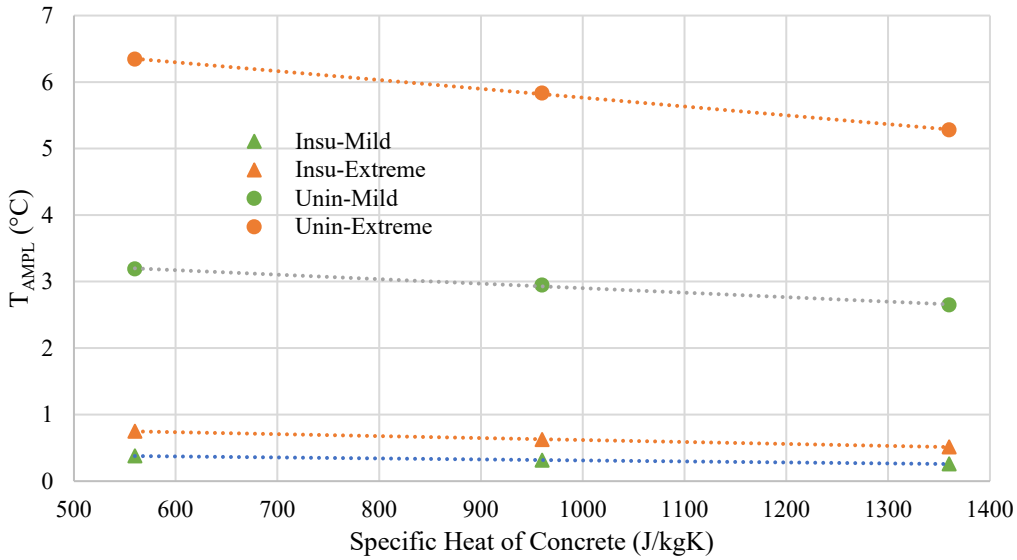

Figure 3-30 Amplitude of Temperature on Interior Surface with Different Specific Heat Wall in Summer Weather

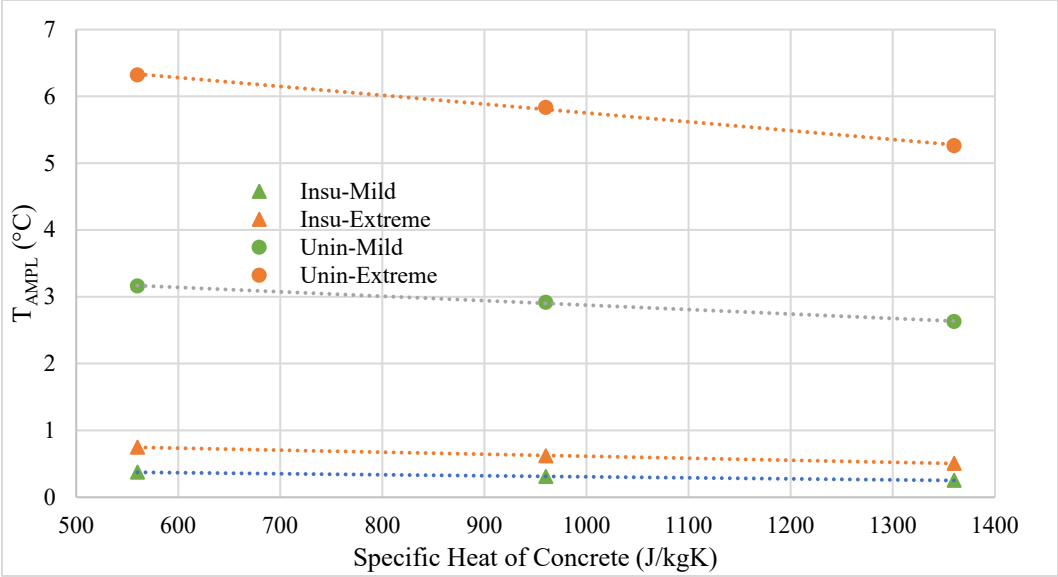

Figure 3-31 Amplitude of Temperature on Interior Surface with Different Specific Heat Wall in Winter Weather

In summary, increases in thermal mass did not affect the $T_{in,\ mean}$ and the $T_{d,\ mean}$, however increases in thermal mass (increases in specific heat) do produced decreases in T_{AMPL} and increases in T_{LAG}. This indicated that higher thermal mass helps decrease the peak demand for cooling or heating and delays the time where peak demand for heating and cooling occurs.

These analyses showed that high thermal mass does have impact on the total heat flux through building envelope. The impact depended on a number of factors including wall assembly U factor, exterior temperature fluctuations and the like. In the next section, OpenStudio models were established to further investigate the influence of thermal mass on yearly energy consumption in seven Climate Zones, using the material response models developed for the mass wall assemblies.

3.3.2. OpenStudio Model Simulation in U.S. Climate Zone Weather Conditions

3.3.2.1. Description for OpenStudio Models that Leverage Thermal Mass

OpenStudio models were created as the baseline configurations of the four prototypes (Large Office, Secondary School, Standalone Retail, Midrise Apartment) as described in Section 3.1.1. To study the impact of thermal mass on buildings, the building envelopes of each building were replaced by several commonly used walls, including a concrete mass wall with different densities. A steel stud wall system was also analyzed with equivalent U values to provide a low mass wall comparison. Densities of the concrete mass walls were taken as 1442 kg/m^3 (90 pcf), or 1922 kg/m^3 (120 pcf), or 2403 kg/m^3 (150 pcf).

Thermal properties of wall materials are listed in Table 3-8. Thermal properties of concrete mass wall were developed based on information in ACI 122R-14 (ACI/TMSCommittee122, 2014). Thermal properties of the lightweight steel stud wall material were developed based on the properties of a steel stud wall assembly with steel studs (6 in.) at a 24 in. spacing and R-19 with R 19 batt insulation ("Building Component Library," 2020). The U factors of the four wall assemblies were adjusted to be the produce prescriptive U factor consistent with each baseline requirement in each climate zone by adding insulation layers for mass walls, respectively, or by changing the conductivity value directly for lightweight steel stud wall.

Table 3-8: Thermal Properties of Exterior Wall Materials

Type of Wall	Aggregate	Conductivity W/mK (Btu·in/hr·ft2·R)	Specific Heat J/gK (Btu/lb·R)

Poured Concrete 90 pcf	Sanded expanded and sintered clay, shale, slate fly ash; sanded pumice, scoria, cinders	0.591 (4.100)	879 (0.210)
Poured Concrete 120 pcf	Limestone	1.139 (7.900)	879 (0.210)
Poured Concrete 150 pcf	Sand and Gravel or Stone	2.149 (14.900)	879 (0.210)
Light weight steel stud wall	-	0.101 (0.699)	670 (0.160)

3.3.2.2. Analytical Results for OpenStudio Models Leverage Thermal Mass

Total energy consumption of the four prototypes: Large Office, Secondary School, Standalone Retail, Midrise Apartment with different wall configurations in the seven Climate Zones were shown in Figures 3-32, 3-33, 3-34, 3-35. Note that the U factors of models with different wall material were the same, however, the thermal mass varied.

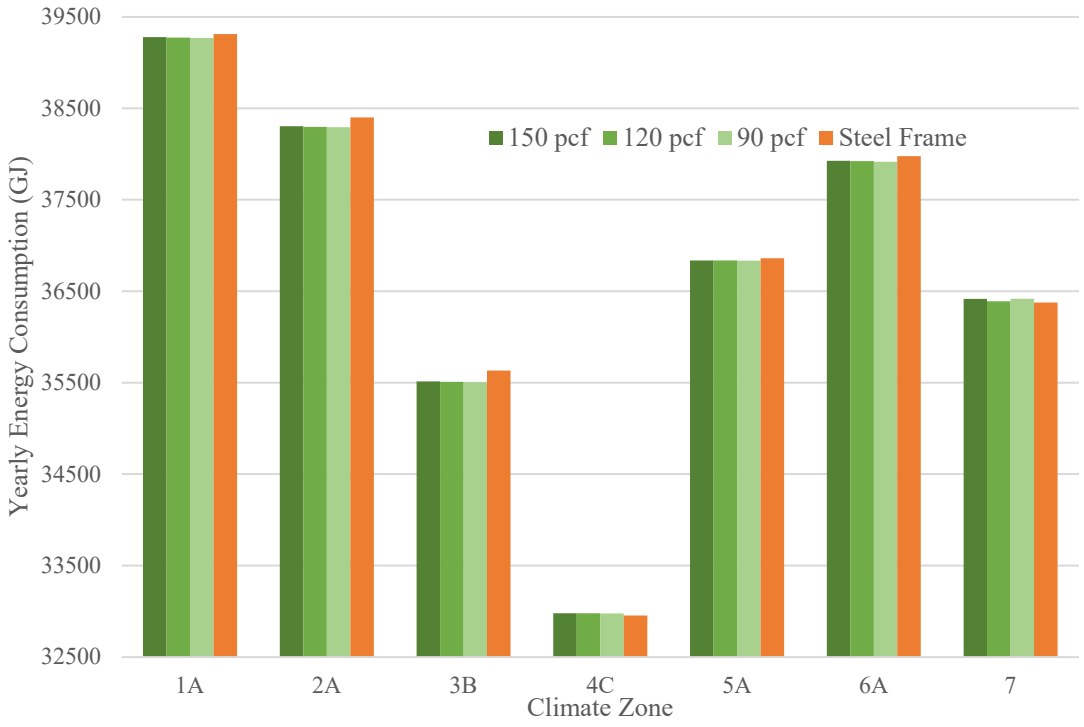

Figure 3-32 Yearly Energy Consumption with Different Wall Configurations (Large Office)

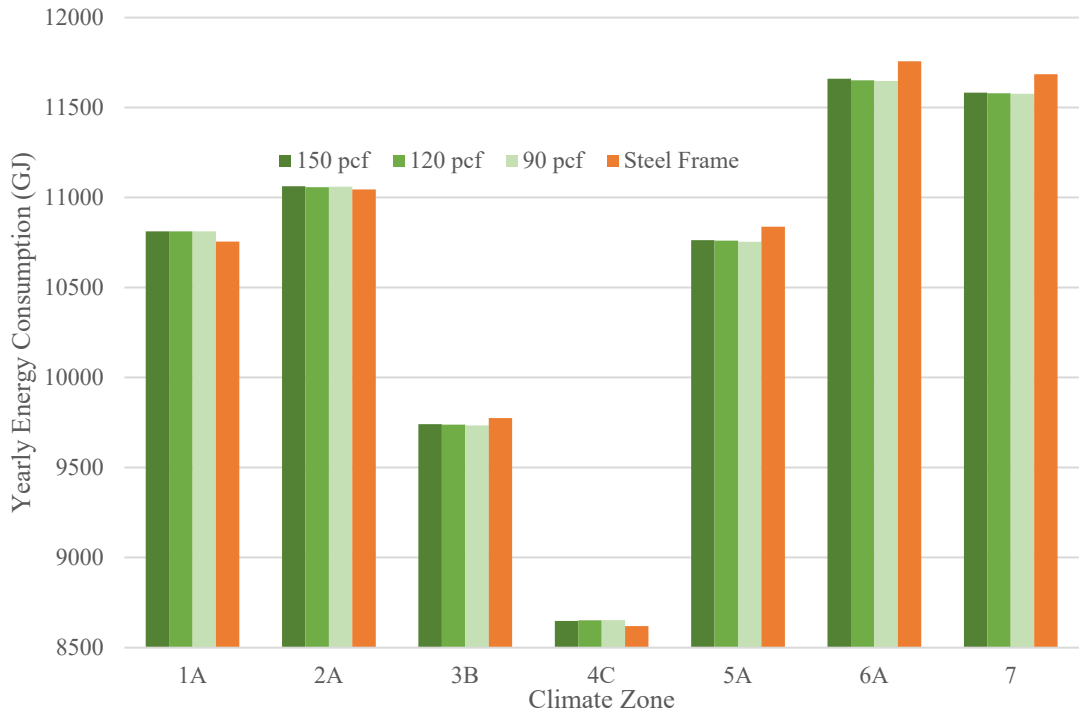

Figure 3-33 Yearly Energy Consumption with Different Wall Configurations (Secondary School)

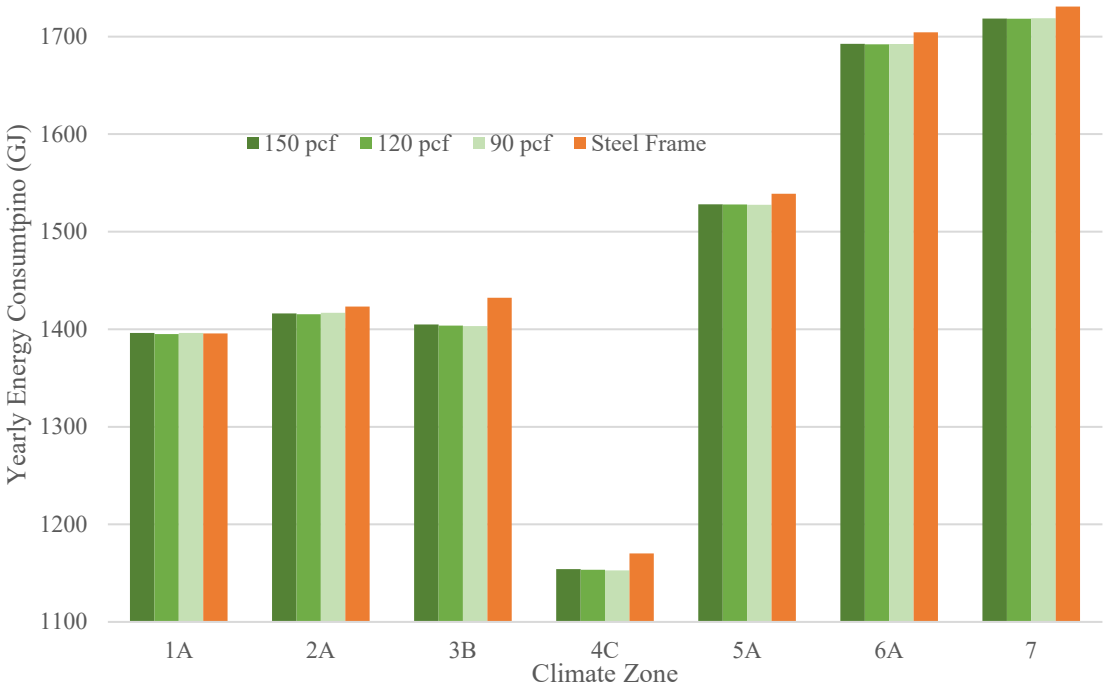

Figure 3-34 Total Energy Consumption with Different Wall Configurations (Standalone Retail)

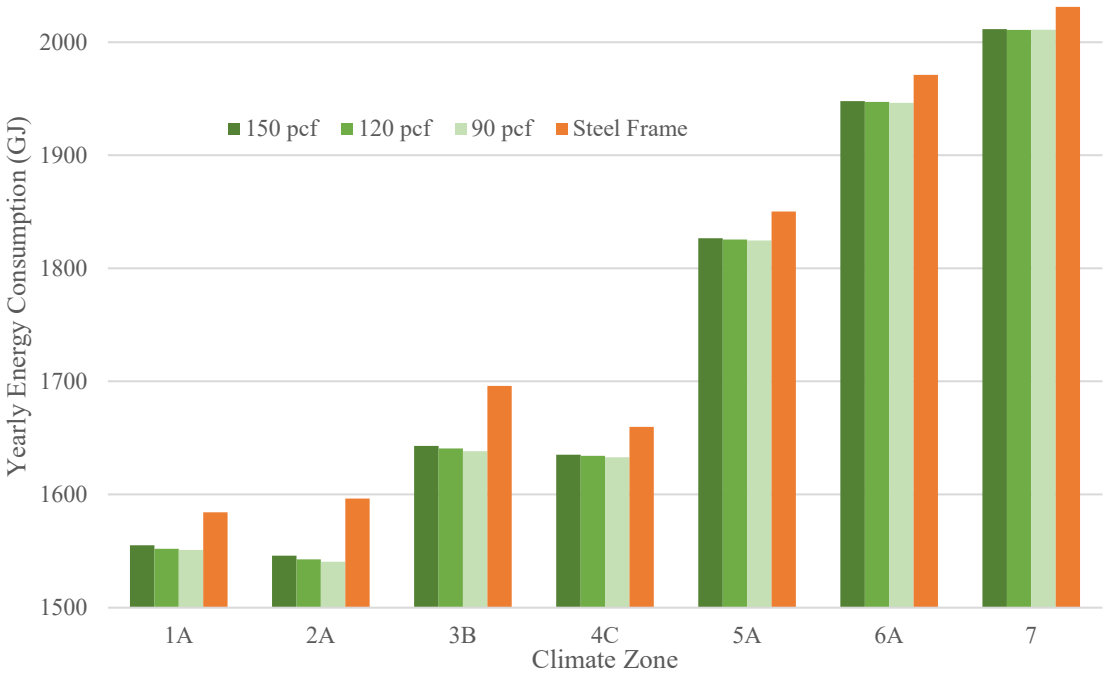

Figure 3-35 Total Energy Consumption with Different Wall Configurations (Midrise Apartment)

As can be seen in Figure 3-32, the influence of thermal mass on energy consumption of the Office building prototytpe varied with Climate Zones. In Climate Zone 1A, 2A, 3B, 5A, 6A, increasing the thermal mass of the exterior walls reduced the energy consumption of the Large Office prototype. In Climate Zones 4C and 7, Large Office buildings constructed with light weight exterior walls consumed the least amount of energy. However, total energy consumption of buildings constructed with different density walls did not change significantly for this building type.

As shown in Figure 3-33, in Climate Zone 3B, 5A, 6A, 7, the use of mass exterior walls reduced the energy consumption in the Secondary School prototype. In Climate Zones 1A, 2A and 4C, the use of mass exterior walls in the Secondary School prototype slightly increased the energy consumption relative to the lightweight steel stud exterior

wall configuration. For mass wall buildings, the density of wall had only a minor effect on total energy consumption, except that in Climate Zone 6A, the difference was around 0.1%, which was the largest percentage difference for the seven Climate Zones.

As can be seen from Figure 3-34, for the Standalone Retail prototype, energy consumption for the mass exterior wall configurations was always lower than the exterior stud wall configuration, except in Climate Zone 1A. For mass wall buildings, total energy consumption of buildings with different density walls did not change significantly and the difference in energy consumption in any case was not large.

As can be seen in Figure 3-35, for Midrise Apartment prototype, higher mass exterior walls significantly reduced energy use when compared to light weight study walls However, lower density mass walls were slightly better than higher density mass walls with respect to reducing building energy consumption.

The analyses also showed that in most Climate Zones, the four prototype buildings with mass wall envelopes consumed less energy over the year than the baseline configurations with exterior light weight steel stud walls (with the same U-factors). The exceptions for this were: the Large Office prototype in Climate Zones 4C and 7, and the Secondary School prototype in Climate Zones 1A, 2A and 4C. The analysis clearly shows that small buildings like the Standalone Retail and Midrise Apartment prototypes should employ mass walls instead of light-weight steel stud walls, in all climates. For large buildings like the Large Office and Secondary School prototypes, light-weight steel stud walls in some Climate Zones may use slightly less energy.

The Energyplus/OpenStudio model analyses also suggested that wall density (or thermal mass) of mass walls has limited impact on total yearly energy consumption. However, in most cases, an exterior mass walls with lower thermal mass may use slightly less energy than other configurations. Moreover, as the conductivity of concrete increases with the increase of density, high thermal mass walls will have higher the U factors, thus thicker insulation is needed to make the wall assembly code compliant. This will increase initial cost. In most cases, lower density mass walls perform better than higher ones, except for the Large Office prototype in Climate Zone 4C and 7, the Secondary School prototype in Climate Zone 4C, the Standalone Retail prototype in Climate Zone 1A, 2A, 6A and 7, the Midrise Apartment prototype in Climate Zone 7.

3.3.3. Results and Discussion

The Energyplus/OpenStudio building energy analysis and MATLAB analysis energy movement analysis illustrated the effects of thermal mass in two different ways. As we concluded earlier, the MATLAB simulation proved that the increase in thermal mass reduced the T_{AMPL} and barely impact the T_d value. The OpenStudio/EnergyPlus simulations revealed that mass walls were generally more efficient in saving building energy consumption than light weight steel stud walls, although mass walls with lower density performed slight better than those with higher density. However, the research results did not provide clear trend as there were conditions where light weight steel stud walls performed better than mass walls. The impact of thermal mass on building energy consumption appears to depend on a number of factors including weather conditions, thermostat settings, exterior wall U factor, and internal loads.

Since the MATLAB model showed that increases in thermal mass decreases the T_{AMPL}, many may assume that it would reduce peak energy consumption. However, EnergyPlus/OpenStudio model results showed that buildings with higher mass walls sometimes had higher peak demand for heating and cooling. For example, the peak electricity demand for Large Office prototype in Climate Zone 1A with 90 pcf, 120 pcf, 150 pcf concrete wall was 1845.5 kW, 1846.0 kW and 1846.5 kW, respectively. This result indicates that that the perception that high thermal mass is always good may not always true.

In addition, the MATLAB models evaluated thermal energy flow through the exterior wall cross section over a 24-hour period, under ideal conditions. Furthermore, in MATLAB modelling, room temperature was set to a constant value with no tolerances or range, with ambient temperature assumed to be a cyclic sine curve. The OpenStudio models, on the other hand, evaluated holistically energy use in the building throughout the year, using actual weather files based on realistic weather conditions in specific regions. In addition, these models define interior loads and temperature swings use schedules. These additional energy flows often dominate the energy flows through the exterior walls and thus made the more simplistic MATLAB models less accurate when these flows dominated the building behavior.

It is recommended that holistic energy analyses be used to determine building energy consumption when determining the impacts of thermal mass in building envelopes. In addition, further research is needed in the economics of thermal mass application. MATLAB simulations proved the ability of thermal mass walls to shift peak energy

demand times. However, the energy use impact and cost implications must be researched further.

3.4. Active Thermal Insulation Wall Systems in Typical Summer/Winter Condition

In this research, the performance of a novel composite energy conservation strategy (active thermal mass/insulation wall system) was investigated in addition to the conventional energy conservation strategies studied previously. The active thermal mass/insulation wall system uses a pipe system that circulates heating or cooling fluid within the wall. This configuration is intended engage the thermal mass of the wall and possibly couple the walls to ground heat or solar heat, thus achieving more efficient building heating and cooling.

3.4.1. Model Descriptions of Active Thermal Insulation (Mass) Wall System and Four Conventional Wall Systems

To evaluate the performance of active thermal insulation (mass) wall system, the author simulated the thermal performance of ATIWS and four types of conventional grouted masonry assembly configurations. These models were analyzed under typical summer and winter temperature regimes to observe their energy conservation potentials. The Mild Summer and Mild Winter temperature conditions shown in Figure 3-26 were used as the ambient temperature conditions for the analysis. The indoor temperature conditions (indoor set point) were set to 22°C, unless stated otherwise.

The proposed four conventional wall configurations included: a solid grouted CMU wall, a grouted CMU wall with an air gap in the cells, a grouted CMU wall with rigid insulation insert in the cells, and a grouted CMU wall with rigid reflective insulation insert in the cells (see Figures 3-36, 3-37, 3-38, 3-39).

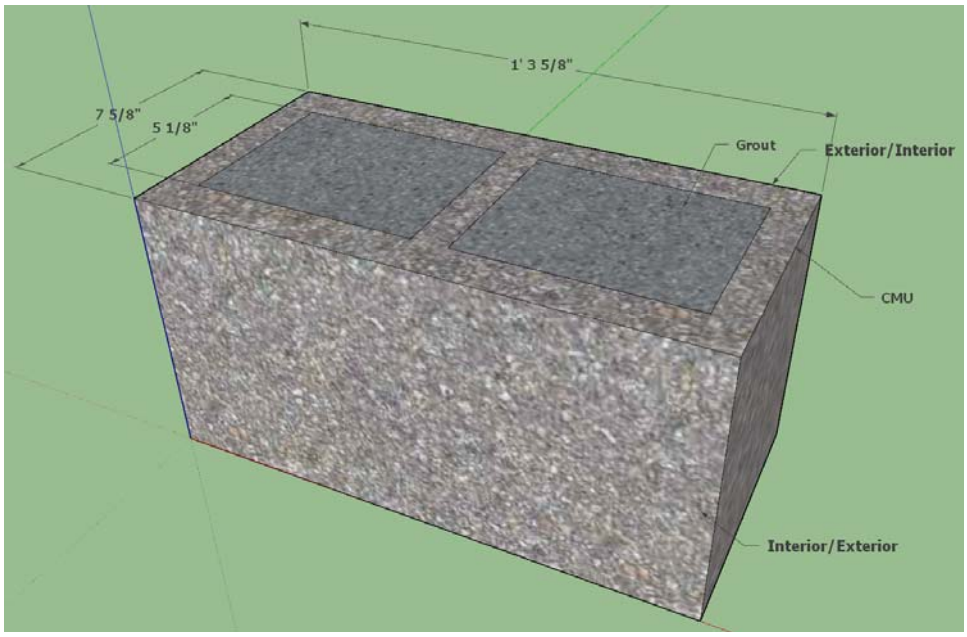

Figure 3-36 Solid Grouted CMU Wall

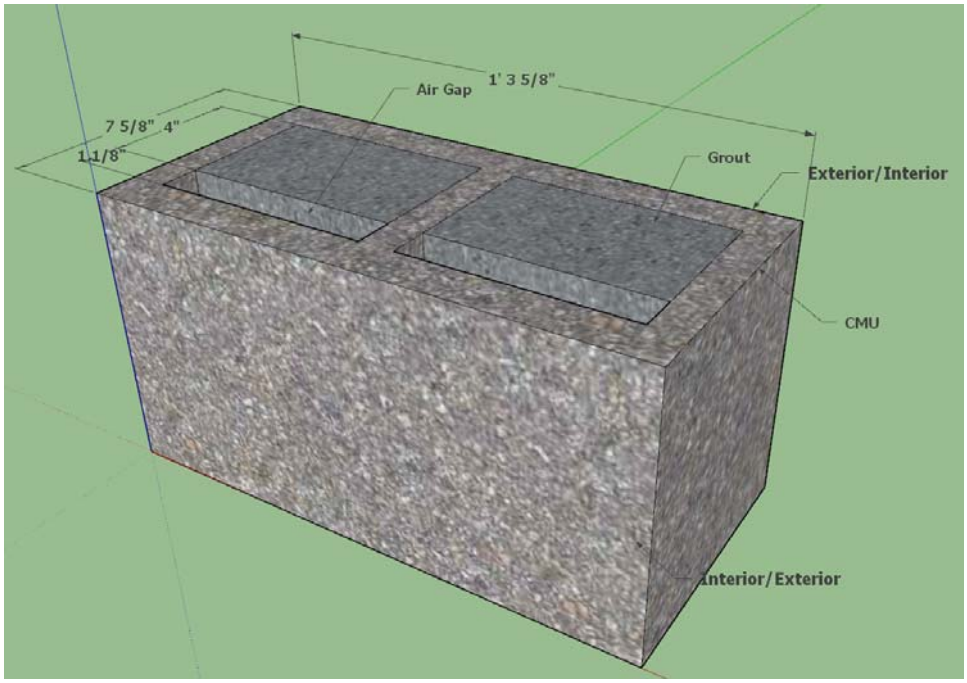

Figure 3-37 Grouted CMU Wall with Air Gap

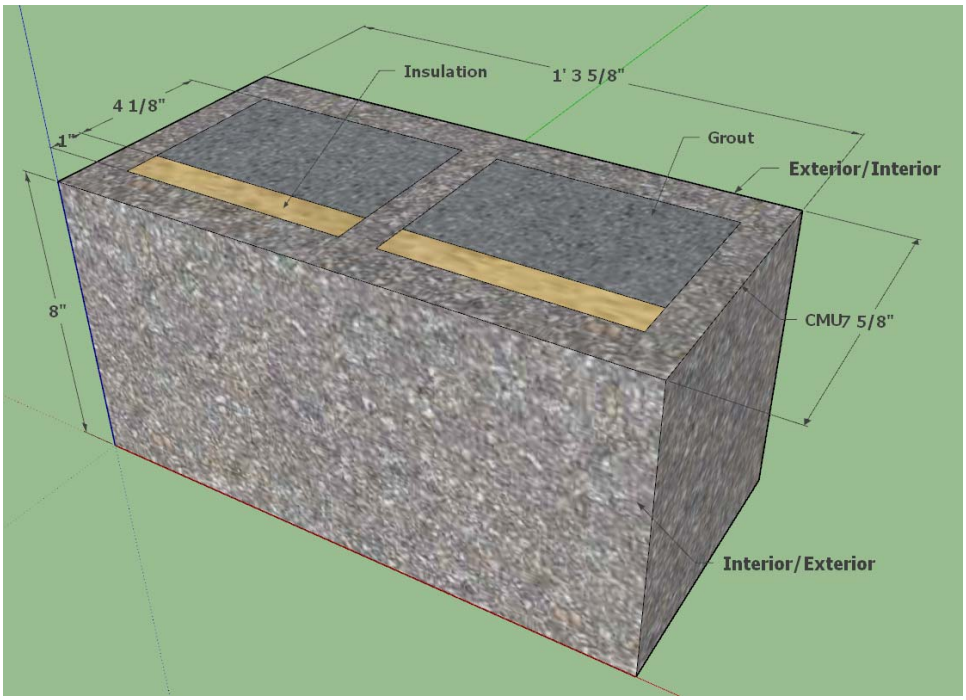

Figure 3-38 Grouted CMU Wall with Rigid Insulation Insert

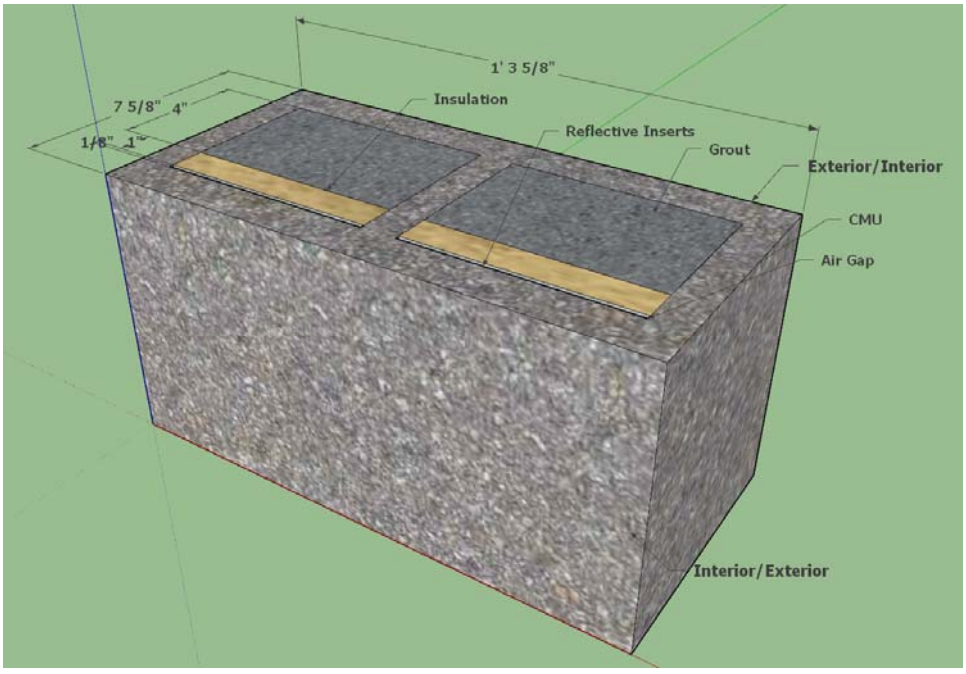

Figure 3-39 Grouted CMU Wall with Rigid Reflective Insulation Insert

The proposed active thermal insulation wall model was shown in Figure 3-40. In the first phase of analysis, the width of wall section (pipe spacing) was assumed to be 16

inches (0.4064 m). To evaluate pipe location effects, the distribution pipe was located in three possible locations: near the exterior ("NE") side of the grouted cell wall, at the middle ("M") of the grouted cell and near the interior ("NI") side of the grouted cell wall. The analysis of the active thermal insulation (mass) wall sections with different fluid temperatures, indoor temperatures and summer and winter temperature regimes were conducted. The optimum pipe location was determined from these analyses.

The impact of pipe spacing and fluid temperature were also evaluated. The active thermal insulation (mass) models were assumed to be uninsulated (zero insulation thickness). It was noted that if insulation was utilized, the temperature dispersion of the wall sample would be over a rather small temperature range, thus not conducive to measurement and lead to a larger measurement error. Furthermore, the ATIWS was intended to replace traditional wall insulation.

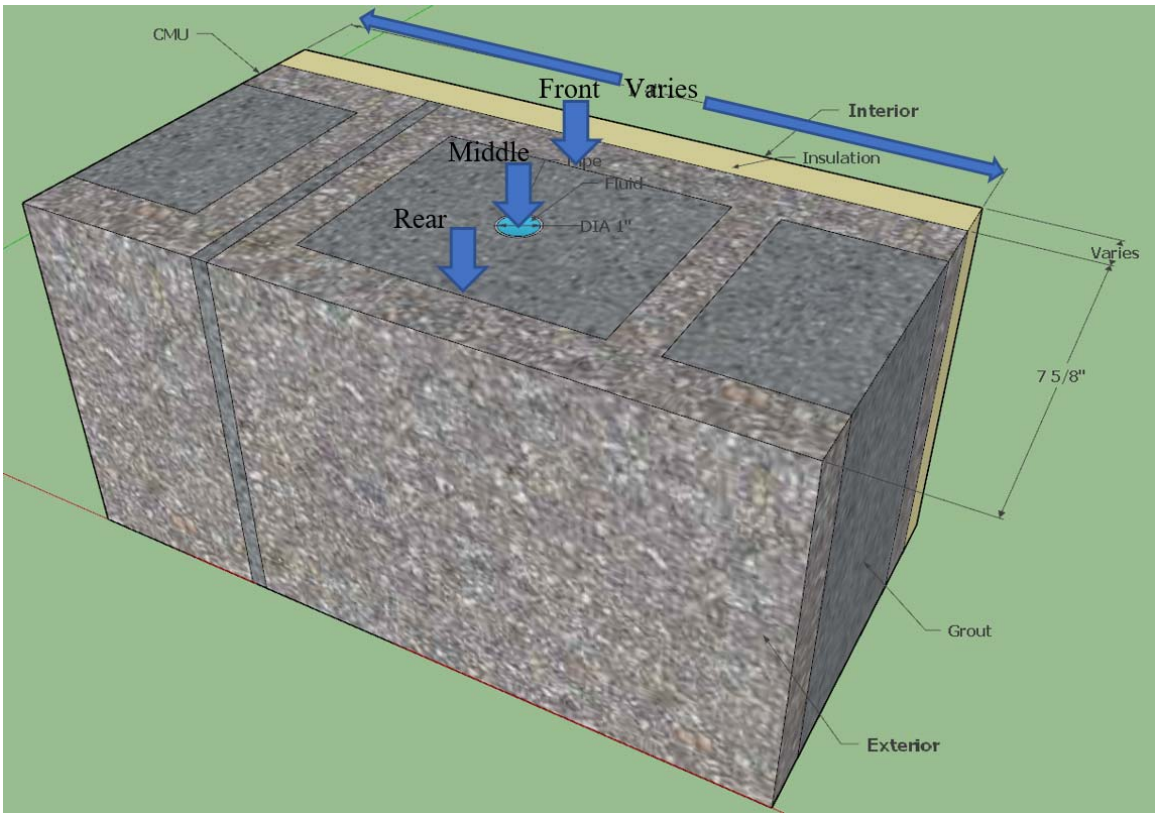

Figure 3-40 General Active Thermal Insulation (mass) Wall Model

MATLAB models were developed for each wall assembly configuration shown in Figures 3-36 through 40 with variable widths (spacing) and no insulation. Details of the models are presented Chapter 3.1.2.

3.4.2. Analytical Results of the Conventional Wall System

The results of analyses of the solid grouted wall in summer were shown in Figure 3-41 and it are representative of all four of the proposed conventional wall system configurations. The average temperature of the two surfaces (interior and exterior surface of CMU), the indoor temperature, and the ambient temperature, were plotted for the 24-hour period. By comparing the difference of the interior surface temperature to the interior

temperature curve (T_d), the effective insulating ability of these wall systems can be evaluated.

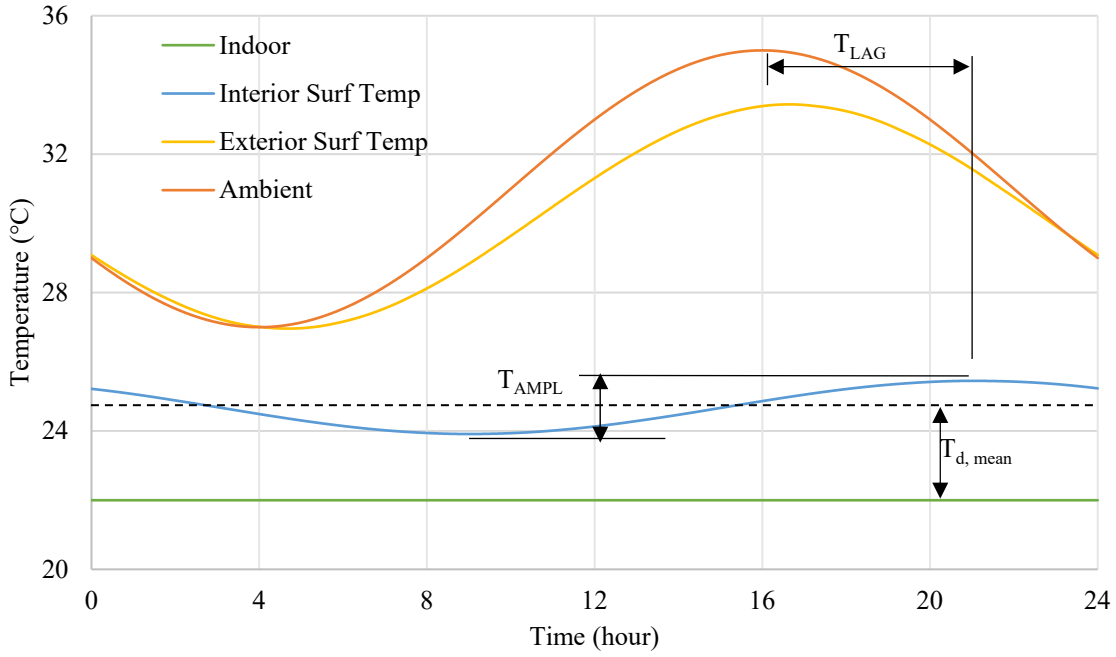

Figure 3-41 Temperature of CMU Surfaces (Solid Grouted)

T_d, the difference between average temperature at interior surface of the CMU and the indoor temperature of the four conventional wall systems were shown in Figure 3-42 and 3-43. This temperature difference determines the heat flux drive to and from the interior space and thus is proportional to the heating or cooling energy demand of the space. Lower T_d means results in lower heating or cooling demand. These figures showed that solid grouted walls have the highest T_d and thus the greatest heat flux (loss) through the walls. The rest of four conventional wall configurations performed in a similar manner. The present of a reflective insulation insert did not show any significant advantage either in summer or winter conditions when compared to a rigid insulation insert alone. This indicated that a reflective middle layer in the wall configuration has limited impact on the

thermal performances. The T_{LAG} value of solid grouted wall was slightly lower than the other three, indicate that U factor of walls impact the T_{LAG} value as well.

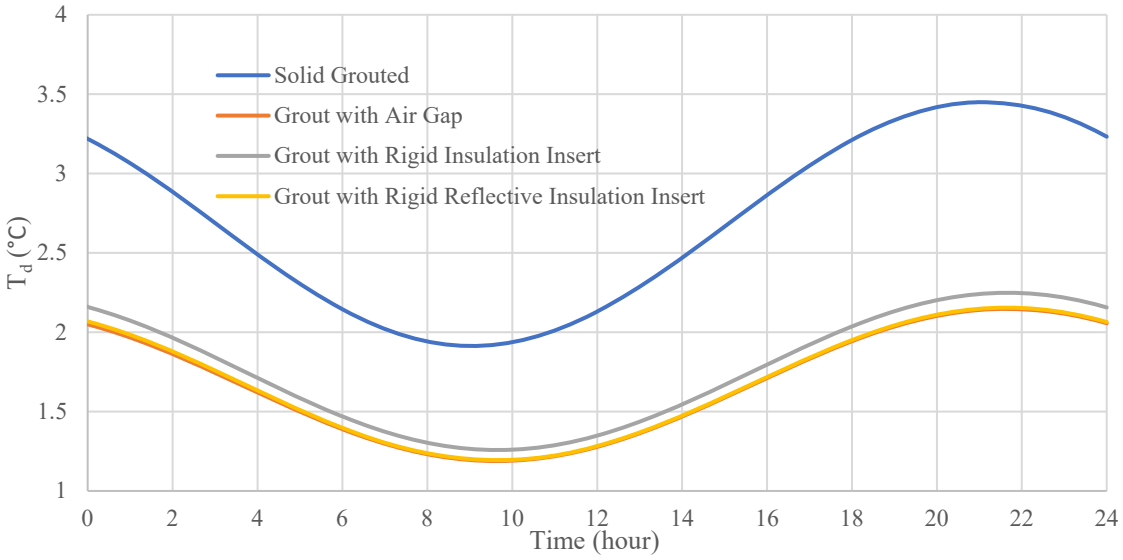

Figure 3-42 T_d of the Four Conventional Walls in Summer

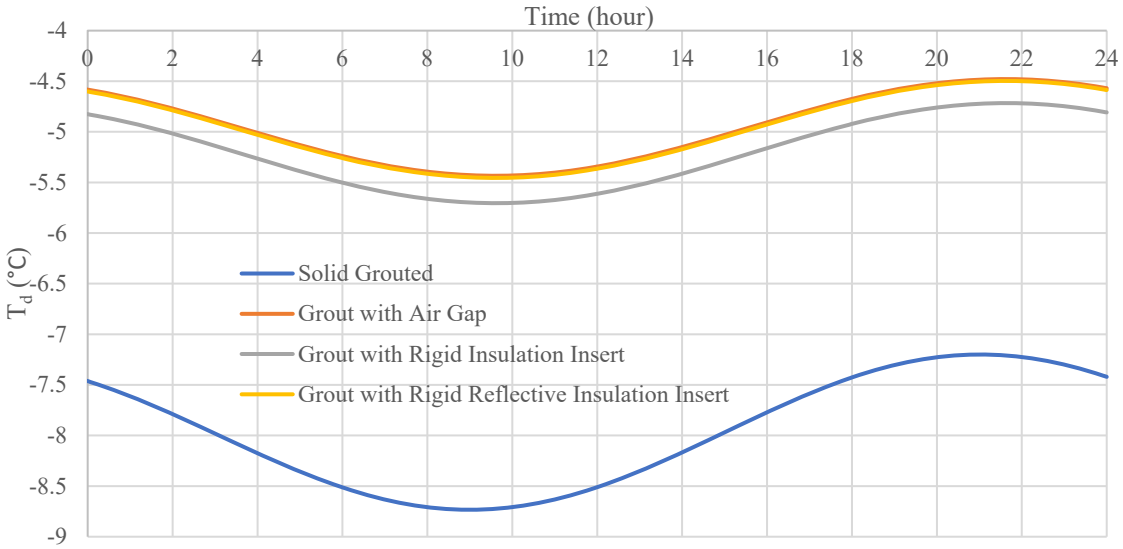

Figure 3-43 T_d of the Four Conventional Walls in Winter

In this analysis, the performance of the "Grout with Air Gap" wall and "Grout with Rigid Reflective Insulation Insert" were almost identical. However, further study is needed

to verify this result. In this analytical model, the air cavity was treated as a solid with the thermal properties of air, resulted in neglecting the convection in the air cavity, and likely resulting in less accurate results. In fact, the thermal performance of walls with air cavity is likely not as good as shown.

3.4.3. Analytical Results of Fixed Spacing ATIWS

The simulation matrix for the fixed width (16-inch) ATIWS simulations are shown in Table 3-9. The measured thermal performance of the active wall systems with pipes at 16-inch spacing, with the indoor temperature held at 22°C or 24°C in Mild Summer and Mild Winter as shown in Figure 3-26. For the convenience of discussion, each test was numbered and named.

Table 3-9: Simulation Matrix for 16-inch Active Thermal Insulation Wall

No.	Weather	Indoor Temperature (°C)	Pipe Location	Fluid Temperature (°C)	Designation
1_1	Summer	22	Near Interior (NI)	16	S_22_16_NI_Fluid16
1_2		22	NI	22	S_22_16_NI_Fluid22
1_3		22	NI	28	S_22_16_NI_Fluid28
1_4		22	Middle (M)	16	S_22_16_M_Fluid16
1_5		22	M	22	S_22_16_M_Fluid22
1_6		22	M	28	S_22_16_M_Fluid28
1_7		22	Near Exterior (NE)	16	S_22_16_NE_Fluid16
1_8		22	NE	22	S_22_16_NE_Fluid22
1_9		22	NE	28	S_22_16_NE_Fluid28
1_10		24	NI	16	S_24_16_NI_Fluid16
1_11		24	NI	22	S_24_16_NI_Fluid22
1_12		24	NI	28	S_24_16_NI_Fluid28
1_13		24	M	16	S_24_16_M_Fluid16
1_14		24	M	22	S_24_16_M_Fluid22
1_15		24	M	28	S_24_16_M_Fluid28
1_16		24	NE	16	S_24_16_NE_Fluid16
1_17		24	NE	22	S_24_16_NE_Fluid22
1_18		24	NE	28	S_24_16_NE_Fluid28

1_19		22	NI	16	W_22_16_NI_Fluid16
1_20		22	NI	22	W_22_16_NI_Fluid22
1_21		22	NI	28	W_22_16_NI_Fluid28
1_22		22	M	16	W_22_16_M_Fluid16
1_23		22	M	22	W_22_16_M_Fluid22
1_24		22	M	28	W_22_16_M_Fluid28
1_25		22	NE	16	W_22_16_NE_Fluid16
1_26		22	NE	22	W_22_16_NE_Fluid22
1_27	Winter	22	NE	28	W_22_16_NE_Fluid28
1_28		24	NI	16	W_24_16_NI_Fluid16
1_29		24	NI	22	W_24_16_NI_Fluid22
1_30		24	NI	28	W_24_16_NI_Fluid28
1_31		24	M	16	W_24_16_M_Fluid16
1_32		24	M	22	W_24_16_M_Fluid22
1_33		24	M	28	W_24_16_M_Fluid28
1_34		24	NE	16	W_24_16_NE_Fluid16
1_35		24	NE	22	W_24_16_NE_Fluid22
1_36		24	NE	28	W_24_16_NE_Fluid28

Note: the first term stands for the Summer by “S” or Winter by “W”, the second term stands for the room temperature, the third term stands for the pipe spacing, the fourth term indicates the pipe location, “NE” for near exterior, “NI” for near interior, “M” for middle, the fifth term stands for the fluid temperature.

Figure 3-44 shows the typical isotherm determined from of the model output for simulation No. 1-5, at Time=16.3 hours. This example is similar to the results from the other simulations. In this figure, the impact of the circulation pipes can be clearly observed. The relatively low temperature fluid in pipes reduced the temperature around the pipe, thereby reducing the heat energy transfer between the interior and the exterior of this section of wall.

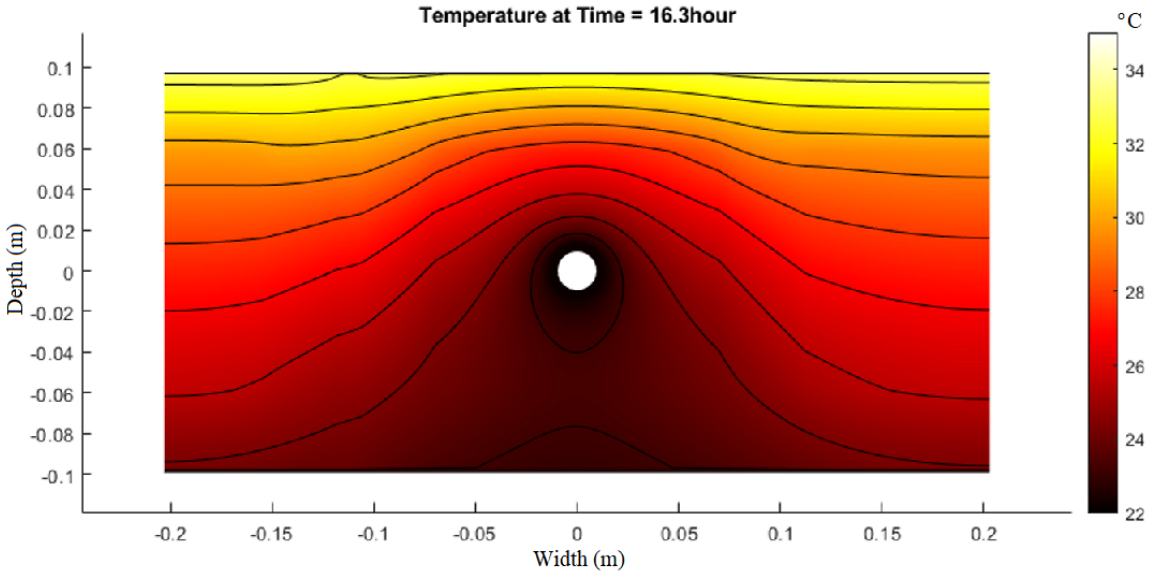

Figure 3-44 Isotherm at Time=16.3h of ATIWS Simulation No. 1-5

Figure 3-45 showed the average temperature on surfaces determined from simulations No.1-4, 1-5 and 1-6. These responses are representative of the range of the responses of all the wall configuration models. The average surface temperature of these varied wall configurations were shown in Figure 3-45. The average interior surface temperature of the wall varied significantly when the circulation fluid temperature changed.

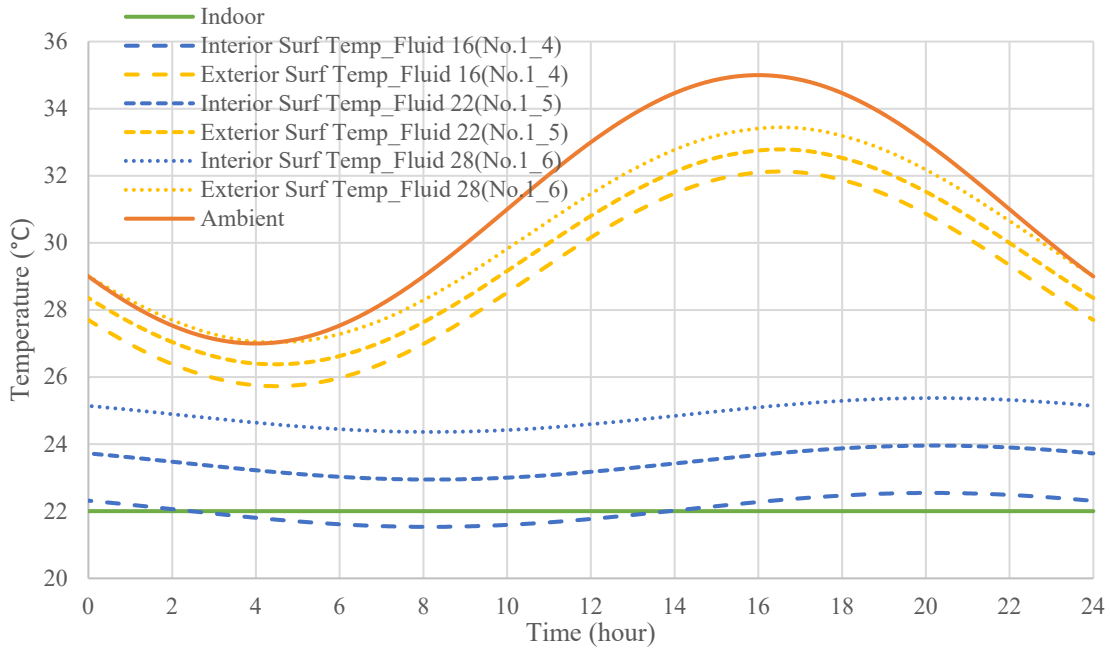

Figure 3-45 Temperature Response at Surfaces of ATIWS, Pipe at Middle, Pipe Spacing16 inches, Summer

As stated previously, the temperature difference between interior surface of wall and indoor temperature (T_d) is proportional to the heat loss and gain through the walls. The relationships between T_d and other factors like fluid temperature, pipe spacing, pipe location were similar to the relationships between those factors and heat flux through the walls. These relationships were evaluated in the following analyses. Figure 3-46 presented the T_d curves of simulations No. 1_1 through 1_9.

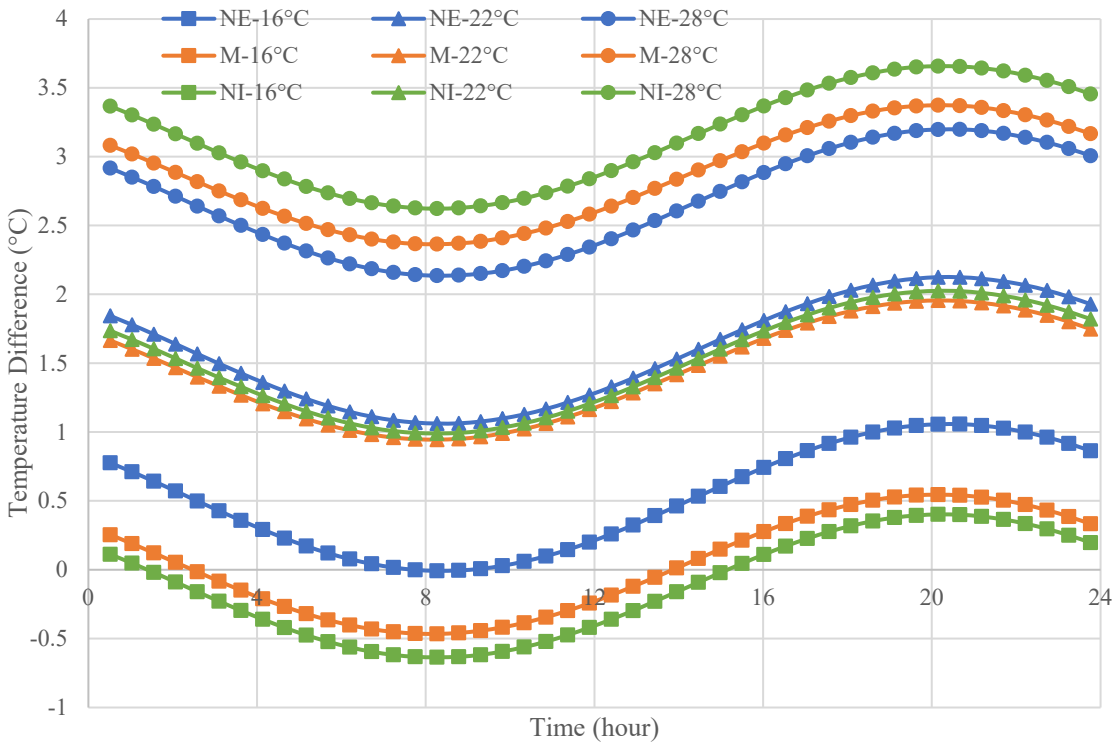

Figure 3-46 T_d Response of Simulations No 1_1 to 1_9 (Summer, Indoor 22°C, 16 inches Spacing)

The factors derived from the T_d curves include $T_{d,\,mean}$, T_{AMPL} and T_{LAG}. The temperature response (T_d) results in Figure 3-46 show that the variation of fluid temperature hardly affected the T_{LAG} value. Thus, T_d curves for each simulation were not plotted. Instead, the $T_{d,\,mean}$ value was used to represent the temperature response curves of interior surfaces, thus the thermal flow impact of each system. The T_{LAG} value of the ATIWS configurations are similar to the other solid grouted wall configuration. The T_{LAG} value shows the ability of wall assembly to shift the time that HVAC energy consumption will begin. A higher T_{LAG} value indicated a significant shift in peak energy demand. The variation in fluid temperature did not change the total thermal mass of the wall assembly, it can be shown that the change in circulation speed of fluid would affect the T_{LAG} value, however, this influence would be minor. Therefore, the embedded pipes have very limited

impact on the peak energy consumption times. However, the author infers that for lightweight walls (e.g., wood stud wall, steel frame wall), the embedded pipe system would have considerable positive impact on peak demand times, although further research on this needs to be done.

Simulated $T_{d, mean}$ results were shown in Figure 3-47. Note that this quantity is the temperature difference between the indoor set point and interior surface of wall, and thus represents the driving demand/load of HVAC systems. The closer the $T_{d, mean}$ was to zero, the lower energy demand for heating or cooling.

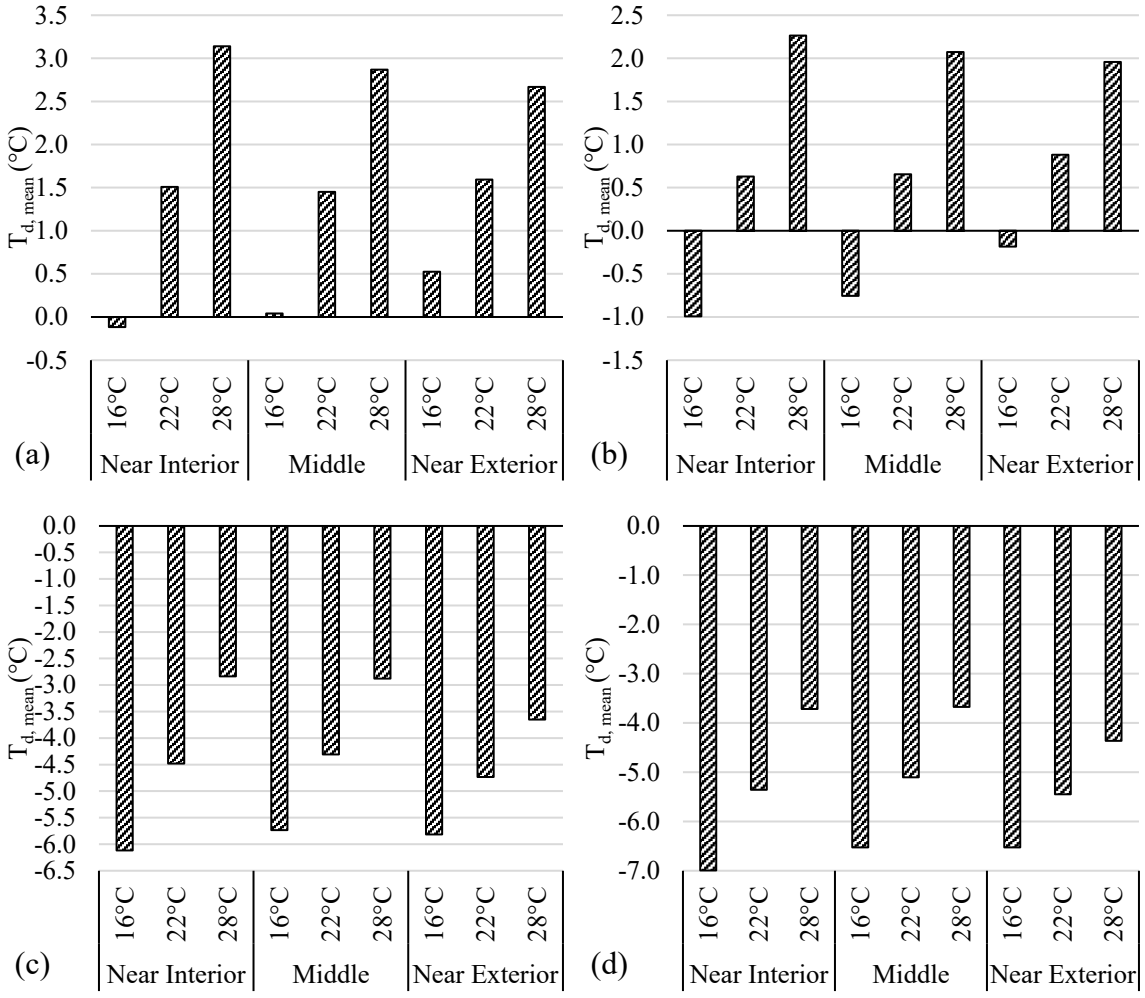

Figure 3-47 $T_{d,\,mean}$ with Variable Pipe Location and Fluid Temperature of 16-inch Pipe Spacing in (a) Summer Set Point 22°C; (b) Summer Set Point 24°C; (c) Winter Set Point 22°C; (d) Winter Set Point 24°C

The impact of fluid temperature on $T_{d,\,mean}$ was roughly linear for both summer and winter conditions. Due to the need to evaluate the performance of ATIWS DX systems, the fluid temperature was often lower than 28°C. The analysis showed that for an equivalent to code compliant performance in winter, the fluid temperature should be at around 40°C, way higher than the simulated temperature (28°C).

In summer, when fluid temperature was 16°C (lower than indoor set point), the near-interior-located pipes had greatest impact on the $T_{d,\,mean}$, although the middle-located pipes had a comparable performance. The performance of near-exterior-located pipes was appeared to be less effective than the other two pipe locations; when fluid temperature was 22°C (close to indoor set point), the results was similar to the other pipe locations; when fluid temperature was 28°C (higher than indoor set point), the near-exterior-located pipes resulted in the lowest $T_{d,\,mean}$ value. Note that the near-interior-located pipes resulted in a highest $T_{d,\,mean}$ values while the middle-located pipes typical resulted in thermal performance in between the other two locations. Moreover, overcooling was found in some cases. This suggests that the pipe systems could overheat or overcool the indoor environment when fluid temperature was not carefully controlled. In winter, except for the fact that no overheating occurred in the temperature range studied, the simulated performance was similar.

In general, the performance of near-interior-located pipes and middle-located pipes were similar, however, middle-located pipes showed a larger tolerance interval and thus would likely have fewer chances of overcooling than a near-interior-located pipe. In cold

regions where heating load dominates, it appears that it would be best to locate the pipes near interior because the near-interior-pipes perform slightly better than middle-located pipes, and overheating is a rare phenomenon and the impact is minor.

In colder regions like Climate Zone 6A and 7, heating demands are significantly larger than cooling demand. While in warmer regions like Climate Zone 1A, 2A and 3B, cooling demand dominates. In Climate Zone 4C and 5A, the demands for both heating and cooling are high. Therefore, in Climate Zone 1A, 2A and 3B, pipes may be located at the front side (close to the interior) or middle of the wall. In other Climate Zones, pipes should be located at middle layer of the wall. In this research, for the simplicity of simulation later in Chapter 5, pipes are assumed to located at middle.

3.4.4. Analytical Results of Variable Spacing ATIWS

MATLAB simulations of ATIWS in the Mild Summer (fluid temperature 16°C and indoor set point 24°C) and in the Mild Winter (fluid temperature 16°C and indoor set pint 22°C) with various pipe spacing were conducted to investigate the relationship between pipe spacing and the $T_{d,\ mean}$ values. The Mild Summer and Mild Winter temperature conditions were defined in Figure 3-26. The results were shown in Figure 3-48. Performance of uninsulated solid grouted walls were shown as straight dash lines as references. The results showed that larger pipe spacing led to lower impacts on $T_{d,\ mean}$. In the summer, overcooling occurred when pipe spacing was less than about 22 inches (0.559 m), the change in $T_{d,\ mean}$ value was significantly less when spacing was moved above 25 inches (0.635 m), both in summer and winter. The analyses also showed that the $T_{d,\ mean}$ value slowly approached the control (solid grouted, the straight dash line) with the increase of pipe spacing.

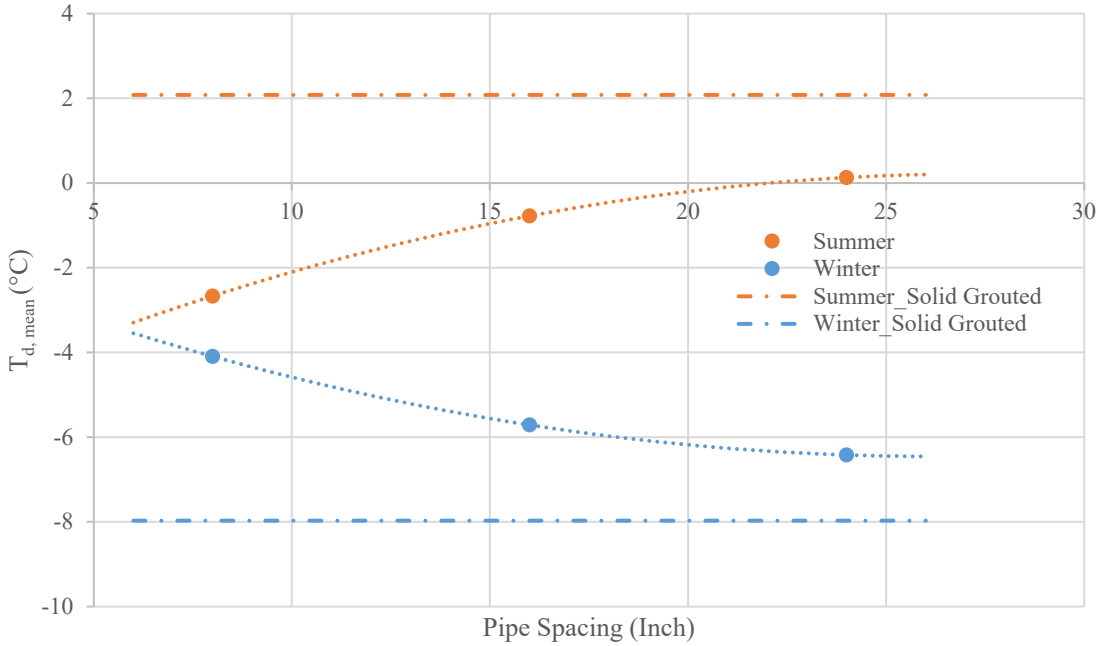

Figure 3-48 $T_{d,\,mean}$ VS. Pipe Spacing (Fluid Temperature 16°C, Indoor 24°C in Summer, Indoor 22°C in Winter)

3.4.5. Discussion

The pipe system showed significant reduction in the heat flux moving through the building envelope. Generally, pipes should be located at center, since middle-located pipes had a comparable thermal performance with interior side-located pipes, and will not cause overheating or overcooling. The pipes will hardly affect the heat flux beyond 12 inches (0.3048 m) from the pipe center. This distance is affected by the thermal property of concrete and the pipe. Therefore, for mass walls, pipe should be spaced from 16 to 24 inches (0.4064 ~ 0.6096 m) of center, for maximum effect.

CHAPTER 4

TESTING PROGRAM

4.1. Specimen Description and Testing Configurations

In Chapter 3, MATLAB Models were used to analyze the thermal performance of the four conventional wall configurations and the active thermal insulation wall system configuration. In this Chapter, hot box testing was conducted to observe the temperature dispersion over the sections of specimen, evaluate the thermal performance of specimens and validate the MATLAB models.

Four types of conventional wall specimens were cast, each with a number of replicants. These included a solid grouted CMU specimen, a grouted CMU with an air gap, a grouted CMU with insulation inserts, and a grouted CMU with reflective inserts and a thin air gap. Nine active thermal insulation wall specimens were also cast. These included 8 inch, 16 inch and 24 inch grouted wall specimens with pipe embedded at near interior, middle or near exterior side of core.

4.1.1. Materials

The thermal properties of the CMU, grout and insulation used for the specimen fabrication are listed in Table 4-1, these properties are the same as those listed in Table 3-14 and used in MATLAB modelling. The CMU blocks used in the tests (half blocks and knockout blocks) are shown in Figure 4-1. Insulation inserts are OWENS CORNING 1-

inch R-5 XPS insulation, the reflective insulation inserts were 1-inch, R-5 insulation with a reflective surface as shown in Figure 4-2. The grout used was a fine masonry grout mixed to the following proportions: 1 volume of cement to 3 sand.

Table 4-1: Thermal Properties of Materials Used in Tests

Material	Density kg/m^3 (lb/ft^3)	Thermal Conductivity W/mK (BTU/h·ft·°F)	Specific heat J/kgK (BTU/lb·°F)
Concrete	1682 (105)	0.73 (0.42)	960 (0.23)
Grout	2000 (124.85)	1.41 (0.82)	800 (0.19)
Insulation	30 (1.87)	0.026 (0.015)	1200 (0.29)
Black Steel Pipe	8050 (502.55)	31.75 (220.14)	510.69 (0.12)
Copper Coil	8960 (559.35)	385 (222.60)	385.11 (0.092)

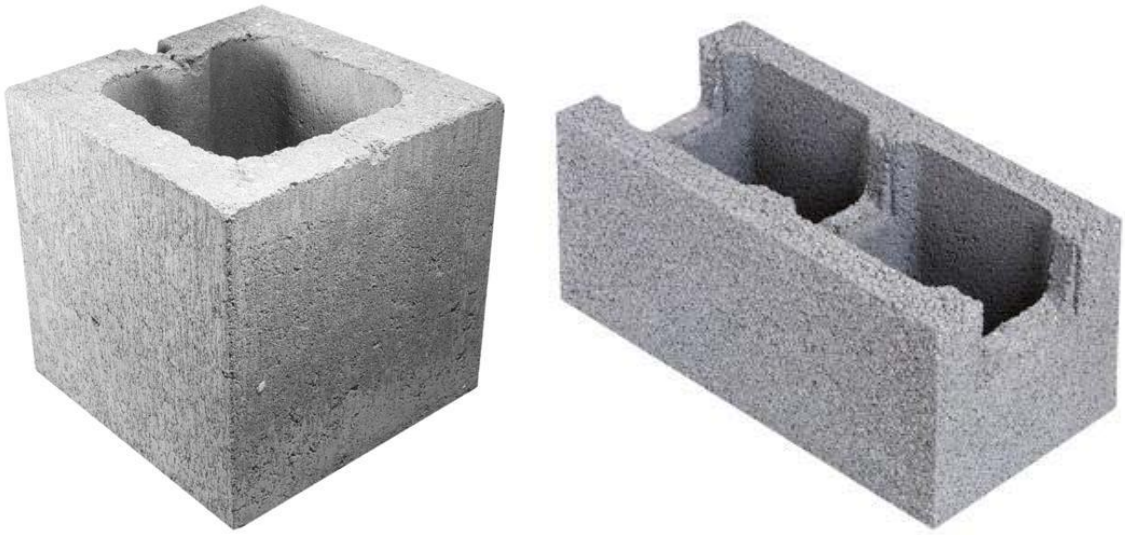

Figure 4-1 CMU Blocks: 8-inch Half Block (Left), 16 inch Knockout Block (Right)

Figure 4-2 Insulation Materials: 1-inch R-5 XPS Insulation (Left), 1-inch R-5 Reflective Inserts (Right)

Figure 4-3 Black Steel Pipes (Left) and Connection Detail (Right)

4.1.2. Specimens

The conventional wall specimens' configurations are listed in Table 4-2. The solid grouted (labelled CONVL_1) and solid grout with 1" reflective insert & ¼" air gap (labelled CONVL_4) specimens had three replicants in order to observe the thermal performance of the three specimens and verify the consistency of their performance. The solid grouted specimens with a 1" air gap (labelled CONVL_2) and the solid grouted

specimens with 1” insulation inserts (labelled CONVL_3) had only two replicants. Additional specimens were cast and were to be tested if significant variability was observed. They were not tested due to the consistency of the other test results.

Table 4-2: List of Specimens (Conventional Wall Specimen)

No.	Description of CMU Cores	Width m (inch)	Replicants
CONVL_1	Solid grouted	0.4064 (16)	3
CONVL_2	Solid grouted with 1" air gap	0.4064 (16)	2
CONVL_3	Solid grouted with 1" insulation	0.4064 (16)	2
CONVL_4	Solid grouted with 1" reflective insert & 1/4" air gap	0.4064 (16)	3

The configurations of the active thermal insulation wall specimens are listed in Table 4-2. To validate the MATLAB model, specimens were designed to cover the expected range of pipe spacing (specimen width). This spacing varied from 0.2032 m (8 inch) to 0.6096 m (24 inch). Three pipe locations, rear, middle and front side of the core are used to observe the influence of pipe positions on thermal response of the wall assembly.

Table 4-3: List of Specimens (Active Thermal Insulation Wall Specimen)

No.	Width m (inch)	Pipe Location	Replicants
ACTV_1	0.2032 (8)	Near Exterior	1
ACTV_2	0.2032 (8)	Middle	1
ACTV_3	0.2032 (8)	Near Interior	1
ACTV_4	0.4064 (16)	Near Exterior	1
ACTV_5	0.4064 (16)	Middle	1

ACTV_6	0.4064 (16)	Near Interior	1
ACTV_7	0.6096 (24)	Near Exterior	1
ACTV_8	0.6096 (24)	Middle	1
ACTV_9	0.6096 (24)	Near Interior	1

The conventional wall specimens and active thermal insulation wall specimens after construction are shown in Figure 4-4 and 4-5, respectively.

Figure 4-4 Specimen Casting (Conventional Wall Specimen)

Figure 4-5 Specimen Casting (Active Thermal Insulation Wall Specimen)

4.1.3. Sensors

There were two type of sensors used in the hot box test. OMEGA T type thermocouples (error: 1.0°C) and OMEGA HFS-5 heat flux sensors (error: 1.0°C) were used on each specimen. These sensors are shown in Figure 4-6 and they were used to monitor the temperature dispersion throughout specimens and verify the temperature predictions produced by MATLAB simulations.

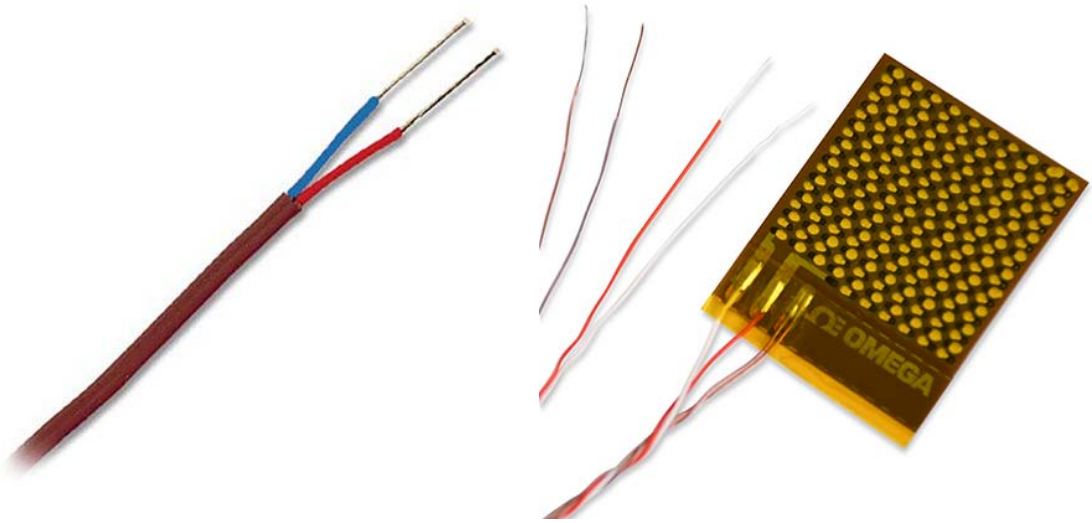

Figure 4-6 OMEGA T Type Thermocouple (Left) and OMEGA HFS-5 Heat Flux Sensor (Right)

Heat flux sensors were attached to interior and exterior surface of each specimen. Thermocouples were attached to interior and exterior surface of each specimen. Thermocouples were also embedded in grout at the interfaces of different materials, note that thermocouples had also been placed at outer surfaces at the middle of pipes, shown in Figure 4-7, inlet and outlet fluid temperatures were also monitored by thermocouples.

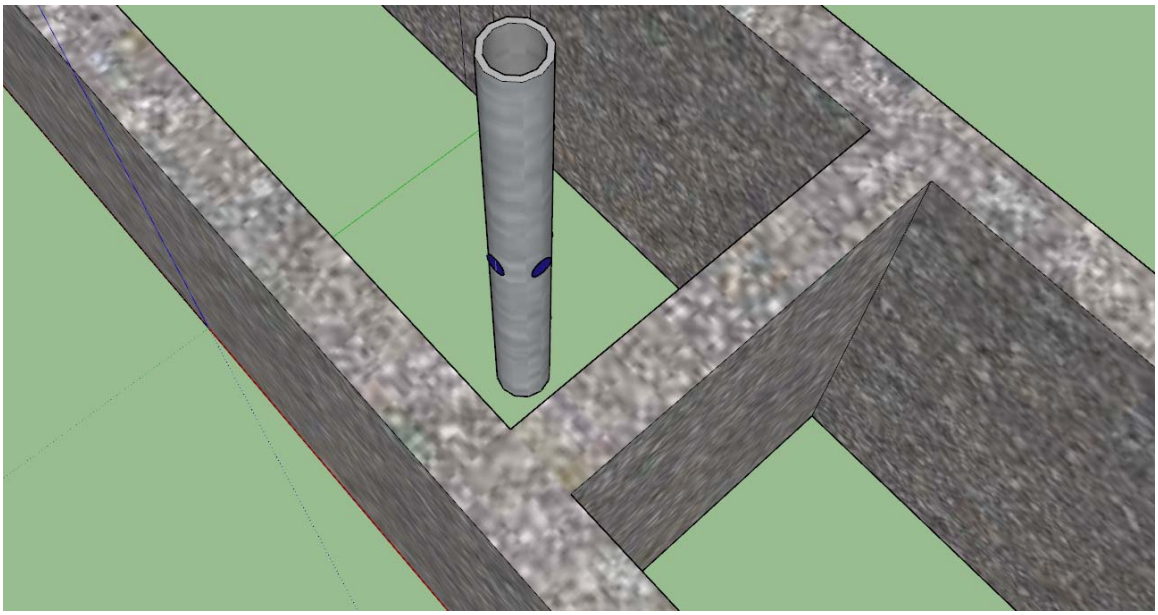

Figure 4-7 Thermocouple Locations on Pipes before Grouted (Demonstration)

The layouts of sensors of each type of specimen are shown in the Figure 4-8. The first type of sensor (heat flux sensor) recorded the temperature on the specimen surfaces. The second type of sensor (thermocouples attached to interior and exterior surfaces) recorded the temperature on active thermal insulation wall specimen surfaces and were used to correct the data obtained by the first type of sensor and get the average of surface temperatures. The thermocouples embedded in grout at interfaces recorded the temperature at interfaces and were also used to validate MATLAB simulations. Note that only data obtained by surface sensors are presented, since the interior surface temperature (and the temperature difference between interior surface temperature and indoor room temperature T_d) is used to assess the thermal performance of blocks. The temperature data obtained from the thermocouples on the pipes were recorded to validate the MATLAB simulation were not presented.

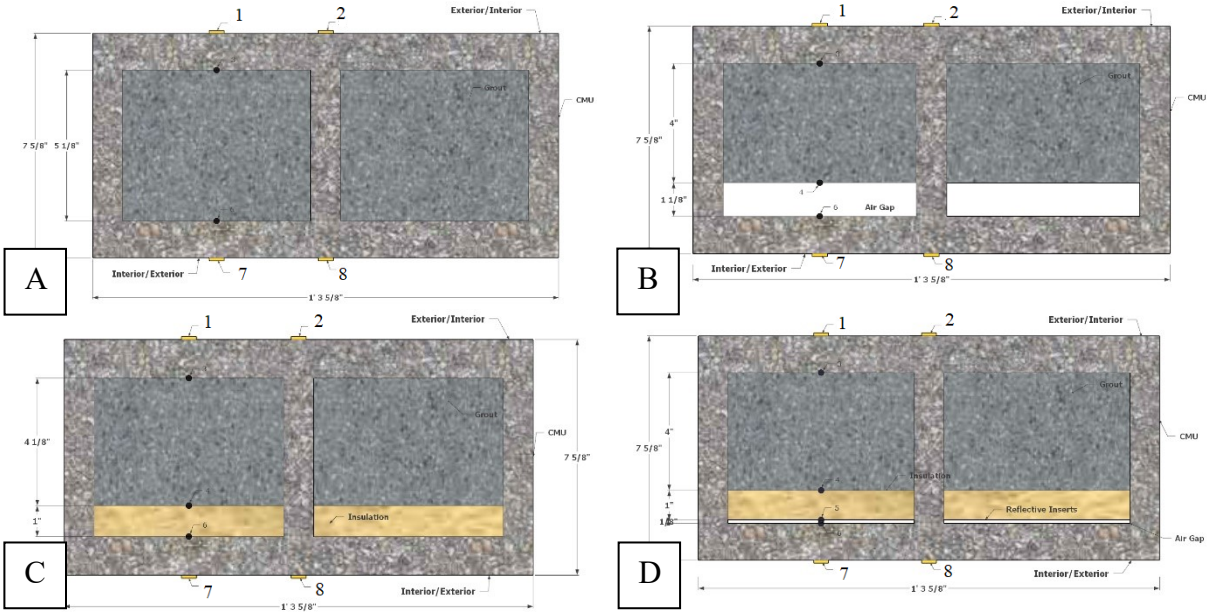

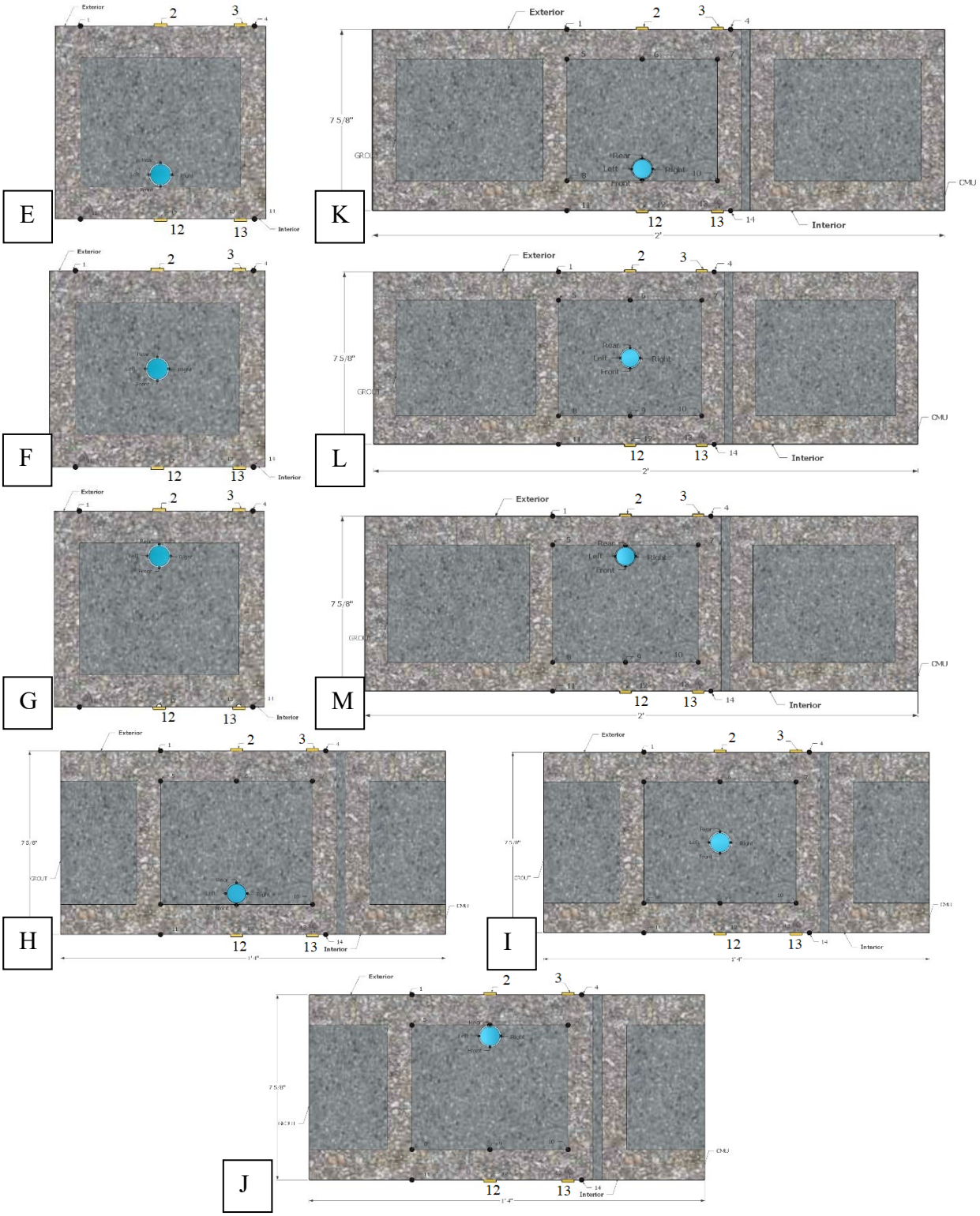

Figure 4-8 Specimens Sensor Layout: CONVL_1, CONVL_2, CONVL_3, CONVL_4, ACTV_1, ACTV_2, ACTV_3, ACTV_4, ACTV_5, ACTV_6, ACTV_7, ACTV_8, ACTV_9 (A, B, C, D, E, F, G, H, I, J, K, L, M)

4.2. Testing Apparatus

Hot box tests were performed to evaluate the thermal performance of the proposed wall assemblies shown in the Simulation Matrix and verify the MATLAB simulations in Chapter 3. The hot box testing device using in this investigation is capable of applying steady state as well as dynamic temperature profiles to a material test sample. The apparatus can perform steady state R-value testing as well as simulate diurnal climate cycling, in addition to performing ramp and step profiles. This allowed testing that simulate both prolonged temperature extremes, temperature cycling, as well as other dynamic profiles needed for testing (Kiesel, 2013).

Analytical models were developed and applied to evaluate the performance of conventional CMU wall systems (with and without inserts) and active the thermal insulation wall systems as described in Chapter 3.

Dynamic hot box testing was implemented to examine and validate the four conventional wall system specimens and the active thermal insulation wall system specimens. The validated analytical MATLAB models were used to find optimal configurations of the active thermal insulation wall system in different Climate Zones.

A sketch of the hot box testing apparatus is shown in Figure 4-9 and a photo of it was shown in Figure 4-10. The climate chamber was used to simulate the ambient (outside) temperature condition (a diurnal curve), the indoor chamber was used to simulate an indoor temperature (at a constant value). The testing specimen was surrounded by the insulation panel to reduce edge effect and induce one-way heat flow. The three part of testing apparatus clamped together and kept airtight.

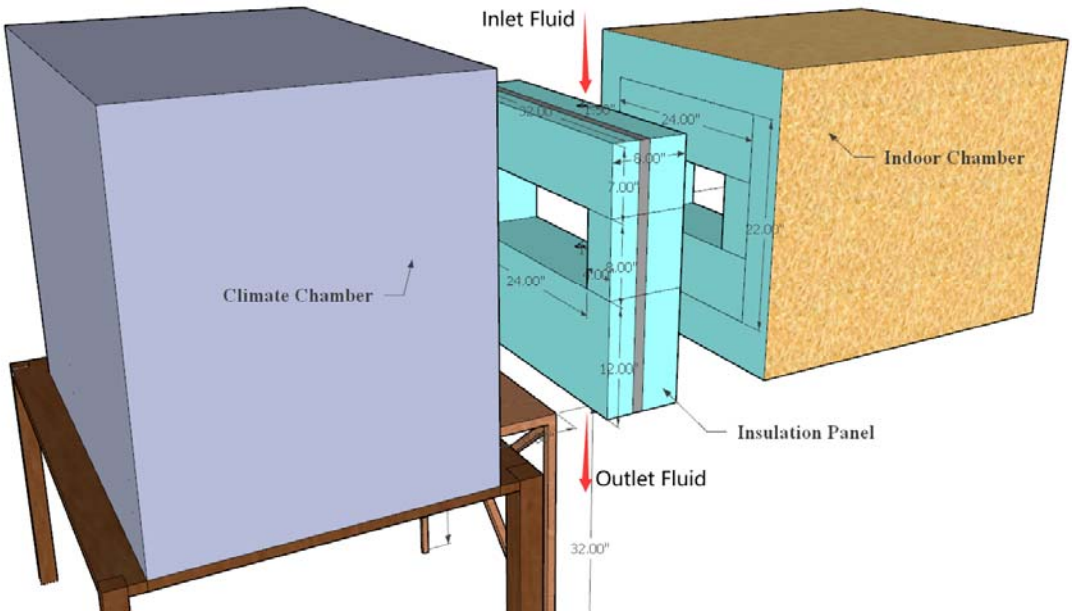

Figure 4-9 Hot Box Test Apparatus Demonstration (by Sketchup)

Figure 4-10 Hot Box Test Apparatus Demonstration

Pipes for the active thermal insulation wall specimens were extended through the insulation panels. The inlet for the pipe fluid was located at the top of the specimen and the

fluid outlet was at the bottom. The circulation pipe was connected to a copper coil which was submerged in a water bath tank. The water in the tank was maintained at the target fluid temperature using a controller, a chiller and heating coil.

4.2.1. Temperature Regimes

The typical summer and winter temperature conditions described in Chapter 3 (section 3.3.1) as Mild Summer and Mild Winter were used in the climate chamber. Note that Climate Zone 5A temperature conditions were used as representatives of other Climate Zones since buildings in Climate Zone 5A require reasonable amount of both heating and cooling. These two temperature diurnal curves were created based on high and low temperatures in July and January weather conditions in in Chicago. Before each test, the system was pre-heated for about half an hour at the temperature of 29°C for Mild Summer and -6.75°C for Mild Winter.

In the hot box tests, ambient temperatures followed the two exterior diurnal temperature curves. During the tests the interior temperatures were held at a constant 22°C or 24°C, to simulate typical winter and summer set points.

4.2.2. Testing Matrix

The test program was divided into four phases. In Phase one, the three replicants of CONVL_1 specimen were tested at the Mild Summer situation to verify the consistency of thermal performance of solid grouted specimens and thus infer the consistency of other models. In Phase two, the other three types of conventional wall specimens (CONVL_2, CONVL_3, CONVL_4) were tested at the Mild Summer situation to compare their thermal performance with solid grouted specimens tested in Phase 1. In Phase three, the 16-inch specimens (ACTV_4, ACTV_5, ACTV_6) were tested at different temperature settings

(circulation fluid and indoor/outdoor temperatures). In Phase four, the 8-inch and 24-inch specimens (ACTV_1, ACTV_2, ACTV_3, ACTV_7, ACTV_8, ACTV_9) were tested at select temperature settings.

The specimens tested in Phase 1 were shown in Figure 4-11. A, B, C and were the three replicants of solid grouted conventional wall specimen CONVL_1. The results of Phase 1 were used as baselines to evaluate the energy saving potential of other specimens.

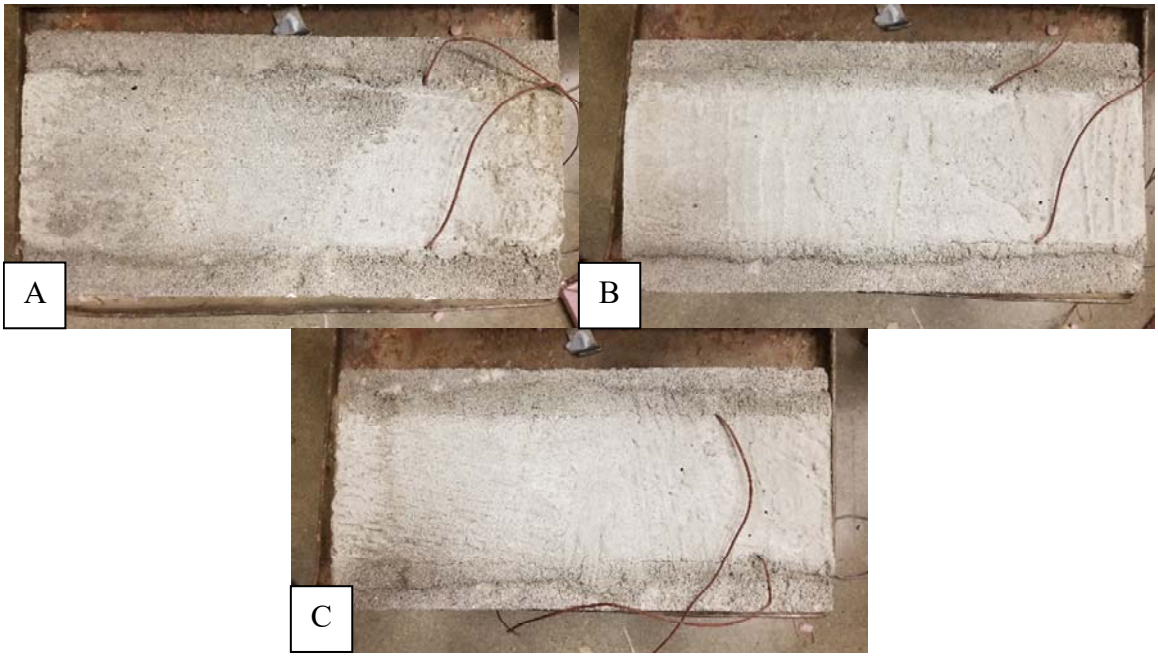

Figure 4-11 Specimens Tested in Hot Box Test Phase One: Three Replicants of CONVL_1 (A, B & C)

The specimens tested in Phase 2 were shown in Figure 4-12. A, B, C and were the three conventional wall specimen CONVL_2, CONVL_3, CONVL_4, respectively. By comparing the results of Phase 2 with Phase 1, the relative performance of these three wall configurations were investigated.

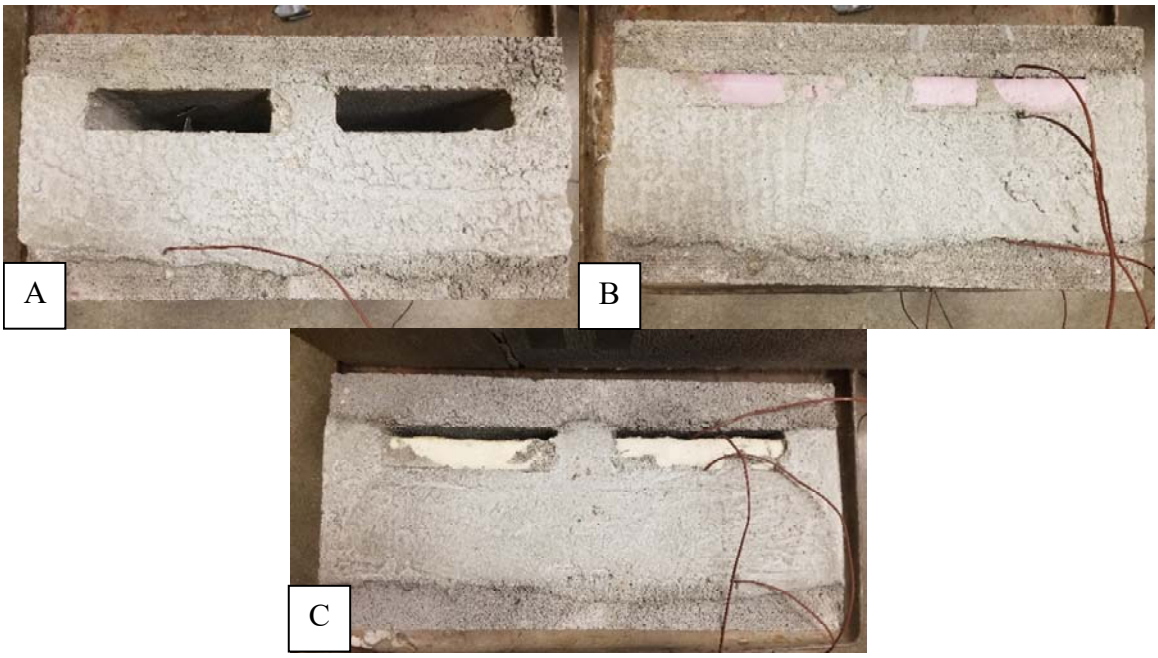

Figure 4-12 Specimens Tested in Hot Box Test Phase Two: CONVL_2, CONVL_3, CONVL_4 (A, B & C)

The specimens tested in Phase 3 were shown in Figure 4-13. A, B, C and were the three active thermal insulation wall specimen ACTV_4, ACTV_5, ACTV_6, respectively. These three specimens were tested at different fluid and indoor temperatures, and at both typical summer and winter conditions. The first goal of these tests was to find the optimal pipe position for different weather and fluid temperatures. The second goal was to get an optimum fluid temperature for the different exterior weather conditions, if possible. The third goal of this phase of tests was to verify if the thermal energy flow effects of this system were significant.

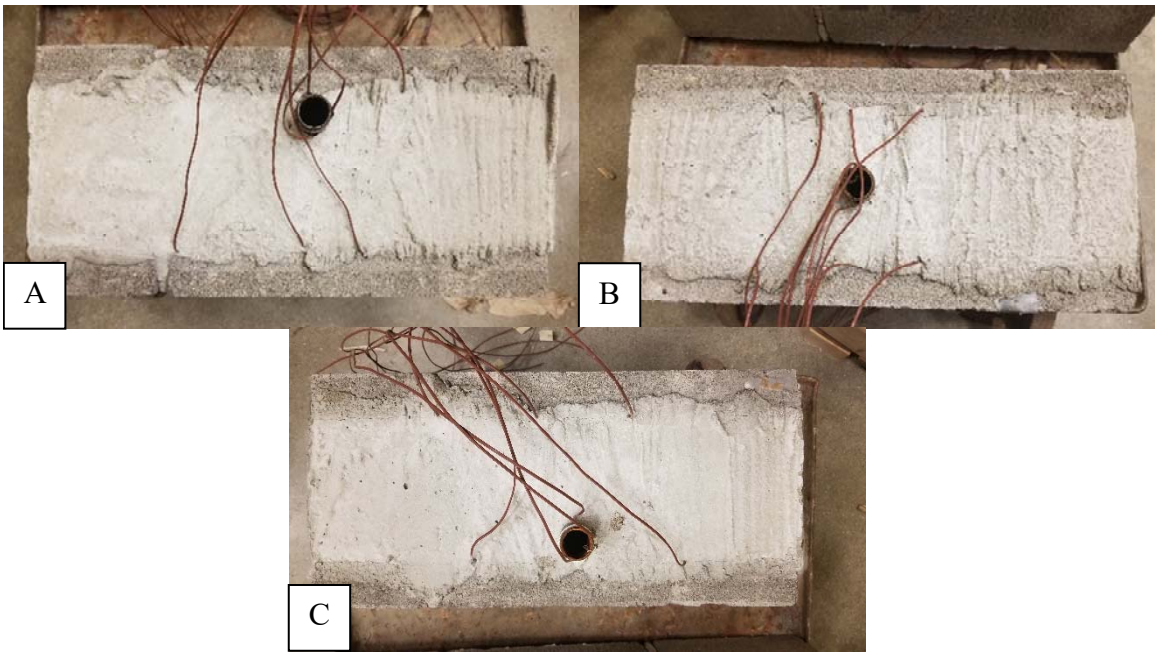

Figure 4-13 Specimens Tested in Hot Box Test Phase Three: ACTV_4, ACTV_5, ACTV_6 (A, B & C)

The specimens tested in Phase 4 were shown in Figure 4-14. A, B, C, D, E, F and were the six active thermal insulation wall specimen ACTV_1, ACTV_2, ACTV_3, ACTV_7, ACTV_8, ACTV_9, respectively. These six specimens were tested at a designated fluid and indoor temperature, with both Mild Summer and Mild Winter climate chamber conditions. The results were compared with the results of Phase 3 to evaluate the influence of pipe spacing for active thermal insulation walls.

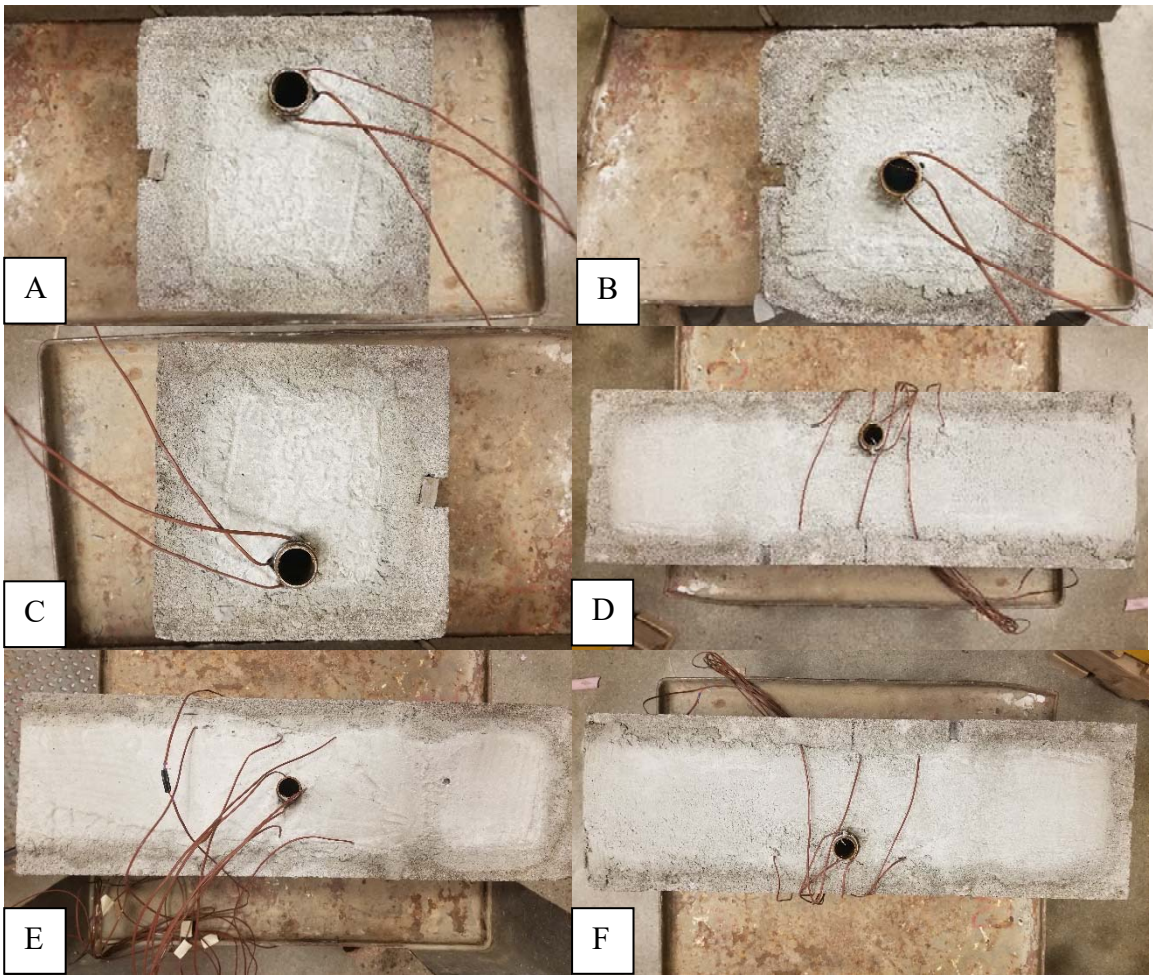

Figure 4-14 Specimens Tested in Hot Box Test Phase Four: ACTV_1, ACTV_2, ACTV_3, ACTV_7, ACTV_8, ACTV_9 (A, B, C, D, E, F)

The testing matrix of hot box tests from Phase 1 to Phase 4 were shown in Table 4-4 to Table 4-7, respectively.

Table 4-4: Hot Box Testing Matrix: Phase 1

Test No.	Ambient Temperature	Indoor Temperature (°C)	Specimen
1_1	Mild Summer	22	CONVL_1
1_2	Mild Summer	22	CONVL_1
1_3	Mild Summer	22	CONVL_1

In Phase 2, the three specimens were also tested in the same surface temperature regimes, but with the specimen flipped so that the air gap or insulation location was reversed. Tests No. 2_1, 2_3 and 2_5 put the air gap, insulation, or reflective insert at the exterior side of core, close to the exterior temperature chamber side. That means the thermal mass was higher at the interior side, not the exterior side. Tests No. 2_2, 2_4 and 2_6 put the air gap, insulation, or reflective insert at the interior side of core, marked as "Flip over specimen".

Table 4-5: Hot Box Testing Matrix: Phase 2

Test No.	Ambient Temperature	Indoor Temperature (°C)	Specimen	Note
2_1	Mild Summer	22	CONVL_2	
2_2	Mild Summer	22	CONVL_2	Flip over specimen
2_3	Mild Summer	22	CONVL_3	
2_4	Mild Summer	22	CONVL_3	Flip over specimen
2_5	Mild Summer	22	CONVL_4	
2_6	Mild Summer	22	CONVL_4	Flip over specimen

In Phase 3, the three 16-inch active thermal insulation wall specimens were tested in both summer and winter condition. The group "α" tests (No. 3_1, 3_2, 3_3, 3_9, 3_10, 3_11, 3_17, 3_18) were used for investigating the influence of pipe location (front, middle, rear side of core) on active thermal insulation wall specimens in summer. The group "β" tests (No. 3_6, 3_7, 3_8, 3_14, 3_15, 3_16, 3_21, 3_22) were used for investigating the behavior in winter. The group "γ" tests (No. 3_4, 3_5, 3_12, 3_13, 3_19, 3_20) were used

to determining whether the thermal barrier effect is significant, or under what circumstances there is a thermal barrier effect. Note that thermal barrier effect is that the thermal performance has an improvement when fluid temperature is the same as indoor temperature.

Table 4-6: Hot Box Testing Matrix: Phase 3

Test No.	Ambient Temperature	Indoor Temperature (°C)	Fluid Temperature (°C)	Specimen	Test Regime
3_1	Mild Summer	22	16	ACTV_6	α
3_2	Mild Summer	22	22		α
3_3	Mild Summer	22	28		α
3_4	Mild Summer	24	22		γ
3_5	Mild Summer	24	24		γ
3_6	Mild Winter	22	10		β
3_7	Mild Winter	22	16		β
3_8	Mild Winter	22	22		β
3_9	Mild Summer	22	16	ACTV_5	α
3_10	Mild Summer	22	22		α
3_11	Mild Summer	22	28		α
3_12	Mild Summer	24	22		γ
3_13	Mild Summer	24	24		γ
3_14	Mild Winter	22	10		β
3_15	Mild Winter	22	16		β

3_16	Mild Winter	22	22		β
3_17	Mild Summer	22	16	ACTV_4	α
3_18	Mild Summer	22	22		α
3_19	Mild Summer	24	22		γ
3_20	Mild Summer	24	24		γ
3_21	Mild Winter	22	16		β
3_22	Mild Winter	22	22		β

In Phase 4, three 8-inch and three 24-inch active thermal insulation wall specimens were tested in the Mild Summer and Mild Winter conditions with various fluid and indoor temperatures. The results of Phase 4 and results of group "α" tests in Phase 3 were used to evaluate the influence of pipe spacing.

Table 4-7: Hot Box Testing Matrix: Phase 4

Test No.	Ambient Temperature	Indoor Temperature (°C)	Fluid Temperature (°C)	Specimen
4_1	Mild Summer	22	16	ACTV_1
4_2	Mild Winter	22	16	
4_3	Mild Summer	22	16	ACTV_2
4_4	Mild Winter	22	16	
4_5	Mild Summer	22	16	ACTV_3
4_6	Mild Winter	22	16	
4_7	Mild Summer	22	16	ACTV_7
4_8	Mild Winter	22	16	

4_9	Mild Summer	22	16	ACTV_8
4_10	Mild Winter	22	16	
4_11	Mild Summer	22	16	ACTV_9
4_12	Mild Winter	22	16	

CHAPTER 5

TEST RESULTS AND OBSERVATIONS

The results of the tests described in Chapter 4 were presented in this Chapter. The plots of hot box test results were shown in APPENDIX A (Figure A-1 to Figure A-17). Figure A-1 is duplicated here for convenience at Figure 5-1.

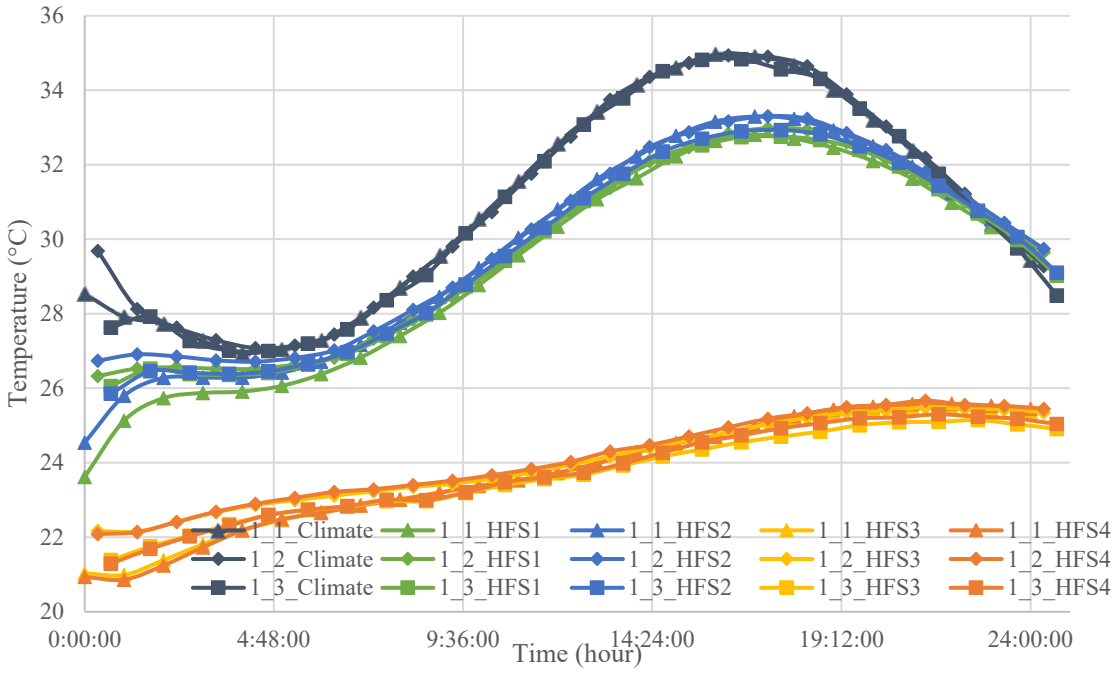

Figure 5-1 Temperature Response of The Three Solid Grouted Specimen Replicates

In these figures, the dark blue curves at top part of the figure were the driving temperatures (the temperature in Climate Chamber during hot box tests). Sensor HFS1 was

located on the block web on exterior surface, sensor HFS2 was located at the center of the core on exterior surface. Sensor HFS3 was located at the center of the core on the interior surface, HFS4 located at the center of the block web on interior surface.

The variations in the driving temperature curves were caused by chamber system instability. However, the overall trend of driving temperature followed the designed testing temperature conditions. Another must point-out was that the sensor which measured the climate temperature was already corrected (the readings were 1.3°C higher than input). For test No. 3-8, the ambient temperature curve was not run as programed at the second half of the test, this was due to equipment problems. Tests No.4_5 and No.4_6 were unavailable since the fluid temperatures were not stable during test.

To describe the temperature response of the specimens, for each test a $T_{d,max}$ and $T_{d,mean}$ were derived from the test data . Typically, the smaller those values were, the greater the effect the wall assembly had on thermal energy flow.

The specimen response indicated that the initial temperature response was dominated by the initial conditions during the first few hours of running in the tests. After a period of time, the temperature response was then dominated by the exterior (driving) temperature regimes. It was thus concluded that it would not be propriate to use only the $T_{d,mean}$ or $T_{in,mean}$ value to describe each specimens' temperature response, since this mean value was affected by the initial conditions, and the initial conditions of many of the specimens were different. To order to minimize the impact of initial condition, a $T_{d,\ max}$' value was used to describe the temperature response of specimens. It is the maximum value of $T_{d,\ max}$ during the last 12 hours of test. Both these temperatures are proportional to the internal HVAC system loading of a space adjacent to this exterior wall system.

The temperature response during the first few hours were dominated by the initial temperature conditions of the specimen, therefore, the observations and discussions were focused on the temperature response after the first few hours.

5.1. Test Results of Conventional Wall Specimens

Figure 5-1 shows that the temperature information measured by the four heat flux sensors for replicate Specimens 1_1 through 1_3 are consistent. The temperature responses were within 0.4°C after the first few hours of operation, while the differences in first few hours were dominated by the different initial temperature conditions. These results show that the thermal properties of the test CMU specimens were quite consistent, thus no additional duplicates were needed for other types of specimens.

The measured $T_{in,\ max}$' was recorded for each test and shown in Table 5-1. These values were measured by the two sensors attached on the interior side of specimens, sensor HFS4 located on interior surface near web, sensor HFS3 located on interior surface near the block core.

Table 5-1: Measured $T_{in,max}$' and Their Average for Conventional Wall Specimens

Test No.	$T_{in,max}$' (°C)			Note
	HFS4	HFS3	Average of Two Sensors	
1_1	25.66	25.58	25.62	
1_2	25.68	25.52	25.60	
1_3	25.34	25.18	25.26	
2_1	24.54	24.63	24.59	CONVL_2
2_2	24.97	24.64	24.81	CONVL_2 Flipover

2_3	24.73	24.16	24.45	CONVL_3
2_4	24.63	24.45	24.54	CONVL_3 Flipover
2_5	24.87	24.81	24.84	CONVL_4
2_6	24.84	24.22	24.53	CONVL_4 Flipover

The measured responses of Tests No.1_1 through No.1_3 shown in the Figure 5-1 and Table 5-1 shows that under the Mild Summer exterior temperature test regime, the average $T_{in, max}$' of the three specimens measured on the interior surface of the specimens did not vary significantly. The average $T_{in, max}$' of Test No.1_1 through No.1_3 measured by HFS3 was 25.43°C and by HFS4 was 25.56°C, roughly at the time of 21:40 hours. This suggested that the temperature at interior surface, corresponding to the core and web locations, are very consistent. The minor difference may be caused by minor differences in thermal properties of the CMU and grout, or just measurement error.

The temperature response of the solidly grouted specimens with the 1" air gap (Test No.2_1, No.2_2) are shown in Figure A-2. The temperature response of the solidly grouted specimens with the 1" insulation inserts (Test No.2_3, No.2_4) are shown in Figure A-3. The temperature response of the solidly grouted specimens with the 1" reflective insert and air gap (Tests No.2_5, No.2_6) are shown in Figure A-4. The results of these tests indicate that thermal performance of all three conventional wall configurations are similar. Given the thermal sensor accuracy, the results did not show a significant difference in behavior, even accounting for the location of the thermal mass with respect to the interior surface. This is probably due to the fact that the thermal mass distribution does not change significantly. Other researchers have found similar effects (Jie et al., 2018; Zhang et al., 2017).

The temperature differences in thermal behavior of the three specimens (CONVL_2, CONVL_3, CONVL_4) were minor, the $T_{in,\ max}$' values were about 1°C lower than the ones of solid grouted specimens (CONVL_1). Furthermore, the measured response and predicted response were comparable. This proved that the air gap and presence of insulation inserts reduces the energy flow through these wall systems compared to solid grouted walls. However, the presence of a high reflectivity film on the insulation insert did not appear to improve the thermal resistance of the assembly significantly. Some researchers (Nathaniel C. Huygen & Sanders, 2019) showed that heat flux through a masonry veneer wall section may be significantly reduced with the use of reflective radiation barriers. The test results in this investigation suggests that, for cells of block walls, this effect may not be significant. Moreover, the normal insulation inserts produced a slightly lower $T_{in,\ max}$' value than reflective insulation inserts, which suggests these reflective insulation inserts worked no better than normal insulation inserts.

All those findings were based on the measured data. However, due to the limit on the accuracy of the thermal sensors (1.0°C), further tests should be done to verify these conclusions.

5.2. Test Results of Active Thermal Insulation Wall Specimens

The temperature response of the 16-inch active thermal insulation wall specimens with pipes embedded at interior side of the block core are shown in Figures A-5 to A-7. The temperature response of the 16-inch active thermal insulation wall specimens with pipe embedded at middle of the block cores are shown in Figures A-8 to A-10. The temperature response of the 16-inch active thermal insulation wall specimens with pipe embedded at near exterior of block core are shown in Figures A-11 to A-13.

Table 5-2 shows the maximum temperatures measured by the two sensors attached on the interior side of specimens of the active thermal insulation wall specimens with a fixed pipe spacing. Those data are also plotted in Figure 5-2 through 5-4. Note that Sensor 1 was HFS4 and Sensor 2 was HFS3.

Table 5-2: Measured $T_{in,max}$' and Their Average (Fixed Spacing Active Thermal Insulation Wall)

Test No.	$T_{in,max}$' (°C)			Note[1]
	HFS4	HFS3	Average of Two Sensors	
3_1	21.68	19.97	20.83	NI-Summer-22-16
3_2	23.60	22.98	23.29	NI-Summer-22-22
3_3	25.58	26.07	25.82	NI-Summer-22-28
3_4	24.72	23.86	24.29	NI-Summer-24-22
3_5	25.40	24.94	25.17	NI-Summer-24-24
3_6	15.22	14.31	14.77	NI-Winter-22-10
3_7	17.59	17.66	17.63	NI-Winter-22-16
3_8	19.95	21.01	20.48	NI-Winter-22-22
3_9	21.62	20.93	21.28	M-Summer-22-16
3_10	23.52	23.06	23.29	M-Summer-22-22
3_11	25.40	25.18	25.29	M-Summer-22-28
3_12	-	-	-	M-Summer-24-22
3_13	25.48	25.01	25.24	M-Summer-24-24
3_14	15.43	15.16	15.30	M-Winter-22-10
3_15	17.94	17.86	17.90	M-Winter-22-16

3_16	19.74	20.19	19.97	M-Winter-22-22
3_17	22.69	22.34	22.51	NE-Summer-22-16
3_18	24.34	24.33	24.34	NE-Summer-22-22
3_19	24.99	24.80	24.89	NE-Summer-24-22
3_20	25.42	25.33	25.38	NE-Summer-24-24
3_21	16.31	16.23	16.27	NE-Winter-22-16
3_22	17.43	17.59	17.51	NE-Winter-22-22

Note:

1. Brief descriptions of these tests are listed in here. The first term indicates pipe location, “NI” means pipe near interior, “M” means pipe in middle, “NE” means pipe near exterior. The second term indicates the driving temperature, “Summer” means the Mild Summer condition, “Winter” means the Mild Winter, third term indicates the interior temperature, the fourth term indicates the fluid temperature.

2. The Test No. 3-12 data was not recorded due to system failure.

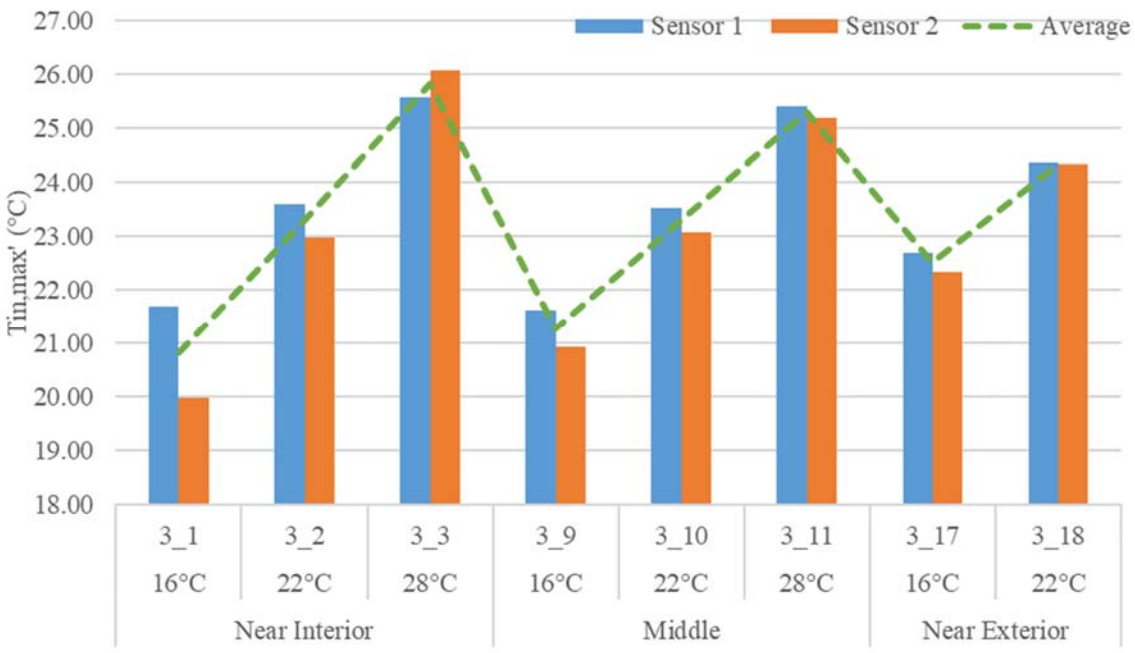

Figure 5-2 Temperature Response of 16-inch Active Thermal Insulation Specimens in Summer Condition with Indoor Temperature of 22°C

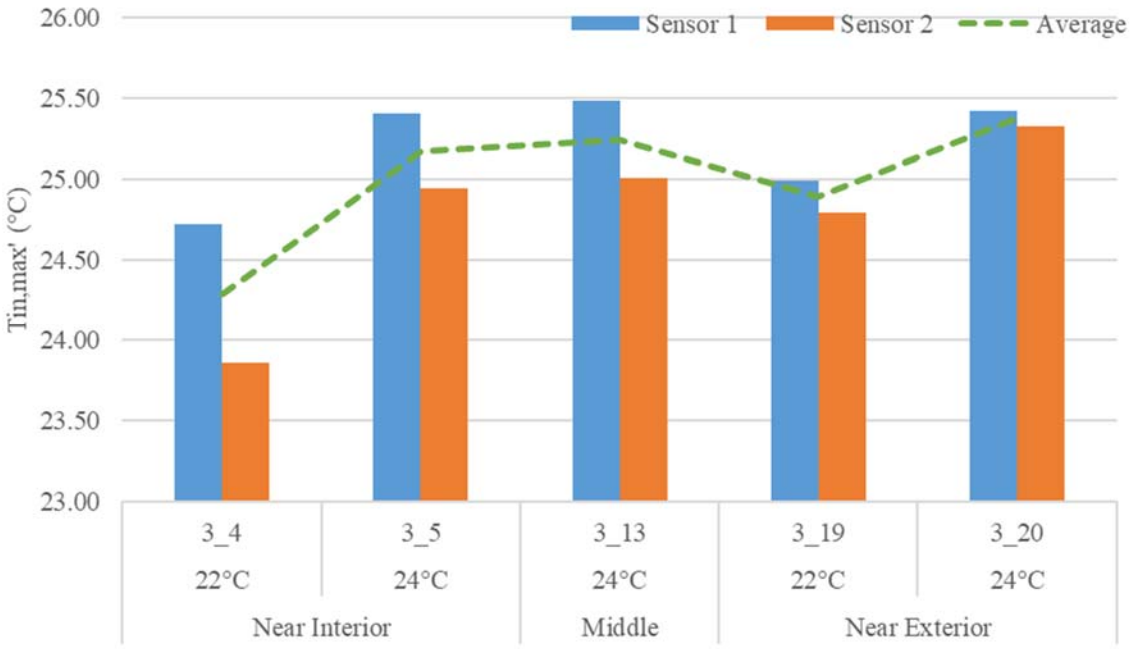

Figure 5-3 Temperature Response of 16-inch Active Thermal Insulation Specimens in Summer Condition with Indoor Temperature of 24°C

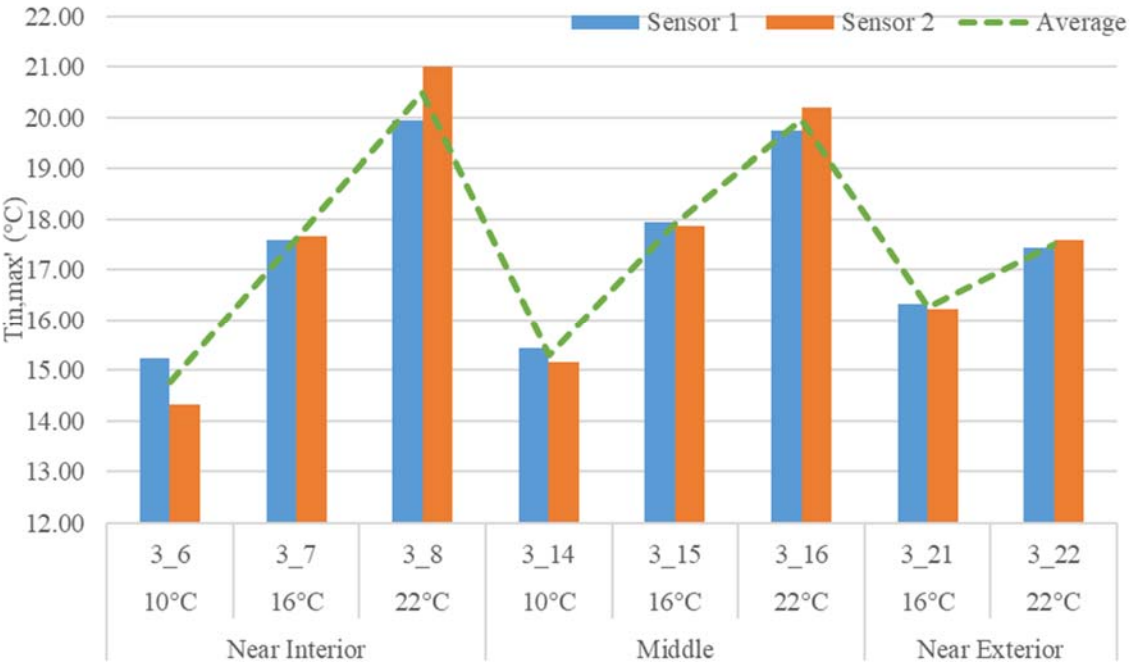

Figure 5-4 Temperature Response of 16-inch Active Thermal Insulation Specimens in Winter Condition with Indoor Temperature of 22°C

Examining the temperature values listed in Table 5-2, suggests that the interior surface temperature recorded by HFS3 was more sensitive to fluid temperature impacts when the pipe is located near interior surface. This result is reasonable because the longer the distance between the pipe and the interior surface, the longer it takes the thermal heat flow to impact the interior surface temperatures. Thus, the interior surface temperature is less influenced by the fluid temperature in those configurations where the pipe is further from the interior surface. This result also suggests that the interior surface temperature could be prone to overheating or overcooling when the pipes are placed near the interior surface.

Under summer conditions, although the $T_{in,\,max}$' recorded by HFS3 (near block core midpoint) was lower when the pipes were located near the interior, $T_{in,\,max}$' recorded by HFS4 (web) of specimens with pipes embedded near the interior surface, or at middle of the block, were very similar. This response made the averages of the two sensors of the two types of specimen close in value. Under winter conditions, similar behavior was observed.

The experimental results also show that when fluid temperatures are the same as the indoor temperature, there was not a noticeable reduction in heat flow and thus no significant increase in thermal resistance. This is consistent with the results predicted by the analytical models presented in the previous chapter.

The results of the active wall system tests on variable pipe and block configurations are shown in Table 5-3 and plotted in Figures 5-5 to 5-6. It shows the maximum temperature measured by the two sensors attached on the interior side of specimens. The

horizontal axis below the bar chart shows the Test No., the fluid temperature and pipe location. As predicted, the $T_{in,\,max}$' value was roughly proportional to the fluid temperature in all cases, both for the Summer or Winter climate test conditions. It is also clear from these graphs that behavior of active thermal insulation specimen when the pipes are located near the interior surface, and middle of the wall, were similar. However, the behavior of the specimens with the pipes located near the exterior surface was quite different. This difference was like due to the fact that when the pipe is near exterior, the heat flow between the pipe and ambient environment was significantly greater than with the other two configurations. It appears that the pipes should be placed in the middle of wall to prevent the internal surface temperature of wall from being noticeable uneven, to avoid overheating or overcooling that can occur in some conditions, and because this location produces comparable heat flow responses to near interior surface location.

Table 5-3: Measured $T_{in,max}$' and Their Average (Variable Spacing Active Thermal Insulation Wall)

Test No.	$T_{in,max}$' (°C)			Note[1]
	HFS4	HFS3	Average of Two Sensors	
4_1	20.76	20.70	20.73	8-NE-Summer
4_2	19.14	18.88	19.01	8-NE-Winter
4_3	20.68	20.18	20.43	8-M-Summer
4_4	18.70	18.41	18.56	8-M-Winter
4_5	-[2]	-	-	8-NI-Summer
4_6	-[2]	-	-	8-NI-Winter
4_7	23.41	22.69	23.05	24-NE-Summer

4_8	16.43	16.57	16.50	24-NE-Winter
4_9	22.07	21.00	21.54	24-M-Summer
4_10	17.90	17.95	17.93	24-M-Winter
4_11	22.27	20.38	21.33	24-NI-Summer
4_12	16.38	17.16	16.77	24-NI-Winter

Note:

1. The first term indicates pipe spacing, “8” means 8-inch, “24” means 24-inch. The second term indicates pipe location, “NI” means pipe near interior, “M” means pipe in middle, “NE” means pipe near exterior. The third term indicates the driving temperature, “Summer” means summer-lowΔT condition, “Winter” means winter-lowΔT.
2. The 8-inch specimen with pipe embedded at near interior side was damaged, thus Tests No.4_5 and No.4_6 were not conducted.

Test results shown in Table 5-3, and some of the results shown in Table 5-2 was plotted in Figures 5-5 to 5-6. The horizontal axis on the bar chart shows the Test No., pipe spacing and pipe location. Sensor 1 was HFS4 and Sensor 2 was HFS3.

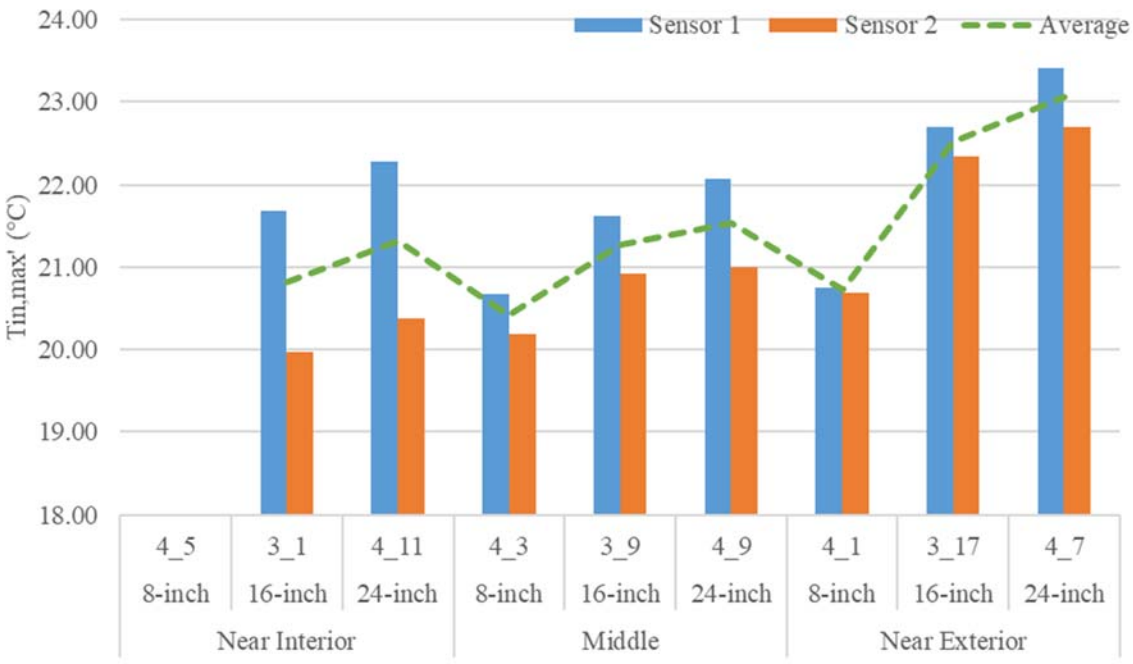

Figure 5-5 Temperature Response of Variable Spacing Active Thermal Insulation Specimens in Summer Condition with Fluid Temperature of 16°C and Indoor Set Point of 22°C

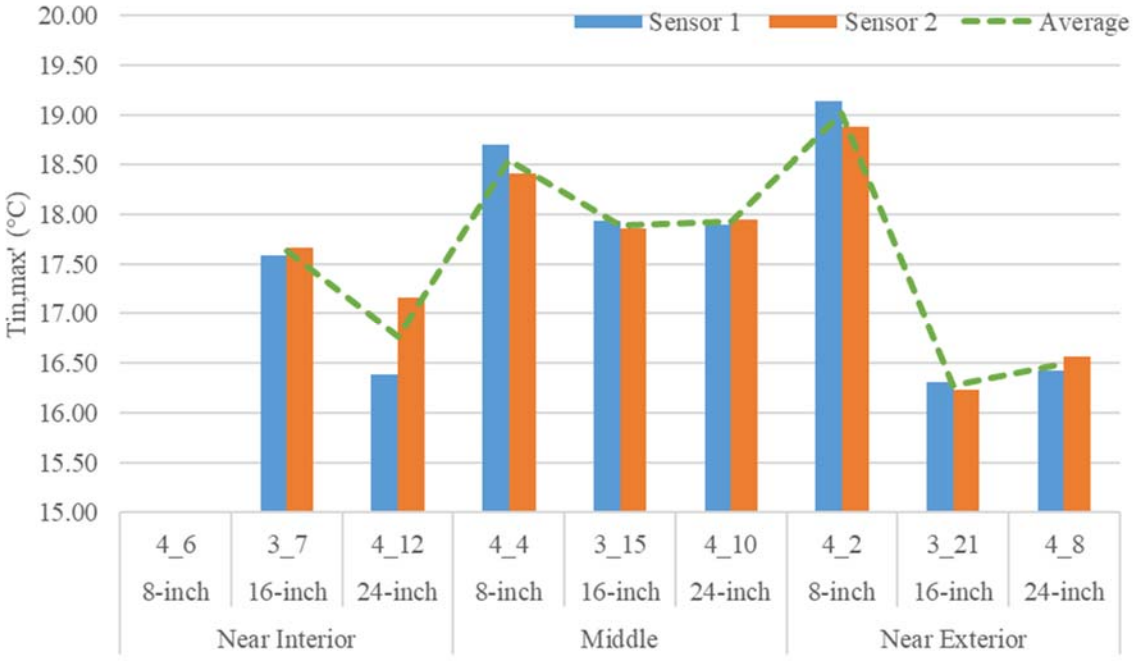

Figure 5-6 Temperature Response of Variable Spacing Active Thermal Insulation Specimens in Winter Condition with Fluid Temperature of 16°C and Indoor Set Point of 22°C

The temperature response of the 8-inch active thermal insulation wall specimens with pipes embedded at different locations are shown in Figures A-17 to A-18. The temperature response of the 24-inch active thermal insulation wall specimens with pipe embedded at different locations are shown in Figures A-19 to A-20.

From Figures 5-5 and 5-6 above, it can be seen that the larger pipe spacing produced higher interior surface temperatures in summer and lower interior surface temperatures in winter. However, this trend becomes less pronounced as the pipe spacing increases. This observation verifies the analytical results as shown in Chapter 3.4.5.

5.3. Validation of MATLAB Model Simulations

The tests were also used to validate The MATLAB Model proposed in Chapter 3. The temperature response of Test No.1-1 (Solid Grouted), Test 2-1 (Solid Grouted with Air Gap), Test 2-3 (Solid Grouted with Insulation Inserts), Test 2-5 (Solid Grouted with Reflective Insulation Inserts), 2-6 (Solid Grouted with Reflective Insulation Inserts Flipped over), and Test 3-9 (16-Inch Active Thermal Insulation Wall with Pipe Embedded in the Middle of the block) were compared to MATLAB Model predictions for these specimen configurations. These comparisons are shown in Figures 5-7, 5-8, 5-9, 5-10, 5-11, 5-12, respectively. Solid lines were the measured data, dash lines were the predictions.

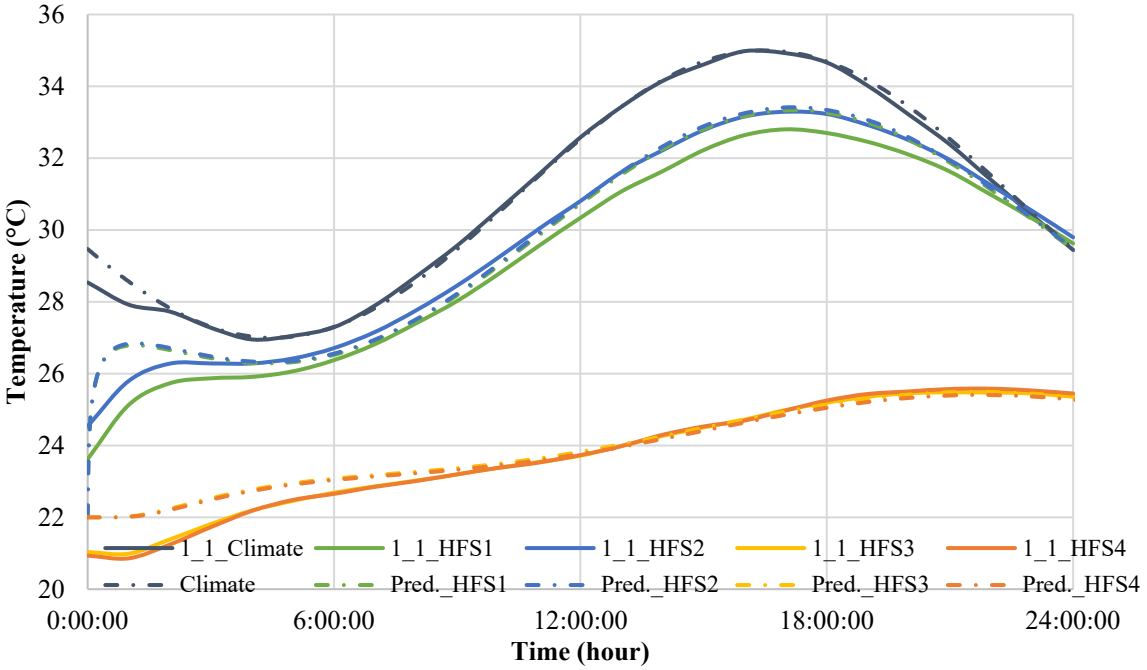

Figure 5-7 MATLAB Model Validation of Solid Grouted Specimen Test No.1_1 Temperature Response

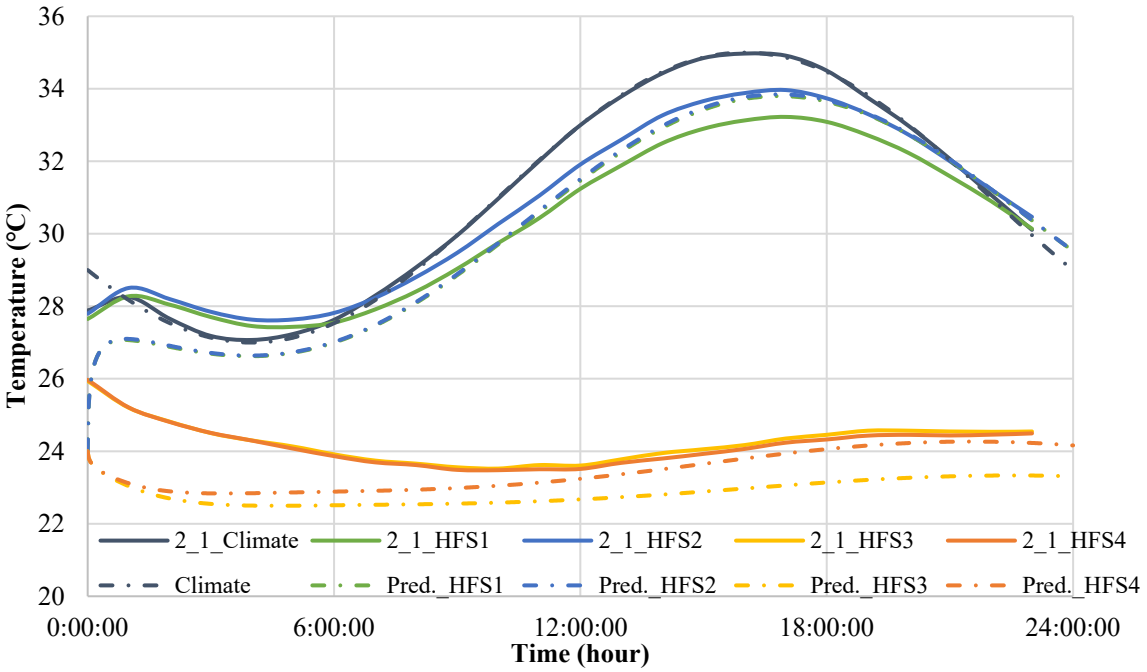

Figure 5-8 MATLAB Model Validation of Solid Grouted with Air Gap Specimen Test No.2_1 Temperature Response

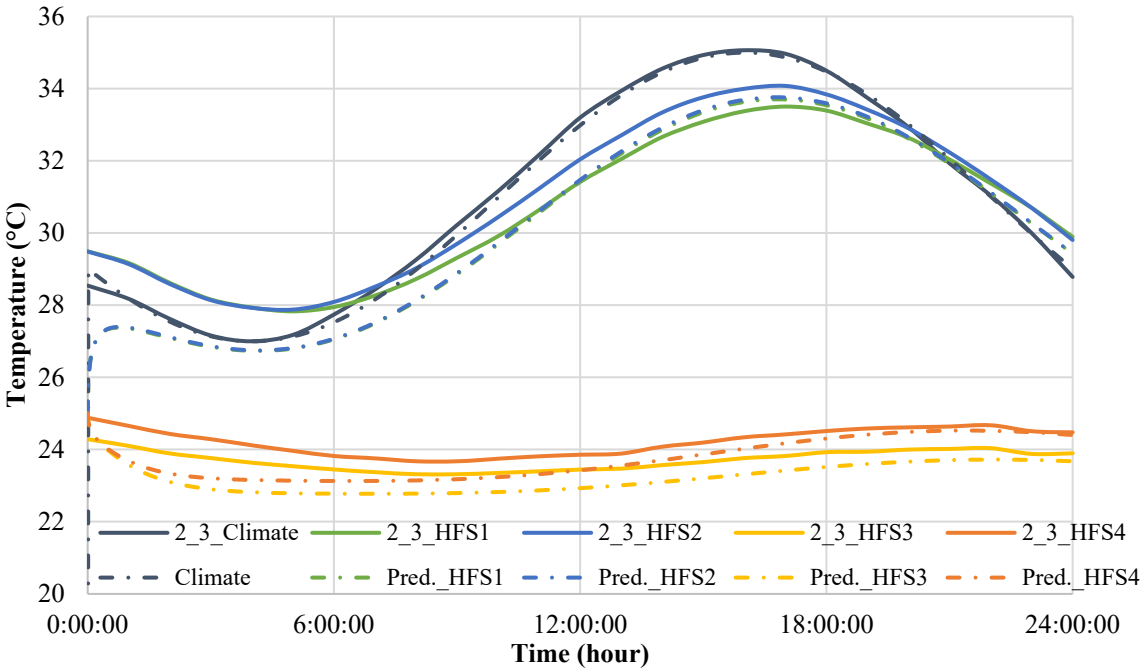

Figure 5-9 MATLAB Model Validation of Solid Grouted with Insulation Inserts Specimen Test No.2_3 Temperature Response

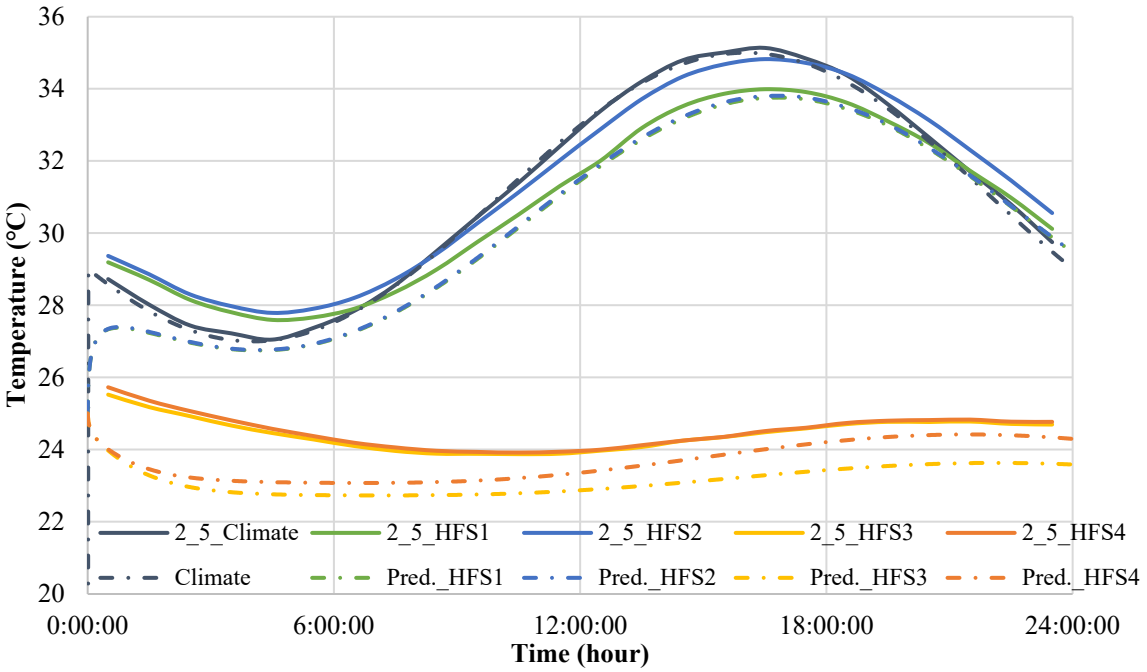

Figure 5-10 MATLAB Model Validation of Solid Grouted with Reflective Inserts Specimen Test No.2_5 Temperature Response

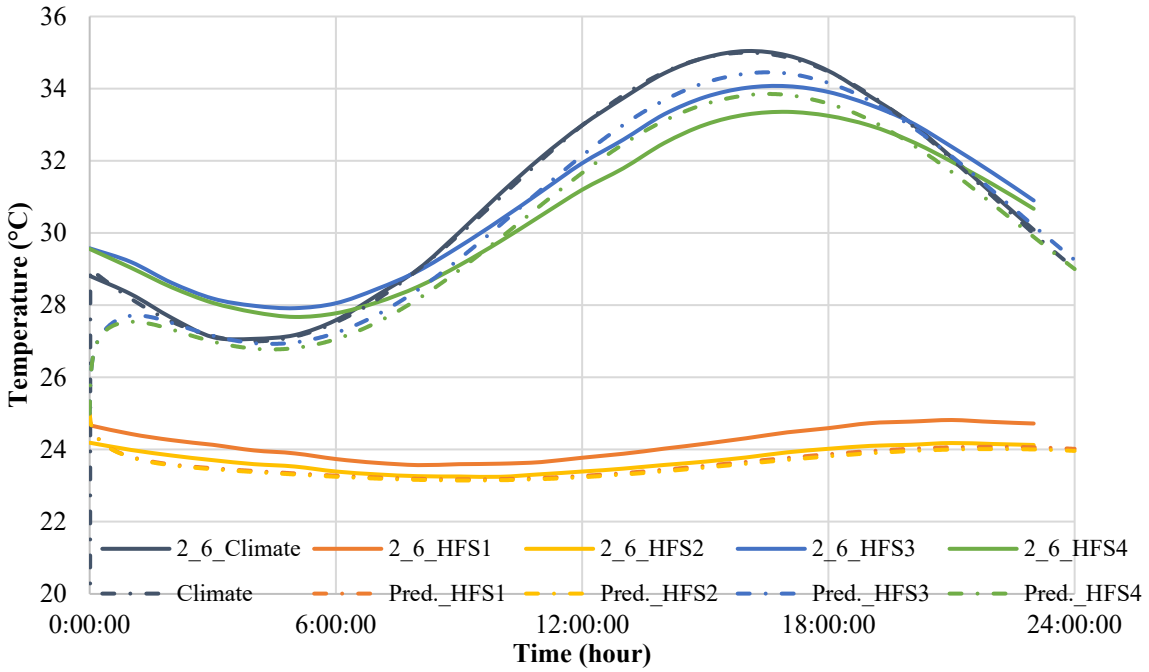

Figure 5-11 MATLAB Model Validation of Solid Grouted with Reflective Inserts Specimen Test No.2_6 (Flipped) Temperature Response

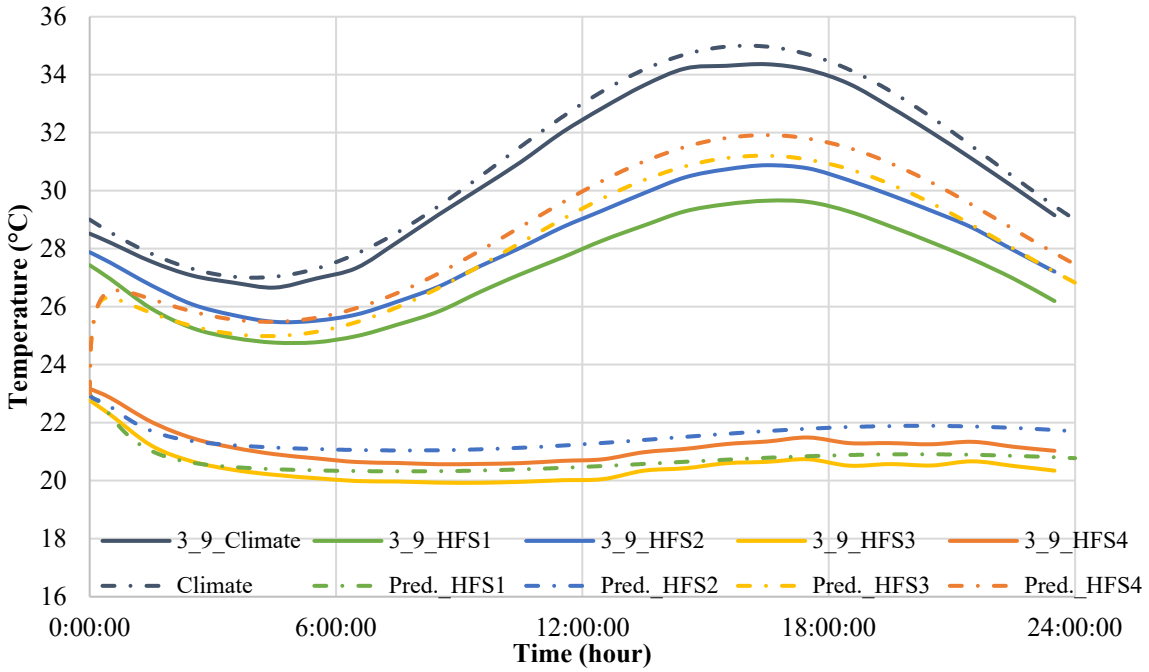

Figure 5-12 MATLAB Model Validation of 16-Inch Active Thermal Insulation Wall Specimen Test No.3_9 Temperature Response

These figures show that the MATLAB model generally predicted the behavior of proposed wall configurations well. The estimates for walls with airgaps were slightly biased. This was expected, as discussed previously, the analytical model ignored convection through the air gap, which may have caused some of the observed difference, with the measured $T_{in,\ max}$' values being higher than the predictions. For walls with reflective inserts, there was a larger difference between measured and predicted surface temperatures (Test 2-5). However, this may have been due to a loose sensor which would reduce the measured values. The temperature responses recorded by the sensors on interior surfaces were obviously slower to respond than other tests.

As $T_{d,\ max}$' value was used as an indicator of how well the wall system reduces heat loss/gain the building, and is proportional to HVAC demand, the predicted $T_{d,\ max}$' values of the tests specimens, along with the measured $T_{d,\ max}$ values are listed in Table 5-4. Note that the tolerance of sensors used in the tests was ±1°C. The difference between the MATLAB Model predictions (difference between measured and predicted temperature) are also listed in the Table 5-4.

Table 5-4: Measured and Predicted $T_{d,\ max}$' and Deviation of the Method

Test No.	Sensor 1			Sensor 2		
	Meas.	Pred.	Diff.	Meas.	Pred.	Diff.
1_1	3.66		**0.25**	3.58		**0.09**
1_2	3.68	3.4079	**0.27**	3.52	3.49	**0.03**
1_3	3.34		**-0.07**	3.18		**-0.31**
2_1	2.54	1.99	**0.55**	2.63	2.05	**0.58**

2_2	2.97	2.41	**0.56**	2.64	1.62	**1.02**
2_3	2.73	2.14	**0.59**	2.16	2.21	**-0.05**
2_4	2.63	2.54	**0.09**	2.45	1.73	**0.72**
2_5	2.87	2.04	**0.83**	2.81	2.11	**0.70**
2_6	2.84	2.43	**0.41**	2.22	1.64	**0.58**
3_1	-0.32	-0.25	**-0.07**	-2.03	-2.45	**0.42**
3_2	1.60	1.67	**-0.06**	0.98	0.66	**0.32**
3_3	3.58	3.58	**-0.01**	4.07	3.77	**0.30**
3_4	0.72	0.75	**-0.03**	-0.14	-0.49	**0.35**
3_5	1.40	1.39	**0.01**	0.94	0.55	**0.39**
3_6	-6.78	-7.08	**0.30**	-7.69	-7.51	**-0.19**
3_7	-4.41	-5.17	**0.76**	-4.34	-4.39	**0.05**
3_8	-2.05	-3.25	**1.20**	-0.99	-1.28	**0.30**
3_9	-0.38	-0.11	**-0.27**	-1.07	-1.09	**0.02**
3_10	1.52	1.57	**-0.05**	1.06	1.09	**-0.03**
3_11	3.40	3.25	**0.15**	3.18	3.28	**-0.10**
3_12	-	-	**-**	-	-	**-**
3_13	1.48	1.31	**0.17**	1.01	0.91	**0.10**
3_14	-6.57	-6.42	**-0.15**	-6.84	-6.49	**-0.35**
3_15	-4.06	-4.74	**0.67**	-4.14	-4.30	**0.16**
3_16	-2.26	-3.06	**0.79**	-1.81	-2.12	**0.31**
3_17	0.69	0.56	**0.13**	0.34	0.05	**0.29**
3_18	2.34	1.81	**0.53**	2.33	1.55	**0.78**

3_19	0.99	1.09	**-0.10**	0.80	0.79	**0.01**
3_20	1.42	1.51	**-0.08**	1.33	1.29	**0.04**
3_21	-5.69	-4.83	**-0.84**	-5.77	-4.59	**-1.16**
3_22	-4.57	-3.59	**-0.96**	-4.41	-3.08	**-1.30**
4_1	-1.24	-0.80	**-0.44**	-1.30	-0.93	**-0.37**
4_2	-2.86	-3.75	**0.89**	-3.12	-3.80	**0.68**
4_3	-1.32	-1.40	**0.08**	-1.82	-1.78	**-0.04**
4_4	-3.30	-3.87	**0.57**	-3.59	-3.82	**0.23**
4_5	-	-	**-**	-	-	**-**
4_6	-	-	**-**	-	-	**-**
4_7	1.41	0.74	**0.67**	0.69	0.17	**0.52**
4_8	-5.57	-5.01	**-0.56**	-5.43	-4.71	**-0.72**
4_9	0.07	0.05	**0.02**	-1.00	-1.01	**0.01**
4_10	-4.10	-4.88	**0.78**	-4.05	-4.38	**0.33**
4_11	0.27	-0.13	**0.40**	-1.62	-2.42	**0.80**
4_12	-5.62	-5.26	**-0.36**	-4.84	-4.42	**-0.42**

Note: The 8-inch specimen with pipe embedded at near interior side was damaged, thus Tests No.4_5 and No.4_6 were not conducted.

In general, the differences between measured and predicted $T_{d,max}$' values were within 0.5°C. In some cases, the difference was between 0.5°C and 1°C, well within the allowable error for the sensors (±1°C). In four of the test cases, out of forty-three tests, the differences were slightly larger than 1°C. The likely causes of the temperature differences are measurement error or faulty installations of the temperature sensors.

The results described above suggest that MATLAB analytical model is reasonably accurate over the range of specimens tested including the novel active thermal insulation system.

5.4. Performance of Active Thermal Insulation Wall System in U.S. Climate Zone Weather Conditions

In previous analyses, the proposed MATLAB models were used to evaluate the ATIWS in typical mild and extreme summer and winter weather conditions. However, these analyses are not sufficient to understand the performance of ATIWS in practice. In this part of the investigation, the verified MATLAB models were used to evaluate the behavior of ATIWS under typical U.S. Climate Zone weather conditions. This was done in an effort to compare the performance of ATIWS walls with conventional mass walls when they are both used to enclose conventionally conditioned spaces. As discussed previously, centrally located pipe with a spacing of 16 inches (0.4064 m) was chosen as an optimal option for ATIWS.

Two types of ATIWS were discussed in Chapter 2, an ATIWS DX and an ATIWS/GCHP. For the ATIWS DX, the fluid temperature can be taken as the yearly average air temperature on site, for ATIWS/GCHP, the fluid temperature can be varied. To investigate the performance of ATIWS/GCHP, two scenarios were assumed. ATIWS/GCHP Scenario A was designed to get match the heat flux of walls configured to meet the prescriptive U factor requirements of the building energy code(ASHRAE, 2019) as conventional insulated walls. ATIWS/GCHP Scenarios B was designed to obtain a zero heat flux through the wall. These two scenarios were designed to evaluate under which circumstances the ATIWS would work more efficiently, or be the most cost effective.

Five series of MATLAB simulations were conducted to evaluate the ATIWS under the two scenarios. These five were:

a). Series 1- Code Compliant: A code compliant exterior solidly grouted 8" CMU wall with insulation,

b). Series 2 – A Bare Wall: A solidly grouted 8" CMU (without insulation),

c). Series 3 - ATIWS DX: A solidly grouted 8" CMU with direct circulation pipes at 16" in center, with fluid temperature the same as the annual air temperature on site,

d). Series 4 - ATIWS/GCHP Scenario A: A solidly grouted 8" CMU with indirect circulation pipes at 16" in center, with a fluid temperature determined by getting equal or less heat flux through wall than the Code Compliant configurations. The fluid was assumed to circulate constantly,

e). Series 5 - ATIWS/GCHP Scenario B: A solidly grouted 8" CMU with indirect circulation pipes at 16" in center, with a fluid temperature determined by achieving near zero heat flux through the wall. The fluid was assumed to circulate constantly.

5.4.1. Temperature Conditions

The temperature conditions of the seven representative cities for the seven Climate Zones shown in Chapter 3 were listed in Table 5-5. Shown are the average high and low temperature of each season measured and recorded by the National Centers for Environmental Information by National Oceanic and Atmospheric Administration (U.S. Department of Commerce National Oceanic & Atmospheric Administration National Environmental Satellite). The stations where these data were generated was also shown in the Table.

Table 5-5: Temperature Condition of Seven Representative Cities by Season (°C)

Station	City	Zone	Season	Designation	Annual Average	Average High	Average Low
CAPE FLORIDA, FL US USC00081306	Miami, FL	1A	Spring	1A-SPG	24.8	27.0	20.9
			Summer	1A-SMR		31.1	25.2
			Autumn	1A-AUT		28.9	23.2
			Winter	1A-WNTR		24.3	17.4
HOUSTON WILLIAM P HOBBY AIRPORT, TX US USW00012918	Houston, TX	2A	Spring	2A-SPG	21.3	26.1	16.3
			Summer	2A-SMR		33.1	23.9
			Autumn	2A-AUT		27.1	17.2
			Winter	2A-WNTR		18.1	8.2
LAS VEGAS MCCARRAN INTERNATIONAL AIRPORT, NV US USW00023169	Las Vegas, NV	3B	Spring	3B-SPG	20.8	26.2	13.9
			Summer	3B-SMR		38.7	25.7
			Autumn	3B-AUT		26.8	14.8
			Winter	3B-WNTR		14.9	4.7
PALMER 3 ESE, WA US USC00456295	Seattle, WA	4C	Spring	4C-SPG	9.9	13.9	4.0
			Summer	4C-SMR		22.2	10.4
			Autumn	4C-AUT		14.9	5.9
			Winter	4C-WNTR		7.2	0.8
PARK FOREST, IL US USC00116616	Chicago, IL	5A	Spring	5A-SPG	10.1	14.8	4.2
			Summer	5A-SMR		27.8	17.1
			Autumn	5A-AUT		16.8	6.3
			Winter	5A-WNTR		0.8	-7.6
MINNEAPOLIS CRYSTAL AIRPORT, MN US USW00094960	Minneapolis, MN	6A	Spring	6A-SPG	7.6	13.6	1.7
			Summer	6A-SMR		27.6	15.4
			Autumn	6A-AUT		14.2	3.2
			Winter	6A-WNTR		-2.9	-12.3

DULUTH INTERNATIONAL AIRPORT, MN US USW00014913	Duluth, MN	7	Spring	7-SPG	4.3	9.2	-1.5
			Summer	7-SMR		23.2	11.7
			Autumn	7-AUT		10.4	1.3
			Winter	7-WNTR		-5.7	-15.0

5.4.2. Simulation Results

The MATLAB Model simulation results for the five series of simulations are shown in Table 5-6 (Solid Grouted Uninsulated Wall, Solid Grouted Insulated Wall-Code Compliant, Active Thermal Insulation Wall). The energy savings potential of the active thermal insulation wall system was evaluated by comparing the T_d at the interior surface of wall and the heat flux through the interior surface of wall for the five series of simulations. Note that a positive heat flux means heat goes from the concrete to the environment or fluid, and vice versa. These results were also plotted in Figures 5-13 to 5-19, for the seven Climate Zones, respectively.

Table 5-6: MATLAB Simulation Results for Active Thermal Insulation Walls in Seven Representative Cities by Season

Ambient Condition	Code Compliant		Solid Grouted		ATIWS DX			ATIWS/GCHP Scenario A				ATIWS/GCHP Scenario B			
	$T_{d,mean}$ (°C)	Heat Flux 1 (W/m^2)	$T_{d,mean}$ (°C)	Heat Flux 1 (W/m)	$T_{d,mean}$ (°C)	Heat Flux 1 (W/m)	Heat Flux 2 (W/m)	$T_{d,mean}$ (°C)	Heat Flux 1 (W/m)	Heat Flux 2 (W/m)	Fld. Temp (°C)	$T_{d,mean}$ (°C)	Heat Flux 1 (W/m)	Heat Flux 2 (W/m)	Fld. Temp (°C)
1A-SPG	0.16	0.7	0.58	5.8	0.97	9.8	9.8	0.16	0.6	-4.4	21.4	0.00	0.0	-6.0	20.7
1A-SMR	0.52	2.1	1.83	18.3	1.65	16.4	16.4	0.52	2.1	-13.7	20.0	0.01	0.0	-18.9	17.9
1A-AUT	0.34	1.4	1.21	12.1	1.31	13.1	13.1	0.35	1.4	-9.1	20.7	0.01	0.0	-12.5	19.3
1A-WNTR	-0.10	-0.4	-0.34	-3.4	0.48	4.9	4.9	-0.10	-0.4	2.5	22.3	-0.01	0.0	3.4	22.7
2A-SPG	-0.07	-0.3	-0.25	-2.5	-0.31	-3.1	-3.1	-0.08	-0.3	1.8	22.2	-0.01	0.0	2.5	22.5
2A-SMR	0.55	2.2	1.94	19.5	0.87	8.6	8.6	0.56	2.2	-14.5	19.9	0.02	0.0	-20.1	17.6
2A-AUT	0.01	0.0	0.03	0.3	-0.15	-1.5	-1.5	0.01	0.0	-0.3	21.9	0.00	0.0	-0.4	21.9
2A-WNTR	-0.75	-3.0	-2.63	-26.4	-1.59	-15.8	-15.8	-0.77	-3.1	19.6	24.8	-0.03	0.0	27.1	27.9
3B-SPG	-0.13	-0.5	-0.57	-5.7	-0.60	-6.0	-6.0	-0.14	-0.6	4.5	22.7	-0.01	0.0	5.8	23.3
3B-SMR	0.69	2.8	3.04	30.5	1.35	13.3	13.3	0.71	2.8	-24.4	18.0	0.02	0.0	-31.4	15.1
3B-AUT	-0.08	-0.3	-0.35	-3.5	-0.48	-4.8	-4.8	-0.09	-0.3	2.7	22.4	-0.01	0.0	3.5	22.8
3B-WNTR	-0.83	-3.4	-3.63	-36.3	-2.24	-22.3	-22.3	-0.86	-3.4	29.0	26.6	-0.04	0.0	37.4	30.1
4C-SPG	-0.75	-3.1	-3.88	-38.9	-4.96	-49.7	-49.7	-0.79	-3.1	32.4	27.5	-0.04	0.0	40.0	30.7

4C-SMR	-0.33	-1.3	-1.68	-16.9	-3.77	-37.9	-37.9	-0.35	-1.3	14.0	24.4	-0.02	0.0	17.3	25.8
4C-AUT	-0.67	-2.7	-3.43	-34.4	-4.72	-47.3	-47.3	-0.70	-2.7	28.7	26.9	-0.04	0.0	35.4	29.7
4C-WNTR	-1.04	-4.2	-5.35	-53.6	-5.75	-57.5	-57.5	-1.08	-4.2	44.7	29.6	-0.05	0.0	55.2	33.9
5A-SPG	-0.62	-2.5	-3.71	-37.2	-4.84	-48.5	-48.5	-0.66	-2.5	32.0	27.7	-0.04	0.0	38.3	30.3
5A-SMR	0.02	0.1	0.13	1.3	-2.77	-28.0	-28.0	0.02	0.1	-1.1	21.8	0.00	0.0	-1.3	21.7
5A-AUT	-0.52	-2.1	-3.10	-31.1	-4.51	-45.2	-45.2	-0.55	-2.1	26.8	26.8	-0.03	0.0	32.0	28.9
5A-WNTR	-1.26	-5.1	-7.55	-75.6	-6.91	-69.0	-69.0	-1.33	-5.1	65.1	33.6	-0.07	0.0	77.9	38.8
6A-SPG	-0.63	-2.6	-4.27	-42.8	-5.72	-57.3	-57.3	-0.67	-2.6	37.6	28.9	-0.04	0.0	44.0	31.5
6A-SMR	-0.02	-0.1	-0.14	-1.4	-3.50	-35.3	-35.3	-0.03	-0.1	1.2	22.2	-0.01	0.0	1.4	22.3
6A-AUT	-0.59	-2.4	-3.96	-39.7	-5.56	-55.7	-55.7	-0.63	-2.4	34.9	28.4	-0.04	0.0	40.9	30.9
6A-WNTR	-1.31	-5.3	-8.80	-88.2	-8.17	-81.5	-81.5	-1.38	-5.3	77.6	36.2	-0.09	0.0	90.8	41.6
7-SPG	-0.71	-2.9	-5.39	-54.0	-7.12	-71.3	-71.3	-0.76	-2.9	48.4	31.1	-0.05	0.0	55.6	34.0
7-SMR	-0.18	-0.7	-1.35	-13.5	-4.94	-49.7	-49.7	-0.19	-0.7	12.0	24.3	-0.02	0.0	13.8	25.0
7-AUT	-0.63	-2.6	-4.80	-48.1	-6.80	-68.2	-68.2	-0.68	-2.6	43.2	30.1	-0.05	0.0	49.5	32.7
7-WNTR	-1.27	-5.1	-9.62	-96.4	-9.40	-93.9	-93.9	-1.35	-5.2	86.5	38.2	-0.09	0.0	99.2	43.4

Note:

1. Heat Flux was average heat flux through the interior surface of wall, per effective width (0.4064 m), therefore the unit is W/m.
2. Heat Flux 1 was the heat flux through the interior surface of wall, Heat Flux 2 was the heat flux through the pipe.
3. Fld. Temp was fluid temperature required to get such performance.

The floating bar plots of Figures 5-13 through 5-19 show the range of T_d obtained from the simulations of each configuration ($T_{d,\,min}$ to $T_{d,\,max}$). The dashed line indicates the heat flux through interior surface of wall. The scatter data points are the fluid temperatures required to get the stated performance in each ATIWS/GCHP case.

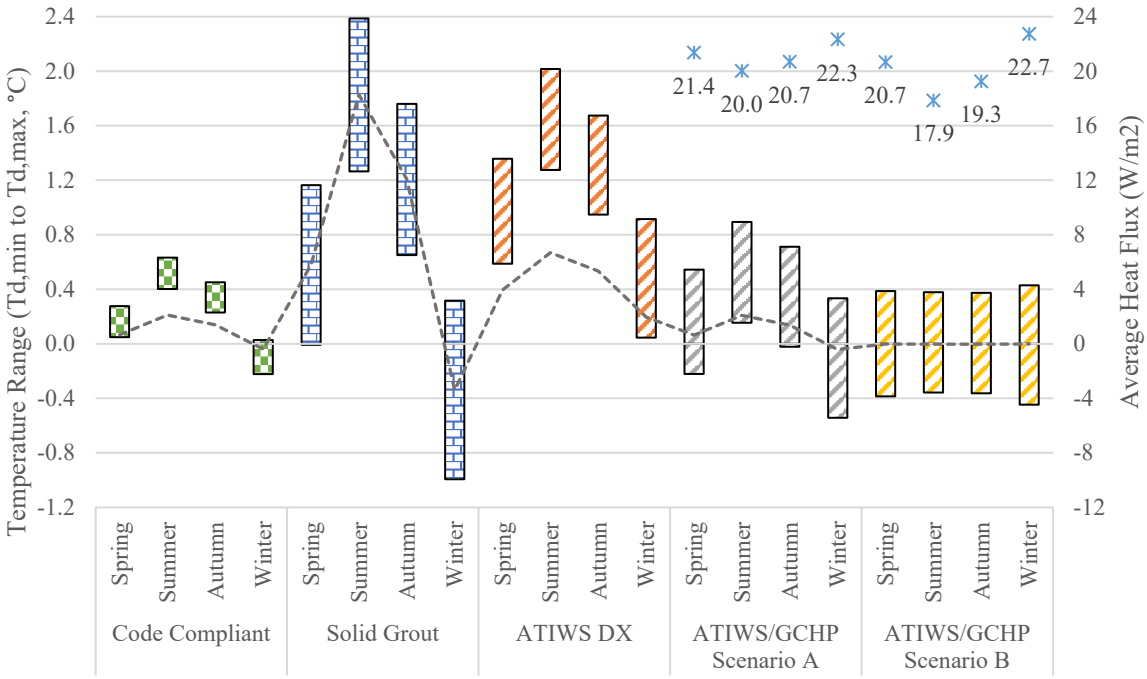

Figure 5-13 MATLAB Simulation of the Five Proposed Wall's Performance in Climate Zone 1A

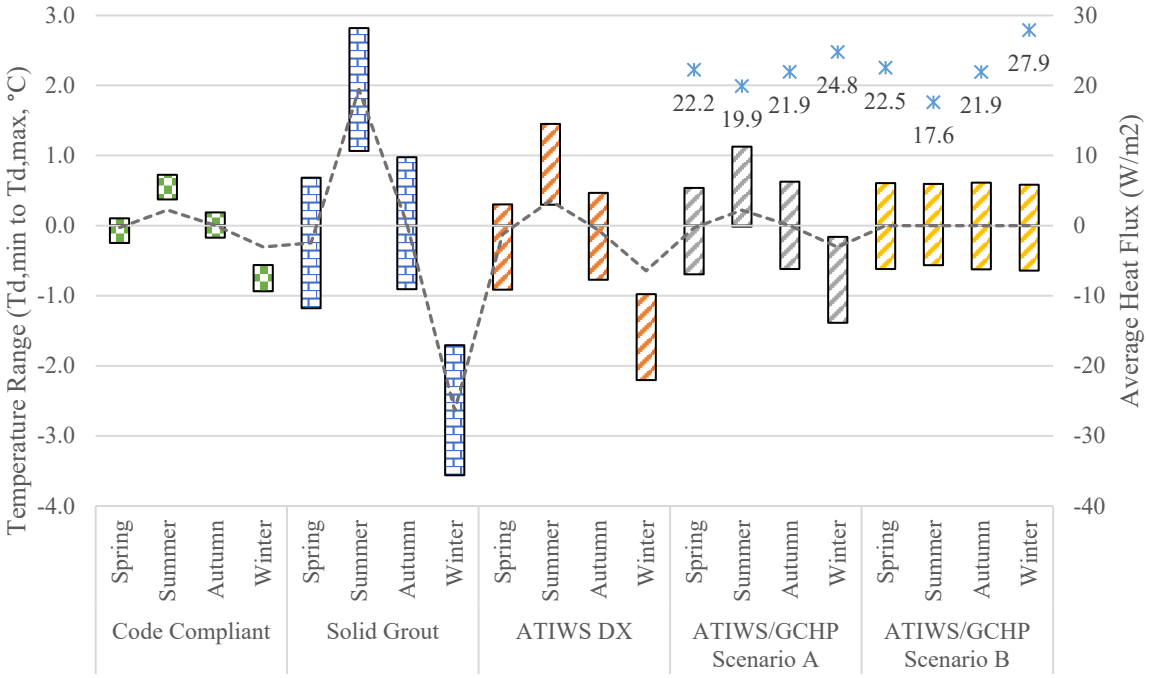

Figure 5-14 MATLAB Simulation of the Five Proposed Wall's Performance in Climate Zone 2A

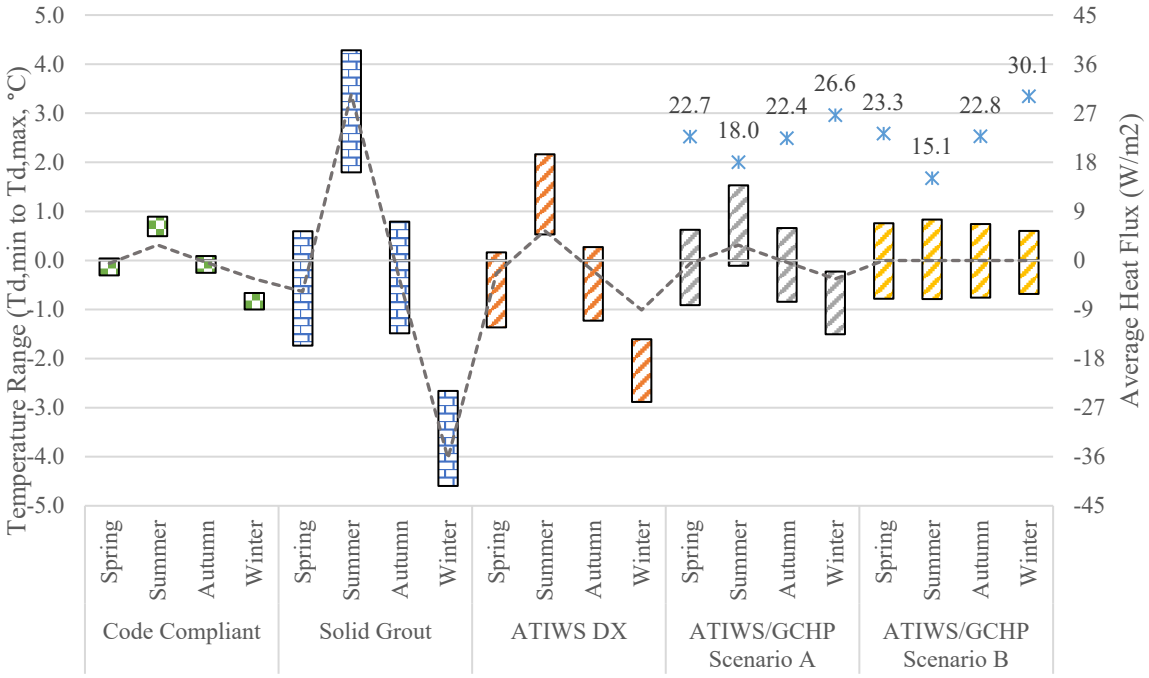

Figure 5-15 MATLAB Simulation of the Five Proposed Wall's Performance in Climate Zone 3B

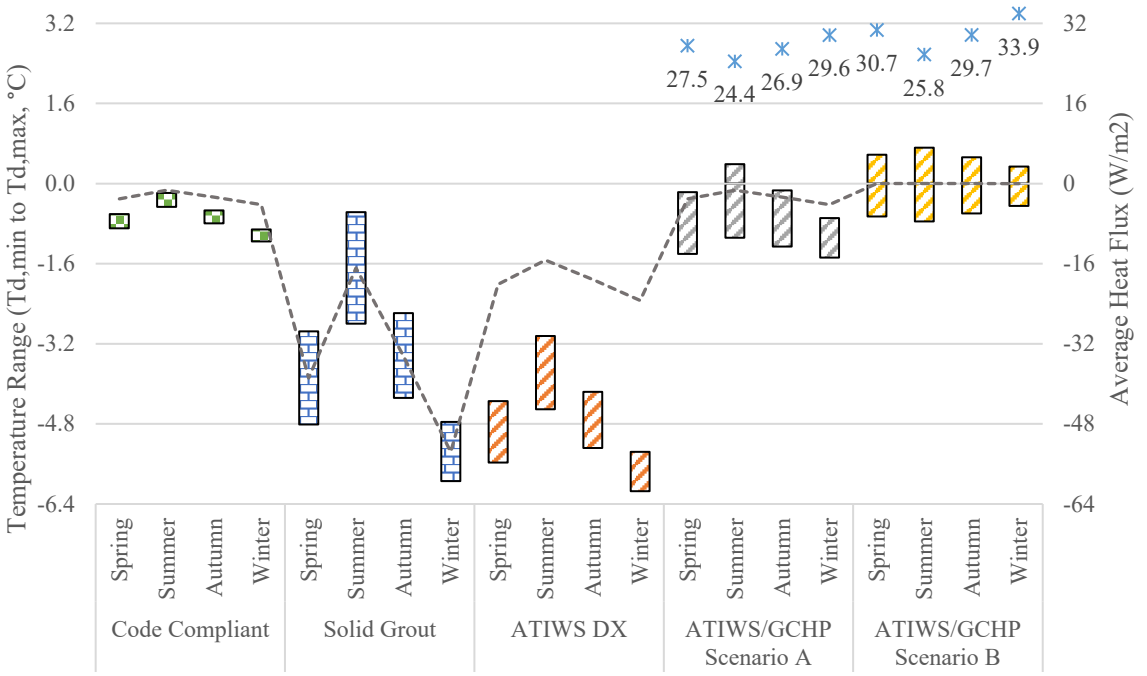

Figure 5-16 MATLAB Simulation of the Five Proposed Wall's Performance in Climate Zone 4C

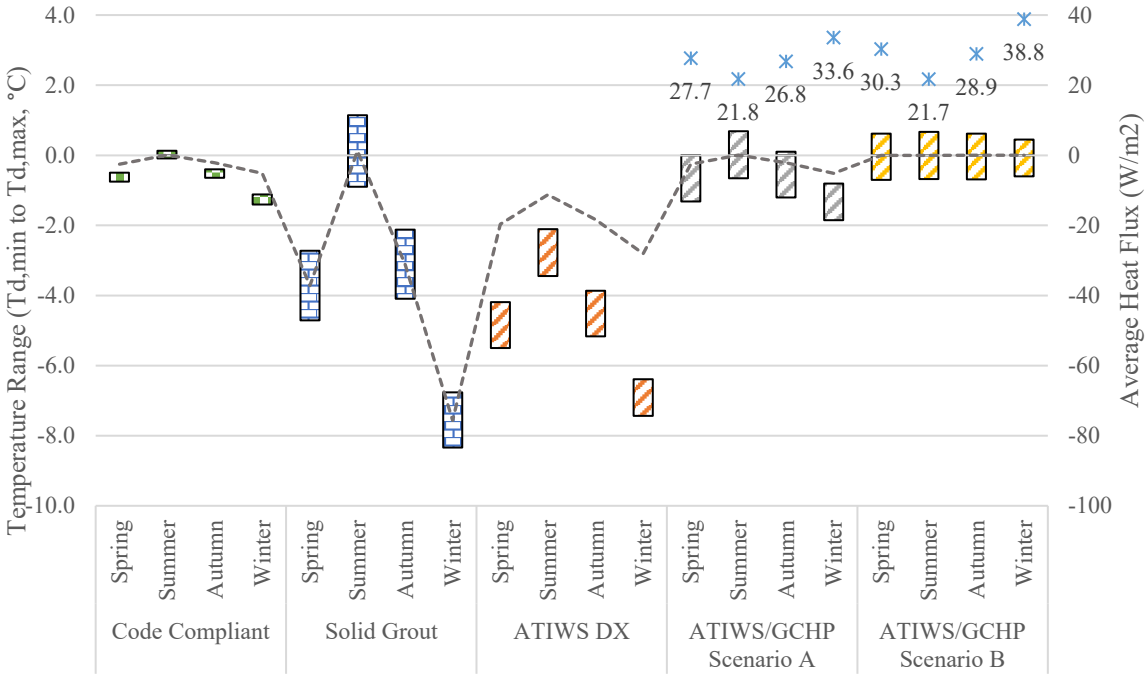

Figure 5-17 MATLAB Simulation of the Five Proposed Wall's Performance in Climate Zone 5A

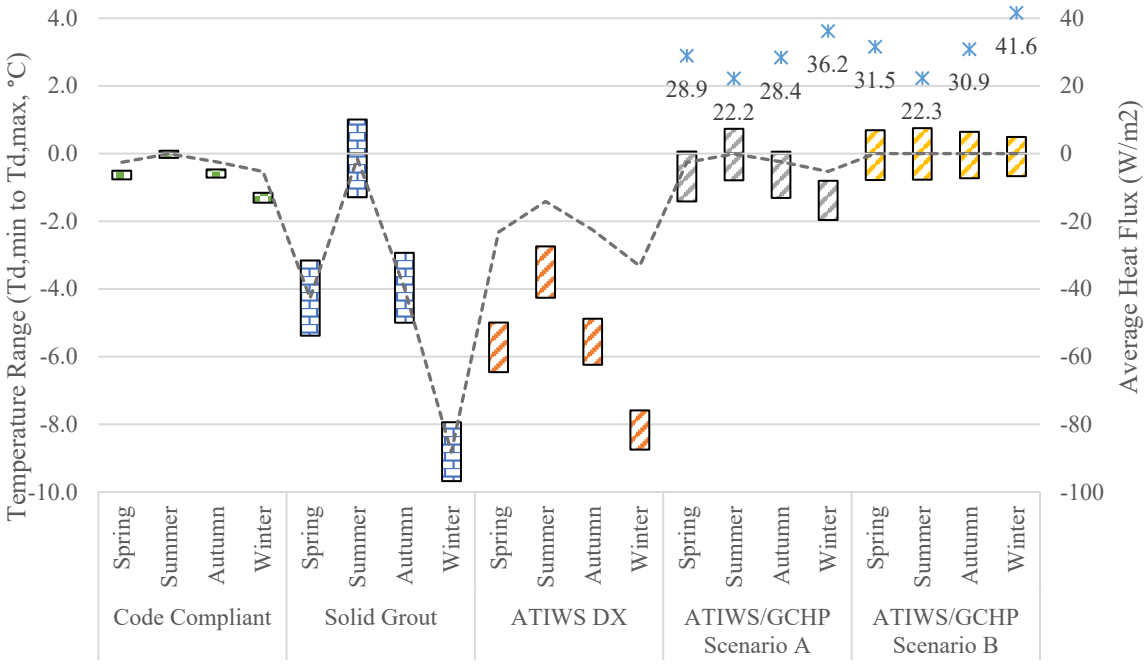

Figure 5-18 MATLAB Simulation of the Five Proposed Wall's Performance in Climate Zone 6A

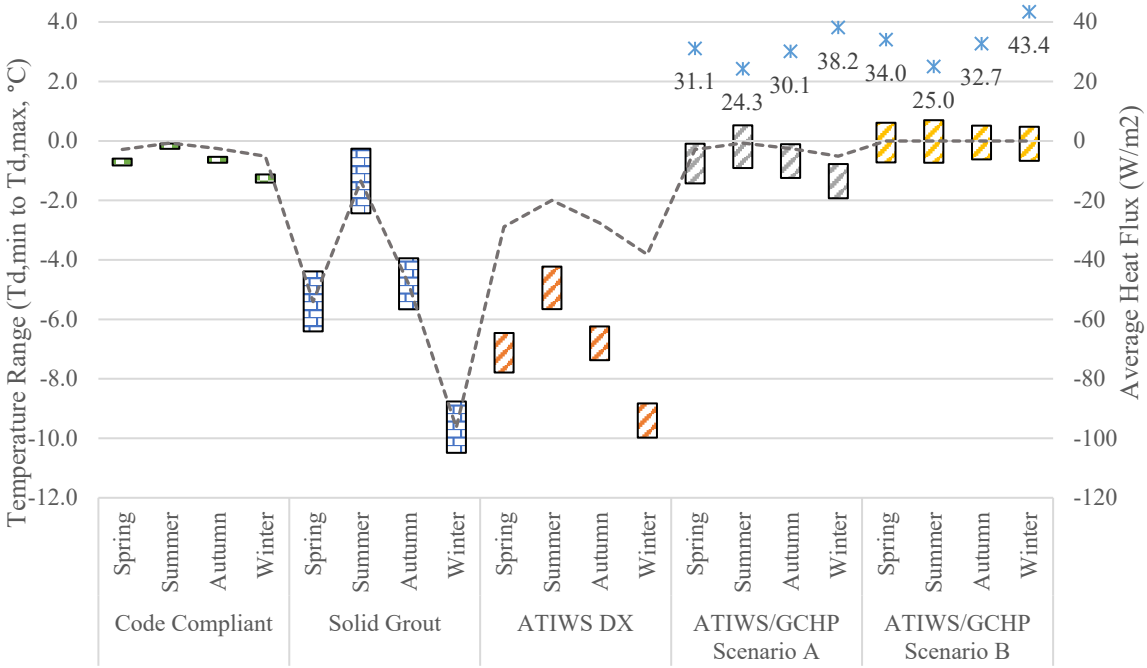

Figure 5-19 MATLAB Simulation of the Five Proposed Wall's Performance in Climate Zone 7

Examining the data in Table 5-6 and the plots in Figures 5-13 through 5-19 suggests that, for all Climate Zones three observations can be made. First, the Solidly Grouted (uninsulated) wall configurations and ATIWS DX (ground loop) showed less ability to maintain the indoor set point than the ATIWS/GCHP Scenario A and ATIWS/GCHP Scenario B. Second, the two ATIWS/GCHP scenarios could get equivalent or less heat flux through the walls compared to Code Compliant wall configurations with the noted fluid temperatures were used. Finally, walls without insulation allowed significantly larger fluctuations in the interior surface temperature did insulated wall configurations, although the fluctuation was within 2°C of the ATIWS configurations. This level of fluctuation will not seriously impact indoor comfort.

In Climate Zones 1A, the summer heat flux for the Solid Grout wall configuration in summer was positive, and for the ATIWS DX wall configuration was negative. This indicates that if fluid circulating speed and time was controlled instead of a constantly circulated, the total heat flux through the wall could reach a net zero condition. It was also seen that for this climate, fluid temperature of the two ATIWS/GCHP configurations was close to the annual average air temperature (24.8 °C).

In Climate Zones 2A, although the heat flux of ATIWS DX configurations was less than the Solid Grout configurations, it was still much higher than the Code Compliant baselines. Fluid temperatures for the two ATIWS/GCHP configurations were also close to the annual average air temperature (21.3 °C). In Climate Zones 3B, although the heat flux of the ATIWS DX configurations was less than Solid Grout configurations, it was still much higher than the Code Compliant baselines. The Fluid temperatures of the two ATIWS/GCHP configurations were not near the annual average air temperature (20.8 °C).

In Climate Zones 4C, heat flux of the ATIWS DX configurations was more than the Solid Grout configurations, which means the direct pumping system had negative impact on energy conservation. The fluid temperatures of the two ATIWS/GCHP configurations were at least 15°C higher than the annual average air temperature (9.9 °C). Solar panels may be able to heat up the fluids, but ground temperatures alone could not meet the demand, further investigation is needed.

In Climate Zone 5A, observations similar to those in for Climate Zone 4C can be made, except in summer. The summer heat flux of the Solid Grout case was positive and that of the ATIWS DX configuration was negative. This indicates that if fluid circulating speed and time was adjusted for the ATIWS DX configuration, the wall heat flux could be adjusted to zero. The fluid temperature of the two ATIWS/GCHP configurations were at least 10°C higher than the annual average air temperature (10.1 °C) and could not be achieved by ground coupling alone.

In Climate Zone 6A, observations similar to those described for Climate Zone 4C can be made. The fluid temperatures of the two ATIWS/GCHP configurations were at least 15°C higher than the annual average air temperature (7.6 °C), again not ground loop obtainable.

In Climate Zone 7, observations similar to those described for Climate Zone 4C can be made. The fluid temperature of the two ATIWS/GCHP configurations was at least 20°C higher than the annual average air temperature (4.3 °C) and not obtainable by ground loop coupling alone.

5.5. Discussion

As a result of the previous analyses, it can be concluded that the ATIWS DX wall system could be used in buildings to achieve code compliance in Climate Zone 1A in winter and Climate Zone 5A in summer. In these two Climate Zones, the ATIWS DX system can reduce the heat flux through walls to zero with only water pumping energy with variable pumping speeds or schedules. However, this system could also be used in other Climate Zones to at least reduce heating or cooling energy using only pumping energy. For example, this system could be used in places where the average annual temperature is higher than 22 °C and the winter temperature is lower than 22 °C, such as in Climate Zone 1A. It could also be used in places where average annual temperature is lower than 22 °C and winter temperature is lower than 22 °C, such as in Climate Zone 5A

However, MATLAB models do not give a compete assessment of the performance of the ATIWS DX wall system. A holistic building analysis must be used to further evaluate the performance of ATIWS DX and to observe how heating and cooling load it can take from conventional HVAC systems. As a result of the current study, we only know that the ATIWS DX system can reduce heat flux through the exterior walls and this reduce this part of a conventional HVAC load.

The analysis also shows that an ATIWS/GCHP system could be used in most building configuration to produce code compliant energy performance without significant wall insulation, especially with buildings that could take advantage of geothermal or solar heating or cooling resources. However, economic analyses are needed to determine if this system should be used to replace conventional systems.

CHAPTER 6

PAYBACK ANALYSIS

In previous analyses, yearly energy consumption used by buildings that incorporated various energy conservation measures was studied. However, the reduction in utility bills and initial investments on these measures were not addressed. Although some measures clearly had high energy conservation potential, high initial investment in these technologies and/or long payback periods would likely prevent owners or designers from adopting these measures. To determine the cost effectiveness of each conservation measure, payback analyses were conducted and used to evaluate the cost effectiveness of the proposed conventional energy conservation measures. Also investigated was the anticipated payback periods for the proposed ATIWS systems.

6.1. Payback Analysis Assumptions

6.1.1. Payback Analysis Assumptions for Conventional Energy Conservation Measures

32W T8 fluorescent lighting was one of the most common type of lights used in commercial buildings, therefore in this research, 32W T8s were assumed to be used in all proposed baseline models. However, prices of these lighting systems also varied. Typical costs for 32W T8 lighting was listed in Table 6-1. The average unit price of these T8 tubes

was $1.82 and life of 22500 hours, these values were used to calculate the cost of baseline prototypes on a per bulb per year. The time that the lighting was on was about 10 hours a day in the four prototypes studied.

Table 6-1: Available Lighting Bulbs for Baseline Prototypes

Brand	Type	Watt	Unit Price	Lumens	Average Life Hours
Sylvania	FO32/V41/ECO	32	$1.79	2450	22500
Sylvania	FO32/V35/ECO	32	$1.68	2450	22500
Sylvania	FO32/V65/ECO	32	$1.85	2400	22500
Sylvania	FO32/V50/ECO	32	$1.94	2450	22500
Average		32	$1.82	2437.5	22500

Average yearly cost for one lighting tube in Table 6-1 is $\frac{\$1.82}{22500/(365\times24\times(10/24))} = \$0.295$., normalized for the life of the bulb.

In this research, 25W T8 linear fluorescent lighting tubes were considered as a lighting upgrade and will achieve a 20% improvement in lighting efficiency. Fixtures and other accessories remain unchanged with these new bulbs, and was assumed to be the lowest cost lighting improvement available. Table 6-2 indicates the cost sand outputs of the improved lighting elements (25W T8 linear fluorescent lighting tubes). It should be noted that equivalent lumens as the baseline configuration with an average unit price of $3.64 and life of 30000 hours. These values were used to calculate the cost of proposed lighting efficiency improvements.

Table 6-2: Available Lighting Bulbs for Lighting Improved Prototypes

Brand	Type	Watt	Unit Price	Lumens	Average Life Hours

Philips	281238 F32T8/ADV841/XLLALTO25W	25	$7.18	2425	36000
Philips	282095 F32T8/ADV835/XEW/ALTO25W	25	$3.10	2500	30000
Philips	280792 F32T8/ADV850/XEW/ALTO25W	25	$2.01	2400	30000
SATCO/NUVO	F32/25WT8/850/ES /ENV	25	$4.31	2375	30000
Havells	1906	25	$0.99	2500	24000
Philips	13781-0	25	$2.94	2500	30000
SATCO/NUVO	F32/25WT8/841/ES /ENV	25	$4.31	2400	30000
SATCO/NUVO	F32/25WT8/835/ES/ENV	25	$4.31	2400	30000
Average		25	$3.64	2437.5	30000

Average yearly cost for one lighting tube in Table 6-2 is $\frac{\$3.64}{30000/(365\times24\times(10/24))} =$ $0.443 normalized for the life of the bulb.

The cost of HVAC system equipment varies widely, therefore the result of this study should only be used as an indicator of approximate performance. The cost of heat pumps, air conditioners, furnaces were based on Trane brand equipment and developed using Trane's online estimators(Trane, 2020). The unit prices for the baseline and upgraded systems are listed in the Tables 6-3 and 6-4 below. The payback analysis of boilers and chillers were not conducted because the price of this equipment varies greatly, there were not many types with different COPs available on market, and the efficiency curves of the equipment varies with occupancy and is thus hard to determine a COP increase. Payback analysis of furnaces were not conducted either because of the extra investment required to go from 80% to 90% to 95% efficiency will be hard to justify, as claimed by US DOE(Saver, 2020).

Table 6-3: Unit Price of Trane Heat Pumps

SEER	14	16	17	17	17.25	18	18	19.5	20
Price($/Ton)	1600	1667	2267	2267	2200	2733	3583	3750	4000

Table 6-4: Unit Price of Trane Air Conditioner

SEER	16	17	17	18	18	18	22
Price($/Ton)	1467	1867	1733	2067	2417	3000	3500

The price of heat pumps and air conditioners used in each building configuration were calculated using the unit prices provided in Tables 6-3 and 6-4 and the system configurations provided in the prototype building models. The SEER value nearest to the target COP value (configuration COP) and the corresponding unit price were used to determine the unit prices for these equipment.

All other costs, such as increased insulation, glasses and reflective paintings, and increment changes from the baseline configuration were based on national averaged installed costs listed in the 2018 Building Construction Costs with RSMeans data (76^{th} annual edition) (hereinafter called "RSMeans data") (Plotner & Company, 2018). Data from RSMeans addresses the price difference between cities and this index was used to adjust the estimates for the representative cities. The cost of the insulation changes thus varied with Climate Zone. Other costs were obtained directly from the manufacturers websites and did not vary with Climate Zones.

An example calculation of the differential cost for the wall insulation for Large Office Prototype Buildings in Climate Zone 1A is shown below. The city index was taken as 82/100, total wall area was 131,143 ft^2, the unit price including installation for R-5

insulation was \$1.08/ft^2 and for R-10 insulation was \$1.7/ft^2 (RSMeans, 2018). The extra cost for insulation upgrades for the Large Office prototype in Climate Zone 1A was:

$$131143 ft^2 \times (1.7 - 1.08)\, \$/ft^2 \times 82/100 = \$66{,}673$$

The rest of the incremental cost were determined using similar calculations.

6.1.2. Payback Analysis Assumptions for ATIWS

The costs of ATIWS systems were assumed to include both initial costs and running costs. For the ATIWS DX system, the initial costs included the cost of pipes, water pumps, and a reduction in wall insulation, as a negative cost. The running costs included the electrical consumption for water pumps balanced by any energy savings for the HVAC systems. For the ATIWS/GCHP systems, the initial costs included the cost of pipes, water pumps, heat pumps, the conventional HVAC system and reduction in wall insulation cost as a negative cost. Running costs included the electrical consumption for heat pumps and balanced by any energy savings with HVAC systems.

Payback analysis for ATIWS was conducted based on the simulations conducted in Chapter 5.4, using the MATLAB simulations. With the limitation of the analyses for these systems (circulating constant temperature fluids), the ATIWS DX did not support a complete replacement of the conventional HVAC systems, in most cases. This system configuration was only viable for providing all heating and cooling in buildings in Climate Zone 1A during winter, and in Climate Zone 5A during summer. Therefore, payback analysis for ATIWS DX was only conducted in buildings in these two Climate Zones.

6.1.2.1. Assumptions for ATIWS

In this analysis, we assumed there was a main loop for the ATIWS, subsystems were then connected to the main loop in order to provide additional heating or cooling, as needed to maintain fluid temperatures. The fluid temperatures of subsystem were assumed to be the same as the main loop, both for the inlet and outlet. In order to simplify the calculations, the maximum lifting head of the fluid for the four prototype buildings was assumed to be 100 meters (ground water harvesting).

Pipes were assumed to be 1-inch black steel pipes; the unit price is $18.95 per linear feet including labor.

In ATIWS/GCHP Scenario B configurations, the average heat flux through wall was designed to be zero, therefore, HVAC load was reduced in these configurations. In previously analyses, the ESPs of wall conventional insulation were used to determine how much energy the ATIWS DX and ATIWS/GCHP system can save in typical HVAC energy consumption. In ATIWS/GCHP Scenario A configurations, the HVAC energy consumption was assumed to be the same as the Code Compliant baselines, as their average heat flux values were very similar. In ATIWS DX configurations, the ATIWS DX was assumed to reduce the heating HVAC load and thus conventional HVAC system energy use in Climate Zone 1A by 50% in the winter and the HVAC cooling load by 50% in Climate Zone 5A in the summer. The pumps were only assumed to run 50% of the year.

As mentioned previously, Guohui Feng et.al. stated in their study that 60~70% of the heat loss of the envelope was through the wall when investigating buildings in a cold region in China (Feng et al., 2016). Haie Huo et. al. suggested that 55% of the total energy was lost through the walls in their research of buildings in four different climatic regions

in China (Huo et al., 2017). These investigations suggest that, if the heat flux through wall could be completely prevented, the tonnage of HVAC system would be less than half of baselines. Thus, the cost of HVAC systems for ATIWS DX and ATIWS/GCHP Scenario B configurations were assumed to be half that of baselines. Note that this estimate was very approximate.

6.1.2.2. Pumping Energy Calculation

To estimate the cost of water pumps, a total head loss of the pipeline system was calculated for each prototype buildings. The total length of pipelines in a building was the total area (A_{wall}) divide the effective width of pipeline (0.4064 m). The total head loss was estimated using the Hazen-Williams Equation shown below (2004a), the head loss per 100 feet was:

$$h_{100ft} = 0.2083(100/c)^{1.852} q^{1.852} / d_h^{4.8655}$$

Where the Hazen-Williams roughness constant c was 140 for ductile iron pipe, Volume flow (q) was in gal/min, the inside hydraulic diameter (d_h) was in inches.

For SI units, the head loss per 100 meters was:

$$h_{100m} = 0.7110(100/c)^{1.852} q^{1.852} / d_h^{4.8655}$$

Where the Hazen-Williams roughness constant c was 140, Volume flow (q) was in m^3/s, the inside hydraulic diameter (d_h) was in meters.

Pumping energy demanded to circulate the fluid was estimated using the equation provided by The Engineering Toolbox (EngineeringToolBox, 2009):

$$E_{pump} = q \cdot \rho \cdot g \cdot ht/\mu_p\mu_m = \rho g V \left(\frac{\pi D^2}{4}\right)\left(100 + \frac{A_{wall}}{0.4064} h_{100m}/100\right)/\mu_p\mu_m$$

To get a rough idea of the pipe pumping costs, both the pumping efficiency (μ_p) and motor efficiency (μ_m) were assumed to be about 0.9. Note that Volume flow (q) was in m^3/s, mean velocity of the fluid (V) was assumed as 0.25 m/s, the density (ρ) of the fluid was 997 kg/m^3, acceleration of gravity (g) was 9.81 m/s^2, differential head (ht) was in meters, pipe inner diameter (D) was 0.01905 m (0.75 inch), area of the wall (A_{wall}) was in m^2. E_{pump} was in watts.

In this analysis, since the pipe system was quite long, the differential head created by water lifting and total head loss of the system were considered. The total head loss of the four prototype buildings was assumed to be 100 meters, in practice, the head loss will likely be much lower than this value.

6.1.2.3. Power of Each Subsystem

To maintain the temperature of fluid at a reasonable range, it was assumed the ATIWS consisted of a main loop with sub-piping systems, and for each of these subsystems, the outlet fluid temperature was assumed to be 1°C lower than the inlet fluid temperature. The number of subsystems was varied with the building configurations and weather conditions. Based on these assumptions, the energy each pipe system can provide of as power (Watts, Power, "P_{sub}") is:

$$P_{sub} = \rho q c_p \Delta T_{i,o} = \rho V \left(\frac{\pi D^2}{4}\right) c_p \Delta T_{i,o}$$

The density (ρ), volume flow (q), mean velocity of the fluid (V) and pipe inner diameter (D) were defined previously, specific heat capacity (c_p) was 4.182 kJ/kg·K, $\Delta T_{i,o}$ was the temperature difference between the inlet and outlet temperature (1°C).

Based on the equation above, each pipe subsystem can provide a total wattage of 291 W. This value was used to with the heating and cooling demand to calculate the number of subsystems needed and thus the total pumping energy of the system.

6.1.2.4. Cost of GCHP and Water Pump

In ATIWS/GCHP Configurations, it was assumed that the GCHP was the source used to heat or cool the fluid. In Table 5-6, the heat flux through the pipes were used by the ATIWS in a number of ways. The heat flux through the pipes was used to determine the power (tonnage) of provided by the GCHP, the sum of heat flux through the pipes over a typical season temperature were used to estimate the electricity needed for the GCHP. The price and efficiency of GCHP varied, in this analysis, assumed unit cost of the GCHP was taken $3000/ton (or $3000/3517Watt) including pipelines embedded underground (PickHvac, 2021), the COP of GCHP was assumed to be 4.

It was also assumed that the price of water pumps was $1200 per 10000 gal/hour size (PondUSA.com, 2021).

6.1.2.5. Energy Saved in HVAC Energy Consumption When Using An ATIWS

As described at the beginning of this Chapter, the ESP of the exterior wall insulation configurations for the four prototype buildings were used to derive HVAC energy saved by ATIWS DX or ATIWS/GCHP configurations when the heat flux through wall was zero.

The equation to calculate this ESP was shown in Chapter 3.2.2, and the maximum ESPs values are listed in Table 6-5.

Table 6-5: The Maximum ESP of Wall Insulation in Seven Climate Zones

Climate Zone	Large Office	Secondary School	Standalone Retail	Midrise Apartment
1A	0.40%	1.98%	4.78%	3.59%
2A	0.33%	0.80%	3.73%	4.11%
3B	0.51%	1.39%	4.85%	6.89%
4C	0.71%	1.25%	4.62%	7.76%
5A	1.20%	2.76%	8.46%	8.26%
6A	1.62%	3.49%	9.33%	10.23%
7	1.19%	3.51%	9.35%	10.28%

Please note that this assumption is likely quite conservative, but it was done this way to conservatively assess the performance of these systems. The difference between using ATIWS and increasing wall insulation (to a value to achieve the listed maximum ESP) is that the ATIWS will also heat/cool the indoor environment. The wall insulation just reduces the rate of heat flux through the wall. However, the analysis conducted in this investigation was not sophisticated enough to assess this difference more accurately.

Figure 3-6 and Figure 3-7 shows that the heating and cooling energy for the prototype buildings was about 15% to 30% of the total yearly energy consumption, and this varied with building type and weather conditions. As stated previously, studies showed that about 50%, or more, of total heat flux through envelope was through the walls.

However, the ESP of wall insulation was less than 2% for the Large Office buildings, and also very small for other prototypes in warmer climate zones. Thus, it was assumed that the energy saving effect of ATIWS should be between the maximum ESP of wall insulation and half the percentage of the total energy used by the HVAC system in a year.

6.1.2.6. An Example for ATIWS/GCHP

For the Large Office prototype building, in Climate Zone 1A, with a ATIWS/GCHP Scenario A, the increase in initial cost included the cost of GSHP and pipes, and the decrease in initial cost for the less insulation. The increase in running costs (electricity) included the GCHP and pumping.

The final increase in initial cost was:

$$Cost_{initial} = Cost_{GHE} + Cost_{Pipe} + Cost_{Pump} - Saving_{Insulation}$$

The maximum heat flux through pipe is -13.68 W/m per width (pipe spacing is 16 inches) of the wall, therefore is -33.66 W/m^2. The total wall area of Large Office prototype is 12183.6 m^2, the minimum tonnage required was thus 408,318 W (117 tons). The cost of the GCHP is taken as $351,000.

The unit cost of pipe was $18.95/ft, and the city index was 82/100. The total length of pipeline is 12183.6/0.4064=29979 m. Total cost for pipeline is 18.95×82/100×(1/0.3048) ×29979=$1,528,376.

The power of each subsystem was 291 W, the minimum tonnage required is 408318 W, resulted in a total of 1403 subsystems. The size required for the pump is (0.25×π×

(0.01905/2)^2) × 1403=0.1 m^3/s=95102 Gal/hour. The cost of this pump is 1200 × 10=$12,000.

The unit cost of the insulation was $1.08/$ft^2$, and the city index is 82/100. The Total cost for pipes is 1.08×82/100×(1/0.092903)×12183.6=$116140.

Therefore, the total increase in initial cost is $351000+$1528376+$12000-$116140=$1775236.

The final increase in electricity cost is:

$$Bill = Bill_{GCHP} + Bill_{Pumping}$$

The average heat flux through pipe was (4.37+13.68+9.07+2.46)/4=7.39 W/m per effective width, therefore 18.20 W/m^2. Total yearly energy consumed by GCHP was 18.20 ×12183.6×365×24/4=485487 kWh.

The total head loss of system was 29979/100×0.7110×(100/140)^1.852×(0.25×π ×(0.01905/2)^2)^1.852/ 0.01905^4.8655 = 558 m. The pumping energy required for the system was 997×9.81×0.25×π×(0.01905/2)^2×(100+558)/(0.9×0.9)=566 W. The yearly consumption for pumping was 566×365×24/1000=4959 kWh

Therefore, the total yearly energy consumption saving was -485487-4959=-490446 kWh

The initial cost and running costs both increased, so no payback period could be determined, and the economics of this systems is questionable within the constraints of the analysis.

6.2. Payback Analysis Results

6.2.1. Large Office

The total lighting power budget for the Large office baseline prototype was 408842W (compact fluorescent lamps) based on the OpenStudio analysis, resulted a total of 12777 count of 32 W fluorescent tubes. The HVAC systems equipment used in Large Office baseline prototype included four heat pumps with COP of 3.4 (one 100~117-ton unit, two 3-ton units, one 22~23-ton unit), one 614~734-ton chiller with a COP of 5.5, and two boilers with an efficiency of 0.8 (one 124~143-ton, one 344~672-ton. The efficiency and tonnages varied with Climate Zones.

The result of the payback analysis for the Large Office prototype configuration, in all seven Climate Zones, are shown in Table 7-6. In all Climate Zones, switching to higher efficiency lighting tubes saves a considerable amount of energy and money with a small yearly initial investment. Other than that, improved air conditioner COP significantly increased initial investment but produce only a small reduction in yearly electricity bills, with paid backs up to 20 years in Climate Zones 1A & 2A, and within 30 years in Climate Zones 3B, 5A, 6A. The payback periods in the other climate zones, and for the other energy conservation measures are more than 40 years.

The payback analysis for ATIWS/GCHP Scenario A and B showed that both initial costs and running costs increased, thus no payback could be calculated. However, these results are likely due, at least in part, from the very conservative assumptions used in the analyses. The actual saving in HVAC systems energy would likely be much higher than assumed. Furthermore, the ESP of the wall insulation that was used to establish the HVAC energy saving of the ATIWS, this likely much too conservative. This result was found to

be similar for other three protypes, as well. However, the ATIWS DX system worked well with a relatively short payback period in Climate Zone 5A. This result was consistent with the other three prototype buildings, as well, especially when a saving in conventional reinforcement rebar was considered.

Table 6-6: Payback Analysis for the Large Office Prototype in Seven Climate Zones

Climate Zone	Description	Total Site Energy (GJ)	Electric Consumption (kWh)	Gas Consumption (k ft3)	Percentage Difference (%)	Extra Cost ($)	Energy Saved ($/Year)	Payback Period (Year)
1A	Baseline	39271.8	10791269.4	401.2	0.00%			
	Wall Insulation R 5 to 10 Btu/ft·h°F	39205.1	10773227.8	399.4	0.17%	66673	1378	48.4
	Roof Insulation R 20 to 40 Btu/ft·h°F	39260.0	10788469.4	399.6	0.03%	71704	229	313.0
	Lighting Tubes 32W to 25 W	38320.1	10526850.0	401.4	2.42%	1891/yr	19909	*[a]
	Peak Lighting Demand reduced by 30%	38380.2	10543277.8	402.3	2.27%	-[b]	18661	-
	COP 3.4 to 4.17	38329.8	10529591.7	401.2	2.40%	275200	19704	14.0
	COP 5.5 to 6.05	38892.0	10685755.6	401.2	0.97%	-	7945	-
	Boiler efficiency 0.8(normal) to 0.92(high efficiency)	39269.6	10791269.4	399.1	0.01%	-	24	-
	Glass thickness 3.9 to 7.8, 8.6 to 17.2 mm & Air gap double	39167.4	10765455.6	390.3	0.27%	2637127	2066	1276.3
	Set Point [21, 24] to [23, 26] °C	38311.4	10514936.1	433.7	2.45%	-	20444	-
	Set Point [21, 24] to [20, 25] °C	38680.4	10632161.1	383.6	1.51%	-	12178	-
	Reflectance value 0.3 to 0.7	39163.0	10760158.3	404.2	0.28%	164532	2309	71.3
	ATIWS DX	39251.8	10785773.8	401.0	0.05%	1417036	416	3405.4
	ATIWS/GCHP Scenario A	41037.4	11281716.5	401.2	-4.50%	1775236	-36931	-
	ATIWS/GCHP Scenario B	41545.7	11423372.3	399.6	-5.79%	1809636	-47579	-
2A	Baseline	38295.6	10451288.9	635.9	0.00%	0	0	0.0
	Wall Insulation R 5 to 10 Btu/ft·h°F	38240.9	10444072.2	608.7	0.14%	69113	731	94.5
	Roof Insulation R 25 to 50 Btu/ft·h°F	38275.1	10448627.8	625.6	0.05%	88997	272	327.7
	Lighting Tubes 32W to 25 W	37364.8	10190430.6	643.8	2.43%	1891	19930	*

	Peak Lighting Demand reduced by 30%	37458.0	10212150.0	658.0	2.19%	-	18174	-
	COP 3.4 to 4.17	37303.2	10175605.6	636.0	2.59%	288100	21117	13.6
	COP 5.5 to 6.05	38030.5	10377650.0	635.9	0.69%	-	5641	-
	Boiler efficiency 0.8(normal) to 0.92(high efficiency)	38267.5	10451288.9	609.3	0.07%	-	175	-
	Glass thickness 3.9 to 7.8, 8.6 to 17.2 mm & Air gap double	38139.6	10433069.4	550.3	0.41%	2733608	1957	1397.0
	Set Point [21, 24] to [23, 26] ℃	37552.4	10187733.3	830.8	1.94%	-	18912	-
	Set Point [21, 24] to [20, 25] ℃	37654.1	10313283.3	498.8	1.68%	-	11469	-
	Reflectance value 0.3 to 0.7	38231.2	10428413.9	652.9	0.17%	170552	1641	103.9
	ATIWS/GCHP Scenario A	40453.3	11050639.0	635.9	-5.63%	1981703	-45910	-
	ATIWS/GCHP Scenario B	41149.6	11244673.3	633.8	-7.45%	2075503	-60760	-
	Baseline	35508.3	9619611.1	831.9	0.00%			
	Wall Insulation R 5 to 10 Btu/ft·h°F	35427.6	9609869.4	788.7	0.23%	84561	989	85.5
	Roof Insulation R 25 to 50 Btu/ft·h°F	35477.3	9616911.1	811.7	0.09%	108891	327	332.6
	Lighting Tubes 32W to 25 W	34631.7	9359933.3	887.1	2.47%	1891	18546	*
	Peak Lighting Demand reduced by 30%	34622.3	9366430.6	856.0	2.50%	-	18275	-
	COP 3.4 to 4.17	34914.1	9454563.9	831.9	1.67%	296700	12015	24.7
3B	COP 5.5 to 6.05	35344.1	9574002.8	831.9	0.46%	-	3320	-
	Boiler efficiency 0.8(normal) to 0.92(high efficiency)	35457.0	9619611.1	783.3	0.14%	-	315	-
	Glass thickness 3.9 to 7.8, 8.6 to 17.2 mm & Air gap double	35285.9	9586241.7	734.9	0.63%	3344649	3058	1093.6
	Set Point [21, 24] to [23, 26] ℃	34633.4	9287252.8	1136.7	2.46%	-	22217	-
	Set Point [21, 24] to [20, 25] ℃	34832.5	9459047.2	739.3	1.90%	-	12290	-
	Reflectance value 0.3 to 0.7	35462.8	9596941.7	866.1	0.13%	208675	1428	146.1
	ATIWS/GCHP Scenario A	36958.6	10022475.7	831.9	-4.08%	2557328	-29329	-

	ATIWS/GCHP Scenario B	37190.7	10088216.0	827.6	-4.74%	2670128	-34087	-
4C	Baseline	32975.5	8630075.0	1807.7	0.00%			
	Wall Insulation R 10 to 20 Btu/ft·h°F	32866.4	8636813.9	1681.3	0.33%	157278	335	470.1
	Roof Insulation R 30 to 60 Btu/ft·h°F	32947.3	8630863.9	1778.3	0.09%	128304	148	865.5
	Lighting Tubes 32W to 25 W	32208.0	8377819.4	1941.0	2.33%	1891	21857	*
	Peak Lighting Demand reduced by 30%	32220.1	8393858.3	1897.8	2.29%	-	20727	-
	COP 3.4 to 4.17	32718.2	8558602.8	1807.7	0.78%	309600	6475	47.8
	COP 5.5 to 6.05	32929.3	8617250.0	1807.7	0.14%	-	1162	-
	Boiler efficiency 0.8(normal) to 0.92(high efficiency)	32800.1	8630075.0	1641.5	0.53%	-	1243	-
	Glass thickness 6 to 12 mm	32947.2	8632858.3	1771.4	0.09%	3485605	20	178684.3
	Set Point [21, 24] to [23, 26] ℃	32994.6	8445613.9	2455.3	-0.06%	-	11868	-
	Set Point [21, 24] to [20, 25] ℃	32779.1	8517644.4	2005.2	0.60%	-	8709	-
	Reflectance value 0.3 to 0.7	32988.1	8621947.2	1847.4	-0.04%	211083	439	480.5
	ATIWS/GCHP Scenario A	40075.8	10602369.9	1807.7	-21.53%	2910658	-178690	-
	ATIWS/GCHP Scenario B	41501.4	11002132.2	1794.9	-25.86%	3070858	-214813	-
5A	Baseline	36834.9	9215544.4	3468.0	0.00%			
	Wall Insulation R 10 to 20 Btu/ft·h°F	36631.1	9215533.3	3274.9	0.55%	180152	1359	132.6
	Roof Insulation R 30 to 60 Btu/ft·h°F	36782.5	9215247.2	3419.3	0.14%	146964	370	397.7
	Lighting Tubes 32W to 25 W	36058.9	8957225.0	3614.0	2.11%	1891	22791	*
	Peak Lighting Demand reduced by 30%	36098.0	8980205.6	3572.5	2.00%	-	20963	-
	COP 3.4 to 4.17	36402.8	9095766.7	3467.2	1.17%	309600	11050	28.0
	COP 5.5 to 6.05	36715.8	9182411.1	3468.2	0.32%	-	3054	-
	Boiler efficiency 0.8(normal) to 0.92(high efficiency)	36433.9	9215544.4	3088.0	1.09%	-	2672	-

	Glass thickness 6 to 12 mm	36783.9	9217761.1	3412.1	0.14%	3992542	189	21174.9
	Set Point [21, 24] to [23, 26] ℃	36534.2	9013827.8	3871.3	0.82%	-	15763	-
	Set Point [21, 24] to [20, 25] ℃	36157.5	9099172.2	3223.1	1.84%	-	12451	-
	Reflectance value 0.3 to 0.7	36869.6	9205369.4	3535.6	-0.09%	241782	463	522.0
	ATIWS DX	33425.9	8362658.2	3147.1	9.25%	2153827	80892	26.6
	ATIWS/GCHP Scenario A	44240.7	11272709.4	3468.0	-20.11%	3700520	-189671	-
	ATIWS/GCHP Scenario B	45245.3	11563907.2	3426.6	-22.83%	3920120	-216228	-
6A	Baseline	37923.6	9044783.3	5082.6	0.00%			
	Wall Insulation R 10 to 20 Btu/ft·h°F	37632.9	9044500.0	4808.0	0.77%	158324	1974	80.2
	Roof Insulation R 30 to 60 Btu/ft·h°F	37853.9	9044208.3	5018.4	0.18%	129157	515	250.6
	Lighting Tubes 32W to 25 W	37269.1	8788625.0	5336.3	1.73%	1891	25510	*
	Peak Lighting Demand reduced by 30%	37239.9	8814891.7	5219.0	1.80%	-	23541	-
	COP 3.4 to 4.17	37542.9	8939047.2	5082.5	1.00%	311800	11272	27.7
	COP 5.5 to 6.05	37826.0	9017638.9	5082.7	0.26%	-	2893	-
	Boiler efficiency 0.8(normal) to 0.92(high efficiency)	37303.9	9044783.3	4495.2	1.63%	-	4159	-
	Glass thickness 6 to 12 mm	37825.5	9046322.2	4984.3	0.26%	3508798	532	6600.8
	Set Point [21, 24] to [23, 26] ℃	37752.6	8858902.8	5554.7	0.45%	-	16472	-
	Set Point [21, 24] to [20, 25] ℃	37004.1	8934205.6	4588.4	2.42%	-	15286	-
	Reflectance value 0.3 to 0.7	37967.9	9035952.8	5154.7	-0.12%	212488	431	493.5
	ATIWS/GCHP Scenario A	46882.1	11533257.9	5082.6	-23.62%	3789745	-265271	-
	ATIWS/GCHP Scenario B	47788.8	11809271.1	5000.2	-26.01%	4022745	-294111	-
7	Baseline	36406.3	8781966.7	4541.2	0.00%			
	Wall Insulation R 12.5 to 25 Btu/ft·h°F	36200.5	8786897.2	4329.3	0.57%	173025	975	177.5

Roof Insulation R 35 to 70 Btu/ft·h°F	36328.0	8781850.0	4467.4	0.22%	145405	535	271.8
Lighting Tubes 32W to 25 W	35428.9	8530300.0	4473.5	2.68%	1891	27307	*
Peak Lighting Demand reduced by 30%	35624.9	8553475.0	4580.2	2.15%	-	24081	-
COP 3.4 to 4.17	36136.7	8704466.7	4550.1	0.74%	313900	8199	38.3
COP 5.5 to 6.05	36344.7	8764486.1	4542.5	0.17%	-	1855	-
Boiler efficiency 0.8(normal) to 0.92(high efficiency)	35867.4	8781966.7	4030.4	1.48%	-	3617	-
Glass thickness 6 to 12 mm & Air gap 6 to 12 mm	35744.3	8806950.0	3828.5	1.82%	3349759	2383	1405.7
Set Point [21, 24] to [23, 26] ℃	36238.8	8599052.8	5006.6	0.46%	-	16204	-
Set Point [21, 24] to [20, 25] ℃	35506.9	8668661.1	4075.4	2.47%	-	15377	-
Reflectance value 0.3 to 0.7	36443.8	8773836.1	4604.5	-0.10%	202856	419	484.7
ATIWS/GCHP Scenario A	47658.3	11907504.7	4541.2	-30.91%	2021980	-333182	-
ATIWS/GCHP Scenario B	48886.6	12264539.1	4487.3	-34.28%	2042780	-370860	-

Note:

a. Since the lights often won't last 20 years, extra cost for lighting tubes is calculated as extra cost per year, not one-time cost as other renovation methods, thus no payback period needed for lighting tubes retrofit.

b. If there was no cost, or the payback period was negative, it was shown a "-".

6.2.2. Secondary School

The yearly lighting energy power demand for the baseline prototype was 196,022 W, based on the OpenStudio analysis. Thus, the total number of lighting tubes installed was 6126. HVAC systems equipment used in the Secondary School baseline prototype in Climate Zones 1A & 2A were six heat pumps with COP's ranging from 3.466 to 3.865 (two 9.0~9.5-ton units, two 10~10.5-ton units and two 31.5~33.5-ton units), two 336~345-ton chillers with COP of 5.766 to 6.280. The HVAC systems used in Climate Zone 3B, 4C, 5A, 6A, 7 were three air conditioners with COP's ranging from 3.4 to 3.8 (two 10~12-ton, one 29.5 to 37-ton), two 214 to 374-ton chiller with COP's of 5.329, eight boiler with efficiency of 0.8 (four 7.5~18.5-ton, two 39~66.5-ton, two 146~279-ton). Efficiencies and tonnages vary with Climate Zones. Not that no paybacks were determine for the bailer systems as discussed previously.

The payback analysis for Secondary School prototype in the seven Climate Zones are shown in Table 7-7. In all Climate Zones, switching to higher efficiency lighting tubes saves considerable amounts of energy and money with a relatively small initial investment. Other than that, in Climate Zone 1A, doubling the baseline wall insulation may result in a paid back of up to 19 years. Increased exterior wall reflectance (typically using coatings) can reduce electricity consumption in warmer regions (Climate Zone 1A & 2A), and payback periods for these coatings produce paybacks of roughly 27 or 28 years. The data shows that the cost of adopting higher efficiency air conditioners in Climate Zone 7 can be recovered in about 38 years. The payback periods of other energy conservation measures are more than 40 years.

Table 6-7: Payback Analysis for Secondary School Prototype in Seven Climate Zones

Climate Zone	Description	Total Site Energy (GJ)	Electric Consumption (kWh)	Gas Consumption (k ft3)	Percentage Difference (%)	Extra Cost ($)	Energy Saved ($/Year)	Payback Period (Year)
1A	Baseline	10811.8	2748119.4	870.6	0.00%			
	Wall Insulation R 5 to 10 Btu/ft·h°F	10728.2	2724955.6	870.4	0.77%	31590	1747	18.1
	Roof Insulation R 20 to 40 Btu/ft·h°F	10758.5	2733388.9	870.4	0.49%	235588	1112	211.9
	Lighting Tubes 32W to 25 W	10250.4	2592344.4	870.1	5.19%	907	11736	*
	Peak Lighting Demand reduced by 30%	10334.8	2615613.9	870.7	4.41%	-	9977	-
	All Heat Pump COP changed to 4.22	10739.8	2728105.6	870.6	0.67%	221900	1507	147.2
	Chiller COP 6.28 to 6.908	10586.1	2685422.2	870.6	2.09%	-	4721	-
	Glass thickness 3.9 to 7.8, 8.6 to 17.2 mm & Air gap double	10765.7	2735277.8	870.7	0.43%	1188243	966	1229.9
	Set Point [21, 24] to [23, 26] ℃	9372.4	2348286.1	870.6	13.31%	-	30107	-
	Set Point [21, 24] to [20, 25] ℃	10029.9	2531013.9	870.4	7.23%	-	16351	-
	Reflectance value 0.3 to 0.7	10673.4	2709616.7	870.8	1.28%	77955	2897	26.9
	ATIWS DX	10803.8	2746078.4	870.0	0.07%	671512	161	4172.6
	ATIWS/GCHP Scenario A	11649.8	2980887.9	870.6	-7.75%	843112	-17527	-
	ATIWS/GCHP Scenario B	11750.8	3013997.0	853.4	-8.68%	821378	-19827	-
2A	Baseline	11056.4	2801027.8	921.9	0.00%			
	Wall Insulation R 5 to 10 Btu/ft·h°F	11021.0	2791038.9	922.5	0.32%	32745	762	43.0
	Roof Insulation R 25 to 50 Btu/ft·h°F	11037.0	2795613.9	922.0	0.18%	292406	414	706.4
	Lighting Tubes 32W to 25 W	10472.1	2638716.7	921.9	5.28%	907	12433	*
	Peak Lighting Demand reduced by 30%	10558.1	2662550.0	922.2	4.51%	-	10606	-

	All Heat Pump COP changed to 4.22	10997.9	2784766.7	921.9	0.53%	211600	1246	169.9
	Chiller COP 5.7655 to 6.3421	10792.1	2727566.7	922.0	2.39%	-	5626	-
	Glass thickness 3.9 to 7.8, 8.6 to 17.2 mm & Air gap double	11041.0	2796616.7	922.4	0.14%	1231716	335	3677.1
	Set Point [21, 24] to [23, 26] ℃	9944.1	2492080.6	921.8	10.06%	-	23666	-
	Set Point [21, 24] to [20, 25] ℃	10393.3	2616847.2	921.9	6.00%	-	14109	-
	Reflectance value 0.3 to 0.7	10923.0	2763830.6	922.4	1.21%	80807	2846	28.4
	ATIWS/GCHP Scenario A	12080.1	3085394.1	921.9	-9.26%	941991	-21782	-
	ATIWS/GCHP Scenario B	12381.2	3171190.7	914.5	-11.98%	942124	-28306	-
3B	Baseline	9738.0	2301152.8	1378.0	0.00%			
	Wall Insulation R 5 to 10 Btu/ft·h°F	9675.1	2289958.3	1356.5	0.65%	40065	954	42.0
	Roof Insulation R 25 to 50 Btu/ft·h°F	9645.9	2285988.9	1342.5	0.95%	357767	1334	268.1
	Lighting Tubes 32W to 25 W	9265.2	2155219.4	1427.8	4.86%	907	10301	*
	Peak Lighting Demand reduced by 30%	9326.8	2170219.4	1435.0	4.22%	-	9162	-
	All Heat Pump COP changed to 4.22	9699.9	2290569.4	1378.0	0.39%	118500	770	153.8
	Chiller COP 5.3287 to 5.8617	9569.5	2254344.4	1378.0	1.73%	-	3407	-
	Boiler efficiency 0.8(normal) to 0.92(high efficiency)	9679.0	2301152.8	1322.1	0.61%	-	363	-
	Glass thickness 3.9 to 7.8, 8.6 to 17.2 mm & Air gap double	9655.8	2282636.1	1363.2	0.84%	1507040	1444	1043.9
	Set Point [21, 24] to [23, 26] ℃	9388.8	2092391.7	1759.3	3.59%	-	12723	-
	Set Point [21, 24] to [20, 25] ℃	9331.5	2186638.9	1383.4	4.17%	-	8301	-
	Reflectance value 0.3 to 0.7	9682.6	2278705.6	1402.1	0.57%	98869	1477	66.9
	ATIWS/GCHP Scenario A	10426.6	2492425.0	1378.0	-7.07%	1214629	-13925	-
	ATIWS/GCHP Scenario B	10487.1	2514861.9	1358.8	-7.69%	1262129	-15433	-
4C	Baseline	8648.2	1664927.8	2516.0	0.00%			

	Wall Insulation R 10 to 20 Btu/ft·h°F	8600.6	1667413.9	2462.4	0.55%	74517	176	423.7
	Roof Insulation R 30 to 60 Btu/ft·h°F	8589.0	1665141.7	2459.1	0.68%	421549	406	1038.7
	Lighting Tubes 32W to 25 W	8294.1	1529433.3	2642.7	4.09%	907	11328	*
	Peak Lighting Demand reduced by 30%	8377.8	1544683.3	2669.9	3.13%	-	9743	-
	All Heat Pump COP changed to 4.22	8640.8	1662858.3	2516.0	0.09%	99800	187	532.3
	Chiller COP 5.3287 to 5.8617	8611.9	1654791.7	2516.1	0.42%	-	918	-
	Boiler efficiency 0.8(normal) to 0.92(high efficiency)	8441.0	1664927.8	2319.6	2.40%	-	1469	-
	Glass thickness 6 to 12 mm	8638.5	1666058.3	2502.9	0.11%	1570552	-4	-
	Set Point [21, 24] to [23, 26] ℃	9250.5	1556105.6	3458.1	-6.96%	-	2812	-
	Set Point [21, 24] to [20, 25] ℃	8546.6	1599675.0	2642.3	1.18%	-	4967	-
	Reflectance value 0.3 to 0.7	8661.3	1657033.3	2555.3	-0.15%	100010	422	237.3
	ATIWS/GCHP Scenario A	12013.8	2599789.8	2516.0	-38.92%	1378894	-84699	-
	ATIWS/GCHP Scenario B	12691.7	2797312.5	2484.6	-46.76%	1462294	-102359	-
5A	Baseline	10762.6	2161930.6	2824.1	0.00%			
	Wall Insulation R 10 to 20 Btu/ft·h°F	10621.3	2159841.7	2697.4	1.31%	85355	1084	78.8
	Roof Insulation R 30 to 60 Btu/ft·h°F	10511.9	2155455.6	2608.7	2.33%	482858	2112	228.7
	Lighting Tubes 32W to 25 W	10327.7	2025661.1	2877.0	4.04%	907	12193	*
	Peak Lighting Demand reduced by 30%	10364.0	2041438.9	2857.5	3.70%	-	10875	-
	All Heat Pump COP changed to 4.22	10740.3	2155750.0	2824.1	0.21%	113200	570	198.6
	Chiller COP 5.3287 to 5.8617	10643.1	2128647.2	2824.5	1.11%	-	3066	-
	Boiler efficiency 0.8(normal) to 0.92(high efficiency)	10516.3	2161930.6	2590.7	2.29%	-	1641	-
	Glass thickness 6 to 12 mm	10739.9	2162780.6	2799.8	0.21%	1798969	93	19370.1
	Set Point [21, 24] to [23, 26] ℃	10438.6	2030805.6	2964.5	3.01%	-	11103	-

	Set Point [21, 24] to [20, 25] ℃	9998.6	2082416.7	2371.3	7.10%	-	10515	-
	Reflectance value 0.3 to 0.7	10739.2	2152425.0	2834.4	0.22%	114556	804	142.4
	ATIWS DX	9355.8	1879348.0	2455.0	13.07%	1021103	28649	35.6
	ATIWS/GCHP Scenario A	14272.8	3137003.7	2824.1	-32.62%	1752246	-89902	-
	ATIWS/GCHP Scenario B	14660.6	3267532.1	2746.3	-36.22%	1859946	-101389	-
6A	Baseline	11649.7	2073952.8	3965.2	0.00%			
	Wall Insulation R 10 to 20 Btu/ft·h°F	11455.8	2070105.6	3794.5	1.66%	75013	1618	46.4
	Roof Insulation R 30 to 60 Btu/ft·h°F	11274.8	2065319.4	3639.3	3.22%	424354	3227	131.5
	Lighting Tubes 32W to 25 W	11242.0	1941491.7	4030.7	3.50%	907	13656	*
	Peak Lighting Demand reduced by 30%	11265.8	1957166.7	3999.8	3.30%	-	12204	-
	All Heat Pump COP changed to 4.22	11632.1	2069055.6	3965.2	0.15%	116200	522	222.6
	Chiller COP 5.3287 to 5.8617	11549.6	2046022.2	3965.6	0.86%	-	2975	-
	Boiler efficiency 0.8(normal) to 0.92(high efficiency)	11249.2	2073952.8	3585.6	3.44%	-	2688	-
	Glass thickness 6 to 12 mm	11616.9	2074405.6	3932.6	0.28%	1581003	183	8656.2
	Set Point [21, 24] to [23, 26] ℃	11431.0	1960044.4	4146.6	1.88%	-	10858	-
	Set Point [21, 24] to [20, 25] ℃	10694.6	1999872.2	3312.7	8.20%	-	12516	-
	Reflectance value 0.3 to 0.7	11639.8	2066425.0	3981.5	0.08%	100676	687	146.6
	ATIWS/GCHP Scenario A	15895.6	3253378.7	3965.2	-36.45%	1796536	-125727	-
	ATIWS/GCHP Scenario B	16209.8	3381224.5	3826.7	-39.14%	1906836	-138375	-
7	Baseline	36406.3	8781966.7	4541.2	0.00%			
	Wall Insulation R 12.5 to 25 Btu/ft·h°F	36200.5	8786897.2	4329.3	0.57%	173025	975	177.5
	Roof Insulation R 35 to 70 Btu/ft·h°F	36328.0	8781850.0	4467.4	0.22%	145405	535	271.8
	Lighting Tubes 32W to 25 W	35428.9	8530300.0	4473.5	2.68%	1891	27307	*

Peak Lighting Demand reduced by 30%	35624.9	8553475.0	4580.2	2.15%	-	24081	-
COP 3.4 to 4.17	36136.7	8704466.7	4550.1	0.74%	313900	8199	38.3
COP 5.5 to 6.05	36344.7	8764486.1	4542.5	0.17%	-	1855	-
Boiler efficiency 0.8(normal) to 0.92(high efficiency)	35867.4	8781966.7	4030.4	1.48%	-	3617	-
Glass thickness 6 to 12 mm & Air gap 6 to 12 mm	35744.3	8806950.0	3828.5	1.82%	3349759	2383	1405.7
Set Point [21, 24] to [23, 26] ℃	36238.8	8599052.8	5006.6	0.46%	-	16204	-
Set Point [21, 24] to [20, 25] ℃	35506.9	8668661.1	4075.4	2.47%	-	15377	-
Reflectance value 0.3 to 0.7	36443.8	8773836.1	4604.5	-0.10%	202856	419	484.7
ATIWS/GCHP Scenario A	16912.0	3329144.5	4670.0	-46.05%	960018	-157903	-
ATIWS/GCHP Scenario B	17292.9	3482954.2	4506.2	-49.34%	967951	-173140	-

6.2.3. Standalone Retail

From the holistic energy analyses, the total lighting power of the Secondary School baseline prototype is 32473W. The total number of lighting tubes is thus 1015. The HVAC systems equipment used in the baseline prototype in Climate Zones 1A & 2A are eight heat pumps with COP's ranging from 3.4 ranging to 4.1 (four 4.5~6-ton, two 10-ton and two 40.5-ton units).The HVAC equipment used in Climate Zone 3B, 4C, 5A, 6A, 7 were four air conditioners with COP's ranging from 3.339 to 4.117 (two 5.5~7-ton, one 8 to 11.5-ton, one 35.5 to 50-ton units), four boilers were used with and efficiency of 0.8 (three 6~12-ton and one 41~57-ton unit). Efficiency and tonnages varied with Climate Zones.

Payback analysis for Standalone Retail prototype in seven Climate Zones are shown in Table 7-8. In all Climate Zones, switching to higher efficiency lighting tubes saves considerable amounts of energy and money, with small initial investment. Other than that, payback periods for doubling exterior wall insulation in Climate Zones 1A, 2A & 3B are less than 20 years. Payback periods of increasing reflectance valued\s of exterior wall in Climate Zone 1A & 2A are less than or equal to 20 years. The payback periods of the other measures are more than 40 years.

Table 6-8: Payback Analysis for Standalone Retail Prototype in Seven Climate Zones

Climate Zone	Description	Total Site Energy (GJ)	Electric Consumption (kWh)	Gas Consumption (k ft3)	Percentage Difference (%)	Extra Cost ($)	Energy Saved ($/Year)	Payback Period (Year)
1A	Baseline	1395.6	387672.2	0.0	0.00%			
	Wall Insulation R 5 to 10 Btu/ft·h°F	1367.4	379838.9	0.0	2.02%	6441	590	10.9
	Roof Insulation R 20 to 40 Btu/ft·h°F	1385.6	384880.6	0.0	0.72%	46165	210	219.6
	Lighting Tubes 32W to 25 W	1277.6	354888.9	0.0	8.46%	150	2469	*
	Peak Lighting Demand reduced by 30%	1273.3	353694.4	0.0	8.76%	-	2559	-
	All Heat Pump COP changed to 4.22	1329.3	369252.8	0.0	4.75%	115900	1387	83.6
	Glass thickness 3.9 to 7.8, 8.6 to 17.2 mm & Air gap double	1392.9	386902.8	0.0	0.20%	47750	58	824.1
	Set Point [21, 24] to [22, 25] ℃	1318.9	366363.9	0.0	5.50%	-	1605	-
	Set Point [21, 24] to [20, 25] ℃	1226.8	340786.1	0.0	12.09%	-	3531	-
	Reflectance value 0.3 to 0.7	1354.9	376372.2	0.0	2.91%	15895	851	18.7
	ATIWS DX	1395.2	387558.3	0.0	0.03%	137631	9	16048.7
	ATIWS/GCHP Scenario A	1568.6	435733.4	0.0	-12.40%	173631	-3619	-
	ATIWS/GCHP Scenario B	1566.3	435077.5	0.0	-12.23%	127860	-3570	-
2A	Baseline	1415.7	393236.1	0.0	0.00%			
	Wall Insulation R 5 to 10 Btu/ft·h°F	1395.4	387616.7	0.0	1.43%	6677	430	15.5
	Roof Insulation R 25 to 50 Btu/ft·h°F	1416.2	393380.6	0.0	-0.04%	57298	-11	-5178.6
	Lighting Tubes 32W to 25 W	1295.8	359955.6	0.0	8.46%	150	2549	*
	Peak Lighting Demand reduced by 30%	1290.8	358544.4	0.0	8.82%	-	2657	-
	All Heat Pump COP changed to 4.22	1352.2	375613.9	0.0	4.48%	120800	1350	89.5

	Glass thickness 3.9 to 7.8, 8.6 to 17.2 mm & Air gap double	1410.0	391661.1	0.0	0.40%	49497	121	410.3
	Set Point [21, 24] to [22, 25] ℃	1449.2	402550.0	0.0	-2.37%	-	-713	-
	Set Point [21, 24] to [20, 25] ℃	1272.8	353550.0	0.0	10.09%	-	3040	-
	Reflectance value 0.3 to 0.7	1378.0	382777.8	0.0	2.66%	16476	801	20.6
	ATIWS/GCHP Scenario A	1626.5	451818.1	0.0	-14.90%	194822	-4487	-
	ATIWS/GCHP Scenario B	1653.2	459218.6	0.0	-16.78%	156289	-5054	-
3B	Baseline	1404.1	381897.2	27.7	0.00%			
	Wall Insulation R 5 to 10 Btu/ft·h°F	1372.4	374733.3	22.2	2.26%	8169	558	14.6
	Roof Insulation R 25 to 50 Btu/ft·h°F	1378.2	377388.9	18.5	1.85%	70106	388	180.7
	Lighting Tubes 32W to 25 W	1298.7	350622.2	34.6	7.50%	150	2232	*
	Peak Lighting Demand reduced by 30%	1292.1	349052.8	33.6	7.98%	-	2353	-
	All Heat Pump COP changed to 4.17 or 4.22	1357.0	368811.1	27.7	3.35%	127900	953	134.3
	Glass thickness 3.9 to 7.8, 8.6 to 17.2 mm & Air gap double	1395.4	379822.2	26.6	0.62%	60561	159	381.8
	Set Point [21, 24] to [22, 25] ℃	1394.4	374630.6	43.3	0.69%	-	428	-
	Set Point [21, 24] to [20, 25] ℃	1284.4	351161.1	19.1	8.53%	-	2294	-
	Reflectance value 0.3 to 0.7	1384.1	374125.0	35.3	1.42%	20159	517	39.0
	ATIWS/GCHP Scenario A	1546.7	421497.4	27.7	-10.15%	247434	-2883	-
	ATIWS/GCHP Scenario B	1518.6	414093.4	26.4	-8.15%	193759	-2335	-
4C	Baseline	1153.6	288922.2	107.5	0.00%			
	Wall Insulation R 10 to 20 Btu/ft·h°F	1130.1	287855.6	89.0	2.03%	15194	236	64.5
	Roof Insulation R 30 to 60 Btu/ft·h°F	1126.5	288061.1	84.8	2.35%	82604	248	332.9
	Lighting Tubes 32W to 25 W	1081.6	261933.3	131.4	6.24%	150	2267	*
	Peak Lighting Demand reduced by 30%	1079.0	261091.7	131.8	6.47%	-	2340	-

	All Heat Pump COP changed to 4.17 or 4.22	1144.7	286455.6	107.5	0.77%	97000	223	434.0
	Glass thickness 6 to 12 mm	1153.0	288927.8	107.0	0.05%	63114	4	16828.1
	Set Point [21, 24] to [22, 25] ℃	1191.3	287622.2	147.7	-3.27%	-	-183	-
	Set Point [21, 24] to [20, 25] ℃	1058.2	269183.3	84.5	8.27%	-	1961	-
	Reflectance value 0.3 to 0.7	1152.0	286119.4	115.6	0.14%	20392	194	105.3
	ATIWS/GCHP Scenario A	1841.9	480139.4	107.5	-59.68%	282568	-17324	-
	ATIWS/GCHP Scenario B	1948.8	511287.9	102.5	-68.94%	251521	-20109	-
5A	Baseline	1528.7	337630.6	296.9	0.00%			
	Wall Insulation R 10 to 20 Btu/ft·h°F	1470.0	331233.3	263.0	3.84%	17404	828	21.0
	Roof Insulation R 30 to 60 Btu/ft·h°F	1466.9	330602.8	262.3	4.04%	94618	891	106.2
	Lighting Tubes 32W to 25 W	1457.6	309094.4	326.8	4.65%	150	2420	*
	Peak Lighting Demand reduced by 30%	1455.2	308163.9	327.7	4.81%	-	2500	-
	All Heat Pump COP changed to 4.17 or 4.22	1499.2	329455.6	296.9	1.93%	141500	754	187.7
	Glass thickness 6 to 12 mm	1527.0	337525.0	295.6	0.11%	72293	18	3930.2
	Set Point [21, 24] to [22, 25] ℃	1574.9	336933.3	343.0	-3.02%	-	-260	-
	Set Point [21, 24] to [20, 25] ℃	1408.6	311780.6	271.3	7.86%	-	2563	-
	Reflectance value 0.3 to 0.7	1530.5	334366.7	309.7	-0.12%	23358	210	111.0
	ATIWS DX	1341.8	296359.9	260.6	12.22%	211755	4060	52.2
	ATIWS/GCHP Scenario A	2246.6	1933.4	313.2	-46.96%	359022	-18386	-
	ATIWS/GCHP Scenario B	2256.9	1970.2	286.7	-47.64%	319221	-19152	-
6A	Baseline	1692.2	334869.4	461.2	0.00%			
	Wall Insulation R 10 to 20 Btu/ft·h°F	1618.9	327975.0	415.3	4.33%	15295	1060	14.4
	Roof Insulation R 30 to 60 Btu/ft·h°F	1611.7	328194.4	407.7	4.76%	83154	1091	76.3

	Lighting Tubes 32W to 25 W	1632.9	306444.4	502.0	3.50%	150	2741	*
	Peak Lighting Demand reduced by 30%	1631.8	305458.3	504.4	3.57%	-	2830	-
	All Heat Pump COP changed to 4.17 or 4.22	1668.5	328300.0	461.2	1.40%	138300	700	197.5
	Glass thickness 6 to 12 mm	1690.4	334741.7	460.0	0.11%	63533	22	2826.3
	Set Point [21, 24] to [22, 25] ℃	1760.8	339505.6	510.5	-4.06%	-	-843	-
	Set Point [21, 24] to [20, 25] ℃	1569.6	310300.0	428.9	7.25%	-	2848	-
	Reflectance value 0.3 to 0.7	1700.1	332400.0	477.2	-0.47%	20528	150	136.5
	ATIWS/GCHP Scenario A	2560.1	575952.9	461.2	-51.29%	367077	-25699	-
	ATIWS/GCHP Scenario B	2549.3	585557.2	418.2	-50.65%	334477	-26419	-
	Baseline	1718.2	311863.9	564.4	0.00%			
	Wall Insulation R 10 to 20 Btu/ft·h°F	1642.6	306086.1	512.5	4.40%	16715	984	17.0
	Roof Insulation R 35 to 70 Btu/ft·h°F	1639.4	307019.4	506.3	4.59%	93614	928	100.9
	Lighting Tubes 32W to 25 W	1669.0	284358.3	611.6	2.87%	150	2598	*
	Peak Lighting Demand reduced by 30%	1668.2	283411.1	614.1	2.91%	-	2681	-
7	All Heat Pump COP changed to 4.17 or 4.22	1707.5	308886.1	564.4	0.62%	125500	317	395.4
	Glass thickness 6 to 12 mm & Air gap 6 to 12 mm	1698.3	310688.9	549.5	1.16%	60654	231	263.0
	Set Point [21, 24] to [22, 25] ℃	1790.9	317475.0	614.2	-4.23%	-	-951	-
	Set Point [21, 24] to [20, 25] ℃	1606.0	290086.1	532.4	6.53%	-	2548	-
	Reflectance value 0.3 to 0.7	1731.0	310227.8	582.1	-0.74%	19597	49	397.9
	ATIWS/GCHP Scenario A	2807.7	614491.7	564.4	-63.41%	197468	-32260	-
	ATIWS/GCHP Scenario B	2807.5	629915.8	511.7	-63.40%	137868	-33531	-

6.2.4. Midrise Apartment

Based on the holistic energy analyses, the total lighting power for the baseline Midrise Apartment prototype is 43161W. The total number of lighting tubes is thus 1349. The HVAC system equipment used for the baseline prototype is thirty-two air conditioner units with COP of 4.1, tonnages varying from 1 to 2.5-ton, and sixty-four gas heating coils with efficiencies of 0.8 and tonnage varying from 1.5 to 5.

Payback analysis for Midrise Apartment prototype in seven Climate Zones are shown in Table 7-9. In all Climate Zones, switching to higher efficiency lighting tubes saves considerable amounts of energy and yearly energy costs, with only a small initial investment. Other than that, payback periods for doubling exterior wall insulation in Climate Zone 1A, 2A & 3B are less than 14 years, and in Climate Zone 6A is about 25 years. Payback periods of increasing exterior wall reflectance in Climate Zones 1A & 2A are less than 22 years. The payback periods of other energy conservation measures are more than 30 years.

Table 6-9: Payback Analysis for Midrise Apartment Prototype in Seven Climate Zones

Climate Zone	Description	Total Site Energy (GJ)	Electric Consumption (kWh)	Gas Consumption (k ft3)	Percentage Difference (%)	Extra Cost ($)	Energy Saved ($/Year)	Payback Period (Year)
1A	Baseline	1552.0	430894.4	0.7	0.00%			
	Wall Insulation R 5 to 10 Btu/ft·h°F	1528.0	424283.3	0.5	1.55%	8439	654	12.9
	Roof Insulation R 20 to 40 Btu/ft·h°F	1543.3	428547.2	0.5	0.56%	15770	235	67.0
	Lighting Tubes 32W to 25 W	1513.6	420197.2	0.8	2.47%	200	1049	*
	Peak Lighting Demand reduced by 30%	1523.0	422836.1	0.8	1.86%	-	791	-
	Air Conditioner COP 4.1171 to 4.22	1543.6	428569.4	0.7	0.54%	9100	229	39.8
	Boiler efficiency 0.8(normal) to 0.92(high efficiency)	1551.9	430894.4	0.6	0.01%	-	2	-
	Glass thickness 3.9 to 7.8, 8.6 to 17.2 mm & Air gap double	1537.5	426930.6	0.5	0.93%	174595	395	442.5
	Set Point [21, 24] to [23, 26] ℃	1423.5	392813.9	8.8	8.28%	-	3568	-
	Set Point [21, 24] to [20, 25] ℃	1480.5	411213.9	0.1	4.61%	-	1947	-
	Reflectance value 0.3 to 0.7	1516.6	420936.1	1.2	2.28%	20825	968	21.5
	ATIWS DX	1551.2	430689.0	0.7	0.05%	179951	20	8906.8
	ATIWS/GCHP Scenario A	1777.8	493630.1	0.7	-14.55%	226151	-6167	-
	ATIWS/GCHP Scenario B	1806.4	501565.8	0.7	-16.39%	175713	-6946	-
2A	Baseline	1542.5	419713.9	29.9	0.00%			
	Wall Insulation R 5 to 10 Btu/ft·h°F	1515.1	414997.2	20.0	1.77%	8748	670	13.1
	Roof Insulation R 25 to 50 Btu/ft·h°F	1531.3	417794.4	25.8	0.72%	19573	273	71.6
	Lighting Tubes 32W to 25 W	1508.8	409391.7	33.1	2.18%	200	1202	*
	Peak Lighting Demand reduced by 30%	1516.3	411775.0	32.1	1.70%	-	927	-

	Air Conditioner COP 4.1171 to 4.22	1536.2	417961.1	29.9	0.41%	9800	210	46.7
	Boiler efficiency 0.8(normal) to 0.92(high efficiency)	1538.4	419713.9	26.0	0.27%	-	26	-
	Glass thickness 3.9 to 7.8, 8.6 to 17.2 mm & Air gap double	1521.8	415902.8	23.2	1.34%	180983	527	343.2
	Set Point [21, 24] to [23, 26] ℃	1487.6	389236.1	81.8	3.56%	-	3097	-
	Set Point [21, 24] to [20, 25] ℃	1468.6	403530.6	15.0	4.79%	-	2097	-
	Reflectance value 0.3 to 0.7	1519.4	410536.1	39.3	1.49%	21587	998	21.6
	ATIWS/GCHP Scenario A	1818.0	496233.7	29.9	-17.86%	253691	-9167	-
	ATIWS/GCHP Scenario B	1858.6	507889.8	28.6	-20.50%	205766	-10550	-
3B	Baseline	1640.6	431894.4	81.3	0.00%			
	Wall Insulation R 5 to 10 Btu/ft·h°F	1590.7	424666.7	58.7	3.04%	10703	1040	10.3
	Roof Insulation R 25 to 50 Btu/ft·h°F	1620.6	429113.9	71.8	1.22%	23949	408	58.7
	Lighting Tubes 32W to 25 W	1612.2	421961.1	88.3	1.73%	200	1068	*
	Peak Lighting Demand reduced by 30%	1618.7	424388.9	86.1	1.34%	-	811	-
	Air Conditioner COP 4.1171 to 4.22	1634.9	430311.1	81.3	0.35%	11000	181	60.8
	Boiler efficiency 0.8(normal) to 0.92(high efficiency)	1629.4	431894.4	70.7	0.68%	-	101	-
	Glass thickness 3.9 to 7.8, 8.6 to 17.2 mm & Air gap double	1601.6	425744.4	65.4	2.38%	221437	854	259.3
	Set Point [21, 24] to [23, 26] ℃	1629.9	404122.2	165.9	0.65%	-	2368	-
	Set Point [21, 24] to [20, 25] ℃	1561.2	416902.8	57.2	4.84%	-	1941	-
	Reflectance value 0.3 to 0.7	1635.0	423197.2	105.7	0.34%	26413	762	34.7
	ATIWS/GCHP Scenario A	1826.6	483544.5	81.3	-11.33%	326308	-5898	-
	ATIWS/GCHP Scenario B	1765.9	468343.2	75.7	-7.64%	272008	-4109	-
4C	Baseline	1633.7	390155.6	217.2	0.00%			
	Wall Insulation R 10 to 20 Btu/ft·h°F	1576.0	390144.4	162.5	3.53%	19907	538	37.0

	Roof Insulation R 30 to 60 Btu/ft·h°F	1611.9	389213.9	199.8	1.33%	28218	264	106.8
	Lighting Tubes 32W to 25 W	1614.8	380441.7	232.4	1.16%	200	810	*
	Peak Lighting Demand reduced by 30%	1618.3	382641.7	228.2	0.95%	-	634	-
	Air Conditioner COP 4.1171 to 4.22	1632.1	389711.1	217.2	0.10%	8800	44	200.6
	Boiler efficiency 0.8(normal) to 0.92(high efficiency)	1603.9	390155.6	188.9	1.83%	-	278	-
	Glass thickness 6 to 12 mm	1628.8	390452.8	211.5	0.30%	230770	27	8674.6
	Set Point [21, 24] to [23, 26] ℃	1726.0	370244.4	372.6	-5.65%	-	439	-
	Set Point [21, 24] to [20, 25] ℃	1547.1	379155.6	172.6	5.31%	-	1524	-
	Reflectance value 0.3 to 0.7	1639.6	385180.6	239.7	-0.36%	26717	270	99.0
	ATIWS/GCHP Scenario A	2534.8	640453.1	217.2	-55.15%	370298	-24704	-
	ATIWS/GCHP Scenario B	2618.0	668493.1	200.4	-60.24%	338873	-27306	-
5A	Baseline	1826.3	432863.9	254.0	0.00%			
	Wall Insulation R 10 to 20 Btu/ft·h°F	1756.7	431547.2	192.6	3.81%	22802	680	33.5
	Roof Insulation R 30 to 60 Btu/ft·h°F	1800.1	431372.2	234.2	1.44%	32322	370	87.4
	Lighting Tubes 32W to 25 W	1802.1	422886.1	265.1	1.32%	200	1317	*
	Peak Lighting Demand reduced by 30%	1807.2	425188.9	262.1	1.05%	-	1017	-
	Air Conditioner COP 4.1171 to 4.22	1822.8	431894.4	254.0	0.19%	10000	137	73.2
	Boiler efficiency 0.8(normal) to 0.92(high efficiency)	1791.4	432863.9	220.9	1.91%	-	267	-
	Glass thickness 6 to 12 mm	1820.6	433069.4	247.9	0.31%	264332	20	12920.2
	Set Point [21, 24] to [23, 26] ℃	1851.1	411505.6	350.4	-1.35%	-	2236	-
	Set Point [21, 24] to [20, 25] ℃	1755.3	421238.9	226.4	3.89%	-	1862	-
	Reflectance value 0.3 to 0.7	1828.9	427752.8	273.9	-0.14%	30603	560	54.6
	ATIWS DX	1683.3	398963.8	234.1	7.83%	273179	4940	55.3

	ATIWS/GCHP Scenario A	2766.1	693903.7	254.0	-51.46%	470475	-36807	-
	ATIWS/GCHP Scenario B	2798.0	708930.6	233.0	-53.20%	435675	-38756	-
6A	Baseline	1946.8	432197.2	370.5	0.00%			
	Wall Insulation R 10 to 20 Btu/ft·h°F	1854.4	431694.4	284.6	4.75%	20040	815	24.6
	Roof Insulation R 30 to 60 Btu/ft·h°F	1911.4	430800.0	341.7	1.82%	28406	441	64.4
	Lighting Tubes 32W to 25 W	1927.3	422344.4	385.6	1.00%	200	1219	*
	Peak Lighting Demand reduced by 30%	1931.2	424636.1	381.5	0.80%	-	941	-
	Air Conditioner COP 4.1171 to 4.22	1943.8	431386.1	370.5	0.15%	10000	111	89.9
	Boiler efficiency 0.8(normal) to 0.92(high efficiency)	1895.8	432197.2	322.1	2.62%	-	420	-
	Glass thickness 6 to 12 mm	1938.0	432422.2	361.4	0.45%	232305	48	4817.3
	Set Point [21, 24] to [23, 26] ℃	1998.2	411958.3	488.3	-2.64%	-	1751	-
	Set Point [21, 24] to [20, 25] ℃	1868.0	421094.4	333.6	4.05%	-	1842	-
	Reflectance value 0.3 to 0.7	1958.0	427897.2	395.8	-0.58%	26895	370	72.7
	ATIWS/GCHP Scenario A	3083.0	747829.2	370.5	-58.37%	480352	-43273	-
	ATIWS/GCHP Scenario B	3076.5	757124.3	332.6	-58.03%	457252	-44218	-
7	Baseline	2010.8	429666.7	439.8	0.00%			
	Wall Insulation R 10 to 20 Btu/ft·h°F	1913.9	430719.4	344.4	4.82%	21900	685	32.0
	Roof Insulation R 35 to 70 Btu/ft·h°F	1975.0	428800.0	408.8	1.78%	31979	389	82.3
	Lighting Tubes 32W to 25 W	1993.2	419852.8	456.6	0.88%	200	1200	*
	Peak Lighting Demand reduced by 30%	1996.6	422066.7	452.2	0.71%	-	934	-
	Air Conditioner COP 4.1171 to 4.22	2008.7	429069.4	439.8	0.11%	9000	82	109.9
	Boiler efficiency 0.8(normal) to 0.92(high efficiency)	1950.3	429666.7	382.5	3.01%	-	499	-
	Glass thickness 6 to 12 mm & Air gap 6 to 12 mm	1926.0	433266.7	347.1	4.22%	221776	312	710.5

Set Point [21, 24] to [23, 26] ℃	2067.2	410780.6	557.7	-2.80%	-	1565	-
Set Point [21, 24] to [20, 25] ℃	1935.3	419319.4	403.5	3.76%	-	1734	-
Reflectance value 0.3 to 0.7	2023.3	425716.7	465.1	-0.62%	25676	322	79.8
ATIWS/GCHP Scenario A	3437.4	825933.7	439.8	-70.94%	257382	-54328	-
ATIWS/GCHP Scenario B	3441.0	840182.0	394.6	-71.12%	200382	-55889	-

6.3. Payback Analysis Summary

It appears that doubling the exterior wall insulation is less effective in buildings with low surface volume ratio, for example, in the Large Office building prototype, the payback period of doubling the exterior wall insulation is longer than 40 years in all Climate Zones. In addition, increasing exterior wall insulation is a more economical solution in warmer regions than in colder regions, payback periods of Secondary School, Standalone Retail and Midrise Apartment prototypes are mostly shorter than 20 years in Climate Zones 1A & 2A, while the payback periods are much longer in other Climate Zones. This proves that although the energy conservation potential of doubling wall insulation in warmer regions are low, as shown in Chapter 3.1.2.2, however, doubling wall insulation in warmer regions is still economical. In colder regions, since the insulation is already very thick, it is not economical to further increase the thickness of insulations.

Replacing lights with higher efficiency ones will save energy with only a small extra investment in all prototype buildings and all climate zones.

Using air conditioner units with higher COP in Large Office prototype in Climate Zone 1A & 2A appears to be cost effective, but is not very effective in other three prototypes studied. In the Secondary School, Standalone Retail, and Midrise Apartment prototypes, changing the exterior wall reflectance using coatings shows more than a 1% reduction in total energy in Climate Zone 1A & 2A, analysis and the corresponding payback periods are less than 30 years.

US DOE showed that changing the efficiency of furnaces and boilers used for heating from 80% to 90%, or 95% efficiency may be hard to justify in mild climates, while in cold climate it was usually recommended to invest in highest-efficiency system.

An evaluation of the energy conservation potential the ATIWS system presented in this investigation was very limited. Further economic analysis is needed, but the ATIWS was shown to be able to meet some, or all of the, exterior heat flux demand, and showed potential to heat/cool buildings. The ATIWS system work to produce close to a zero heat flux through walls in Climate Zone 5A, and can be used as a supplementary method to cool buildings. However, when considering using a ATIWS/GCHP system, it may be best to use these systems to replace the HVAC systems and just change the fluid temperatures to provide all or most of the building cooling an heating demand. This will likely be more cost effective as initial costs of the ATIWS were high.

Overall, the following general observations can be made:

1. Buildings like the Secondary School, Standalone Retail, Midrise Apartment prototypes should consider thickening exterior wall insulation in warmer regions like Climate Zone 1A & 2A. The payback periods for increasing exterior wall insulation over the code baseline configurations are significantly longer in mild and colder regions, thus should not be encouraged.
2. Using high efficiency lighting and reducing lighting demands are cost effective energy conservation measures in all building prototypes, in all Climate Zones. In this research, compared to normal T8 lighting tubes, high efficiency T8 lighting can significantly reduce energy use and thus, electricity bills. Reduction in lighting demands can be achieved in different ways, such as intelligent lighting controls to adjust lighting level during different time of the day or adopting nature light compensation systems.

3. Adopting more efficient air conditioners and heat pumps in the Large Office prototypes is cost effective in warmer regions like Climate Zone 1A & 2A, however, it is not cost effective in mild and colder regions, nor in the other three prototype buildings studied. The reason is that Large Office prototypes in warmer regions mainly rely on air conditioners and heat pumps for cooling. In other regions or other building prototypes, chillers are used for cooling.
4. Adjusting HVAC setpoints by increasing setpoint deadband width or shifting setpoint values have high energy conservation potential in all prototypes and all Climate Zones. By changing the thermostat settings to get a custom HVAC setpoint range does not require any extra investment, and is considered a no-cost energy conservation measure in most conditions.
5. Higher wall reflectance values use less cooling energy. Since in many regions natural gas is used for heating and electricity is for cooling, it is found that in some cases in colder regions, higher reflectance values actually led to a higher yearly energy consumption, but the total utility bill is always lower because natural gas is a cheaper than electricity.
6. It is not economical to further enhance of the roof insulation or the resistance of window glazing all four of the prototypes in all climates.
7. ATIWS wall systems can be used effectively in Climate Zone 5A for cooling buildings, although many conservative assumptions were made in the economic analysis. Further in-depth research is recommended to explore the practicality of this ATIWS DX system.

CHAPTER 7

SUMMARY, CONCLUSION AND RECOMMENDATIONS

In this research, conventional energy conservation strategies were evaluated, as well as a novel active thermal insulation wall system. The energy saving potential (ESP) of each measure for different prototype buildings in the seven U.S. Climate Zones were also investigated.

The performance of active thermal insulation wall systems (ATIWS) was evaluated using thermal flow simulations in a MATLAB environment. These simulations were validated by ANSYS numerical modelling and hot box tests. These hot box tests evaluated active thermal insulation wall specimen with different configurations. The test results showed good agreement with MATLAB predictions.

Using the validated numerical models, the active thermal insulation wall was investigated under variable weather conditions and configurations, the simulations showed that ATIWS coupled with ground loops (ATIWS DX) was effective in producing low to no heat flux through the exterior walls systems in Climate Zone 1A, in the winter, and Climate Zone 5A, in summer. This ATIWS DX system thus has a potential to prevent heat transfer through exterior walls using only the pumping energy needed to circulate the fluids.

The analyses also showed that the ATIWS systems, when coupled with ground

source heat pumps (GCHP) demonstrated its ability to prevent heat flux through exterior walls and to heat and cool the indoor environment. However, preliminary payback analysis conducted in this research showed that this configuration may not be economical in a typical installation. Holistic building energy simulations are needed to accurately assess this type of application and optimize their design. This must be done before a comprehensive economic analysis of the ATIWS/GCHP system can be completed.

According to the analyses presented in this research, the greatest impact on yearly building energy consumption is obtained by widening the setpoint deadband range. The amount of energy saved by this energy conservation strategy varies with building type and Climate Zone, but it saves significant amounts of energy in most scenarios. The increase of deadband width reduces equipment running time and thus reduces energy consumed by HVAC system. This is also a zero-cost strategy. However, this strategy will affect occupancy comfort and may negatively impact occupant productivity and comfort.

The investigation also identified another energy conservation strategy that works in most scenarios, that is to improve lighting systems. This can be accomplished by either simply using higher efficiency lights or reducing lighting demand. There are different ways to reduce lighting demand. One way to do this is to bring more sunlight into the indoor environment resulting in less lighting demand. This can be accomplished by having larger areas of fenestrations, using certain type of fenestrations (light shelves, transparent insulation material in window hollows) to distribute daylight more evenly in the room, and/or using daylight harvesting equipment like lighting pipes. Smart control systems such as occupancy sensors can also reduce lighting consumption based on occupancy status. Control system with photosensors can also be used to reduce lighting energy use by

detecting the lighting level and then controlling the amount of light provided by the fixtures to maintain a fixed lighting level. The costs of these measures vary with buildings and locations. Generally, this strategy saves significant energy with relatively low initial investments.

The area ratio occupied by window frame and glazing beyond code mandated minimums has only a small impact on energy use, as does adjusting the fenestration SHGC value.

Increase the reflectance of building envelope is encouraged in all buildings. Although this measure increases total energy consumption in some buildings in cold regions, it is an economical choice since in those cases gas is likely used for heating and gas is cheaper than electricity. From a purely energy saving prospective, higher reflectance on the exterior of the building envelopes should be used in all warmer regions.

Mass exterior walls are recommended for most buildings from an energy use perspective over conventional lightweight steel frame walls of equal thermal resistance. However, for some large buildings with high occupancy density and small surface volume ratio like a secondary school, steel frame walls can produce slightly better performance in Climate Zones 1A, 2A, or 4C. That indicates that lightweight frame walls may behave better in buildings with high heat production and slow heat dissipation ability. In other buildings, a lightweight exterior concrete wall will perform better. It should be noted that that for mass exterior walls, lighter weight concrete walls perform better than higher weight ones.

Increasing the thickness of wall insulation has similar effects to increasing thermal mass of wall. It has greater impact on buildings with low occupancy density and large surface volume ratios. From an economic point of view, doubling wall insulation can have a greater impact on building energy usage in warmer regions due to the low amount of mandated insulation. Although doubling wall insulations in cold regions saves larger amount of energy in colder regions, the larger baseline insulation requirements make these increases uneconomical.

The impact of increases in roof insulation will vary with the relative area occupied by roof. However, these increases are generally not economical as the reduction in energy use is not sufficient to justify the cost of the additional insulation.

The ATIWS wall system was shown to be quite effective in reducing heat flow through exterior walls. It appeared to have a greater impact on small buildings with larger surface volume ratios. The use of the ATIWS was able to reduce the exterior wall insulation required to achieve code compliant performance, in some cases even allowing no insulation to be used. Exterior wall insulation increases costs and reduces interior volumes, an additional 2-inches of thickness on exterior walls would reduce the total interior area by about 1% in a typical 1500 ft^2 building. Another advantage of this ATIWS is that it maintains the wall at a comfortable warm temperature in all season thus prevent condensation problems.

The results of this investigation also suggest the following avenues of further research:

1. The thermal performance of CMU's wall systems with air gaps were investigated without accounting for convection in the air cavity. The impact of convention should be investigated as it may be significant.

2. Window frames were conducted to have minor impact on building energy conservation. However, in some cases, it is believed that the thermal bridges in window systems can have adverse effects in building energy conservation. The impact of window thermal bridging is need.

3. Combinations of conventional energy conservation strategies can be investigated achieving the best energy saving effect. Preliminary research by author have shown that some strategies may not save as much energy as expected, however, the energy saving effects of some strategies are linearly superimposed. Therefore, future research can be done in investigating the energy saving effect of different combinations of strategies.

4. The MATLAB model does not include radiation on the exterior surfaces. This simulation model exams the heat transfer through an exterior wall section and the boundary condition of the interior side is a fixed indoor temperature. To better simulate the exterior walls, a larger scale model can be developed. The larger scale model should include the entire exterior walls system and the internal information (including thermal mass of indoor environment). In this way, the influence of the building envelope on the indoor temperature will be simulated more accurately.

5. The pipes used in the ATIWS wall system could potentially function as wall reinforcing. This would act to lower the costs of the ATIWS walls systems and needs to be explored further.

6. The used of ATIWS/GCHP and conventional HVAC systems is not cost effective due to the high initial cost of providing both systems. Use of higher temperature ATIWS to both reduce wall heat flow and heat and cool the building should be explored.

7. This ATIWS can be coupled with waste and geothermal heat storage systems to reduce the cost of these systems. Further research is needed to further develop this system.

REFERENCES

McGinley, W. , Mark , "Active Enamel Coatings and Applications to Civil Engineering Infrastructure – Coated Fibers, Proceedings of the Porcelain Enamel Institute – Tech Forum 2016, Louisville KY , 2016

ASTM A307-14e1, Standard Specification for Carbon Steel Bolts, Studs, and Threaded Rod 60 000 PSI Tensile Strength, ASTM International, West Conshohocken, PA, 2014, www.astm.org

ASTM C348-14, Standard Test Method for Flexural Strength of Hydraulic-Cement Mortars, ASTM International, West Conshohocken, PA, 2014, www.astm.org

ASTM C109 / C109M-16a, Standard Test Method for Compressive Strength of Hydraulic Cement Mortars (Using 2-in. or [50-mm] Cube Specimens), ASTM International, West Conshohocken, PA, 2016, www.astm.org

ACI/TMSCommittee122. (2014). Guide to Thermal Properties of Concrete and Masonry Systems.

Allen, K., Connelly, K., Rutherford, P., & Wu, Y. (2017). Smart windows—Dynamic control of building energy performance. *Energy and Buildings, 139*, 535-546. doi:10.1016/j.enbuild.2016.12.093

Andersen, R. K., Fabi, V., & Corgnati, S. P. (2016). Predicted and actual indoor environmental quality: Verification of occupants' behaviour models in residential buildings. *Energy and Buildings, 127*, 105-115. doi:10.1016/j.enbuild.2016.05.074

Andujar Marquez, J. M., Martinez Bohorquez, M. A., & Gomez Melgar, S. (2016). Ground Thermal Diffusivity Calculation by Direct Soil Temperature Measurement. Application to very Low Enthalpy Geothermal Energy Systems. *Sensors (Basel), 16*(3), 306. doi:10.3390/s16030306

ASHRAE. (2013). ASHRAE 90.1-2013 Energy Standard for Buildings Except Low-Rise Residential Buildings.

ASHRAE. (2019). ASHRAE 90.1-2019 Energy Standard for Buildings Except Low-Rise Residential Buildings.

Atam, E., & Helsen, L. (2016a). Ground-coupled heat pumps: Part 1 – Literature review and research challenges in modeling and optimal control. *Renewable and Sustainable Energy Reviews, 54*, 1653-1667. doi:10.1016/j.rser.2015.10.007

Atam, E., & Helsen, L. (2016b). Ground-coupled heat pumps: Part 2—Literature review and research challenges in optimal design. *Renewable and Sustainable Energy Reviews, 54*, 1668-1684. doi:10.1016/j.rser.2015.07.009

Baetens, R., Jelle, B. P., & Gustavsen, A. (2010). Phase change materials for building applications: A state-of-the-art review. *Energy and Buildings, 42*(9), 1361-1368. doi:10.1016/j.enbuild.2010.03.026

Bottarelli, M., Bortoloni, M., Su, Y., Yousif, C., Aydın, A. A., & Georgiev, A. (2015). Numerical analysis of a novel ground heat exchanger coupled with phase change materials. *Applied Thermal Engineering, 88*, 369-375. doi:10.1016/j.applthermaleng.2014.10.016

Boyano, A., Hernandez, P., & Wolf, O. (2013). Energy demands and potential savings in European office buildings: Case studies based on EnergyPlus simulations. *Energy and Buildings, 65*, 19-28. doi:10.1016/j.enbuild.2013.05.039

Building Component Library. (2020). Retrieved from https://bcl.nrel.gov/. from Building Component Library https://bcl.nrel.gov/

Chen, C., Ling, H., Zhai, Z., Li, Y., Yang, F., Han, F., & Wei, S. (2018). Thermal performance of an active-passive ventilation wall with phase change material in solar greenhouses. *Applied Energy, 216*, 602-612. doi:10.1016/j.apenergy.2018.02.130

Choi, B.-E., Shin, J.-H., Lee, J.-H., Kim, S.-S., & Cho, Y.-H. (2017). Establishment of Passive Energy Conservation Measure and Economic Evaluation of Fenestration System in Nonresidential Building of Korea. *International Journal of Polymer Science, 2017*, 1-9. doi:10.1155/2017/8681737

Chung, J. T., & Choi, J. M. (2012). Design and performance study of the ground-coupled heat pump system with an operating parameter. *Renewable Energy, 42*, 118-124. doi:10.1016/j.renene.2011.08.054

Crawley, D. B., Hand, J. W., Kummert, M., & Griffith, B. T. (2008). Contrasting the capabilities of building energy performance simulation programs. *Building and Environment, 43*(4), 661-673. doi:10.1016/j.buildenv.2006.10.027

Deru, M., Field, K., Studer, D., Benne, K., Griffith, B., Torcellini, P., . . . Crawley, D. (2011). *U.S. Department of Energy Commercial Reference Building Models of the National Building Stock*. Retrieved from

DOE, U. S. (2009). Summary of Results: Round 9 of Product Testing. *DOE Solid-State Lighting CALiPER Program*.

DOE, U. S. (2010). Summary of Results: Round 11 of Product Testing. *DOE Solid-State Lighting CALiPER Program*.

DOE, U. S. (2011). LED APPLICATION SERIES: LINEAR FLUORESCENT REPLACEMENT LAMPS. *Energy Efficiency & Renewable Energy*.

El Mankibi, M., Zhai, Z., Al-Saadi, S. N., & Zoubir, A. (2015). Numerical modeling of thermal behaviors of active multi-layer living wall. *Energy and Buildings, 106*, 96-110. doi:10.1016/j.enbuild.2015.06.084

EngineeringToolBox. (2004a). Hazen-Williams Equation - calculating Head Loss in Water Pipes. Retrieved from https://www.engineeringtoolbox.com/water-pumping-costs-d_1527.html

EngineeringToolBox. (2004b). Water - Dynamic and Kinematic Viscosity. Retrieved from https://www.engineeringtoolbox.com/water-pumping-costs-d_1527.html

EngineeringToolBox. (2009). Pumping Water - Energy Cost Calculator. Retrieved from https://www.engineeringtoolbox.com/water-pumping-costs-d_1527.html

EngineeringToolBox. (2018). Water - Thermal Conductivity. Retrieved from https://www.engineeringtoolbox.com/water-pumping-costs-d_1527.html

Fabi, V., Andersen, R. V., & Corgnati, S. P. (2013). Influence of occupant's heating set-point preferences on indoor environmental quality and heating demand in residential buildings. *HVAC&R Research, 19*, 635–645. doi:10.1080/10789669.2013.789372

Fadejev, J., Simson, R., Kurnitski, J., & Bomberg, M. (2017). Thermal mass and energy recovery utilization for peak load reduction. *Energy Procedia*.

Fayazbakhsh, M. A., Bagheri, F., & Bahrami, M. (2015). Gray-box model for energy-efficient selection of set point hysteresis in heating, ventilation, air conditioning, and refrigeration controllers. *Energy Conversion and Management, 103*, 459-467. doi:10.1016/j.enconman.2015.06.071

Feng, G., Sha, S., & Xu, X. (2016). Analysis of the Building Envelope Influence to Building Energy Consumption in the Cold Regions. *Procedia Engineering, 146*, 244-250. doi:10.1016/j.proeng.2016.06.382

Fumo, N. (2014). A review on the basics of building energy estimation. *Renewable and Sustainable Energy Reviews, 31*, 53-60. doi:10.1016/j.rser.2013.11.040

Ghaith*, F. A., Shakhshir, F. S. A., Nour, M., & Lagtah, N. A. (2017). Thermal Performance of an Integrated Earth-Air Tunnel System with Building's External Wall in UAE. *International Journal of Engineering Research & Technology, 6* (07).

GROUT FOR CONCRETE MASONRY, TEK 09-04A. (2005). *National Concrete Masonry Association*.

Hoyt, T., Arens, E., & Zhang, H. (2015). Extending air temperature setpoints: Simulated energy savings and design considerations for new and retrofit buildings. *Building and Environment, 88*, 89-96. doi:10.1016/j.buildenv.2014.09.010

Huo, H., Shao, J., & Huo, H. (2017). Contributions of energy-saving technologies to building energy saving in different climatic regions of China. *Applied Thermal Engineering, 124*, 1159-1168. doi:10.1016/j.applthermaleng.2017.06.065

Jie, P., Zhang, F., Fang, Z., Wang, H., & Zhao, Y. (2018). Optimizing the insulation thickness of walls and roofs of existing buildings based on primary energy consumption, global cost and pollutant emissions. *Energy, 159*, 1132-1147. doi:10.1016/j.energy.2018.06.179

Kang, J., Ahn, K., Park, C., & Schuetze, T. (2015). Assessment of Passive vs. Active Strategies for a School Building Design. *Sustainability, 7*(11), 15136-15151. doi:10.3390/su71115136

Kiesel, J. D. (2013). Development of concrete incorporating phase change materials for enhanced energy efficiency. *Electronic Theses and Dissertations, Paper 746*. doi:10.18297/etd/746

Kisilewicz, T., Fedorczak-Cisak, M., & Barkanyi, T. (2019). Active thermal insulation as an element limiting heat loss through external walls. *Energy and Buildings, 205*. doi:10.1016/j.enbuild.2019.109541

Kneifel, J., & Webb, D. (2016). Predicting Energy Performance of a Net-Zero Energy Building: A Statistical Approach. *Appl Energy, 178*, 468-483. doi:10.1016/j.apenergy.2016.06.013

Konuklu, Y., Ostry, M., Paksoy, H. O., & Charvat, P. (2015). Review on using microencapsulated phase change materials (PCM) in building applications. *Energy and Buildings, 106*, 134-155. doi:10.1016/j.enbuild.2015.07.019

Krecké, E. D. (2004). Passive House Building Technology ISOMAX.

Krzaczek, M., & Kowalczuk, Z. (2011). Thermal Barrier as a technique of indirect heating and cooling for residential buildings. *Energy and Buildings, 43*(4), 823-837. doi:10.1016/j.enbuild.2010.12.002

Laverge, J., Van Den Bossche, N., Heijmans, N., & Janssens, A. (2011). Energy saving potential and repercussions on indoor air quality of demand controlled residential ventilation strategies. *Building and Environment, 46*(7), 1497-1503. doi:10.1016/j.buildenv.2011.01.023

Lenz, K. (2015). The Foundations of a Sustainable Resort. *gb&dmagazine*.

Li, X., Lin, A., Young, C.-H., Dai, Y., & Wang, C.-H. (2019). Energetic and economic evaluation of hybrid solar energy systems in a residential net-zero energy building. *Applied Energy, 254*. doi:10.1016/j.apenergy.2019.113709

Liu, M., & Heiselberg, P. (2019). Energy flexibility of a nearly zero-energy building with weather predictive control on a convective building energy system and evaluated with different metrics. *Applied Energy, 233-234*, 764-775. doi:10.1016/j.apenergy.2018.10.070

McGinley, W. M., & Liu, L. (2021). *Alternative Energy Code Compliant Designs for Single Wythe Masonry Structures in Hawaii.* Paper presented at the 14th Canadian Masonry Symposium, Montreal, Canada.

Nathaniel C. Huygen, & Sanders, J. P. (2019). Dynamic Thermal Performance Measurements of Residential Wall Systems Part II, with Numerical Validation ofSteady-State Performance. *Proceedings of the Thirteenth North American Masonry Conference*.

Olsthoorn, D., Haghighat, F., Moreau, A., & Lacroix, G. (2017). Abilities and limitations of thermal mass activation for thermal comfort, peak shifting and shaving: A review. *Building and Environment, 118*, 113-127. doi:10.1016/j.buildenv.2017.03.029

Park, C.-S., Kang, J.-E., Ahn, K.-U., & Schuetze, T. (2015). *A Case Study on Passive vs. Active Strategies for an Energy-Efficient School Building Design*. Paper presented at the Proceedings of 8th Conference of the International Forum on Urbanism (IFoU).

Partial Differential Equation Toolbox™ User's Guide. (2020). The MathWorks, Inc.

Plotner, S. C., & Company, R. S. M. (2018). *Building construction costs with RSMeans data 2018*.

Rackes, A., & Waring, M. S. (2017). Alternative ventilation strategies in U.S. offices: Comprehensive assessment and sensitivity analysis of energy saving potential. *Building and Environment, 116*, 30-44. doi:10.1016/j.buildenv.2017.01.027

Ramamurthy, P., Sun, T., Rule, K., & Bou-Zeid, E. (2015). The joint influence of albedo and insulation on roof performance: An observational study. *Energy and Buildings, 93*, 249-258. doi:10.1016/j.enbuild.2015.02.040

Rodrigues, E., Fernandes, M. S., Gaspar, A. R., Gomes, Á., & Costa, J. J. (2019). Thermal transmittance effect on energy consumption of Mediterranean buildings with different thermal mass. *Applied Energy, 252*. doi:10.1016/j.apenergy.2019.113437

Sadineni, S. B., Madala, S., & Boehm, R. F. (2011). Passive building energy savings: A review of building envelope components. *Renewable and Sustainable Energy Reviews, 15*(8), 3617-3631. doi:10.1016/j.rser.2011.07.014

Shazmin, S. A. A., Sipan, I., Sapri, M., Ali, H. M., & Raji, F. (2017). Property tax assessment incentive for green building: Energy saving based-model. *Energy, 122*, 329-339. doi:10.1016/j.energy.2016.12.078

SIEDER, E. N., & TATE, G. E. (1936). Heat Transfer and Pressure Drop of Liquids in Tubes. *INDUSTRIAL AND ENGINEERING CHEMISTRY, 28*.

Šimko, M., Krajčík, M., Šikula, O., Šimko, P., & Kalús, D. (2018). Insulation panels for active control of heat transfer in walls operated as space heating or as a thermal barrier: Numerical simulations and experiments. *Energy and Buildings, 158*, 135-146. doi:10.1016/j.enbuild.2017.10.019

Sozer, H. (2010). Improving energy efficiency through the design of the building envelope. *Building and Environment, 45*(12), 2581-2593. doi:10.1016/j.buildenv.2010.05.004

Sun, X., Gou, Z., & Lau, S. S.-Y. (2018). Cost-effectiveness of active and passive design strategies for existing building retrofits in tropical climate: Case study of a zero energy building. *Journal of Cleaner Production, 183*, 35-45. doi:10.1016/j.jclepro.2018.02.137

Sun, Y., Wilson, R., & Wu, Y. (2018). A Review of Transparent Insulation Material (TIM) for building energy saving and daylight comfort. *Applied Energy, 226*, 713-729. doi:10.1016/j.apenergy.2018.05.094

Tian, W. (2013). A review of sensitivity analysis methods in building energy analysis. *Renewable and Sustainable Energy Reviews, 20*, 411-419. doi:10.1016/j.rser.2012.12.014

Tosun, İ. (2002). Chapter 4 - Evaluation of Transfer Coefficients: Engineering Correlations. In İ. Tosun (Ed.), *Modelling in Transport Phenomena* (pp. 65-131). Amsterdam: Elsevier.

Treado, S., & Chen, Y. (2013). Saving Building Energy through Advanced Control Strategies. *Energies, 6*(9), 4769-4785. doi:10.3390/en6094769

Tsikra, P., & Andreou, E. (2017). Investigation of the Energy Saving Potential in Existing School Buildings in Greece. The role of Shading and Daylight Strategies in Visual Comfort and Energy Saving. *Procedia Environmental Sciences, 38*, 204-211. doi:10.1016/j.proenv.2017.03.107

Tudiwer, D., & Korjenic, A. (2017). The effect of living wall systems on the thermal resistance of the façade. *Energy and Buildings, 135*, 10-19. doi:10.1016/j.enbuild.2016.11.023

U.S. Department of Commerce National Oceanic & Atmospheric Administration National Environmental Satellite, D., and Information Service. 1981-2010 Station Normals of Temperature, Precipitation, and Heating and Cooling Degree Days. *https://www.ncdc.noaa.gov/cdo-web/*.

Villarino, J. I., Villarino, A., & Fernández, F. Á. (2017). Experimental and modelling analysis of an office building HVAC system based in a ground-coupled heat pump and radiant floor. *Applied Energy, 190*, 1020-1028. doi:10.1016/j.apenergy.2016.12.152

WHITAKER, S. (1972). Forced Convection Heat Transfer Correlations for Flow in Pipes, Past Flat Plates, Single Cylinders, Single Spheres, and for Flow in Packed Beds and Tube Bundles. *AlChE Journal 18*, 361-371.

Xie, J.-l., Zhu, Q.-y., & Xu, X.-h. (2012). An active pipe-embedded building envelope for utilizing low-grade energy sources. *Journal of Central South University, 19*(6), 1663-1667. doi:10.1007/s11771-012-1190-3

Xu, L., Pan, Y., Yao, Y., Cai, D., Huang, Z., & Linder, N. (2017). Lighting energy efficiency in offices under different control strategies. *Energy and Buildings, 138*, 127-139. doi:10.1016/j.enbuild.2016.12.006

Yang, J., & Tang, J. (2017). Influence of envelope insulation materials on building energy consumption. *Frontiers in Energy, 11*(4), 575-581. doi:10.1007/s11708-017-0473-7

Yang, L., Yan, H., & Lam, J. C. (2014). Thermal comfort and building energy consumption implications – A review. *Applied Energy, 115*, 164-173. doi:10.1016/j.apenergy.2013.10.062

Yu, N., Salakij, S., Chavez, R., Paolucci, S., Sen, M., & Antsaklis, P. (2017). Model-based predictive control for building energy management: Part II – Experimental validations. *Energy and Buildings, 146*, 19-26. doi:10.1016/j.enbuild.2017.04.027

Yun, G. Y., Kim, H., & Kim, J. T. (2012). Effects of occupancy and lighting use patterns on lighting energy consumption. *Energy and Buildings, 46*, 152-158. doi:10.1016/j.enbuild.2011.10.034

Zhang, L. Y., Jin, L. W., Wang, Z. N., Zhang, J. Y., Liu, X., & Zhang, L. H. (2017). Effects of wall configuration on building energy performance subject to different climatic zones of China. *Applied Energy, 185*, 1565-1573. doi:10.1016/j.apenergy.2015.10.086

Zhang;, L., Jin;, M., Liu;, J., & Zhang;, L. (2017). Simulated study on the potential of building energy saving using the green roof. *10th International Symposium on Heating, Ventilation and Air Conditioning*.

Zhou, Z., Feng, L., Zhang, S., Wang, C., Chen, G., Du, T., . . . Zuo, J. (2016). The operational performance of “net zero energy building”: A study in China. *Applied Energy, 177*, 716-728. doi:10.1016/j.apenergy.2016.05.093

APPENDIX A. Plots of Hot Box Test Results

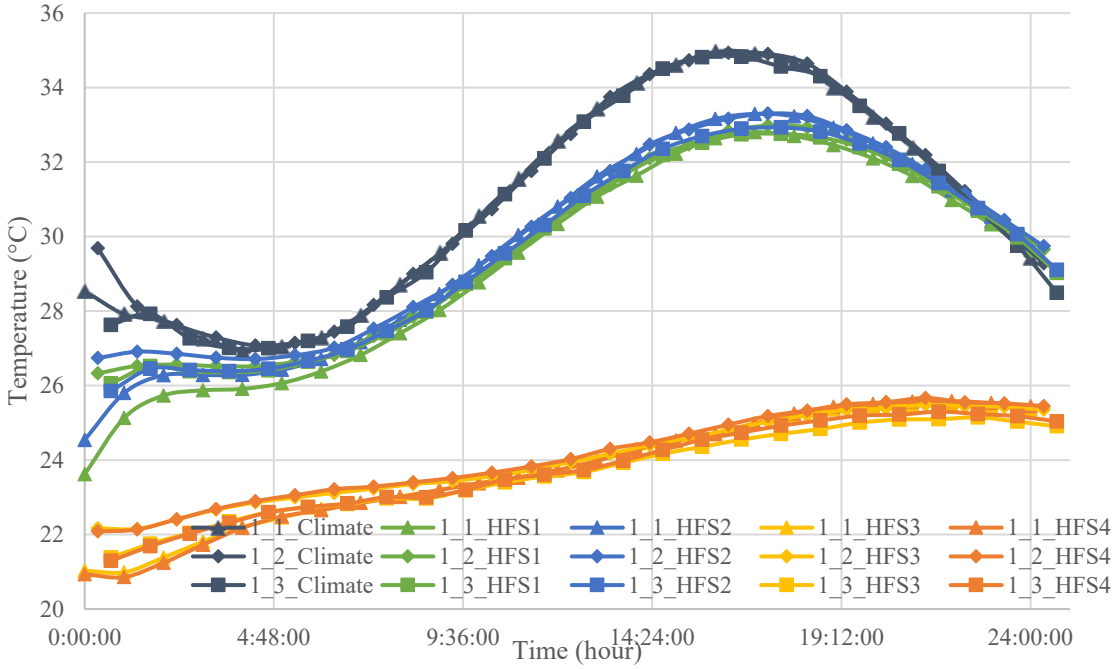

Figure A-1 Temperature Response of The Three Solid Grouted Specimen Replicates

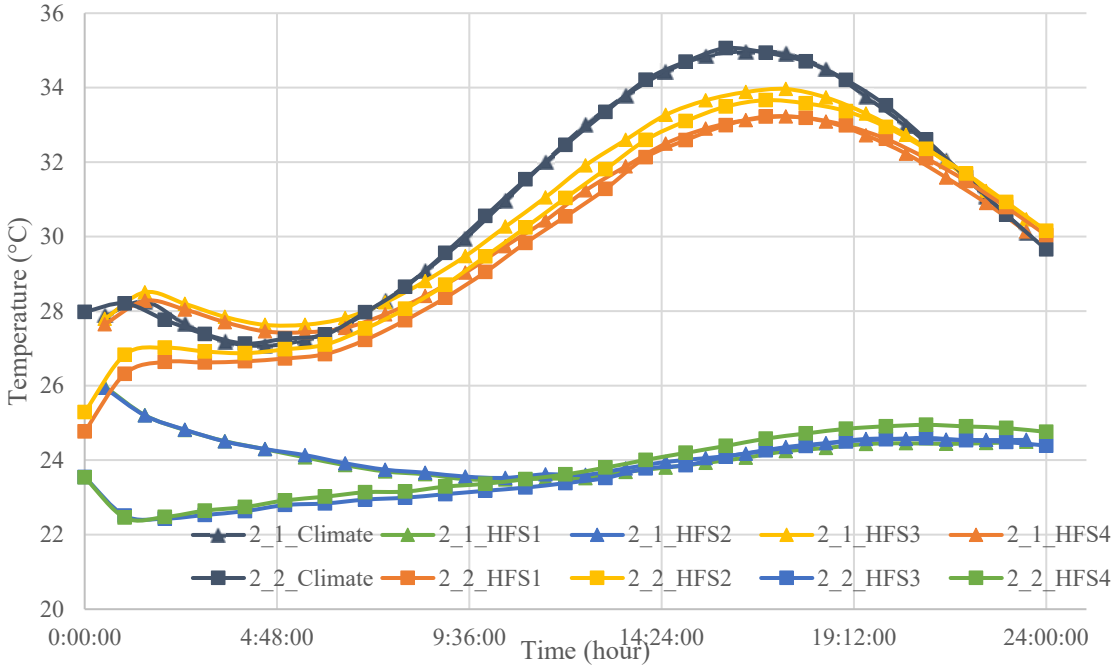

Figure A-2 Temperature Response of The Solid Grouted with Air Gap Specimen (Both Directions)

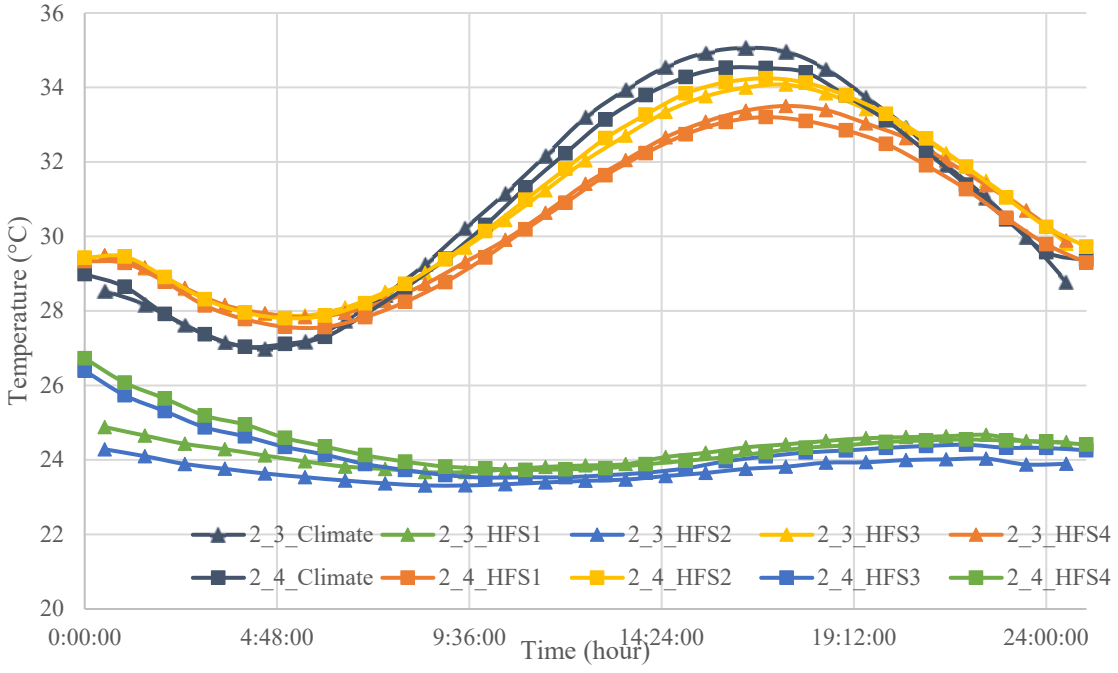

Figure A-3 Temperature Response of The Solid Grouted with Insulation Insert Specimen (Both Directions)

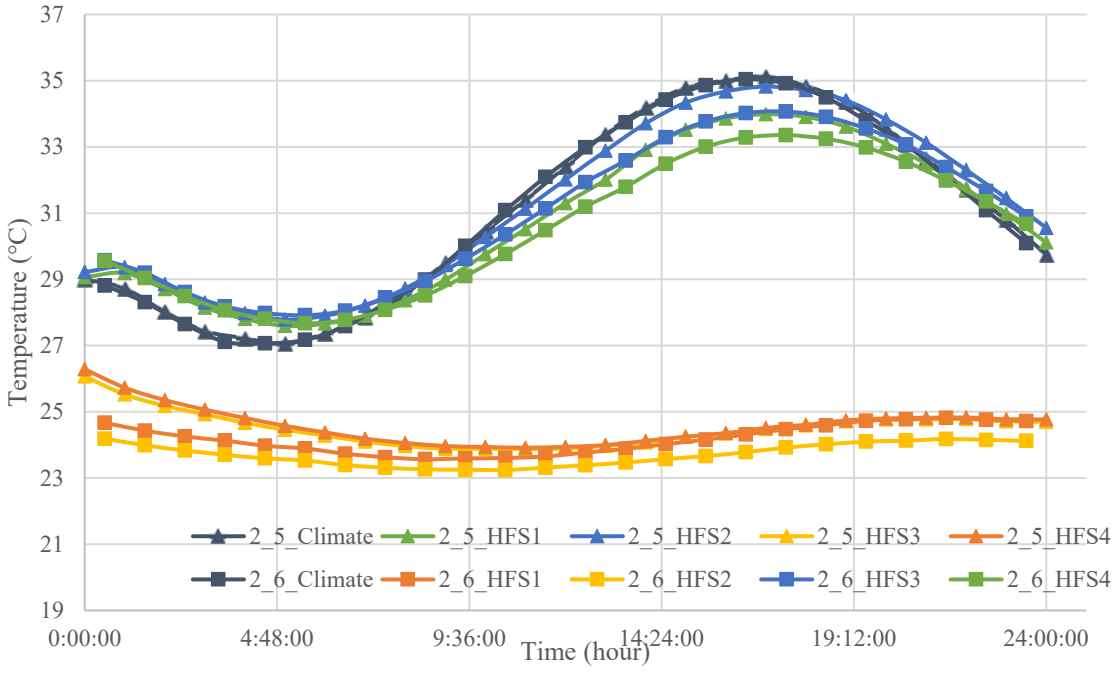

Figure A-4 Temperature Response of The Solid Grouted with Reflective Insert & Air Gap Specimen (Both Directions)

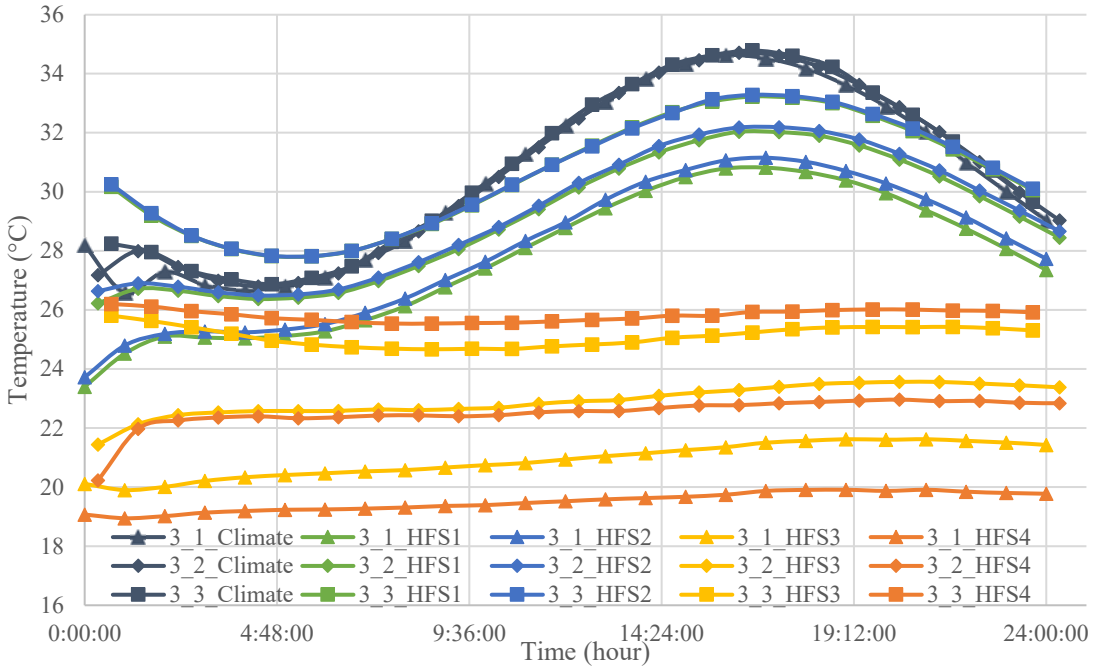

Figure A-5 Temperature Response of The Active Thermal Insulation Specimen (16-inch specimen, pipe near interior) in Summer Condition (Test No.3_1, No.3_2, No.3_3)

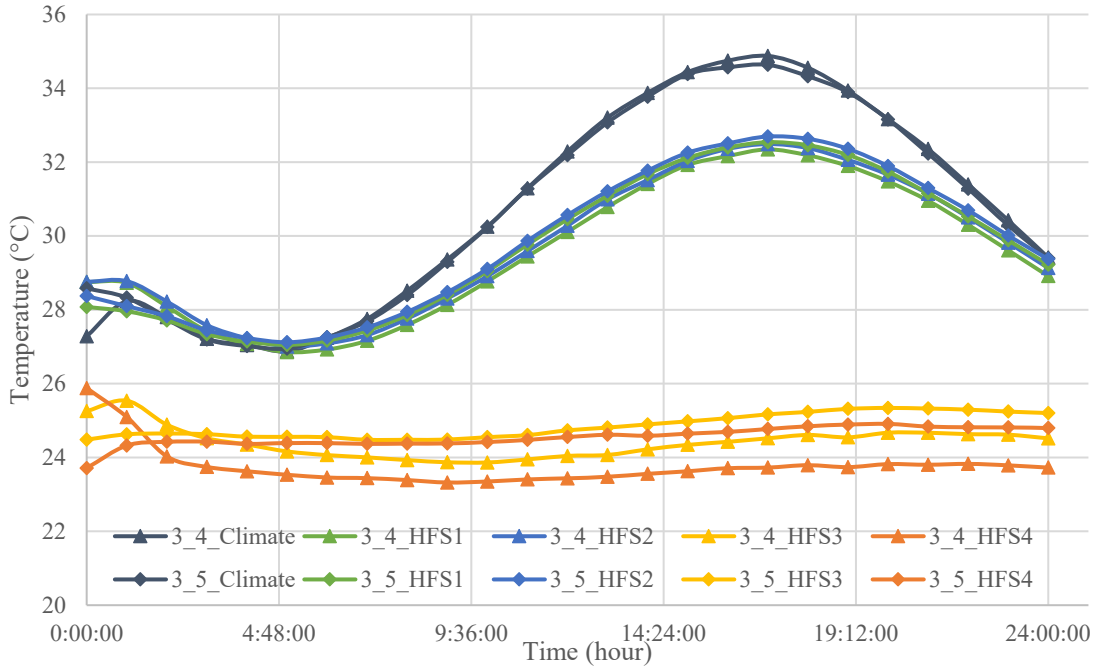

Figure A-6 Temperature Response of The Active Thermal Insulation Specimen (16-inch specimen, pipe near interior) in Summer Condition (Test No.3_4, No.3_5)

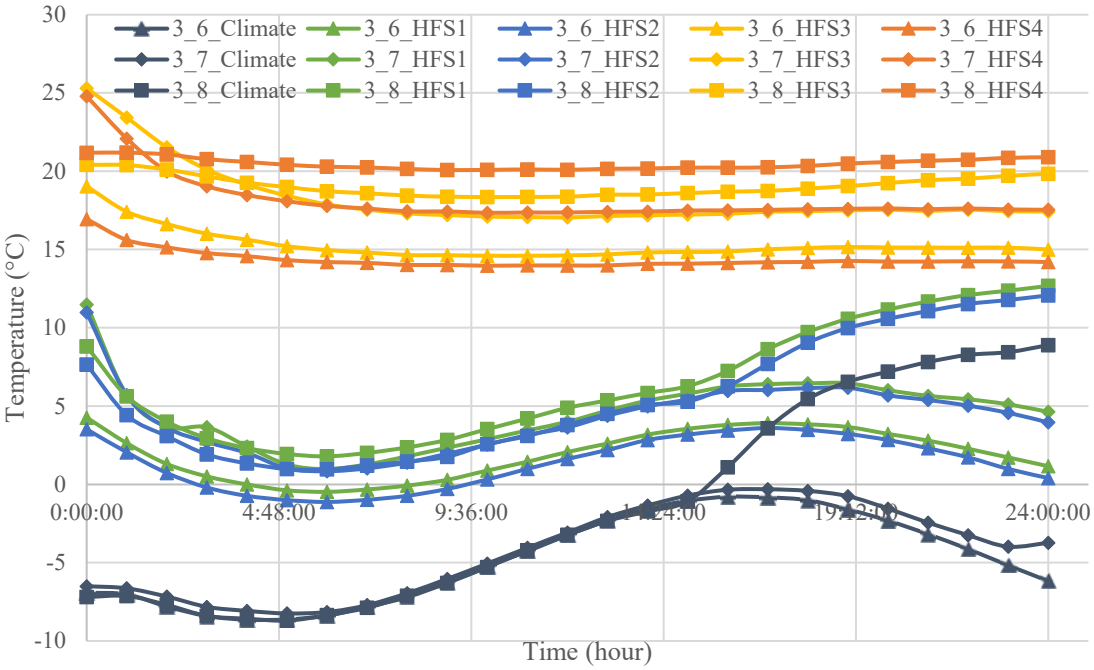

Figure A-7 Temperature Response of The Active Thermal Insulation Specimen (16-inch specimen, pipe near interior) in Winter Condition (Test No.3_6, No.3_7, No.3_8)

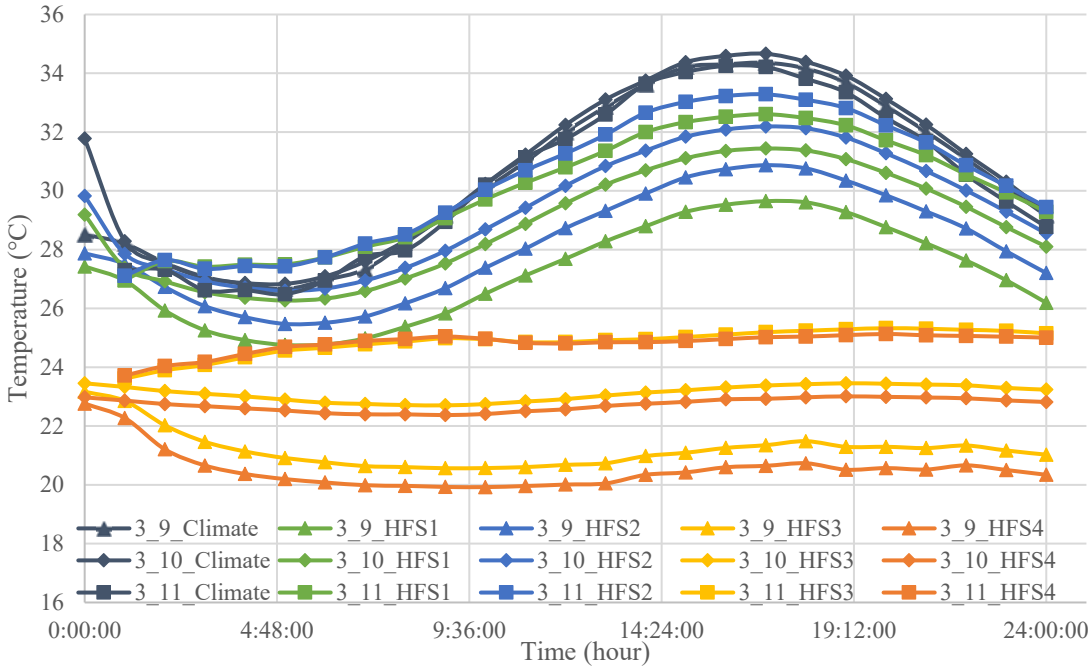

Figure A-8 Temperature Response of The Active Thermal Insulation Specimen (16-inch specimen, pipe in middle) in Summer Condition (Test No.3_9, No.3_10, No.3_11)

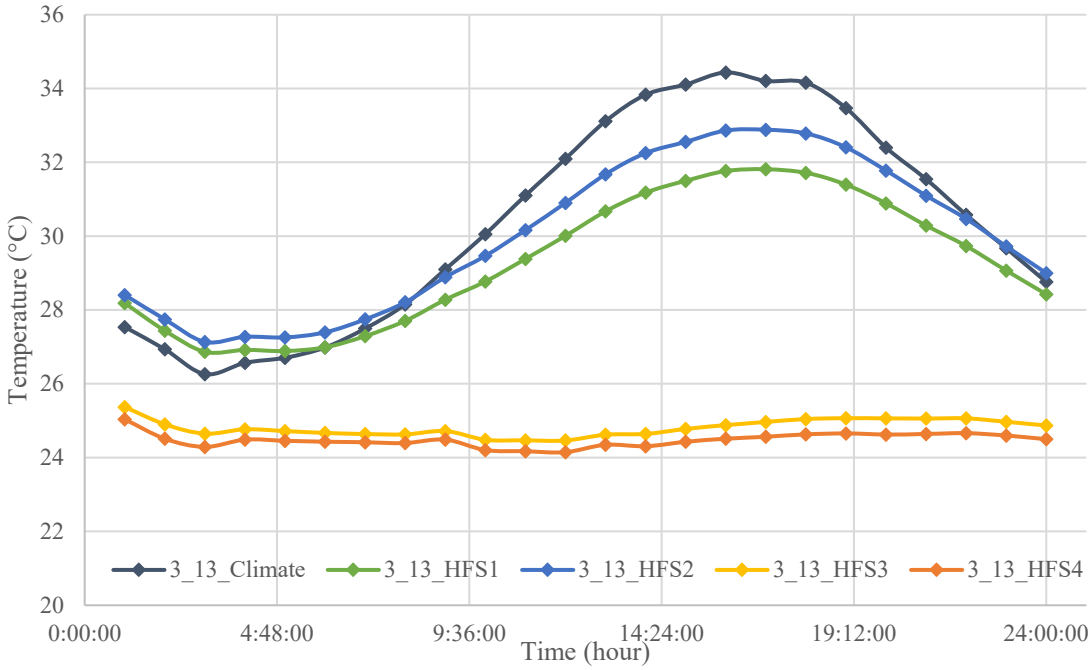

Figure A-9 Temperature Response of The Active Thermal Insulation Specimen (16-inch specimen, pipe in middle) in Summer Condition (Test No.3_13)

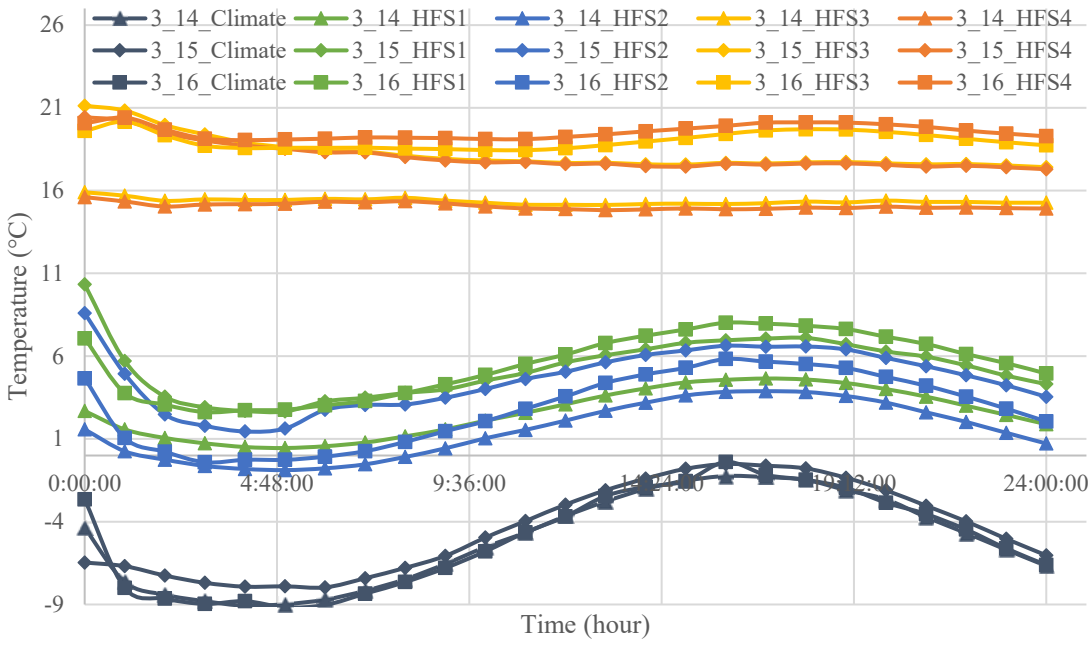

Figure A-10 Temperature Response of The Active Thermal Insulation Specimen (16-inch specimen, pipe in middle) in Winter Condition (Test No.3_14, No.3_15, No.3_16)

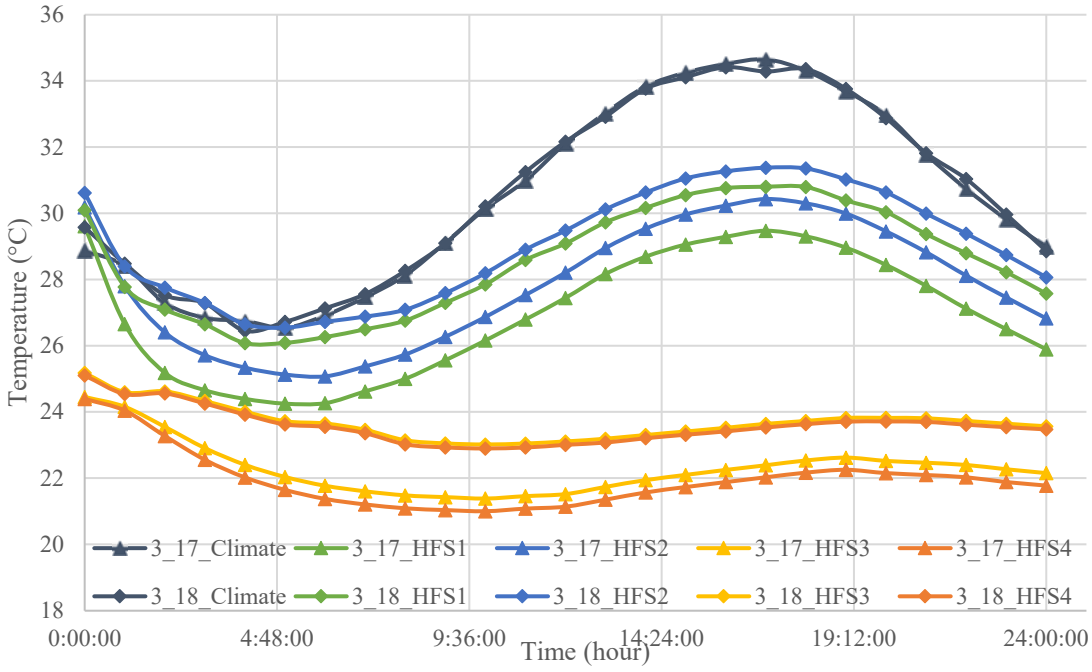

Figure A-11 Temperature Response of The Active Thermal Insulation Specimen (16-inch specimen, pipe near exterior) in Summer Condition (Test No.3_17, No.3_18)

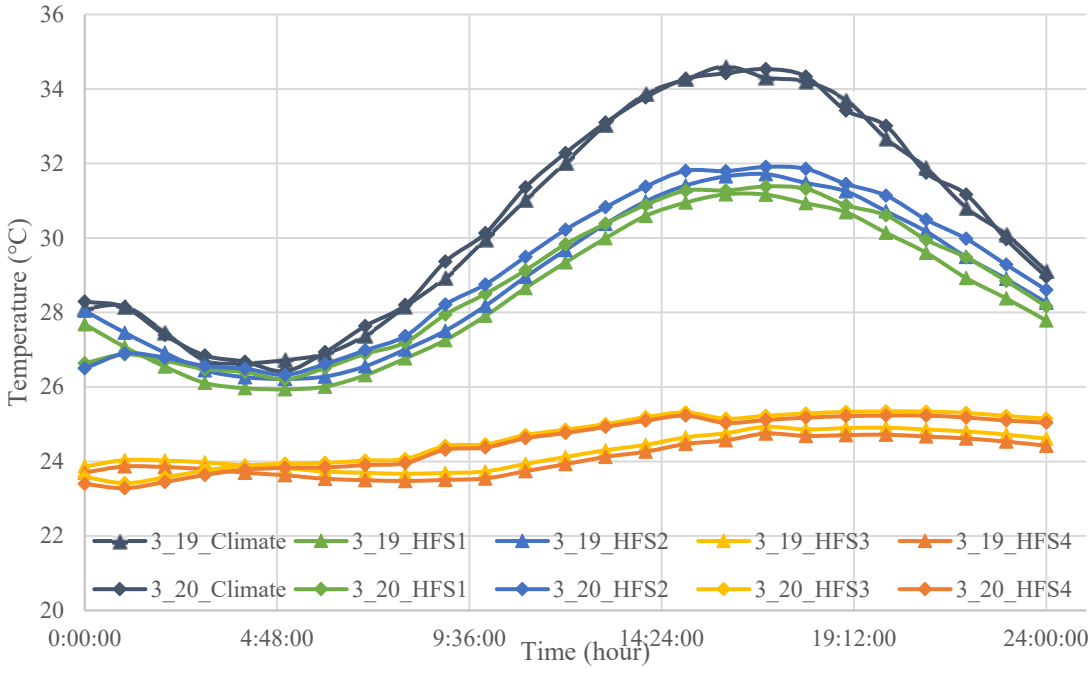

Figure A-12 Temperature Response of The Active Thermal Insulation Specimen (16-inch specimen, pipe near exterior) in Summer Condition (Test No.3_19, No.3_20)

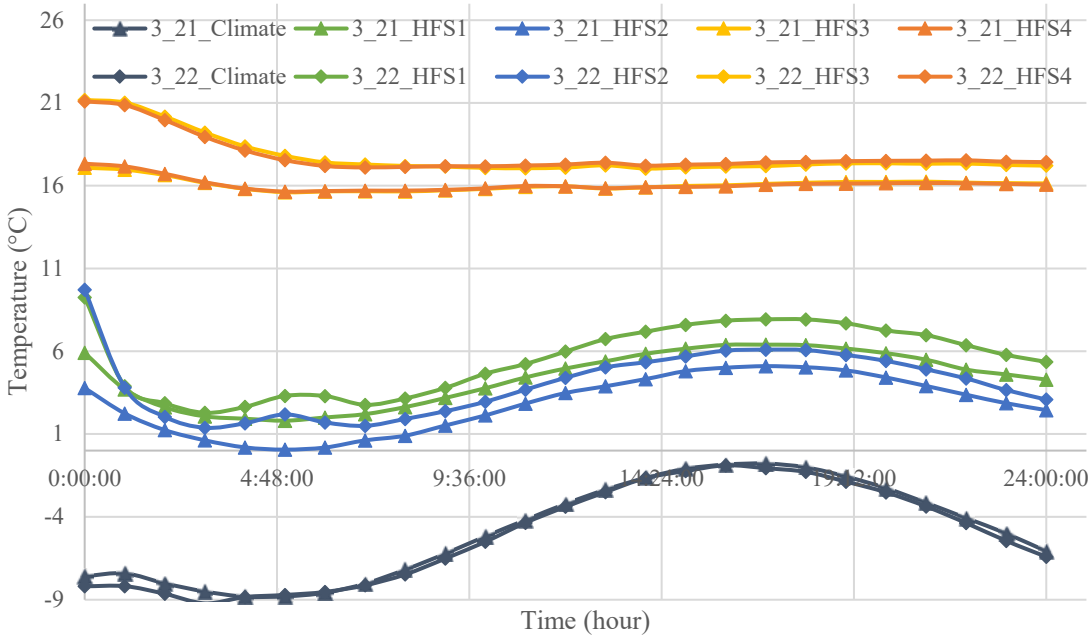

Figure A-13 Temperature Response of The Active Thermal Insulation Specimen (16-inch specimen, pipe near exterior) in Winter Condition (Test No.3_21, No.3_22)

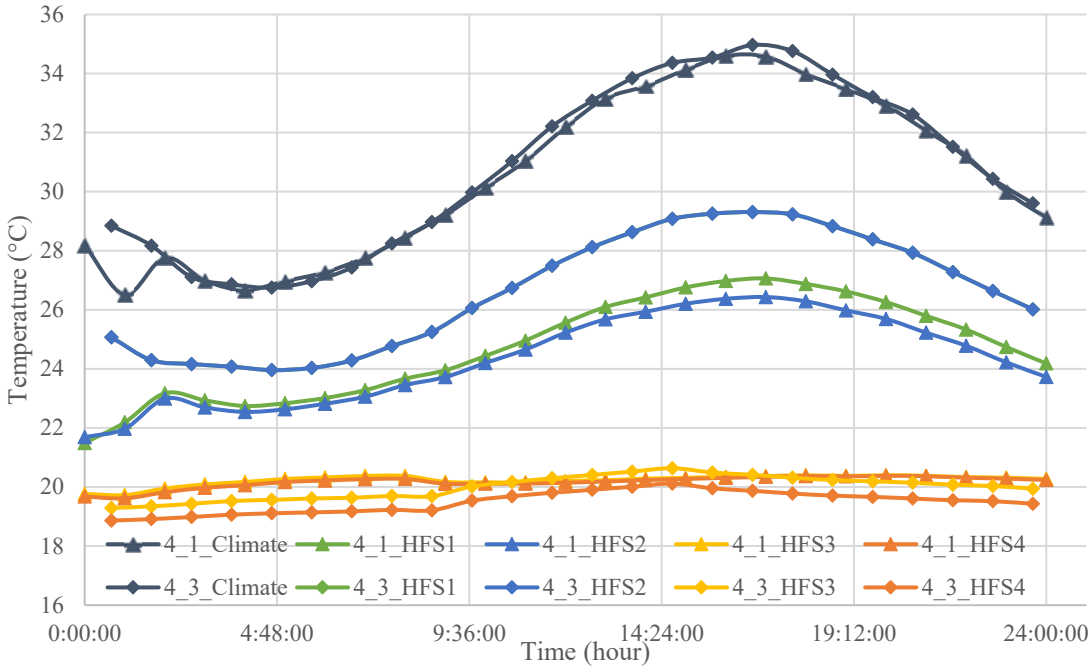

Figure A-14 Temperature Response of The Active Thermal Insulation Specimen (8-inch specimen) in Summer Condition (Test No.4_1, No.4_3)

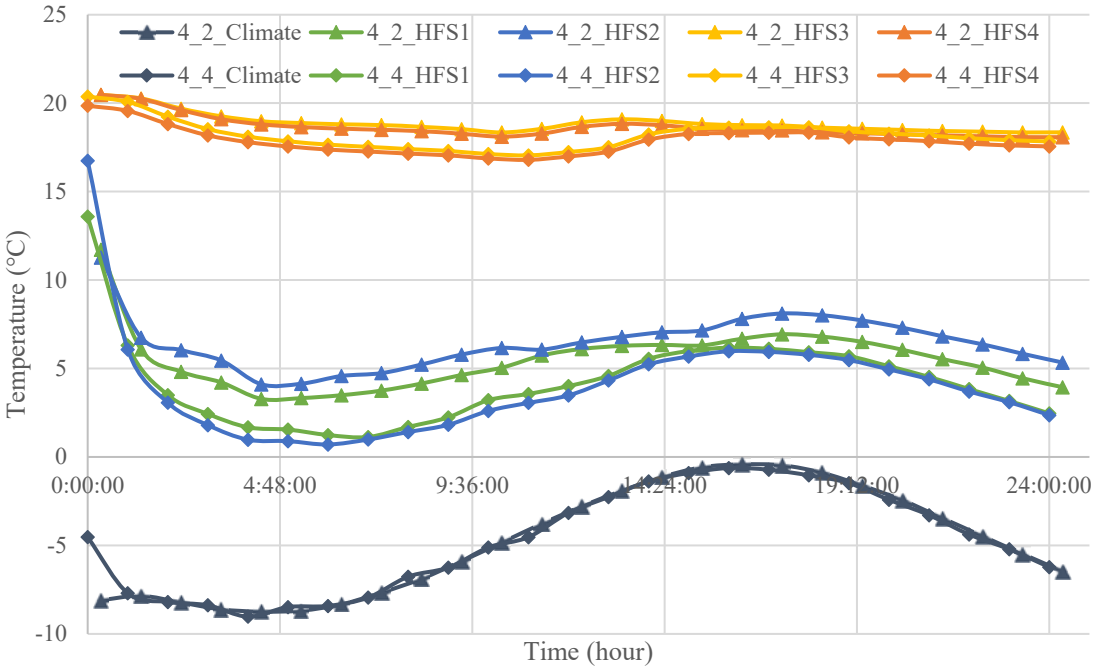

Figure A-15 Temperature Response of The Active Thermal Insulation Specimen (8-inch specimen) in Winter Condition (Test No.4_2, No.4_4)

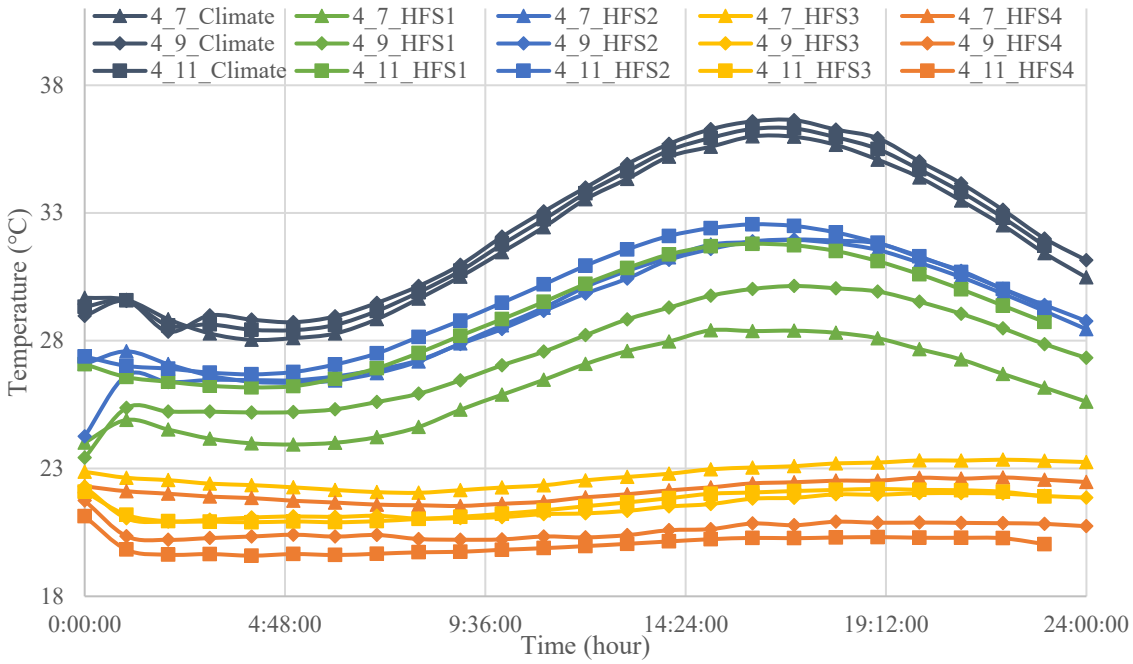

Figure A-16 Temperature Response of The Active Thermal Insulation Specimen (24-inch specimen) in Summer Condition (Test No.4_7, No.4_9, No.4_11)

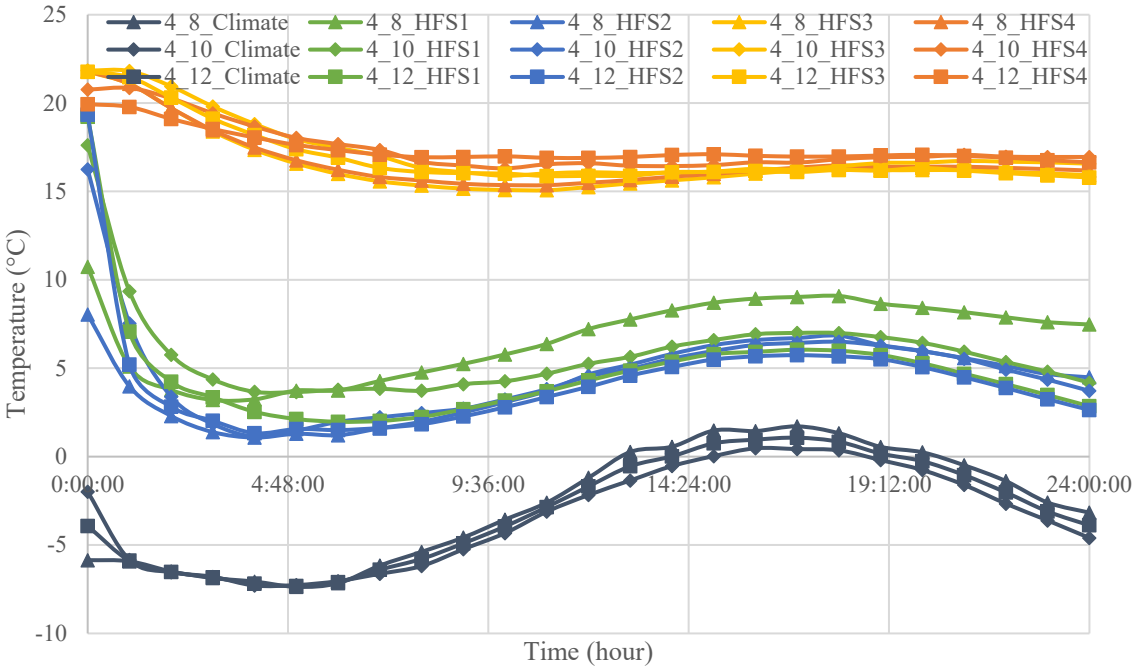

Figure A-17 Temperature Response of The Active Thermal Insulation Specimen (24-inch specimen) in Winter Condition (Test No.4_8, No.4_10, No.4_12)

APPENDIX B. MATLAB Code

An Example Function of ATIWS (16 inch spacing, pipe in middle), used in Chapter 5.4.

```
function [a,b,c,d,e]=FunctionATWIS(x,y)

% SI units (meter,kg,Kelvin,second,Joules,Watt)
% % % % %  INPUT PROPERTIES OF SPECIMEN (START) % % % % %

ZoneSeasonIndex=x;
FluidTemp=y;

% Dimensions (unit, inch) (convert to meter)
CMUwidth=16*0.0254;
CMUthickness=7.625*0.0254;
PIPEdiameter=0.75*0.0254;            % diameter of pipe
PIPEthickness=0.15*0.0254;           % thickness of pipe
CoreHeight=4.625*0.0254;             % height of core
CoreWidth=5.5*0.0254;              % width of core
PIPEdistance=0;   % distance from center
% PIPEdistance=0*0.0254;             % distance from center
% PIPEdistance=CoreHeight/2-PIPEdiameter/2-PIPEthickness   % distance from center
INSUthickness=0*0.0254;
MaxMesh=0.2*0.0254;                  % maximum mesh size
timestep=60;                    % timestep, unit,sec

% Thermal properties (unit, UNKNOWN)
CMUthermalconduc=0.726;   % thermal properties of CMU block, W/m*K  say 105pcf concrete
CMUmassdensity=1682;    % mass density, kg/m3
CMUspecificheat=960;    % specific heat, J/kg*K

GRTthermalconduc=1.41;   % thermal properties of grout, W/m*K
GRTmassdensity=2000;    % mass density, kg/m3
GRTspecificheat=800;    % specific heat, J/kg*K; Assumed

INSUthermalconduc=0.026;  % thermal properties of insulation, foam
INSUmassdensity=30;
INSUspecificheat=1200;    % ASSUMED

PIPEthermalconduc=385;
PIPEmassdensity=8960;
PIPEspecificheat=385;
% PIPEconvecfactor=1500;       % convection of pipe inner surface
```

```
PIPEconvecfactor=0.0002*FluidTemp^3-0.044*FluidTemp^2+15.591*FluidTemp+903.59;

% % % % % % % Fluid Temperature % % % % % % %
% ClimateZone1ASpring/Summer/Autumn/Winter Fahrenheit

% ZoneSeasonIndex=28;
% FluidTemp=43.642;

TempPool=[80.6 87.9 84.1 75.8 78.9 91.6 80.7 64.5 79.2 101.7 80.3 58.9 57 72 58.9 44.9 58.6 82 62.2 33.5
56.4 81.7 57.5 26.7 48.6 73.8 50.7 21.7;
   69.6 77.4 73.7 63.3 61.3 75.1 62.9 46.8 57.1 78.3 58.7 40.4 39.2 50.8 42.7 33.5 39.6 62.7 43.4 18.3 35.1
59.8 37.7 9.9 29.3 53.1 34.3 5.0];        % Average high&low temperature in four seasons and seven climate
zones in F
% FluidTempPool=[76.6 70.3 69.4 49.9 50.1 45.7 39.7];
% % % Initial Conditions
% FluidTempInF=FluidTempPool(ceil(ZoneSeasonIndex/4));      % Fahrenheit
% FluidTemp=(FluidTempInF-32)*5/9;      % Celsius

% % % % % % % Fluid Temperature % % % % % % %

InternalTemp=22;
MeanTempofCMU=22;

TempHigh=TempPool(1,ZoneSeasonIndex);
TempLow=TempPool(2,ZoneSeasonIndex);

% Convert to Celsius
MeanTemp=((TempHigh+TempLow)/2-32)*5/9;
AmplTemp=(((TempHigh-32)*5/9)-((TempLow-32)*5/9))/2;

% ExternalTemp=MeanTemp+AmplTemp*sin((t-28800)/86400);

% Virtual thermal properties of Internal/External air film (unit, UNKNOWN)
INAIFMthickness=0.10*0.02435;        % to make up the R value of air film 0.68(I-P units) or say 0.12(SI
units)
AIFMthermalconduc=0.02435;         % thermal conductivity of air
AIFMmassdensity=1.225;
AIFMspecificheat=1;               % normaly it's this value

EXAIFMthickness=0.03*0.02435;        % to make up the R value of air film 0.17(I-P units) or say 0.03(SI
units)

% % % % %  INPUT PROPERTIES OF SPECIMEN (END) % % % % %

% % % % % % % % % % CREATE GEOMETRY (START) % % % % % % % % % %
xlimitlow = -0.5*CMUwidth;
xlimithigh = 0.5*CMUwidth;
ylimitlow = -0.5*CMUthickness-INSUthickness-INAIFMthickness;
ylimithigh = 0.5*CMUthickness+EXAIFMthickness;

% CMU block
Rect1 = [3                % 3 indicates a rectangle
   4                   % 4 indicates the number of line segments
```

```
    -CMUwidth/2            % line 3 to 6 show x-coordinate of edge starting points
    CMUwidth/2
    CMUwidth/2
    -CMUwidth/2
    -CMUthickness/2        % line 7 through 10 show y-coordinate of edge starting points
    -CMUthickness/2
    CMUthickness/2
    CMUthickness/2];
% Grout left
Rect2 = [3              % 3 indicates a rectangle
    4                   % 4 indicates the number of line segments
    -CMUwidth/2            % line 3 to 6 show x-coordinate of edge starting points
    -CoreWidth/2-2*(CMUwidth-2*CoreWidth)/3
    -CoreWidth/2-2*(CMUwidth-2*CoreWidth)/3
    -CMUwidth/2
    -CoreHeight/2          % line 7 through 10 show y-coordinate of edge starting points
    -CoreHeight/2
    CoreHeight/2
    CoreHeight/2];
% Grout middle
Rect3 = [3              % 3 indicates a rectangle
    4                   % 4 indicates the number of line segments
    -CoreWidth/2           % line 3 to 6 show x-coordinate of edge starting points
    CoreWidth/2
    CoreWidth/2
    -CoreWidth/2
    -CoreHeight/2          % line 7 through 10 show y-coordinate of edge starting points
    -CoreHeight/2
    CoreHeight/2
    CoreHeight/2];
% Grout right
Rect4 = [3              % 3 indicates a rectangle
    4                   % 4 indicates the number of line segments
    CoreWidth/2+(CMUwidth-2*CoreWidth)/3        % line 3 to 6 show x-coordinate of edge starting points
    CMUwidth/2
    CMUwidth/2
    CoreWidth/2+(CMUwidth-2*CoreWidth)/3
    -CoreHeight/2          % line 7 through 10 show y-coordinate of edge starting points
    -CoreHeight/2
    CoreHeight/2
    CoreHeight/2];
% Grout narrow
Rect5 = [3              % 3 indicates a rectangle
    4                   % 4 indicates the number of line segments
    -CoreWidth/2-(CMUwidth-2*CoreWidth)/3-1/4*0.0254        % line 3 to 6 show x-coordinate of edge
starting points
    -CoreWidth/2-(CMUwidth-2*CoreWidth)/3+1/4*0.0254
    -CoreWidth/2-(CMUwidth-2*CoreWidth)/3+1/4*0.0254
    -CoreWidth/2-(CMUwidth-2*CoreWidth)/3-1/4*0.0254
    -CMUthickness/2        % line 7 through 10 show y-coordinate of edge starting points
    -CMUthickness/2
    CMUthickness/2
    CMUthickness/2];
% Internal air film
Rect6 = [3
    4
```

```
    -CMUwidth/2
    CMUwidth/2
    CMUwidth/2
    -CMUwidth/2
    -CMUthickness/2-INSUthickness-INAIFMthickness
    -CMUthickness/2-INSUthickness-INAIFMthickness
    -CMUthickness/2-INSUthickness
    -CMUthickness/2-INSUthickness];
% External air film
Rect7 = [3
    4
    -CMUwidth/2
    CMUwidth/2
    CMUwidth/2
    -CMUwidth/2
    CMUthickness/2
    CMUthickness/2
    CMUthickness/2+EXAIFMthickness
    CMUthickness/2+EXAIFMthickness];
C1 = [1                                 % 1 indicates a circle
    0         % x cordinate of circle center
    PIPEdistance                        % y cordinate of circle center
    PIPEdiameter/2];                      % Radius of circle
C1 = [C1;zeros(length(Rect1)-length(C1),1)];
C2 = [1                                 % 1 indicates a circle
    0         % x cordinate of circle center
    PIPEdistance                        % y cordinate of circle center
    PIPEdiameter/2+PIPEthickness];              % Radius of circle
C2 = [C2;zeros(length(Rect1)-length(C2),1)];
gd=[Rect1,Rect2,Rect3,Rect4,Rect5,Rect6,Rect7,C1,C2];
ns = char('Rect1','Rect2','Rect3','Rect4','Rect5','Rect6','Rect7','C1','C2');
ns = ns';
sf = '(Rect1-Rect2-Rect3-Rect4-Rect5)+(Rect3-C2)+Rect2+Rect4+Rect5+Rect6+Rect7+(C2-C1)';
[dl,bt] = decsg(gd,sf,ns);
pdegplot(dl,'EdgeLabels','on','FaceLabels','on');
xlim([1.2*xlimitlow,1.2*xlimithigh]);
ylim([1.2*ylimitlow,1.2*ylimithigh]);
title 'Labeling of Wall Assembly';

% % % % % % % % % % CREATE GEOMETRY (END) % % % % % % % % % %

% % % % % %  ASSIGN ATTRIBUTES TO THERMALMODEL (START)  % % % % % %

Thermalmodel = createpde('thermal','transient');
pg = geometryFromEdges(Thermalmodel,dl);

% Thermal Properties of CMU
thermalProperties(Thermalmodel,'Face',[1,4],...
                        'ThermalConductivity',CMUthermalconduc,...
                        'MassDensity',CMUmassdensity,...
                        'SpecificHeat',CMUspecificheat);
thermalProperties(Thermalmodel,'Face',[2,5,6,8],...
                        'ThermalConductivity',GRTthermalconduc,...
                        'MassDensity',GRTmassdensity,...
                        'SpecificHeat',GRTspecificheat);
```

```
thermalProperties(Thermalmodel,'Face',9,...
                    'ThermalConductivity',PIPEthermalconduc,...
                    'MassDensity',PIPEmassdensity,...
                    'SpecificHeat',PIPEspecificheat);
% % Thermal Properties of INSULATION
% thermalProperties(Thermalmodel,'Face',1,...
%                     'ThermalConductivity',INSUthermalconduc,...
%                     'MassDensity',INSUmassdensity,...
%                     'SpecificHeat',INSUspecificheat);

% Thermal Properties of Internal/External air film
thermalProperties(Thermalmodel,'Face',[3,7],...
                    'ThermalConductivity',AIFMthermalconduc,...
                    'MassDensity',AIFMmassdensity,...
                    'SpecificHeat',AIFMspecificheat);

% Internal Heat Source
  % function(internalHeatSource), but no internal heat source in this model

% Thermal Boundary Condition
thermalBC(Thermalmodel,'Edge',[31,32,33,34],'ConvectionCoefficient',PIPEconvecfactor,'AmbientTemper
ature',FluidTemp);
thermalBC(Thermalmodel,'Edge',[3],'Temperature',InternalTemp);
thermalBC(Thermalmodel,'Edge',[11,12,13,14,15,16,17,18,19,20],'HeatFlux',0);
thermalBC(Thermalmodel,'Edge',[4],'Temperature',@(location,state)(MeanTemp+AmplTemp*sin(2*pi*(st
ate.time-36000)/86400)));
% % ExternalTemp=MeanTemp+AmplTemp*sin((t-28800)/86400);


% % % % %  ASSIGN ATTRIBUTES TO THERMALMODEL (END)  % % % % % %

% % % % % % % % % % MESH THERMALMODEL (START)  % % % % % % % % % %

mesh = generateMesh(Thermalmodel,'Hmax',MaxMesh);
% locate sensors in this model
% sensorlocations
SL=[0,CMUthickness/2;                   %HFS1
   -CoreWidth/2,CMUthickness/2;         %HFS2
   -CoreWidth/2,-CMUthickness/2;        %HFS3
   0,-CMUthickness/2;          %HFS4
   -CoreWidth/2,-CoreHeight/2;          %6
   0,-PIPEdiameter/2-PIPEthickness;    %22
   -PIPEdiameter/2-PIPEthickness,0;         %23
   -CoreWidth/2,CoreHeight/2;          %26
   0,PIPEdiameter/2+PIPEthickness;         %30
   CoreWidth/2,CoreHeight/2;          %31
   0,CoreHeight/2;          %B5
   0,-CoreHeight/2;            %C23
   CoreWidth/2,CMUthickness/2;            %D3
   -CoreWidth/2-(CMUwidth-2*CoreWidth)/6,CMUthickness/2;          %D8
   -CoreWidth/2-(CMUwidth-2*CoreWidth)/6,-CMUthickness/2;         %D10
   CoreWidth/2,-CMUthickness/2;            %D3
   CoreWidth/2,-CMUthickness/2];           %C26
```

```
NodesTempSensors = findNodes(mesh,'nearest',[SL(1,1) SL(2,1) SL(3,1) SL(4,1) SL(5,1) SL(6,1) SL(7,1)
SL(8,1) SL(9,1) SL(10,1) SL(11,1) SL(12,1) SL(13,1) SL(14,1) SL(15,1) SL(16,1) SL(17,1);
   SL(1,2) SL(2,2) SL(3,2) SL(4,2) SL(5,2) SL(6,2) SL(7,2) SL(8,2) SL(9,2) SL(10,2) SL(11,2) SL(12,2)
SL(13,2) SL(14,2) SL(15,2) SL(16,2) SL(17,2)]);
ExteriorMid = findNodes(mesh,'nearest',[0;CMUthickness/2+INAIFMthickness]);
figure
pdeplot(Thermalmodel);
xlim([1.2*xlimitlow,1.2*xlimithigh]);
ylim([1.2*ylimitlow,1.2*ylimithigh]);
title 'Mesh Displayed on Wall Assembly';
hold on
plot(mesh.Nodes(1,NodesTempSensors),mesh.Nodes(2,NodesTempSensors),'or','MarkerFaceColor','g')
% % % % % % % % % % MESH THERMALMODEL (END)  % % % % % % % % % %

% % % % % % % THERMALMODEL INITIAL CONDITION (START)  % % % % % % %

thermalIC(Thermalmodel,MeanTempofCMU);

% % % % % % % THERMALMODEL INITIAL CONDITION (END)  % % % % % % %

% % % % % % % % % % SOLVE THERMALMODEL (START)  % % % % % % % % % %
tlist = 0:timestep:172800;      % max time in seconds
Thermalresults = solve(Thermalmodel,tlist);
Temperature = Thermalresults.Temperature;

% % % % % % % % % % SOLVE THERMALMODEL (END)  % % % % % % % % % %
% % % % % % % % % % PLOT THERMALMODEL (START)  % % % % % % % % % %
% % Get Nodes at sensor location % %
% Temperature Sensors
SensorsTemp =
Temperature([ExteriorMid,NodesTempSensors(1),NodesTempSensors(2),NodesTempSensors(3),NodesTe
mpSensors(4),NodesTempSensors(5),NodesTempSensors(6),NodesTempSensors(7),NodesTempSensors(8
),NodesTempSensors(9),NodesTempSensors(10),NodesTempSensors(11),NodesTempSensors(12),NodesT
empSensors(13),NodesTempSensors(14),NodesTempSensors(15),NodesTempSensors(16),NodesTempSen
sors(17)],:);

Tempmax = max(max(Temperature));
Tempmin = min(min(Temperature));
% plot ambient temperature function
figure;
plot(tlist/3600,Temperature(ExteriorMid, :));
hold all
plot(tlist/3600,Temperature(NodesTempSensors(1), :));
plot(tlist/3600,Temperature(NodesTempSensors(2), :));
plot(tlist/3600,Temperature(NodesTempSensors(3), :));
plot(tlist/3600,Temperature(NodesTempSensors(4), :));
plot(tlist/3600,Temperature(NodesTempSensors(5), :));
plot(tlist/3600,Temperature(NodesTempSensors(6), :));
plot(tlist/3600,Temperature(NodesTempSensors(7), :));
plot(tlist/3600,Temperature(NodesTempSensors(8), :));
plot(tlist/3600,Temperature(NodesTempSensors(9), :));
plot(tlist/3600,Temperature(NodesTempSensors(10), :));
plot(tlist/3600,Temperature(NodesTempSensors(11), :));
plot(tlist/3600,Temperature(NodesTempSensors(12), :));
plot(tlist/3600,Temperature(NodesTempSensors(13), :));
```

```
plot(tlist/3600,Temperature(NodesTempSensors(14), :));
plot(tlist/3600,Temperature(NodesTempSensors(15), :));
plot(tlist/3600,Temperature(NodesTempSensors(16), :));
plot(tlist/3600,Temperature(NodesTempSensors(17), :));
hold off
grid on
legend('Exterior', 'HFS1','HFS2','HFS3','HFS4','6','22','23','26','30','31','B5','C23','D3','D8','D10','D11','C26')
% axis([0 86400 Tempmin Tempmax])
title 'Sensor Temperature as a Function of Time'
xlabel 'Time(Hours)'
ylabel 'Temperature(Celsius)'
% axis([0 24 MeanTemp-AmplTemp-5 MeanTemp+AmplTemp+5])
axis([0 24.5 20 38])

% Calculate the heat flux through insulation surface using 'evaluateHeatFlux'
%  -------------REFERENCE--------------
NodesOnIntFace = findNodes(mesh,'region','Edge',[5,6,7]);       %%Note the Edge number may change
[qx,qy] = evaluateHeatFlux(Thermalresults);
for k = 1:numel(NodesOnIntFace)
   for j = 1:numel(Thermalresults.SolutionTimes)
      HeatFlux(k,j) = qy(NodesOnIntFace(k),j);
      TempInnerSurface(k,j) = Temperature(NodesOnIntFace(k),j);
   end
end
HeatFluxAtTime = sum(HeatFlux);
HeatFluxAtTimeHalf = HeatFluxAtTime(1441:2881);
HeatFluxSum =
sum(HeatFluxAtTimeHalf*(timestep/86400)*CMUwidth/numel(NodesOnIntFace))/CMUwidth;
TempIntAvg = sum(TempInnerSurface)/numel(NodesOnIntFace);

TinSurf = TempIntAvg(1441:2881);
TdinSurf = TinSurf-InternalTemp;
TdmeaninSurf = mean(TdinSurf);
TdmaxinSurf = max(TinSurf)-InternalTemp;
%  -------------REFERENCE--------------

TimeCount=numel(Thermalresults.SolutionTimes);   % count of time
TimeCount0=(TimeCount+1)/2;

% % Calculate the heat flux through insulation surface using 'evaluateHeatRate'
HeatTotalRate = evaluateHeatRate(Thermalresults,'Edge',[5,6,7]);
HeatTotalRateHalf = HeatTotalRate(1441:2881);
HeatTotal = sum(HeatTotalRateHalf*timestep/86400)/CMUwidth;

HeatTotalRate2 = evaluateHeatRate(Thermalresults,'Edge',3);
HeatTotalRateHalf2 = HeatTotalRate2(1441:2881);
HeatTotal2 = sum(HeatTotalRateHalf2*timestep/86400)/CMUwidth;

TotalHeatRate48HourInteriorAir = evaluateHeatRate(Thermalresults,'Edge',3);
TotalHeatRateInteriorAir = TotalHeatRate48HourInteriorAir(TimeCount0:TimeCount);
HeatRateAverageInteriorAir = mean(TotalHeatRateInteriorAir);
PerAreaHeatRateInteriorAir = HeatRateAverageInteriorAir/CMUwidth;
HeatFluxTotalInteriorAir = HeatRateAverageInteriorAir*86400;
```

```
TotalHeatRate48HourExteriorAir = evaluateHeatRate(Thermalresults,'Edge',4);
TotalHeatRateExteriorAir = TotalHeatRate48HourExteriorAir(TimeCount0:TimeCount);
HeatRateAverageExteriorAir = mean(TotalHeatRateExteriorAir);
PerAreaHeatRateExteriorAir = HeatRateAverageExteriorAir/CMUwidth;
HeatFluxTotalExteriorAir = HeatRateAverageExteriorAir*86400;

TotalHeatRate48HourPipeInner = evaluateHeatRate(Thermalresults,'Edge',[31,32,33,34]);
TotalHeatRatePipeInner = TotalHeatRate48HourPipeInner(TimeCount0:TimeCount);
HeatRateAveragePipeInner = mean(TotalHeatRatePipeInner);
HeatFluxTotalPipeInner = HeatRateAveragePipeInner*86400;

a=HeatRateAverageInteriorAir;
b=HeatRateAverageExteriorAir;
c=HeatRateAveragePipeInner;
d=TdmeaninSurf;
e=TdmaxinSurf;
end
% % % % % % % % % % SOLVE THERMALMODEL (END)  % % % % % % % % % %
```

CURRICULUM VITA

NAME: Li Liu

ADDRESS: 132 Eastern Parkway
Department of Civil and Environmental Engineering
University of Louisville
Louisville, KY 40292
l0liu016@louisville.edu

DOB: Wuhan, Hubei, China- May 3, 1990

EDUCATION & TRAINING:

B.S., Civil Engineering, Huazhong University of Science & Technology, 2008-2012

M.S., Civil Engineering, University of Louisville, 2016-2017

Ph.D., Civil Engineering, University of Louisville, 2017-2021

RESEARCH EXPERIENCE:

1. The Performance of Active Porcelain Enamel Coatings for Fiber Reinforced Concrete- Phase 2 SBIR – Army, Feb1 2017 to July 2018.
2. Alternative Energy Code Compliant Designs for Single Wythe Masonry Structures in Hawaii, Masonry Institute of Hawaii, Feb 2018 to May 2019.
3. Evaluation of Single Wythe Masonry Energy Use with Lightweight (Smart Wall) Systems, Expanded Shale, Clay and Slate Institute, November 2018 to June 2019.